Sonochemical modification of polyethylene and poly(vinyl chloride) surfaces

Clifton, Andrew

Award date:
1993

Awarding institution:
University of Bath

Sonochemical Modification of Polyethylene and Poly(vinyl chloride) Surfaces

Submitted by **ANDREW CLIFTON**

for the degree of **PhD**

at the **University of Bath**

1993

ProQuest LLC
789 East Eisenhower Parkway
P.O. Box 1346
Ann Arbor, MI 48106-1346

Sonochemical Modification of Polyethylene and Poly(vinyl chloride) Surfaces

Submitted by ANDREW CLIFTON

for the degree of PhD

at the University of Bath

1993

ACKNOWLEDGEMENTS

My special thanks go to Dr. Gareth Price for his enthusiasm, effort and constant support over the course of the work in this thesis.

I would like also to thank Peter West for his humour and for making sense when nothing else seemed to.

Thanks also to John, Fiona and BICC.

Thanks to SERC for the loan of the Malvern Particle Sizer and to Amanda for her technical assistance.

To my parents for starting this journey.

To so many other people who have made the last three years such fun.

Louise - thanks for being so understanding and giving me so much love and encouragement.

CONTENTS

Chapter Two EXPERIMENTAL

SUMMARY

The work described in this thesis was concerned with the development of ultrasonically promoted surface modification methods for electrical cables having polyethylene or poly(vinyl chloride) sheathing.

In a series of model reactions aqueous suspensions of powders of these and several other polymers were sonicated and a correlation between the hardness, impact strength and fragmentation ability was shown. Sonication caused limited surface erosion of polyethylene films and had no effect on their optical appearence.

Significant levels of oxidation were achieved in a very thin layer ($<<1\mu m$) of polyethylene film surfaces during sonochemical treatment with aqueous solutions of potassium persulphate or hydrogen peroxide at 35°C. Ultrasound was shown to accelerate the decomposition of persulphate by a factor of about 10 at this temperature. At low sonication times the oxygen containing species were found to comprise mostly hydroxyl groups, but extended irradiation led to the formation of mainly carboxylic acids and esters. This oxidation could be used to introduce further functionality onto the surface.

The surface of PVC powder has been effectively coloured by sonication in aqueous solutions of a number dyes. The colour of the final sample could be controlled in some cases by varying the pH of the dye solution, sonication time and presence of oxygen.

Ultrasound was also used to accelerate the base catalysed elimination of HCl from the surface of PVC to generate reactive sequences of conjugated double bonds. In the presence of $FeCl_3$ a crosslinking reaction was observed. Further reaction of these double bonds with a range of compounds gave a convienient method of introducing surface properties different to those of the bulk polymer.

A number of these reactions were then applied to "real" polymer systems where it was found that sonochemical treatment could also be used to successfully to change the surface property.

CHAPTER 1

INTRODUCTION

This thesis describes a programme of work aimed at the development of suitable ultrasonically promoted methods for the modification of polymer surfaces, namely of those polymers used for the sheathing of electrical cables. The project was supported in part by the research division of BICC Cables Ltd.

The surface of a cable is clearly the part in contact with the environment during use and will, therefore, have a major influence on its application and lifetime. The properties of interest for improvement were slippability, abrasion and chemical resistance. In addition, the surface represents a relatively small amount of the whole material so that endowing this, rather than the bulk polymer, with specialist properties would present clear economic benefits.

The majority of cables used at the present time are based on either polyethylene or poly(vinyl chloride) and work has, therefore, been restricted to these two polymers. Consideration of the processes involved in cable manufacture has also restricted the systems studied. For example, whilst good surface properties can be achieved with highly fluorinated polymers such as Teflon, the formation of undesirable products during their combustion renders such materials unsuitable for household and many industrial applications. Existing manufacturing processes involve extrusion of molten polymer cables into a quenching water bath and it was this process stage which provided the major focus of the project. In addition, safety and environmental considerations required the use of aqueous systems so that, again, work has only been performed in this area.

The project, after an introduction to the relevant technology and experimental techniques, has been divided into two phases. Initially, a wide range of systems were studied for polyethylene and poly(vinyl chloride) film and powder modifications. This enabled an understanding of the basic science of the interactions between ultrasound, polymer surfaces and modification reactions to be developed. The second phase of the work was then concerned with the application of some of the most promising systems to "real" cable samples supplied by BICC, also allowing some speculation as to the commercial utility of the developed

systems.

1.1 Nomenclature

A polymer is a large molecule comprised of many covalently bonded smaller molecules or monomers.[1] When only one type of monomeric repeat unit is present the polymer is referred to as a homopolymer. If however, two or more monomer units are present the resulting structure is described as a copolymer. Many natural polymers such as proteins contain more than five different repeat units. Examples of copolymers are shown in figure 1.1.

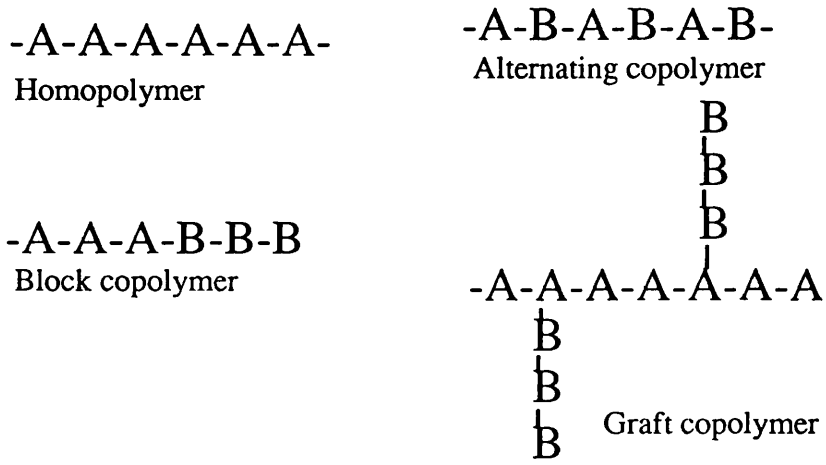

Figure 1.1 Copolymer types

Polymeric systems may have a linear chain-like, branched or crosslinked/network structure as shown in figure 1.2.

Additionally, polymers having asymmetric carbon atoms give rise to three possible stereochemical structures. These are shown in figure 1.3 for polypropylene. Together the skeletal and stereochemical structures control most of the physical properties displayed by polymer materials.

Whilst it is difficult to arrange polymers into precise, well defined groups, three particular categories are evident: thermoplastics, thermosets and rubbers.

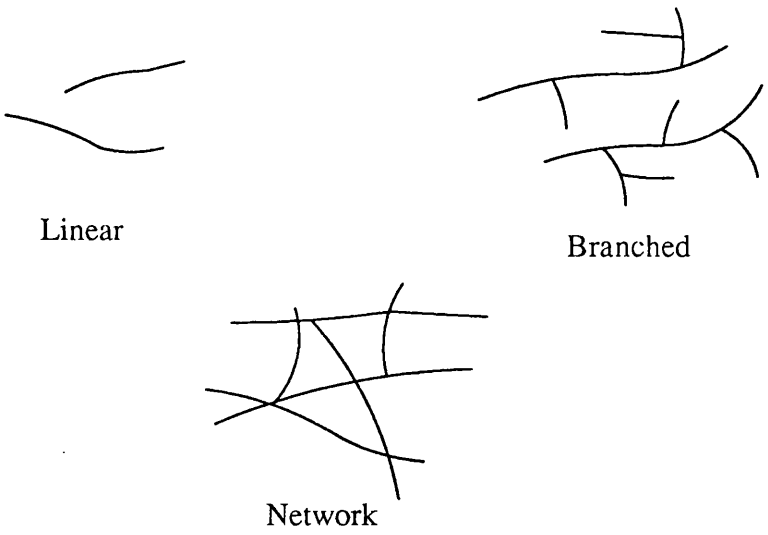

Figure 1.2 Polymer skeletal structures

three particular categories are evident: thermoplastics, thermosets and rubbers. Thermoplastics constitute the largest group of synthetic polymer materials and those studied in the present thesis fall into this category. They may be defined as those plastics which soften and flow upon the application of heat and are comprised of linear and branched macromolecules, such as polyethylene and poly(vinyl chloride).

Thermosets are rigid, highly cross-linked 3D networks which do not melt upon the application of heat, This group includes epoxy resins and natural polymers such as cellulose.

Rubbers exhibit elastomeric properties due to their lightly cross-linked structure and low Tg's, which prevent permanent relative movement of the molecules with respect to each other during deformation. Again, rubbers cannot be melted by heating, but are susceptible to thermal degradation. Examples of rubbers include poly(butadiene) and poly(isoprene).

1.1.1 Uses of Polymers

The use of synthetic polymers in everyday life has grown immensely in the last twenty years. The major reason for this trend must be attributed to the diversity

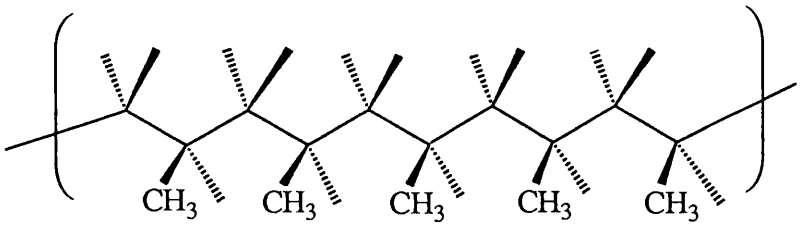

Isotactic polypropylene

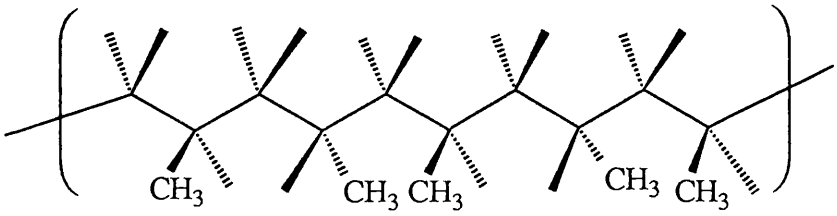

Syndiotactic polypropylene

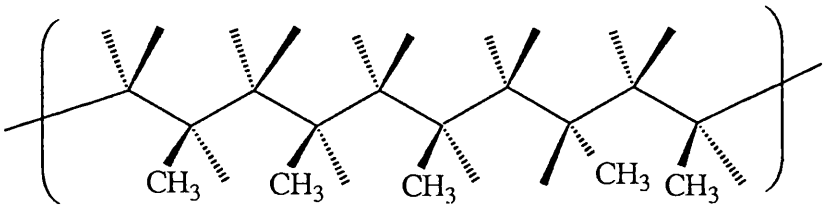

Atactic polypropylene

Figure 1.3 showing the different stereochemical structures in polymers

of properties which can be achieved with these materials. As the mechanical and environmental demands placed upon materials has grown, increasing numbers of workers have applied themselves to the development of both new polymers and also the modification of existing ones. Modification of polymers presents a unique way of manufacturing some polymers for which monomers are unattainable or simply cannot be polymerised.[2]

1.2 Polymer Modification

There are in general two processes by which new polymers can be manufactured. The first involves the synthesis of new monomer units which upon subsequent polymerisation yield new macromolecules. The second method involves chemical modification of a preformed polymer. Whilst the first approach leads to a fully substituted product of known structure, the latter rarely reaches complete functionalisation.[3]

The chemical modification of polymers probably began in 1781 with the isomerisation of natural rubber in the presence of acids.[4] The first reported modification of a totally synthetic polymer was possibly the nitration of polystyrene in reported 1845.[5] Later progress in this area was greatly assisted by Staudinger, who introduced the concept of polymer analogous rections.[6]

The modification of preformed polymers can be further subdivided into homogeneous and heterogeneous reaction systems. Homogeneous transformations generally result in the formation of a statistically modified material or copolymer accordingly:

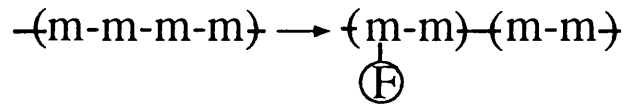

Hence, the new functionality, F, will be distributed throughout the material in a given percentage according to the conditions used. This method is particularly appropriate when synthesis of the monomer unit proves difficult, expensive or if the functional group inhibits polymerisation.[7] Heterogeneous modification on the other hand involves reaction of the polymer in both the solution and solid phase, the latter of which presents a unique method of selectively transforming the outermost regions of a polymer surface. This procedure commonly results in the formation of a material having both the mechanical properties of the base polymer as well as the chemical activity of the modified functionality. In general this procedure also offers

large economic savings, since the materials generated in this way have a wide application range and may be used to replace much more expensive alternatives. In the present thesis work was concerned with the development of heterogeneous sonochemical routes for the modification of both polyethylene and poly(vinyl chloride) surfaces; with particular regard to future commercial application with cables made from these polymers.

1.2.1 Considerations For Heterogeneous Modification

Before considering the techniques available for producing and following chemical transformations at a solid surface it is pertinent to define the term "surface".

A surface may be defined as the perimeter or limits of a material body. In practical terms this represents a monolayer of material at an interface. However, a surface is perhaps more appropriately defined by the resolution of the technique employed for its investigation. The chemistry of a polymer surface will impact on the majority of its applications. The properties achieved at the surface will vary with the depth of the surface chemical layer and an overview of the relation between the thickness of chemical layer and technologically important properties is given in figure 1.4.

In general, heterogeneous reactions are carried out at the interface between a solid substrate and a solvent or vapour containing an appropriate reagent. Each system represents a complex process and a number of considerations must be borne in mind:[8]

a. The unreacted polymer-solvent interface

A solid will interact with a solvent to varying degrees, from not being wetted to ultimately being solvated by it. Thus, the interface ranges from sharp to diffuse

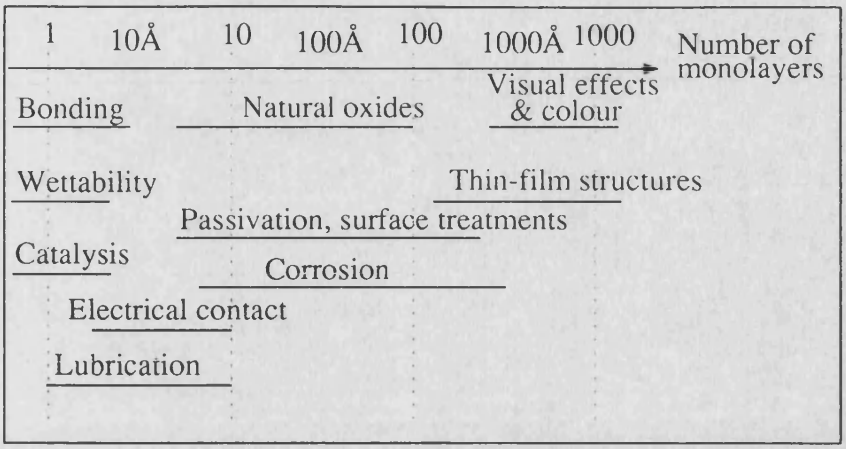

Figure 1.4 showing the relation between depth of chemical layer and technologically important properties

and this will determine the penetration depth of reagent(s) into the solid.

b. The reacted polymer-solvent interface

As the reaction proceeds the chemical nature of the interface is changed. Hence, the modified layer may become more or less compatible with the solvent and this in turn will determine the depth of the modified layer. Ultimately, the modified layer may become soluble and be dissolved away by the solvent.

c. Reagent solubility

The interaction of reagents with the solvent, polymer and modified layer must also be considered. Since, the reagents will partition among the regions of the system and the dynamic partition coefficients will change throughout the course of the reaction also affecting the final product structure.

d. Isolated product structure

Finally, the isolated end polymer may vary greatly from that in contact with the "reactive" solution. The compatibility between the modified and unmodified polymer may induce structural reorganisation. Additionally, surface reorganisation can be induced by the final storage or application atmosphere.

1.3 Polymer Surface Characterisation Methods

Analysis of polymer surfaces often proves difficult because of the low levels of material under investigation and in general, the need to study the surface in situ. Several techniques are available to study a number of properties both chemical and physical and some of these will be dealt with below.

1.3.1 The Interaction of Polymer Surfaces With Liquids: Wetting

The interaction of a solid surface with a liquid brought into contact with it depends on the outermost molecular layer of that surface and as such, is therefore dependent upon the surface structure, both chemical and physical. Accordingly, measurement of this interaction allows very sensitive changes in the surface property to be followed.

1.3.1.1 Thermodynamics of Wetting and Contact Angles

In order to understand the data obtained from contact angle measurements, an appreciation of the thermodynamics of wetting is necessary. A detailed mathematical treatment is beyond the scope of this thesis, but has been dealt with in the literature.[9,10]

When a liquid makes contact with a solid surface that surface is said to be wetted. The extent to which the liquid interacts with the solid to promote wetting is characterised by the contact angle, Θ. The contact angle is defined as the angle through the liquid to the three phase contact point of the liquid droplet in mechanical equilibrium as shown in figure 1.5.

In 1805 Young[11] described the contact angle of a liquid droplet on a solid surface as being due to three surface tensions, shown in figure 1.5, which may be vectorially resolved in a direction parallel to the surface:

$$\gamma_{SV} - \gamma_{SL} = \gamma_{LV} \mathrm{Cos}\Theta \qquad 1.1$$

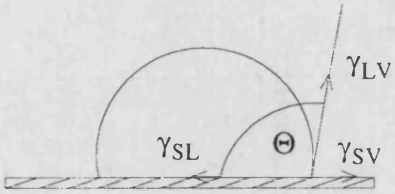

Figure 1.5 Showing the equilibrium contact angle (Θ) of a liquid droplet on a solid surface

Where γ_{SV} is the surface free energy of the solid in a vacuum, γ_{SL} is the interfacial tension and γ_{LV} is the surface tension of the liquid in equilibrium with its vapour.

Problems arise with this treatment because there is no reliable method for the determination of γ_{SV} or γ_{SL} directly. Furthermore, equilibrium between solid, liquid and vapour is seldom achieved because of internal stresses which are frequently present in the surface layers of solids.

In 1937 Bangham and Razouk[12] outlined the importance of adsorption of vapour of the liquid onto the solid surface. This led to the following form of the equations by Young.

$$\gamma_{SV}^{\circ} - \gamma_{SL} = \gamma_{LV}^{\circ}\mathrm{Cos}\Theta \qquad 1.2$$

Where V° is the saturated vapour pressure.

If the solid adsorbs liquid vapour then the solid surface tension becomes reduced to γ_{SV} where:

$$\gamma_{S}^{\circ} = \gamma_{SV}^{\circ} + \pi_{e} \qquad 1.3$$

π_e is known as the spreading pressure.

Values of π_e have been found to be negligible for liquids which have a non-zero contact angle on low surface energy substrates such as polymers.

Consequently, when a liquid spreads on a surface, a solid-liquid interface is formed at the expense of a solid-vapour interface. The free energy change for this

process is then:

$$S = \gamma_{SV}^{\circ} - \gamma_{SL} - \gamma_{LV}^{\circ} \qquad 1.4$$

for spreading $S \geq 0$

For polymers, $\gamma_{SV}^{\circ} < 60\ mJm^{-2}$ so that liquids will spread on polymers only if γ_{LV}° is small.[13]

1.3.1.2 Contact Angle Measurement.

Young's equation (1.1) relates to the equilibrium angle of a liquid on a surface, because it assumes the surface is both chemically homogenous and smooth. Such contact angles are measured from the profiles of liquid drops (Figure 1.6a) or bubbles (Figure 1.6b) resting on a plane surface. These methods are known as the sessile drops and captive bubble methods respectively.[14]

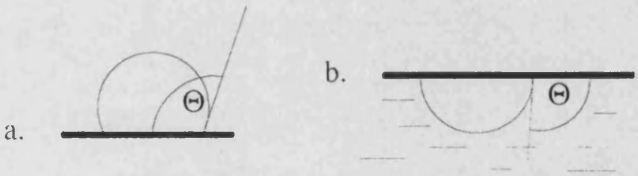

Figure 1.6 Showing the sessile drop, a, and captive bubble, b, methods

The contact angle may be measured directly using a microscope fitted with a goniometer eye piece, or indirectly by drawing a tangent to the profile at the point of three phase contact after the image has been enlarged by photography. Another indirect method involves the measurement of drop dimensions. Provided the drops are sufficiently small ($<10^{-10}\ m^3$) to avoid gravitational distortion,[15] they can then be considered to be the segment of a sphere, hence $\tan(\Theta/2) = 2(h/d)$ where h = height of the drop and d = the diameter of the drop.

In practice, surfaces are seldom smooth or chemically homogenous on a molecular level. As a result, different contact angles may be obtained depending on whether a liquid drop is advanced or withdrawn across the surface. The most common methods are shown in figure 1.7.

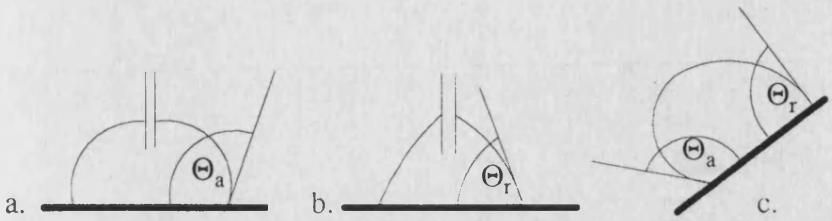

Figure 1.7

Showing, a. Advancing contact angle; b. Receding contact angle and c. Tilted plate methods for a sessile drop.

Advancing and receding contact angles can be measured when a liquid is advanced or withdrawn across the surface by increasing or decreasing the volume dispensed from a syringe needle. The needle remains in the drop during measurement to avoid unnecessary vibrations of the drop.

The advancing and receding contact angles may also be obtained from a sessile drop at the point where the drop begins to move upon increasing the angle of tilt of the surface as shown in figure 1.7c.

1.3.1.3 Hysteresis

The difference between the advancing and receding contact angle is known as the contact angle hysteresis. Zisman[16] has reported that in order to reduce experimental error, the advancing and receding contact angles must be obtained slowly so that equilibrium is maintained as the liquid front moves. Good[17] has described a number of causes of hysteresis which may occur: surface roughness, surface heterogeneity, diffusion, swelling, reorientation and fluid mechanical effects. The most important origins of hysteresis are due to roughness and surface heterogeneity and these will be dealt with below.

A. Surface roughness

This is defined as the ratio of the actual surface area to its expected area if it were perfectly planar. A detailed treatment of surface roughness has been presented by Johnson and Detre.[18] For a rough surface, a drop which wets the entire contact area without the formation of voids will, at equilibrium, adopt a minimum surface

free energy configuration. Under these conditions, the roughness ratio is given by Wenzel's equation:[19]

$$r = \frac{\text{Cos}\phi}{\text{Cos}\Theta} \qquad 1.5$$

Where ϕ is the apparent contact angle of the drop to the horizontal surface and Θ is the intrinsic contact angle (that which would be obtained on an ideally smooth surface). From this equation it can be seen that any liquid with an intrinsic contact angle of $>90^{\circ}$ will have a greater apparent contact angle on a rough surface. Conversely, if the intrinsic contact angle is $<90^{\circ}$ then the apparent value will be reduced on a rough surface. Liquids having high intrinsic contact angles on a solid may not be able to penetrate very rough surfaces and this gives rise to composite surfaces. These surfaces have been dealt with by Johnson and Detre.[18]

B. Surface Heterogeneity

Practical measurements show that even smooth surfaces exhibit contact angle hysteresis, This can arise through either chemical, or structural heterogeneity. The first of these may result from the fragments in the polymer, or in the case of copolymers from phase separation at the surface. The second effect can occur in any polymer system, even those which are chemically homogenous. This feature arises through the presence of crystalline regions, since these have a greater molecular or atomic density and hence a different surface free energy compared with the amorphous regions.

Good and Koo[20] found that contact angle values varied dramatically with droplet size. They attributed this observation to the presence of surface heterogeneity generating droplets with a tortuous perimeter accordingly.

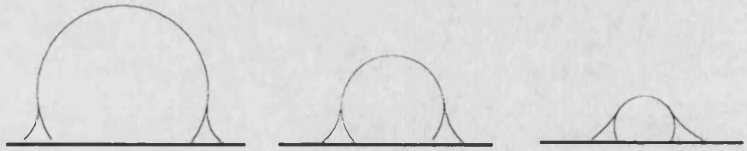

Figure 1.8 Showing sessile drops with a tortuous perimeter

1.3.1.4 Sensitivity Of Contact Angle Measurement

Contact angle measurements probe the first molecular layer of a surface and as such, have a sensitivity to molecular organisation which is far greater than any other analytical method for surface analysis at present. Using contact angle measurement, Bazkin and Ter-Minassian-Saraga[21] were able to follow changes in the surface composition of chemically oxidized polyethylene after heating to 80°C. They reported that during heating the oxidised functionality migrated into the bulk polymer.

Other workers have employed contact angle measurements to follow the ionisation of surface carboxylic acid groups on chemically oxidised polyethylene surfaces.[22]

1.3.2 Infra-Red Spectroscopy

Infrared (ir) spectroscopy is one of the most widely used analytical techniques for the analysis of organic molecules. It is concerned with the detection of transitions between energy levels in molecules which result from vibrations of the interatomic bonds. The vibrational frequencies are characteristic of particular functional groups in molecules, are sensitive to the molecular environment and chain conformations and so afford a useful method of polymer analysis. A comprehensive library of polymer infrared spectra has been published.[23]

1.3.2.1 Background Theory and Equipment.

The infrared region of the electromagnetic spectrum is regarded as extending over the wavelength range 0.5 - 1000 μm. The section of most practical use is that existing between 2.5 and 25 μm (4000 - 400cm^{-1}).

Electromagnetic energy, in this range, from a black body source will only interact with those bonds in which molecular vibration can result in a change of the bond dipole moment. When the vibrating dipole is in phase with the electric vector of the incident radiation the vibrations are enhanced and energy is transferred from

the incident radiation to the molecule. It is the detection of this energy absorption which constitutes ir spectroscopy. In practice, the spectral transitions are detected by scanning through the frequency whilst continuously monitoring the transmitted light intensity. Today, most ir studies are carried out using Fourier transform spectrometers.[24]

One of the major problems with infrared spectroscopy has been the inability to build frequency sensitive detectors. Traditional spectrometers overcame this problem by using monochromators to produce narrow radiation band widths. Fourier transform spectrometers have surmounted this obstacle by converting the information from the infra-red frequencies into audio frequencies where detectors and electronics are able to track both frequency and intensity.

1.3.2.2 Surface Analysis of Polymers by Infra-Red

There are two possible methods for measuring the infrared spectra of polymer surfaces. The first approach, described by Johnson[25] and appraised by Willis and Zichy,[26] involves removal of the surface layers by abrasion; the transmission infrared spectrum of this material then being measured. The second approach, which has found much greater application, is the use of some form of reflection technique.

Incident radiation can be scattered from a solid surface in two ways. If the radiation is reflected towards the detector in the same path that would be followed if the surface were perfectly flat it is termed specular reflectance, while the radiation which is reflected along different pathways constitutes diffuse reflectance.

A. Diffuse Reflectance Infrared Fourier Transform Spectroscopy (DRIFTS)

This technique is particularly useful in the analysis of powders and hard intractable solids which do not lend themselves to ATR analysis (see below), as well as very small samples <9 mm^2.

Diffuse reflectance spectroscopy was initially limited to the ultraviolet and

visible regions of the electromagnetic spectrum due to the relatively low intensity of the irradiation reflected from powders.[27] The development of Fourier transform spectrometers, however, has enabled measurements to be extended into the infrared region although spectral intensities remain weak. Accordingly, measurement of diffuse reflectance spectra requires efficient optical units and systems are generally based on an integrating sphere design. Fuller and Griffiths[28] have described an efficient optical system for DRIFTS measurements. In their work they reported efficient analysis of a number of samples including a study of the oxidation of poly(dimethylfulvene) powder with time.

B. Attenuated Total Reflectance Infrared (ATR-ir)

When light is incident at an interface between materials having different refractive indices (n) such that angle of incidence exceeds the critical angle, α_c, where sin $\alpha_c = n_2/n_1$ then the light is reflected from the surface rather than refracted. See figure 1.9.

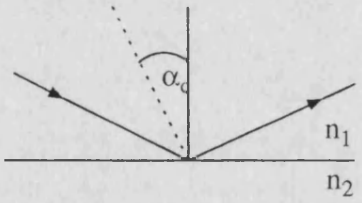

Figure 1.9 Showing the reflection of light from the interface between two materials of different refractive index.

During reflection, some penetration into the sample will take place so that, at energies where selective absorption occurs, the beam is attenuated. In practice the sample is pressed against a suitable internal reflection prism. The relationship between the incident angle, refractive indices of the two materials and the wavelength of the radiation was developed by Harrick[29] and is given by:

$$d_p = \frac{\lambda_0}{2\pi n_1 \left[\mathrm{Sin}^2\Theta - (n_2/n_1)^2 \right]^{1/2}} \qquad 1.6$$

d_p is defined as the distance below the surface at which the amplitude of the electric field is e^{-1} of its initial value.

Where Θ is the angle of incidence, λ_0 is the wavelength of the incident radiation, n_1 is the refractive index of the prism and n_2 is the refractive index of the sample.

Although the refractive index of the prism, n_1, varies only slightly with λ_0, the refractive index of the sample, n_2, may vary considerably in the vicinity of an absorption band. In order to avoid distortion of peak shapes the refractive index of the prism must be much greater than n_2. Typical reflection elements are KRS-5 (TlBr-TlI mixed crystal, n_1=2.4) and Germanium (n_1=4.0). From equation 1.6 it can also be seen that surface sensitivity is increased with decreasing λ_0, increasing Θ and increasing n_1, but the spectral intensity is decreased. This problem can be, to a large extent surmounted by using a multiple reflection element as shown in figure 1.10.

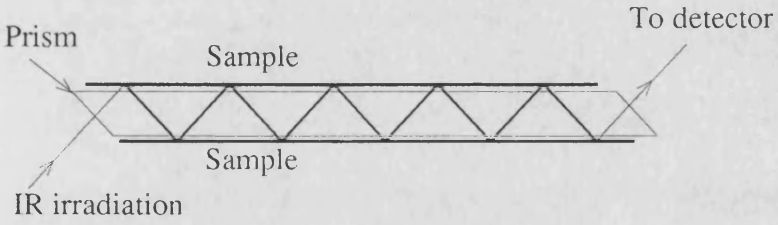

Figure 1.10 Schematic diagram through a multiple internal reflection ATR prism

Ultimately, to obtain good reflection spectra from this technique, very good contact between the sample and crystal is a prerequisite.

The interfacial contact is also of paramount importance when attempting to acquire quantitative information from ATR, since it will determine the thickness of the sampled region. Despite these difficulties Briggs and co workers[30] used atr spectra recorded at different angles of incidence to determine the variation in

oxygen concentration with penetration depth for chromic acid oxidised LDPE. In their work they used long chain hydrocarbons containing isolated ester, acid, and lactone functions to determine the molar extinction coefficients of each oxygen functionality.

Luongo and Schonhorn[31] have studied the surface morphology of LDPE samples nucleated on different energy substrates and found that the crystalline / amorphous ratio could be determined by ratio of the intensity of the bands at 730 and 720 cm^{-1} respectively. Later, Haridoss and Perlman[32] used this method to study the changes in crystallinity when LDPE surfaces were chemically etched.

More recently, Urban and co workers[33] have suggested that the determination of crystallinity gradients requires more detailed polarisation studies to achieve accurate results.

1.3.3 Analysis of Polymers by Optical and Electron Microscopy

Analysis of polymer samples by reflection microscopic methods affords an excellent means of studying surface topography and structures down to ~1 μm. The microscopic techniques and procedures employed for the analysis of polymer surface topography have been well documented.[34,35] Accordingly, only a brief overview will be given in this thesis, and for a more comprehensive treatment the reader is referred to the open literature.[34-36]

1.3.3.1 Optical microscope:

The resolving power, R, of any microscope is governed by the wavelength of the illumination according to equation 1.7.

$$R = \frac{\lambda}{2NA.K} \qquad 1.7$$

Where R is the least distance between two resolvable points, λ is the wavelength of the illumination source, NA is the numerical aperture and K is a

constant depending on the coherence of the illumination.

The numerical aperture, NA, is in turn defined as :

$$NA = n\mathrm{Sin}\Theta \qquad 1.8$$

Where η is the refractive index of the medium occupying the space between the specimen and the front surface of the objective and Θ is the half angular aperture of the objective.

For surface analysis of solid polymer samples it is necessary to use a microscope where the light source is reflected back from the surface of the sample to the objective. Unfortunately, this requirement, together with the need to maximise the depth of field by employing a relatively small aperture objective, seriously limits the maximum magnification and hence resolving power attainable. In practice, this technique is most severely limited by the depth of field which can be obtained.

1.3.3.2 Scanning electron microscope (SEM):

One solution to the resolution problems encountered with optical microscopes is to use an illumination source with much shorter wavelengths. This forms the basis of electron microscopy, where an electron beam having a wavelength of approximately $8x10^{-3}$nm, compared with ~500 nm in the light microscope, is used.

Before outlining the operational procedures for the SEM technique an understanding of the interactions between an electron beam and a solid surface must be made. When an electron beam impinges on a solid surface a number of interactions may arise as shown in figure 1.11

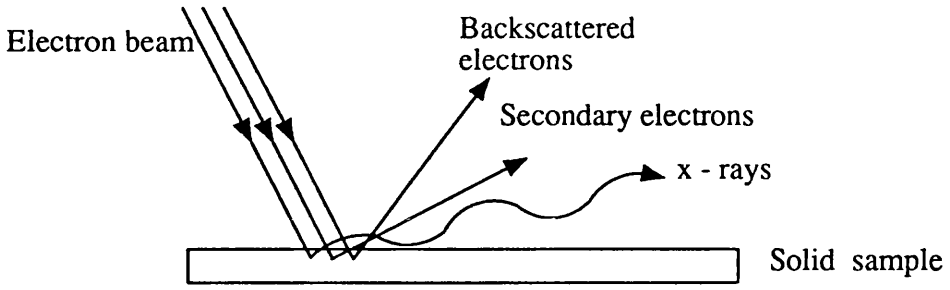

Figure 1.11 Showing the interaction of an electron beam with a solid surface

i. Some electrons may be 'backscattered'.

ii. Some primary beam electrons 'interact directly' with electrons within the atoms of the specimen, knocking them free. These are known as secondary electrons and detection of these provides the commonly displayed images.

iii. After removal of a secondary electron from an inner shell, an outer electron may fall into the resulting 'hole' and emit a photon. These photons are often in the x-ray range of the electromagnetic spectrum and detection of these forms the basis of energy dispersive x-ray analysis or EDX, see 1.3.3.3 below.

Thus, by having suitable detectors present each of these interactions may be recorded.

A schematic representation of a SEM is given in figure 1.12.

The whole of the optical system is contained within an evacuated tube. The source, usually tungsten V, emits a beam of monoenergetic electrons. This electron beam is then accelerated by holding the filament at a large negative potential (typically between 1 and 50 kv) relative to both the anode and sample. The beam passes through a hole in the anode and is then focused onto the specimen using either one or more lenses. After ejection from the surface, the secondary electrons are detected, often a small positive bias is used to attract the electrons to the detector. This signal is then amplified and fed to a monitor which produces an image of the surface being scanned.

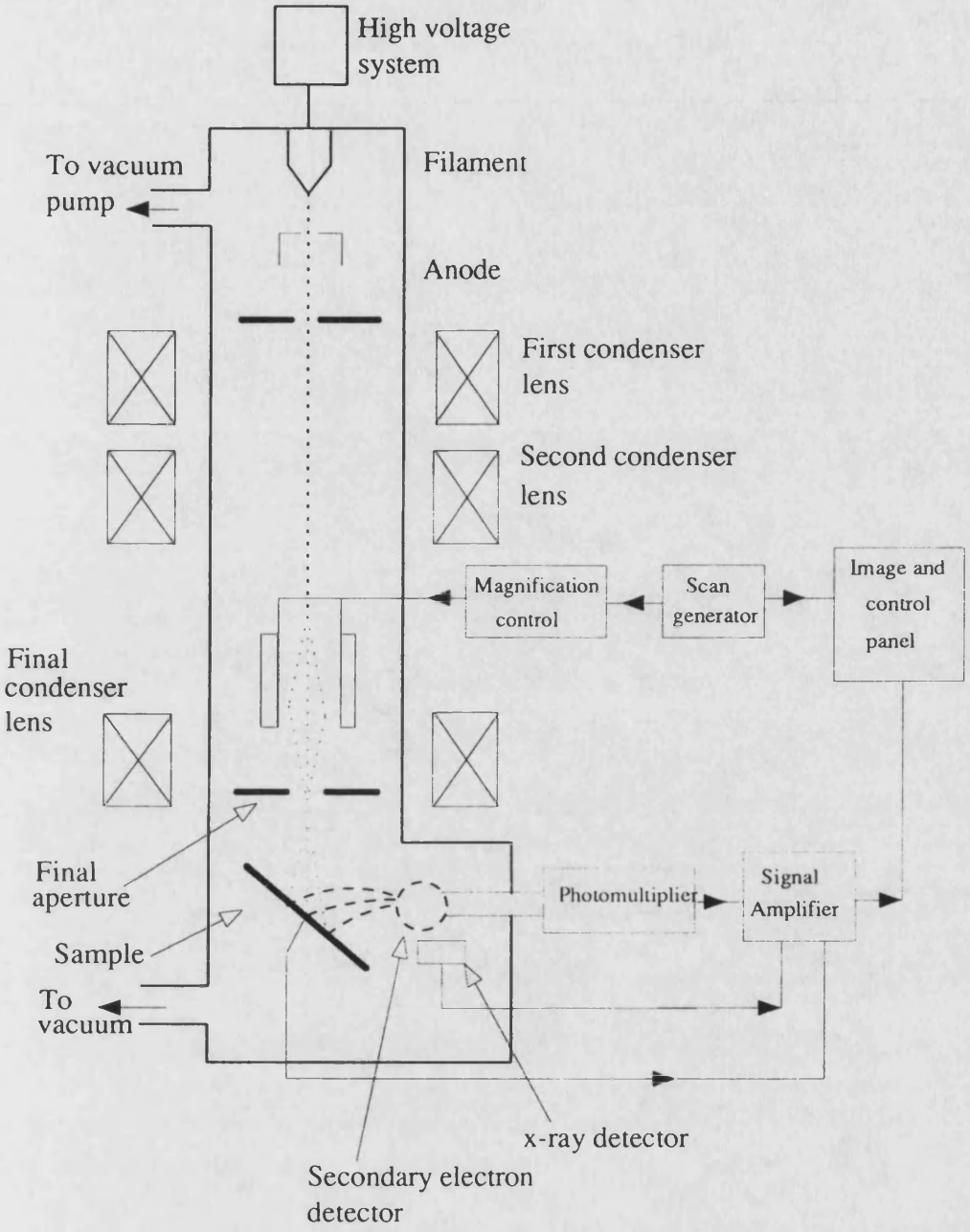

Figure 1.12 Schematic diagram of a scanning electron microscope

The electron beam is then moved over the surface of the sample in a raster pattern by using a variable magnetic field provided by current-carrying 'scan coils'. In order to avoid charge build up during this scanning, most polymer samples need to be coated with a conducting layer (ca 20nm) of usually gold or carbon.

The depth of a field obtained in SEM is extremely good and magnifications

of 50,000+ are possible. Unfortunately, heating effects arise from the interaction of the electron beam with the surface, particularly at high acceleration voltages, and this may result in sample damage with polymers.

1.3.3.3 Energy Dispersion Analysis of X-Rays (EDX)

As described above interaction of an electron beam with a surface may produce x-rays. These x-rays are characteristic of the element from which they arose and hence, their detection affords a useful method of elemental identification.

The x-rays ejected from the sample enter a solid state, Lithium drifted silicon detector. They create electron hole-pairs which cause a pulse of current to flow through the detector circuit. The number of pairs produced being proportional to the energy in each x-ray photon. The pulses are then amplified, sorted by size using a multi-channel analyser and displayed as an energy spectrum. Using this technique it is possible to detect all elements with an atomic number above 6 (carbon) simultaneously.

Furthermore, due to the rastering of the electron beam it is possible to map the elemental composition across a surface. This information can then be used to generate an elemental composition or EDX map.[34]

1.4 Previous Polymer Modification Reactions

This section has been largely devoted to heterogeneous modification routes for polyethylene and PVC, although reference has also been given to analogous polymers and solution phase reactions where appropriate.

1.4.1 Polyethylene

Polyolefins, in particular polyethylene and polypropylene are the most widely used of all synthetic polymers due to their flexibility, inert nature and low production costs. The relative inert character of these materials, however, results in

their forming low energy surfaces which have associated with them a number of adhesion related problems such as poor adhesive joint strength, low print and extrusion coating stability. Although there remain some doubts concerning the origin and nature of adhesive bonding, evidence increasingly suggests that the chemical composition has a much greater effect than either surface topography or weak boundary layers. Thus, to extend the application of polyethylene products it is necessary to generate some chemical functionality on the surface.

It is for these reasons that a large number of workers have investigated surface treatment methods for these polymers. The first appeared over forty years ago[37] and present methods include chemical etching, corona discharge, plasma, photo-oxidation, ozonation and flame treatments.

Polyethylene can be readily chlorinated by replacement of a hydrogen atom. The substitution reaction proceeds via a free radical mechanism and is usually catalysed by ultraviolet light[38] or initiators such as benzoyl or lauroyl peroxides.[39]

If the polymer is crystalline, chlorination is reported to selectively begin in the amorphous areas.[38] In heterogeneous reactions at low temperature traces of crystallinity are found to persist far above 50% chlorine content,[40] for comparison, PVC contains ~56% Cl. Thus, the chlorine must be concentrated in certain regions of the polymer and not evenly distributed across the whole surface.

Puszynski and Godniak[41] have reported that chlorination of polyethylene in suspension may also be catalysed by heavy metal ions such as Cu^{2+}, Co^{2+}, Mn^{2+}, Sn^{2+}, MoO_4^{2-}, and VO_3^-. These metal ions accelerate the decomposition of hydrochlorous acid which is a transitionary product in the reaction. Polyethylene has also been shown to undergo nitration by fuming nitric acid. Reaction was reported to favour the chain folds of crystalline surfaces.[42]

A very important commercial treatment for polyethylene is the simultaneous chlorination and sulphonation.[40] The product from this reaction can be subsequently crosslinked to form a chlorosulphonated polyethylene elastomer. In general this reaction is carried out in homogeneous media using a free radical initiator or

ultraviolet light, although heterogeneous reaction has also been reported.[43] The chlorosulphonated groups may be subsequently hydrolysed to produce poly(ethylene sulphonates).

Polyethylene has also been shown to undergo heterogeneous sulphonation by reaction with gaseous SO_3, fuming sulphuric acid or SO_3 in chlorinated hydrocarbons.[44,45] Recently, Ihata has determined the surface structure of the resulting polymer films and reported the presence of unsaturated sulphonic acid groups.[46]

Olsen and Osteraas have described a method for the modification of polyethylene surfaces involving direct reaction with carbene species.[47,48] The carbene species were generated by in situ pyrolysis of suitable precursors. Reaction was reported to change the surface wettability of the films and the new functionality was shown to undergo secondary organic derivatisation reactions.

More recently, Devi *et al.*[49] have shown that solutions of high density polyethylene (HDPE) in toluene could be grafted with butyl acrylate giving rise to copolymer formation. Reactions were carried out at 100°C using benzoyl peroxide as a free radical initiator and the products were characterised by ir of thin films and thermal methods.

Despite the relatively inert nature of polyolefins, prolonged atmospheric exposure has been shown to cause oxidation. In 1954 Rugg *et al.*[50] used transmission ir of thin films to follow the thermal and photochemical oxidation of polyethylene. They reported that thermal oxidation resulted in the formation of mainly keto groups with some acid and aldehyde groups also evident. Photo oxidation, however, produced similar quantities of all three species. They also found levels of unsaturation in both oxidation methods and postulated that thermal oxidation formed unstable hydroperoxide groups.

Environmentally oxidised polyethylene has recently been shown to form compatible blends with nylon-6 and this has been cited as a possible method for recycling polyethylene.[51]

In order to improve the adhesive properties of polyethylene numerous workers have employed surface treatments, many of which promote oxidation. However, Schonhorn and Ryan[53] melted polyethylene on aluminium and dissolved away the metal with sodium hydroxide solution. They found the resulting polymer surface gave high epoxide joint strength although no oxygen containing species were detected by ATR-ir. This observation led them to conclude that the apparent increase in adhesion arose through the formation of a highly crystalline surface. Later, the same workers exposed polyethylene films to uv radiation and again an increase in joint strength was observed.[54] In this study no surface changes were indicated by either contact angle measurement or ATR-ir and they concluded that the surface became crosslinked. More recently, Briggs and co workers[55] duplicated the earlier work of Schonhorn and Ryan[53] using XPS for analysis and were able to determine that surface oxidation had indeed occurred.

Blais *et al.*[56] have studied the chromic acid oxidation of low density polyethylene (LDPE) at 70°C by ATR-ir and found both hydroxyl and carbonyl groups present. Using the same procedure Wills and Zichy[26] found that alkyl sulphonate and sulphate groups were also generated. In contrast, Rasmussen and co workers[57] reported that chromic acid oxidation of LDPE produced mainly carboxylic acid functionality (60%) with the remaining function due to aldehydes and ketones.

The chromic acid oxidation of LDPE and polypropylene has also been undertaken by Briggs and co workers.[30,58] In their studies both xps and ATR-ir were used to for product analysis. They reported the presence of hydroxyl, carbonyl, carboxyl and $-SO_3H$ groups with both oxidised polymers. Using mild oxidising conditions it was found that the modified layer was less than 100Å thick. It was further reported that oxidation of polypropylene rapidly reaches an equilibrium with low modification depth whilst oxidation increased both in degree and depth in polyethylene. This observation was attributed to the occurrence of chain scission in polypropylene resulting in the outer layers being continually

solvated. In addition, the equilibrium depth of oxidation was too low to be detected by ATR-ir with polypropylene, but the extended oxidation in polyethylene gave rise to assignable infrared bands.

More recently, Haridoss and Perlman[32] have reported the oxidation of polyethylene film samples by permanganic and chromic acids. The resulting films were examined by scanning electron microscopy (SEM) and ATR-ir. Permanganic acid was determined to remove amorphous regions of the surface as indicated by ATR. The modified samples then tested for charge stability and this was found to be due more to the surface morphology than the chemical composition.

Recently, Bergbreiter *et al.*[59] have shown that both polyethylene and polypropylene can be oxidised by Gif-type oxidising agents. The oxidation process was reported to occur by a non radical mechanism, yielding low levels of mainly carbonyl species as determined by contact angle measurements, ATR-ir and derivatisation reactions.

It is recognised that environmental oxidation of polyolefins, in particular polyethylene and polypropylene may be catalysed by transition metal salts such as those of iron and copper.[60] Garton and co workers[61,62] have studied the thermal oxidation of electrical grade polyethylene samples in aqueous media. They reported that oxidation rates were increased by adding aqueous salts such as sodium chloride and sodium nitrate. In addition, it was also shown that oxidation rates were increased even further in the presence of a sodium bicarbonate pH10 buffer, whilst an acidic buffer was found to retard oxidation. Commercial grade cross-linked polyethylene (XLPE) containing antioxidants was also reported to show an increase in oxidation rate. The products of oxidation in each case were carboxylic acids, ketones, aldehydes and carboxylate ions in the case of the pH10 buffer. Surface analysis was carried out by ir and xps.

A large body of information detailing surface modification techniques for polyethylene and other polyolefins is available. Many of the treatments employed

involve the formation of some kind of oxygen containing species to varying degrees and depths into the polymer surface. Only those findings most pertinent to the present work will be reviewed. For a more comprehensive treatment the reader is referred to a recent review.[63]

A. Corona Discharge: This treatment generally occurs in minutes but often results in surface damage. Briggs and co workers[64,65] have shown by xps analysis, that irrespective of the gaseous system used corona discharge treatment leads to the formation of oxygen containing species on the surface of polyolefins. The level of oxidation observed was generally confined to the outer 100Å of the surface. Recently, Gerenser *et al.*[66] have studied gas phase derivatisations of corona discharge treated polyethylene surfaces using XPS for analysis. They found that oxygen levels fell during aging, but reached an equilibrium value after about 3 weeks. However, washing highly oxidised samples with water for 30 seconds reduced the surface oxygen content from its initial value (typically ~18%) to between 9 and 11 atom%. This reduction was apparent, regardless of initial oxygen content (above 11%) and starting contact angle. Spectra recorded before and after washing were reported to be almost identical except for the relative intensity of the neutral carbon peak associated with the polyethylene backbone. They concluded that the soluble and insoluble material fractions were almost identical and that solubilisation arose through chain scission.

B. Plasma: This is also a dry technique and modifies only the top few monolayers of material. The advantage of plasma treatment is that by selectively choosing the gas it is possible to form diverse polar groups.[67] Reactions are generally faster than corona discharge treatment and result in less surface damage.

C. Ozonation: Oxidation of polyethylene by ozone is reported to originate in the amorphous regions of the polymer and, following a slow initiation, extend into the crystalline regions where the rate is much greater.[68] The process has been shown to generate C-O, C=O and CO_2 at nearly equal initial rates, but extended treatment gave rise to a greater proportion of carboxy groups at high depths of

penetration.

D. Photooxidation: This technique has been shown to produce extensive levels of oxidation in an oxygen atmosphere within about 8 hours.[68] The chemically modified surface was found to contain approximately equal amounts of C-O and CO_2 with a lower level of C=O also present.

E. Flame treatment: Briggs and co workers[69] have analysed flame treated polyethylene surfaces by xps and determined that very high levels of oxygenation were generated, similar to severe chromic acid oxidation. The modified layer was found to be very sharp and estimated to be only 40 to 90Å deep.

Polyethylene surfaces have been modified by ultraviolet induced polymerisation of surfactants from an aqueous suspension.[70] The surfactant molecules were expected to accumulate at the polymer-water interface and during irradiation form a crosslinked coating on the polyethylene surface.

Rånby and co workers[71-5] have carried out extensive studies of photografting onto polyethylene and polypropylene films. Reactions were performed in the vapour phase using benzophenone as an initiator. The hydrophilic surface generated by the introduction of acrylic acid groups was reported to undergo structural reorganisation during heating in air to produce a hydrophobic surface.[71] Reheating the films in an aqueous environment was reported to reverse this process and regenerate the hydrophilic surface.

Kubota and co workers have shown that photografting of methacrylic acid onto LDPE could be achieved in aqueous solution, using either triphenylamine or diphenylamine as a photosensitiser previously coated onto the polymer film.[76,77]

Increasingly, workers have attempted to achieve specific surface functionalisation of polyethylene by secondary reaction of oxygen containing species. In this way Batich and Yahiaoui[78] have grafted polyacrylamide onto hydroxylated LDPE surfaces. The hyroxyl rich surface was generated by chromic acid oxidation[57] followed by diborane reduction.[79] Graft polymerisation was carried

out from aqueous solution using Ce^{4+} as an initiator. Bergbreiter and Zhou demonstrated that thiohydroxamic esters could be generated by reaction of the surface carboxyl groups on chromic acid oxidised polyethylene.[80,81] The esters were then used as radical precursors to initiate thermal or photochemical graft polymerisation of vinyl monomers from dimethyl formamide (DMF) onto the polymer surface. More recently, Bergbreiter *et al.*[82] have also shown that surface modification could be achieved by polymerisation of methacrylonitrile onto surface functional groups. Their approach involved the synthesis of terminally functionalised polyethylene oligomers which were incorporated into the base polymer. During solution casting of this material it was reported that the functional groups accumulated at the interface, thereby presenting a more reactive surface. The terminal groups were then used to initiate polymerisation of methacrylonitrile. Reactions were followed by ATR-ir, contact angle measurement and xps.

Margel *et al.*[83] have described a method for generating polyacrolein microspheres on the surface of LDPE. Polyethylene films were again oxidised by chromic acid and reduced by diborane to give an hydroxyl rich starting surface. The hydroxyl groups were then derivatised by a sequence of reactions to produce surface functional amine groups in the ω-position. The polyacrolein microspheres were subsequently bonded to the amines as evidenced by ATR-ir, contact angle measurement, xps and SEM analysis.

1.4.2 Poly(vinyl chloride)

Poly(vinyl chloride) is one of the most widely used commercial thermo plastics at the present time. However, due to the presence of chlorine atoms in the polymer backbone its environmental impact has recently received widespread attention. As a result, much effort has been directed towards the development of more efficient stabilising methods for these polymer systems in order to provide both greater application lifetime and range.

One approach to the problem has been to chemically bond the stabilisers and other additives to the polymer backbone thereby eliminating the traditional leaching processes. Similarly, much interest has focused on surface modification methods since, in most applications the stability of the surface region in contact with its external environment will define the application lifetime of the polymer.

The presence of the alkyl chloride moiety in poly(vinyl chloride), PVC, makes it a potentially reactive polymer. In practice however, the solid polymer is found to be relatively inert.[3] Despite this, the potential for reaction is evident and two main routes can be identified:

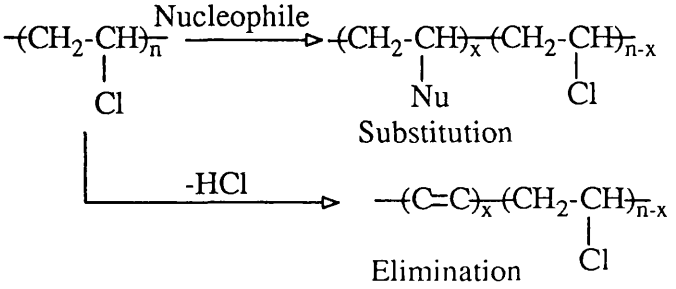

Scheme 1.1

Several workers have proposed that nucleophilic substitution of chlorine atoms could present a useful method for the introduction of groups capable of acting as plasticisers[84] or thermal stabilising agents.[85,86] To effect this aim, Starnes and co workers substituted alkyl tin compounds onto the PVC backbone and found the resulting polymers to have increased thermal stability.[85,86]

Marian and Levin[87] have studied the substitution of chlorine atoms in PVC suspended in water or in solution by nucleophiles such as sodium thiolates ($R\text{-}S^{-}Na^{+}$), where R was an alkyl ether group. High levels of substitution were reported in solution reactions whilst almost no dehydrochlorination was evident. More recently, Levin[88] has introduced the 3[N-2-pyridyl carbamoyl] propylthio residue (1) as an internal antioxidant. The reaction was carried out in water/cyclohexanone using CaO as a base and methyltrioctyl ammonium chloride as a catalyst. In practice the modified polymer(1) was found to be less thermally stable

One approach to the problem has been to chemically bond the stabilisers and other additives to the polymer backbone thereby eliminating the traditional leaching processes. Similarly, much interest has focused on surface modification methods since, in most applications the stability of the surface region in contact with its external environment will define the application lifetime of the polymer.

The presence of the alkyl chloride moiety in poly(vinyl chloride), PVC, make it a potentially reactive polymer. In practice however, the solid polymer is found to be relatively inert.[3] Despite this, the potential for reaction is evident and two main routes can be identified:

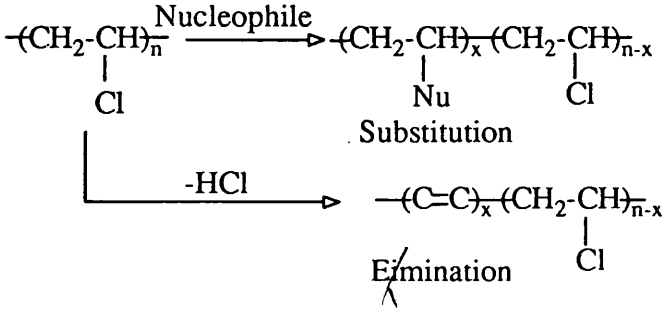

Scheme 1.1

Several workers have proposed that nucleophilic substitution of chlorine atoms could present a useful method for the introduction of groups capable of acting as plasticisers[84] or thermal stabilising agents.[85,86] To effect this aim, Starnes and co workers substituted alkyl tin compounds onto the PVC backbone and found the resulting polymers to have increased thermal stability.[85,86]

Marian and Levin[87] have studied the substitution of chlorine atoms in PVC suspended in water or in solution by nucleophiles such as sodium thiolates ($R\text{-}S^{-}Na^{+}$), where R was an alkyl ether group. High levels of substitution were reported in solution reactions whilst almost no dehydrochlorination was evident. More recently, Levin[88] has introduced the 3[N-2-pyridyl carbamoyl] propylthio residue (1) as an internal antioxidant. The reaction was carried out in water/cyclohexanone using CaO as a base and methyltrioctyl ammonium chloride as a catalyst. In practice the modified polymer(1) was found to be less thermally stable

than PVC owing to the presence of double bond structures formed as side products.

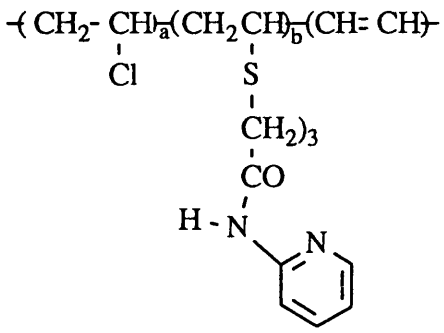

(1)

Takeishi and co workers[89] have reported the successful substitution of chlorine atoms in PVC by azide, thiophenoxide and dithiocarbamate in aqueous solution. In their work, they found that heterogeneous substitution only occurred in the presence of cationic surfactants such as tetrabutyl ammonium bromide and that reaction was suppressed by both methanol and urea. From these observations it was concluded that the surfactant partitioned itself at the surface of the polymer particles and its positive charge attracted the surrounding nucleophiles.

Gilbert[90] has studied the solution phase reaction of sodium azide with PVC in DMF and reported that substitution of up to 60% of the chlorine atoms was possible. Moreover, it was reported that unsaturation also occurred and the end polymer readily crosslinked.

Following the previous literature, Zimmerman *et al.*[91] grafted a thiol substituted hydroxybenzophenone onto the surface of PVC at low temperature. Reaction products were analysed by ultraviolet spectroscopy and the modification layer was reported to be less than 25μm deep. Film samples having the thiol substituted hydroxybenzophenone moiety attached were found to exhibit greater stability towards photochemical oxidation.

Numerous workers have studied the substitution of chlorine atoms by acetoxy groups in PVC.[92-4] Initial work produced only limited success and dehydrochlorination was also apparent. Lewis *et al.*[94] however, have shown that up to 5% of the chlorine atoms in PVC could be replaced by acetoxy groups if reactions were carried out in the presence of 18-crown-6 ether. The presence of the acetoxy

groups in the polymer were, however, found to have a destabilising effect, possibly by providing a favourable neighbouring group effect with respect to hydrogen chloride elimination. A more detailed treatment of the application of phase transfer catalysts to the modification of polymers has been given by Fréchet.[95]

Attempts have also been made to introduce diphenyl phosphine groups into PVC by direct reaction with lithio diphenyl phosphine, for use as catalyst supports.[96] Unfortunately, chain scission and hydrogen chloride elimination were apparent.

Hiratani *et al.*[97] have also reported substitution of chlorine by dithiocarbamate groups. The modified polymers were found to complex metal ions and were stabilised towards γ irradiation.

PVC may also be modified under Friedel-Crafts type conditions. In this way, Gal *et al.*[98] have substituted ferrocene onto PVC using $AlCl_3$ as a catalyst. They reported that modification produced polymers containing upto 62% ferrocene.

Metallation of PVC by alkyl lithium compounds would at first appear to present a useful method for the introduction of functionality. Unfortunately, these reactions prove to be much more complicated than would be expect from consideration of low molecular weight analogues and chlorine can be replaced by both the alkyl group and the metal itself.[3]

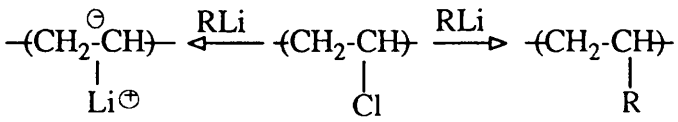

Scheme 1.2

The Lithiated polymer can undergo Wurtz-type coupling leading to a crosslinked product. Despite the difficulties involved with this system functionalised polymers have been prepared by lithiation of PVC.[99] McCarthy and co workers[100-3] have demonstrated that surface selective functionalisation of poly(chlorotrifluoroethylene) could also be achieved.

One substitution reaction of PVC which has been shown to go almost to completion is the dechlorination by lithium aluminium hydride.[104] This reaction has

been used mainly for analytical purposes, since the transformed polymer is simply polyethylene, which can then be studied by infrared to determine the number of chain branches. Conversely however, Starnes and co workers[105] have compared this method with direct nmr interpretation of the initial PVC sample and found it to be inaccurate.

Treatment of PVC with ethanolic KOH saturated with H_2S has been reported to introduce thiol groups with a maximum substitution efficiency of ~25 per 1000 repeat units.[106] Upon oxidation in cyclohexanone with DMSO as a catalyst these groups generated sulphur bound radicals which were able to initiate grafting of methyl methacrylate.

Graft copolymers with PVC backbones have also been prepared in solution by Lechermeier *et al.*[107,108] using butyl lithium in tetrahydrofuran to affect grafting via an anionic mechanism. Conversely, Kennedy and co workers[109,110] have used organoaluminium compounds to carry out both slurry and solution phase cationic grafting reactions onto poly(vinyl chloride) backbones. In their work they used EDAX to follow the apparent reduction in chlorine levels as the polymer surface became grafted.

Finally, although substitution usually occurs through replacement of chlorine atoms, reactions proceeding via hydrogen replacement are also known.[111] This situation arises during the free radical chlorination of PVC in solution. The solvated chlorine radicals are found to attack the polymer backbone primarily at CH_2 groups and, as the reaction proceeds to higher chlorine contents, CCl_2 groups are generated.

The elimination of hydrogen chloride from PVC has, been regarded so far as an unfavourable side reaction, occurring during the thermal and photochemical degradation of the polymer.[112,113]

This elimination of hydrogen chloride can, however, be used positively for the formation of double bonds. In 1939 Marvel *et al.*[114] noted that treatment of halogen containing polymers, such as PVC, with suitable nucleophiles resulted in

the formation of conjugated sequences. Since that time a number of nucleophilic bases have been employed to affect dehydrochlorination; examples include, benzyltrimethyl ammonium hydroxide, 2-ethoxyethanol, potassium amide in liquid ammonia and lithium chloride in dimethyl formamide.[115-7] These systems however, necessitate good solvents for PVC or high temperatures because the reaction rate in heterogeneous systems is low.

Tüdös and co workers[118] have studied the formation of double bonds during the thermal degradation of PVC both in solution and the solid state. They found that the number of double bonds formed was disproportionate to the loss of HCl due to intramolecular cyclization and also showed that the double bonds could be transformed via a Diels-Alder type reaction with chloromaleic anhydride.

More recently, Kise[119] has described a facile two phase dehydrochlorination process involving aqueous sodium hydroxide and a phase-transfer catalyst. Dehydrochlorinations were carried out on both solid (powder and film) and solvated PVC samples. In this investigation the process was reported to be dependent upon the concentrations of base and catalyst, the degree of polymerisation and the reaction temperature. The mechanism was determined to be due to a "zipper-like" elimination with tetrabutyl ammonium bromide being the most efficient catalyst. In principle, selective dehydrochlorination of PVC could lead to the formation of an all-trans polyacetylene structure having conductive properties. In practice such structures cannot be generated due to the intervention of some cis configurations and, more importantly, because of the presence of some unreactive chlorine groups and the occurrence of crosslinking side reactions. Kise and co workers[120] have also applied this system to vinylidene chloride-vinyl chloride copolymers. They were able to detect some carbon triple bonds, but only a small amount of aromaticity through internal ring closure was evident.

Finally, Urban and Salzar-Rojas[121] have studied the application of ultrasound to the base catalysed dehydrofluorination of poly(vinylidene fluoride) surfaces.

They found that the ultrasonic reaction was faster in the initial stages and at lower temperatures (< 40°C), but produced a much thinner modification layer.

1.5 General Principles Of Ultrasound

The term ultrasound refers to sound waves having a frequency between approximately 20 KHz and 10 MHz. Within this broad spectrum there are two distinct areas of ultrasonic application:

i. High frequency, >100 MHz, low power ultrasound. This is used for medical imaging, sonar and non destructive testing.

ii. Lower frequency (20 - 100 kHz), high power ultrasound which may be used for cleaning, dispersing solids, formation of emulsions and welding of thermoplastics. The application of low frequency ultrasound to chemical systems is known as sonochemistry.

Since the velocity of sound in liquids is $\approx$1500 ms^{-1} ultrasound has acoustic wavelengths of about 7.5 to 0.015 cm. Accordingly, no direct coupling of the sound waves on a molecular level can occur.

1.5.1 Propagation of Ultrasound

As ultrasound propagates through a liquid a number of associated phenomena arise. A mathematical treatment of these can be found in the literature,[122,123] but only a qualitative overview is necessary to appreciate the ultrasonic process.

As a sound wave, ultrasound is transmitted through any substance possessing elastic properties. Vibrations from the sound source are communicated to molecules

in the medium, which then move to pass on the motion to the adjoining molecules before returning to their initial, equilibrium position. The sinusoidal motion of the sound waves in liquids gives rise to both longitudinal and transverse waves, but the transverse waves have a very high attenuation with distance and need not be considered here. As the molecules of the medium move to transmit the wave a series of rarefaction and compression cycles are generated. This is shown schematically in figure 1.13.

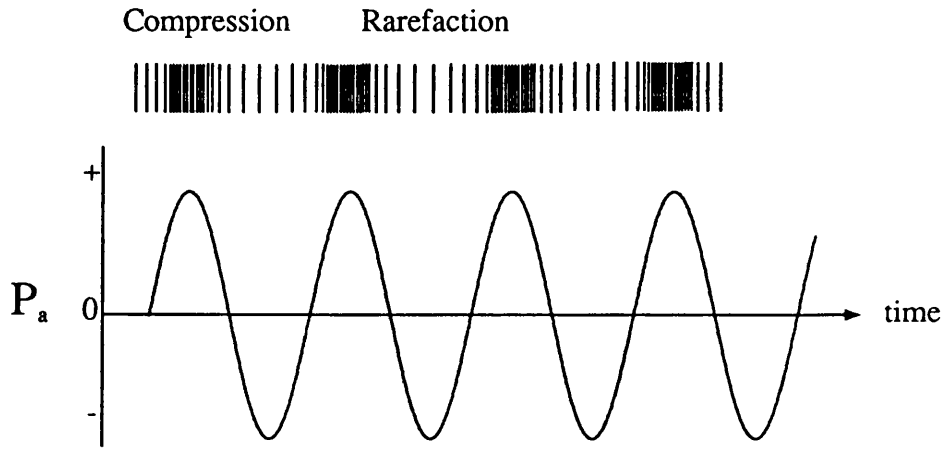

Figure 1.13

This succession of compressions and rarefactions may be described in terms of an acoustic pressure, P_a, which varies with time, t, accordingly;

$$P_a = P_{max} \text{ Sin } (2\pi ft) \qquad 1.9$$

where P_{max} = maximum pressure generated and f is the frequency of the ultrasound. The intensity, I, of the sound wave is defined as the energy transmitted through a unit area of the medium per unit time and is given by:

$$I = \frac{P^2_{max}}{2\rho c} \qquad 1.10$$

where P_{max} is the pressure amplitude, c is the velocity of sound in the liquid

and ρ is the density of the liquid.

During propagation the sound intensity is attenuated due to the transfer of energy to the medium. This energy is lost in the form of heat and generally results in an increase in the bulk temperature during prolonged sonication. The attenuation is be given by:

$$I_d = I_o \exp(-2\alpha d) \qquad 1.11$$

Where I_d is the intensity of sound at a distance, d, from a source radiating at an intensity, I_o. The term α is the absorption coefficient and depends on factors such as the thermal conductivity, specific heat capacity, the density and velocity of sound in the medium.[125]

During the rarefaction cycle large negative pressures are generated and these may be sufficiently powerful to overcome the intermolecular binding forces within the liquid. In this instance, the liquid is torn apart, forming tiny microbubbles and voids. These may then act as ultrasonic cavitation nuclei, and it is this process which is responsible for many of the chemical and mechanical effects promoted by ultrasound.

1.6 Ultrasonic Cavitation

The cavitation process in liquids was first reported in 1895 by Sir John Thornycroft and Sidney Barnaby,[125] who found that incorrect alignment of a ship's propeller resulted in the mechanical shearing of the surrounding water. Subsequently, cavitation was produced with the resulting erosion of the propeller blades.

As outlined above (see section 1.5.1), the propagation of a sound wave through water generates a series of compression and rarefaction cycles which in turn may cause rupturing of the liquid and cavity formation. During subsequent acoustic cycles these cavities may undergo one of a number of fates:

i. Stable Cavitation: This occurs when the cavities grow to an equilibrium size and then oscillate often non-linearly about this size for a number of acoustic cycles.

ii. Transient Cavitation: Transient Cavities usually exist for less than one acoustic cycle. During the rarefaction half cycle they grow rapidly, often to many times their original size, by diffusion into them of liquid and vapour from the bulk. In the subsequent compression half-cycle they then undergo violent adiabatic collapse. Such collapse results in localised regions of intense pressure and temperature, the maximum values being described by equations 1.12 and 1.13 respectively.

$$P_{max} = P\left\{\frac{P_m(\gamma-1)}{P}\right\}^{(\gamma/\gamma-1)} \qquad 1.12$$

$$T_{max} = T_{initial}\left\{\frac{P_{max}(\gamma-1)}{P}\right\} \qquad 1.13$$

Where P_{max} and T_{max} are the maximum pressure and temperature respectively and P is the pressure inside cavity, γ is the polytropic ratio, C_p/C_v, P_m is the pressure in the liquid at the moment of collapse and $T_{initial}$ is the ambient temperature.

From these equations it can be shown that such collapse will result in localised temperatures in the region of 5000 K and pressures of up to 100 atmospheres during irradiation of water at 25°C.[126-128] These temperatures and pressures are sufficiently large to heat the gaseous contents of the bubbles to incandescence, which is observed as sonoluminesence.[129,130] The experimental observation and dependence of this sonoluminescence has been a major driving force in the acceptance of the sonochemical 'hot-spot' reaction theory.

Other workers, however, have reported that upon bubble collapse large electrical discharges are produced and it is these which determine the observed sonochemistry.[131]

Whilst there remains some doubt about the exact origin of ultrasonic reactivity it is widely accepted that transient cavitation is the first step.

1.6.1 Cavitation Thresholds

As explained above, the negative pressures developed by the propagation of sound waves in water results in breakdown of the liquid with the formation of voids. Theoretical calculations for this process in pure water indicate that pressures of the order of thousands of atmospheres would be necessary.[132] In practice however, the actual pressure required for the onset of cavitation is found to be much lower. This observation has been attributed to gas entrapped in small angle crevices of particulate contaminants in the liquid which provide weak spots or nucleation sites for cavitation.[133-5] This is known as the crevice model and is depicted in figure 1.14. This model has been supported by experiments in which ultrafiltration of the

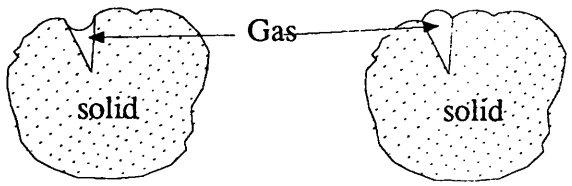

Figure 1.14 Showing gas entrapped in small angle crevices of particulate contaminants

liquid, hence removal of most of the contaminants, greatly increased the cavitation threshold.[136] During the rarefaction cycle gas entrapped in small crevices of the contaminant particles is expelled to produce nucleation sites for cavitation.

1.6.2 Factors Affecting Cavitation

A number of parameters affect the ultrasonic cavitation process and these

will be dealt with below.

a) Solvent Properties

The inter-molecular forces, vapour pressure and surface tension of a solvent will determine both its cavitation intensity and threshold. For reversible adiabatic collapse, the final temperature reached in a collapsing cavity is given by equation 1.13. From this equation it can be seen that solvents with high vapour pressures will yield lower localised temperatures upon bubble collapse.

Care must also be exercised when choosing solvents for sonochemistry as cavitation has been shown to promote fragmentation of a number of solvents, particularly halogenated one such as $CHCl_3$ and CCl_4, giving rise to highly reactive radical and carbene species.[137-9]

b). Intensity

From equation 1.10 it can be seen that raising the ultrasonic intensity increases the pressure amplitude which in turn will give rise to greater sonochemical effects. This relationship does not continue indefinitely, however, since an increase in P_a will also produce an increase in the mean bubble size.[126,134] Ultimately, if the intensity is increased indefinitely the bubbles may become too large to collapse and simply migrate to the surface. In addition, increasing P_a results in the formation of a greater number of bubbles. The presence of sufficient numbers of these bubbles at the irradiating face of an ultrasonic source may result in inefficient coupling of the energy into the medium because of cushioning effects

c). Temperature

In sonochemical reactions it is commonly found that lowering the temperature increases the rate of reaction. This is a direct result of lowering the solvent vapour pressure, with subsequent increase in the final temperature achieved during bubble collapse according to equation 1.13.

In contrast, however, a number of workers have shown that optimal temperatures exist for the sonochemical reactions in a given solvent.[140,141] These observations were rationalised accordingly; the number of cavitation nuclei increase with increasing temperature to the point where solvent vapour pressure dominates the reaction.

d). Dissolved Gases

From equations 1.12 and 1.13 it can be seen that gases with larger γ values (i.e monatomics) will produce greater final temperatures and pressures during bubble collapse, and have increased sonochemical activity.[142,143] Indeed this has been confirmed experimentally.

The dissolved gas concentration and hence solubility, also influences the cavitation process since, an increase in dissolved gas concentration will provide an increased number of cavitation nuclei thereby reducing the cavitation threshold.[144] However, the greater the solubility of the gas the greater the amount which will penetrate into the cavitation bubble and the lower the intensity of the shock wave produced on bubble collapse, thus reducing sonochemical effects.[145]

e). Frequency

Increasing the frequency of ultrasound means that the time between successive rarefaction and compression cycles is decreased. Accordingly, cavitation bubbles have less time to expand before collapse and ultimately, at very high frequency, may not be generated at all.[146,147] Since there is no direct coupling of sound waves on a molecular level, this simply means the size of cavitation bubbles decreases as a function on increasing frequency. Margulis has reported that in practice aqueous sonochemistry remains unchanged over the frequency range in which cavitation occurs, 10 KHz-10 MHz.[148] More recently, however Cum and co workers have studied the affects of frequency on the ultrasonic oxidation of iodide to iodine. In their work it was found that the reaction yield varied with frequency

and that an optimum frequency existed for the oxidation process.[149]

1.7 Generation Of Ultrasound: Piezoelectric effect

The fundamental principles behind the generation of ultrasound are based upon the piezoelectric effect and its inverse, established by the Curies over 100 years ago.[150,151]

In general, ultrasonic transducers employ the inverse effect. That is, when an electrical potential is applied across opposite faces of certain materials, an accompanying change in dimension is observed. If this potential is alternated at high frequencies then the crystal material converts the electrical energy to sound energy. Consequently, at sufficiently high alternating potential ultrasound is produced.

1.7.1 Ultrasonic Equipment

As the number of chemical applications and general interest in ultrasound has increased, so the diversity of equipment available has also grown. However, there remain two basic methods of introducing ultrasound into a laboratory reaction.

i. The reaction vessel may itself be immersed in an irradiated liquid (usually water).
ii. Direct immersion of an ultrasonic source or probe into the reaction.

A number of commercial systems employing one of the above criteria are available, but only the two most relevant to this thesis will be discussed below. For a more comprehensive treatment of ultrasonic equipment the reader is directed elsewhere.[152]

1.7.1.1 Ultrasonic Bath

Ultrasonic Baths are generally the most accessible method of introducing ultrasound into a reaction. They vary greatly in both size and power, but are relatively easy to use and a general guideline procedure has been published.[153]

In these systems, the ultrasonic transducers are mounted on the walls of the bath as shown in figure 1.15

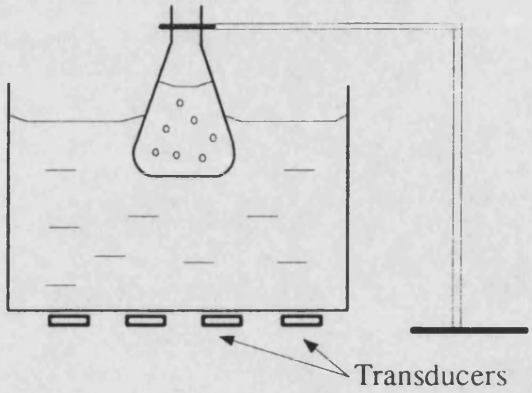

Figure 1.15 Ultrasonic cleaning bath

The ultrasound is then transmitted through the base of the tank and into the bulk liquid. This medium is usually water containing a surfactant in order to reduce energy loss in the bulk. Elaborate reaction apparatus may then be clamped into position in the bath.

A number of drawbacks are however present with such baths:

i. Attenuation of the ultrasound at the reaction vessel/water interface greatly reduces the intensity within the flask and may even eradicate cavitation.

ii. The ultrasonic field produced is non-uniform and it has been shown that maximum intensity occurs at $\lambda/2$ intervals from the transducers.[154]

iii. Temperature control is not easy since cleaning baths exhibit bulk heating effects, particularly over prolonged use.

1.7.1.2 Direct-Immersion Sonic Probe

Ultrasonic Probe Systems comprise an electronically driven transducer mechanically coupled to a probe. The probe amplifies the vibration produced by the transducers and is subsequently able to produce high ultrasonic intensities in excess of 100 Wcm^{-2}. Direct contact of the probe tip with the liquid means that efficient transfer of energy into the reaction medium is possible. Furthermore, by using jacketed reaction vessels temperature control is made easier than with bath type systems. Figure 1.16

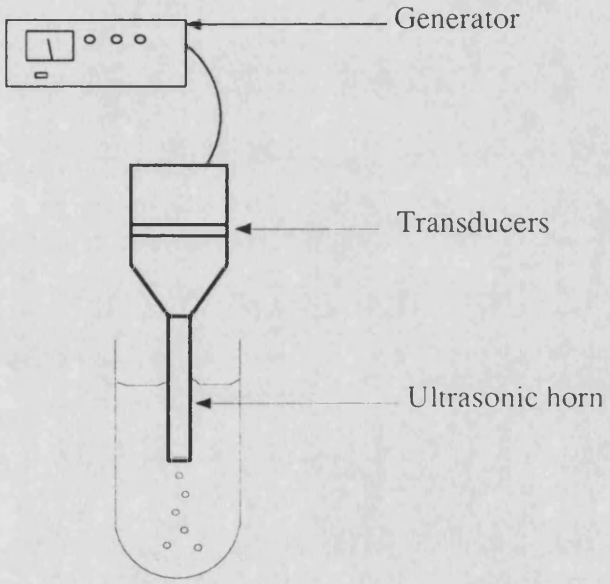

Figure 1.16 Ultrasonic horn(probe) system

The disadvantages of these systems are:

i. The zone of energy is small and centered around the probe tip. Cell design is therefore important, since to obtain effective sonication the reagents must flow through the irradiated region.

ii. Tip erosion may occur during prolonged use and contaminate the reaction system.

iii. Sealing the system can be difficult and may present problems when trying to work under inert atmospheres.

1.7.1.3 Equipment for Scale-Up of Sonochemical Reactions

The success of sonochemistry as an industrially important synthetic procedure for cable modification ultimately depends on the ability of carrying out large-scale or continuous reactions. There are at present a number of possible commercial equipment options, each having advantages and disadvantages. These systems can be broadly categorised into two groups, as outlined below:

a). Batch Reactors

These include large scale 'cleaning baths', immersible transducer set-ups and large sonic probe systems.

b). Continuous Reactors

This group comprises continuous loop reactors and flow-through systems.

Continuous systems are most pertinent to the present work and accordingly a brief treatment of these systems will be given.

Loop-reactors are commonly available and were developed for the biotechnology industry. They incorporate an ultrasonic source into a chemical flow cell as shown in figure 1.17. The reaction solution is then irradiated as it is passed through the cell.

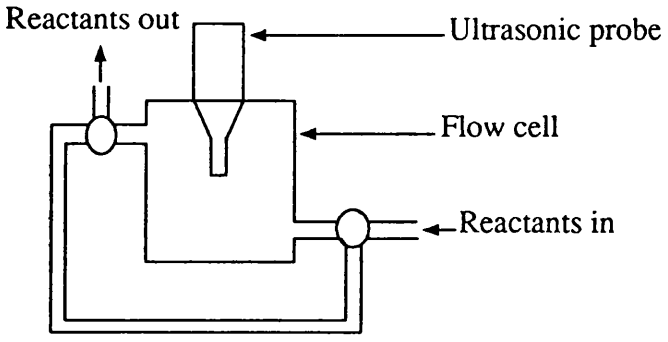

Figure 1.17 Ultrasonic Loop reactor

Flow through systems, on the other hand involve mounting transducers to the outside of a pipe and irradiating the reagents as they pass through the pipe. These systems would appear to be the most appropriate for sonochemical transformations

on the surfaces of preformed cables and commercial equipment is available which can process volumes between 37.8 and 189 l min^{-1}.[155]

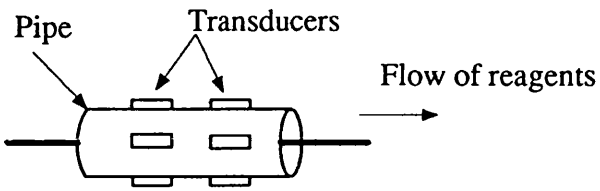

Figure 1.18 Ultrasonic Flow through reactor

Its advantages are:

i). It is non-intrusive, non-evasive and unlikely to contaminate the reaction.

ii). It requires only a small number of transducers.

iii). These systems are relatively cheap and easy to retro-fit into existing pipe work.

1.8 Sonochemistry

The first reported effects of ultrasound on chemical systems was published by Richards and Loomis in 1927.[156] Up to the late 1970's interest was relatively moderate in the chemical world, largely due to the scarcity of reliable ultrasound equipment. Since that time however, interest has expanded rapidly prompting a number of books[157-60] and reviews[161-5] on the subject.

Whilst some workers have viewed ultrasound as a possible way of merely increasing the rate of a chemical reaction, comparable to say, temperature, concentration, catalysts and pressure, this is a somewhat simplistic view. Although it is generally thought that sonochemical effects arise through 'hot-spot' formation, a number of papers have shown that the conditions produced during bubble collapse favour different reaction pathways to those observed in standard thermochemistry. Recently, Luche[166] has described some general guidelines for applying ultrasound to a reaction and suggested that in general, sonochemical transformations favoured radical pathways.

1.8.1 Homogeneous Sonochemistry

Although opinions remain split over the origin of sonochemical reactivity in homogenous media, more recent publications by Suslick concerning the production of sonoluminescence tend to support the 'hot-spot' theory. [167]

1.8.2 Heterogeneous Sonochemistry

The present work was concerned with the modification of preformed polymer cables and accordingly, a more detailed understanding of the events arising during heterogeneous sonochemistry is appropriate.

Heterogeneous systems are known to support an additional cavitational feature to those described previously. As early as 1944, Kornfield and Suvorov proposed that the observed damage and erosion produced by cavitation might arise from liquid jets produced by collapsing bubbles attached to an extended surface.[168] This was supported experimentally in 1961 by Naude and Ellis,[169] and in 1966 by Benjamin and Ellis.[170] Conclusions from their work indicated that non-spherical collapse of cavities occurred near a surface and spherical collapse only at distances from the surface which were too great for damage to occur. In 1971 Chapman and Plesset produced theoretical calculations to support these conclusions.[171] They estimated that little or no effect on the surface would be obtained if the distance between the solid and the collapsing bubble was greater than $b/R_0=1.5$, where b is the distance between the centre of the bubble of radius R_0 and the surface.

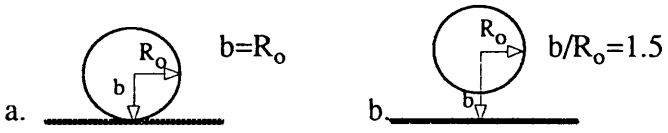

Figure 1.19

Two possible cases were simulated and these are shown in Figure 1.19a and b. Calculations from these models produced jet velocities of 130 and 170ms^{-1}

respectively. The larger value obtained for case b is as expected since a bubble further from a surface will collapse to a smaller size and concentrate its energy over a smaller volume.

Later, using laser generated bubbles, high speed photography and holography, Lauterborn and co workers recorded the growth and collapse of these bubbles near a solid boundary.[172-4] They found that asymmetric bubble collapse and jet formation occurred through distortions of the acoustic field near a solid boundary. Jet formation is also accompanied by Shockwaves of ca. 1-10 bar. These experiments agreed almost entirely with the theory presented by Chapman and Plesset.[171]

Vyas and Preece have studied the collapse of bubble clouds, produced by an ultrasonic horn, near a surface and found that pressures up to 9 bar were generated.[175] It is not surprising therefore that the greatest application of ultrasound has been in heterogeneous systems.

In 1927 Woods and Loomis reported that two non-miscible liquids formed an emulsion during sonication.[176] Later in 1938, Söllner reported the successful dispersion of solids such as a gypsum, mica and haematite in water, producing colloidal or semi colloidal solutions.[177]

These findings have prompted extensive studies over the years in the area of catalysis. Much of this emphasis, however, was focused on improving existing reaction systems. Lindley *et al.*[178] have reported that sonication increased the rate of the Ullmann coupling, of 2-iodonitrobenzene by a factor of 64 and that the mean particle size of the copper catalyst fell from 87 to 25 μm. More recently, Suslick and co workers have carried out studies of the effects of ultrasound on surface morphology of inorganic powders and metals.[179-81] In their work they found that sonication reduced particle sizes to a limiting value beyond which no further reduction was evident. This size reduction was attributed to shock wave induced collisions because the starting particle sizes were less than those observed for a

collapsing cavity and subsequently unlikely to arise through microstreaming. These collisions also produced 'pock-marked' surfaces with surface areas in excess of 10 times their starting value for TaS_2 and MoO_3. More ductile solids such as Nickel however, were found to have a smoother surface after sonication and exhibited only a moderate increase in surface area.

Non-metallic catalysts have also been shown to exhibit increased reactivity during sonication. Indeed, branched alkanes and olefinic hydrocarbons are more efficiently alkylated when the H_2SO_4-hydrocarbon emulsion is sonicated. The reaction is faster, applies to a greater variety of alkane-olefin mixtures and requires 5-50% less acid.[182]

The polymerisation of ethylene and propylene has been shown to be greatly facilitated by ultrasound when catalysed by chromium oxide on silica-alumina as well as several other catalysts.[183] Margulis has also reported that ultrasonically dispersed $TiCl_3$ in a hydrocarbon solution of triethyl aluminium greatly improves the production of polyolefins.[184]

The ability of ultrasound to generate stable emulsions, solid dispersions and improve mass transfer across a solid surface has led to its often being used in place of conventional phase transfer catalysts. Moriguchi, investigating the effects of ultrasound on electrochemical processes found that irradiation eliminated over-voltage effects in the electrolytic reduction of copper sulphate, presumably by removal of the diffusion barrier between the electrode and electrolyte.[185,186]

Lash has shown that ultrasound promoted the oxidation of alkenes by aqueous potassium permanganate, the Bayer Test, eliminating the need for a phase-transfer catalyst.[187]

Regen and Singh[188] have reported the production of dichlorocarbene from the reaction of chloroform and solid sodium hydroxide in the absence of a phase transfer catalyst when ultrasound is used. This transformation is shown in scheme 1.3

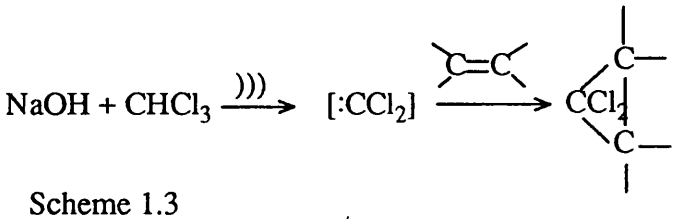

Scheme 1.3

1.8.3 Aqueous Sonochemistry

Almost all of the early work in sonochemistry was carried out in aqueous media, since it was generally believed that organic solvents could not support cavitation.[189]

The production of H_2O_2 during sonication of aqueous systems was first reported by Schmitt *et al.* in 1929.[190] In this paper it was found that sonication of halide ion solutions resulted in the formation of the halogen. Later, Weissler studied the sonication of water and proposed the following mechanism for the production of H_2O_2.

$$H_2O \longrightarrow H^{\bullet} + {}^{\bullet}OH$$

$$2\,OH^{\bullet} \longrightarrow H_2O_2$$

$$2H^{\bullet} \longrightarrow H_2$$

Despite extensive work by a number of researchers,[191-4] it was not until 1982 that conclusive evidence for the production of hydroxyl and hydrogen radical intermediates during sonication was presented.[195,196] In this work Riesz *et al.*[195,196] used standard diamagnetic nitrone and nitroso compounds as spin traps for the short lived H· & OH· radicals accordingly.

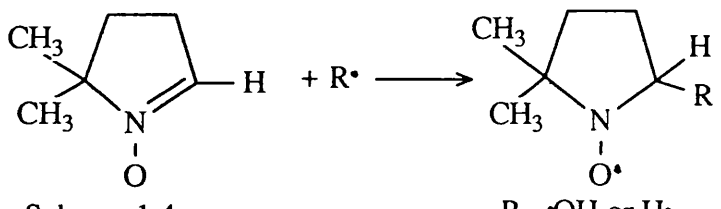

Scheme 1.4

R= ·OH or H·

By analysis of the hyperfine coupling constants in the ESR spectra, they

were able to unambiguously identify both OH· and H· adducts.

Given this facile homolytic cleavage of water during ultrasonic irradiation, a wide range of secondary sonochemistry is to be expected. Indeed, it has been shown that many inorganic species undergo redox reactions during sonication for example;[197]

$$Fe^{2+} \xrightarrow{)))} Fe^{3+}$$
$$Ce^{4+} \xrightarrow{)))} Ce^{3+}$$
$$KMnO_4 \xrightarrow{)))} Mn(OH)_2$$

Many workers have attempted to quantify the production of H· and OH· radicals formed during sonication of water. This has led to the development of a number of dosimeter systems.

a). The Fricke Dosimeter:[198] The oxidation of Fe(II) to Fe(III) can be followed by uv absorbance measurements and has been employed by several workers.[199]

b). The Terephthalate Dosimeter: This system was developed by Armstrong in 1963 for the measurement of ionising irradiation.[200] Alkaline or buffered solutions of terephthalic acid react readily with OH to produce the highly fluorescent hydroxyterephthalic acid according to scheme 1.5

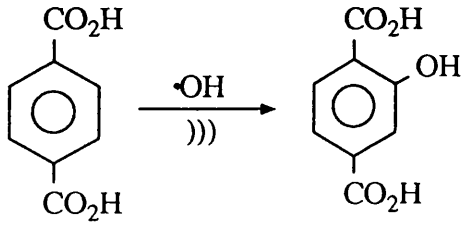

Scheme 1.5

These systems have recently been used by Price and Lenz to quantify the production of hydroxyl radicals in water at several ultrasonic intensities.[201]

Radical production arising from aqueous free radical initiators has also been shown to be facilitated by ultrasound. In 1940, Schumb and Rittner reported a rate enhancement of ~10 % for the decomposition of potassium persulphate during sonication with ultrasound at 8.7 KHz.[202] More recently, Lorimer *et al.*[203] have

reported that ultrasound increases the rate of decomposition of aqueous potassium persulphate below about 75°C.

1.8.3.1 Sonication of Organics in Aqueous Solution

Early work showed that aqueous solutions or suspensions of organic molecules underwent fragmentation during sonication. Weissler showed that aqueous solutions of CCl_4 liberated Cl_2 according to the following sequence:[192]

$$CCL_4 + H_2O \rightarrow Cl_2 + CO + 2HCl \qquad \text{Scheme 1.6}$$

Zechmeister and co workers[204] and more recently Price *et al.*[205] have reported the facile cleavage of aromatic carbon halogen bonds in aqueous solution.

A summary of some of the reported transformations of organic compounds in aqueous media is shown in Table 1.1

Table 1.1

Sonochemistry of organics in aqueous media

Substance	Products
CCl_4	Cl_2, CO_2, HCL, C_2Cl_6, HOCl
CH_3I	CH_4, I_2, CH_3OH, HI, C_2H_6
R_2CHCl	R_2CHOH, HCl
C_6H_5Br	Br^-, C_2H_2
C_6H_5OH	$C_6H_4(OH)_2$
$C_6H_{11}OH$	C_2H_2
RCHO	CO, CH_4, C_2H_4, $C_2H_4O_2$, RCO_2H

1.8.4 The Effect of Ultrasound on Polymers

In 1933, Flosdorf and Chambers,[206] Szalay[207] and Szent-Gyorgi[208] reported

that ultrasonic irradiation reduced the viscosity of solutions of natural polymers, such as starch, gum arabic and gelatin. This reduction in viscosity was later shown to occur through bond breakage with a resultant decrease in the polymer molecular weight.[209,210]

Extensive work over the past fifty years has shown that the rate of ultrasonic polymer degradation decreases with decreasing molecular weight, and approaches a limiting value beyond which no further cleavage is evident. Furthermore, the rate of degradation has also been shown to depend upon the irradiation time, intensity, polymer concentration and the interaction between the polymer and solvent.[160] By selectively varying these parameters Price and co workers have shown that ultrasound could be used to generate polymer solutions of known molecular weight and polydispersity.

Cleavage of σ bonds in the polymer backbone may result in the formation of either two macroradicals or an ion pair accordingly:[211,212]

i. Homolytic: $\mathbf{M\text{-}M\text{-}M\text{-}M \longrightarrow M\text{-}M^{\cdot} + {}^{\cdot}M\text{-}M}$

ii. Heterolytic: $\mathbf{M\text{-}M\text{-}M\text{-}M \longrightarrow M\text{-}M^{-} + M\text{-}M^{+}}$

The most common cleavage observed in ultrasonic degradation is the homolytic bond fission. Evidence for the formation of macroradicals was first presented by Melville and Murray who sonicated polymers in the presence of vinyl monomers,[213] and by Henglein who used 2,2'-diphenylpicrylhydrazyl, DPPH, as a radical scavenger.[212] More recently, evidence of macro radical formation during the sonication of polypropylene, polystyrene, poly(methyl methacrylate) and poly(vinyl acetate) in benzene has been presented by Tabata *et al.*[214,215]

Heterolytic bond fission has been described by Thomas and de Vries during the ultrasonic degradation of poly(dimethyl siloxane), PDMS.[216]

The mechanism by which ultrasonic degradation of polymers occurs is generally accepted as being the result of hydrodynamic forces created by either, the

cavitation event itself, or by the resulting shock waves. Whichever mechanism is responsible, the resulting process is non-random and can lead to the production of relatively mono-disperse polymers.

In the present work it was anticipated that the ability to generate macroradicals from polymers in solution, the capacity for controlling the polymer block length and the characteristic properties of ultrasound at a solid surface might cumulatively present a suitable method for the production of heterogeneous graft copolymers.

Numerous studies have been reported on the use of ultrasound to initiate radical polymerisations, often of aqueous monomers, where the homolysis of water could initiate reaction. More recent work by both Kruus[217,218] and Price *et al.*[219,220] has shown that a number of vinyl monomers could be polymerised in organic solvents using ultrasound in the absence of any further initiating species. The kinetics of polymerisation as a function of experimental conditions were found to be consistent with the initiation mechanism arising from the localised hot spot produced during cavitational collapse. The ability to induce polymerisation at low temperatures using ultrasound was cited as a suitable means of controlling the tacticity of poly(methyl methacrylate).

1.9 Particle Size Measurement

In the present thesis ultrasound has been used for the chemical modification of polymer powders. In view of the nature of this technique it was necessary to establish the physical effects of sonochemical treatment on the polymer particles. One method of characterising powders and other particles is by size distribution and this will be outlined below.

The size of an isotropic, spherical particle is uniquely defined by its diameter. Most particulate systems, however, are comprised of rough, irregularly

shaped particles. With such systems the assigned size is generally dependent upon the method of measurement and a number of size definitions have arisen.

A number of experimental techniques are available for the measurement of particle sizes, but almost all, with the exception of microscopy deal with some kind of size distribution. In the present work discussion will be limited to the method of low angle laser light scattering, but for a more comprehensive review the reader is directed elsewhere.[221]

The light scattering technique utilises the fact that illuminated particles serve as secondary radiation sources in a manner which is related to their size. If the size of the suspended particles is very small with respect to the wavelength of light or their refractive index is close to that of the medium, then the equations of Rayleigh[222] and Rayleigh and Gans can be applied.[223,234] The first condition is generally valid for solvated polymer molecules and hence, in molecular weight determinations by this method. Neither treatment is valid, however, when the suspended particles are greater or equal to the wavelength of the incident radiation. In this instance the more complex Mie theory is generally used.

In practice, light from a low power laser is transmitted through a cell containing suspended particles. The light is diffracted by the interacting particles before passing on to a collection lens where it is focused onto a solid state detector. The detectors are comprised of a number of channels and each detector ring is radially optimised for a particular size band. A typical instrument layout is shown in figure 1.20

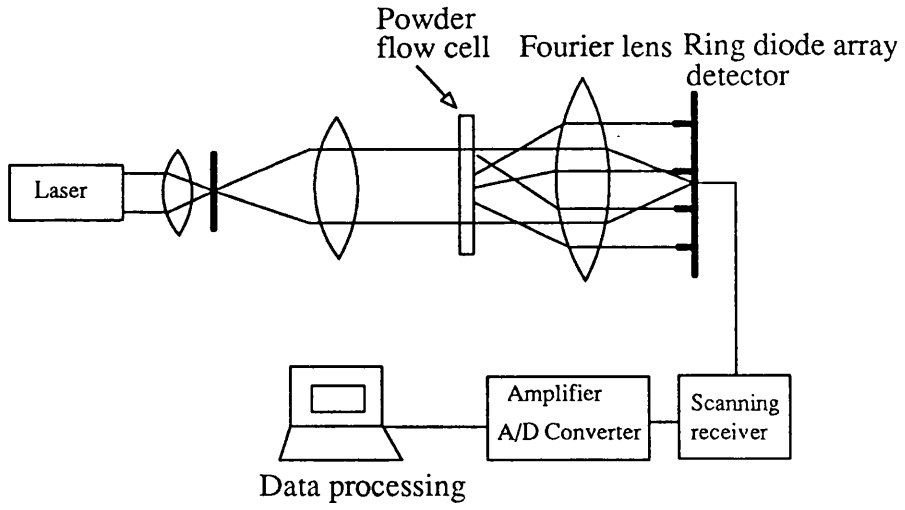

Figure 1.20 Schematic representation of a laser diffraction particle sizer

1.10 TARGETS

The work detailed in this thesis was concerned with the application of ultrasound to the heterogeneous modification of polyethylene and poly(vinyl chloride), PVC, surfaces. Studies were particularly aimed at the development of suitable ultrasonic transformations for the modification of preformed polymeric electrical cables.

In conjunction with BICC cables four main areas for improvement of the existing systems were identified:

(i) It was considered important to increase the chemical resistance of the polymer cables towards attack by oils and similar compounds.

(ii) In order to present a more durable cable it was felt that improvements to the surface toughness of the polymer were necessary.

(iii) The introduction of colour to the polymer surface would allow master batches of white polymer to be used and coloured as desired after fabrication of the cable. This process could present large scale economic savings as well as simplifying the extrusion process through removal of the coloured pigments. Also, the colour stability of such cables would be greatly increased since much of the traditional leaching process would be eradicated.

(iv) An increase in the surface 'slippability' and hardness were cited as suitable methods for improving the handling characteristics of the cables, thereby providing easier unrolling and laying by the consumer.

The approach to (i) was to increase the surface hydrophilicity of the cable by introducing polar groups onto the surface, whilst it was felt that points (ii) and (iv) might be achieved by grafting other polymers onto the cable. To achieve point (iii), however, it was considered necessary to chemically attatch dye molecules to the cable surface.

CHAPTER 2

EXPERIMENTAL

2.1 Materials

Polymers:

Poly(vinyl chloride) was from Aldrich, inherent viscosity 0.92

Polyethylene BPD 2133, Mw= 145,000, γ= 7, was supplied by BICC in 0.2 to 0.3mm melt pressed sheets

Polyethylene cable compound

Very low density polyethylene

Poly(vinyl chloride) cable compound GHI 219

Poly(vinyl chloride) multicore sheathing compound PM 134

Polyacrylamide, Aldrich, d=1.302

Poly(acrylic acid), Aldrich, Mw=1,250,000

Poly(ethylene oxide), Aldrich, Mw=8,000,000

Poly(methyl methacrylate) beads, BDH high Mwt

Polypropylene powder, Amoco, MFI=1.6

Poly(vinyl methyl ether), Aldrich, 50% $^{w}/_{w}$ solution in water

Poly(vinyl alcohol), BDH, 98% hydrolysed Mw=65,000

Monomers:

Acrylamide, Aldrich, (99+%)

Acrylic acid, Aldrich, (99%) inhibited with 200ppm hydroquinone monomethyl ether

Hydroxyethyl methacrylate, Fluka, (95%) inhibited with 300ppm hydroquinone

Methyl methacrylate, Aldrich

Trimethylsilyl methacrylate, Aldrich, (98%)

2-Vinyl naphthalene, Aldrich, (98%)

Dyes:

Brilliant green, Aldrich, dye content (93%)

Bromophenol blue, Aldrich, dye content (90%)

Crystal violet, Aldrich, dye content (98%)

Methylene blue, Aldrich, certified

Rhodamine B, Aldrich

Rose Bengal, Aldrich, certified

Solvents:

Acetone, Aldrich, (99+%)

Decahydronaphthalene , Aldrich, anhydrous 99+% mixture of cis and trans

Dichloromethane, Aldrich, HPLC, (99.9%)

Ethyl acetate, Fisons, (99.5%)

Methanol, Aldrich, HPLC (99.9%)

2-Propanol, Aldrich,

Tetrahydrofuran, Aldrich, (99+% inhibited with 0.025% butylated hydroxy toluene)

Other reagents:

Aluminium chloride hydrated, Aldrich (99.99%)

Ammonium persulphate, Aldrich, (98+%)

4-Bromo-1-aminonaphthalene, Aldrich, (99%)

Chlorosulphonic acid, Aldrich, (99%)

Chromium trioxide, Fisons analar reagent, (>99%)

Hydrogen peroxide, Fisons analar reagent, 100 volumes 30%, 20 volumes 6%

Iron(III) chloride hydrated, Fisons analar reagent, (>98%)

Iron(II) sulphate, BDH, (98%)

Lithium wire (98+%) high sodium content

Maleic anhydride, Fisons analar reagent, (99.5%)

Naphthalene, Aldrich (99%)

Potassium bromide, IR grade, (99+%)

Potassium Persulphate, Aldrich, (99+%)

Sodium dodecyl sulphate, Aldrich, (70%)

Sodium hydroxide, Fisons analar reagent, (98%)

Sodium metabisulfite, Aldrich, (97%)

N-t-Butyl-α-phenlynitrone, Sigma

Tetrabutyl ammonium bromide, Aldrich, (99%)

Trifluoroacetic anhydride, Aldrich, (99+%)

Zinc chloride, Aldrich, (98%)

2.2 Preparation and Purification of Monomers

Acrylic acid was distilled under vacuum to remove the hydroquinone monomethyl ether inhibitor. After distillation the collection flask was stoppered, covered in aluminium foil and stored under refrigeration until required.

Hydroxyethyl methacrylate was passed through a disposable ion exchange column designed for the extraction of hydroquinone and hydroquinone monomethyl ether inhibitors. After collection of the required amount of eluent the flask was stoppered, wrapped in aluminium foil and stored under refrigeration before use.

2.3 Preparation of Glassware

All glassware used in the present work was thoroughly cleaned according to the following procedure, unless stated otherwise. Glassware was soaked in chromic acid solution, rinsed with copious amounts of distilled water, acetone and then dried in an oven.

2.4 Sonication Experiments

The ultrasound was introduced into reaction systems by either a Kerry 'pulsatron' PUL 325 ultrasonic bath or a Sonics and Materials VC600 ultrasonic probe.

2.4.1 Cell Design

It has been reported that both the shape and position of a reaction vessel can effect the ultrasonic intensity reaching the reactants in an ultrasonic bath.[152] Some workers have also reported that the shape of the reaction vessel influences sonochemical reactions performed with an immersed probe.[225] It was essential therefore, to develop suitable reaction cells which could be used reproducibly throughout each series of sonochemical reactions, in order to maintain comparable results.

a) Ultrasonic Probe

A significant amount of heat can be generated during prolonged ultrasonic irradiation with a probe. A jacketed reaction vessel was therefore employed with a circulating thermostat. Temperature control in the present system was typically to within ±1°C. Furthermore, long term exposure, typically several months of continued use, results in the erosion of reaction vessels and a thick-walled glass cell was therefore necessary.

Two cell types have been used in the present work, depending upon the reaction medium (that is, films or powders), and these are shown in figures 2.1a and 2.1b. The larger jacketed beaker was used as depicted for all film reactions and without the film holder for calibration of the probe intensity (see section 2.4.2) and potassium persulphate decomposition kinetics (see section 2.8). In most film reactions the probe was clamped at a distance of 3 cm from film surface although this distance could be varied.

b) Ultrasonic Bath

Due to attenuation of the sound waves at the water-vessel interface a large amount of ultrasonic intensity is lost in this system. Many workers have reported that flat bottomed reaction vessels are to be preferred for use in ultrasonic baths.[153]

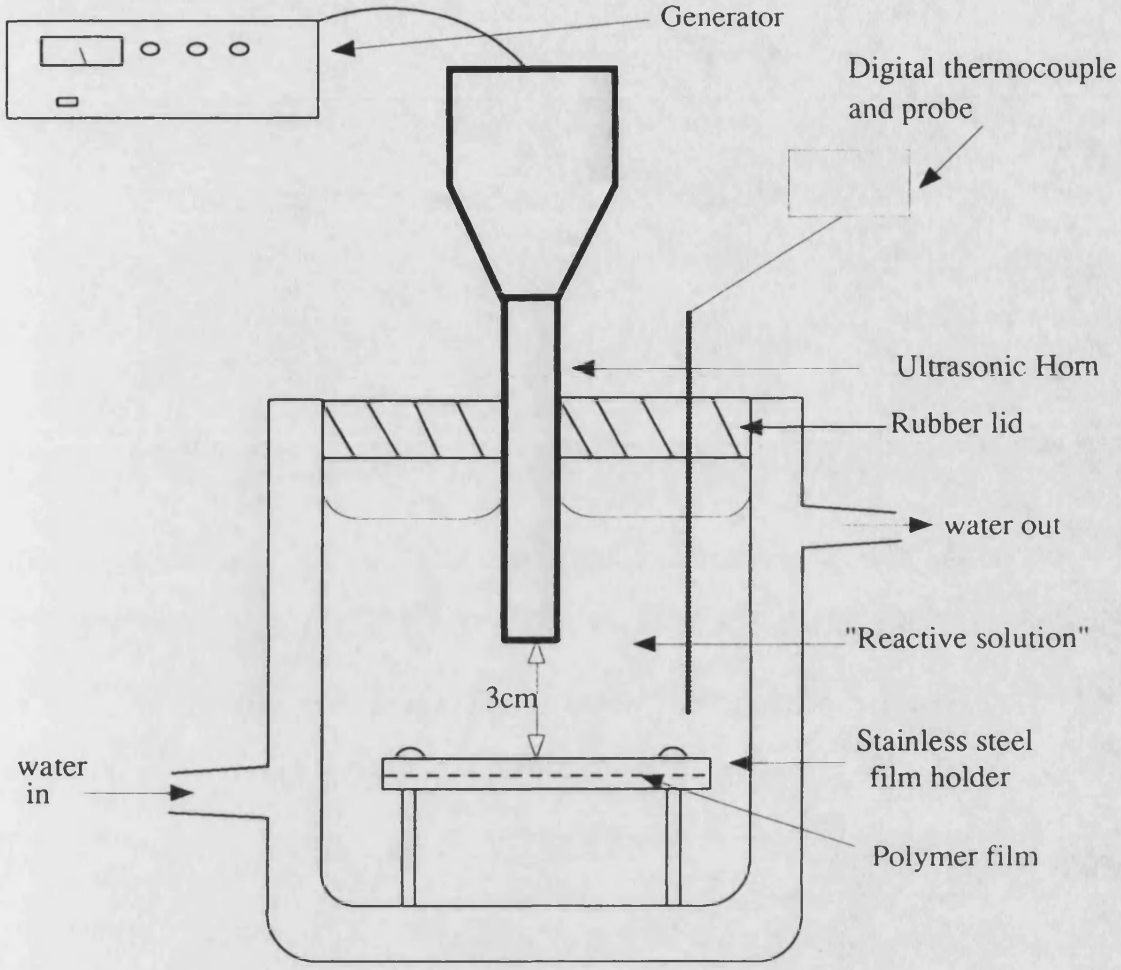

Figure 2.1a Ultrasonic film reactor (250 cm^3)

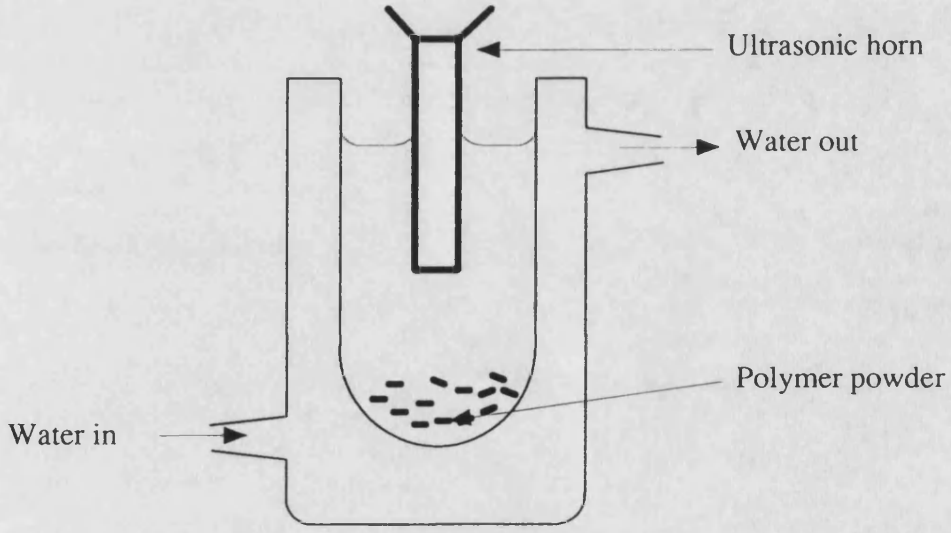

Figure 2.1b Ultrasonic reaction cell for powders (100 cm^3)

Accordingly, in the present work all reactions were performed in 50 cm^3 conical

flasks. Furthermore, a large amount of energy is lost through viscous interactions between molecules in the bulk liquid during the propagation of ultrasound. In order to reduce this effect surfactant solution was added to the bulk, distilled water, prior to sonication. Additionally, to reduce temperature rise during prolonged sonication, experiments were carried out with a copper cooling coil immersed in the ultrasonic bath, see figure 2.2.

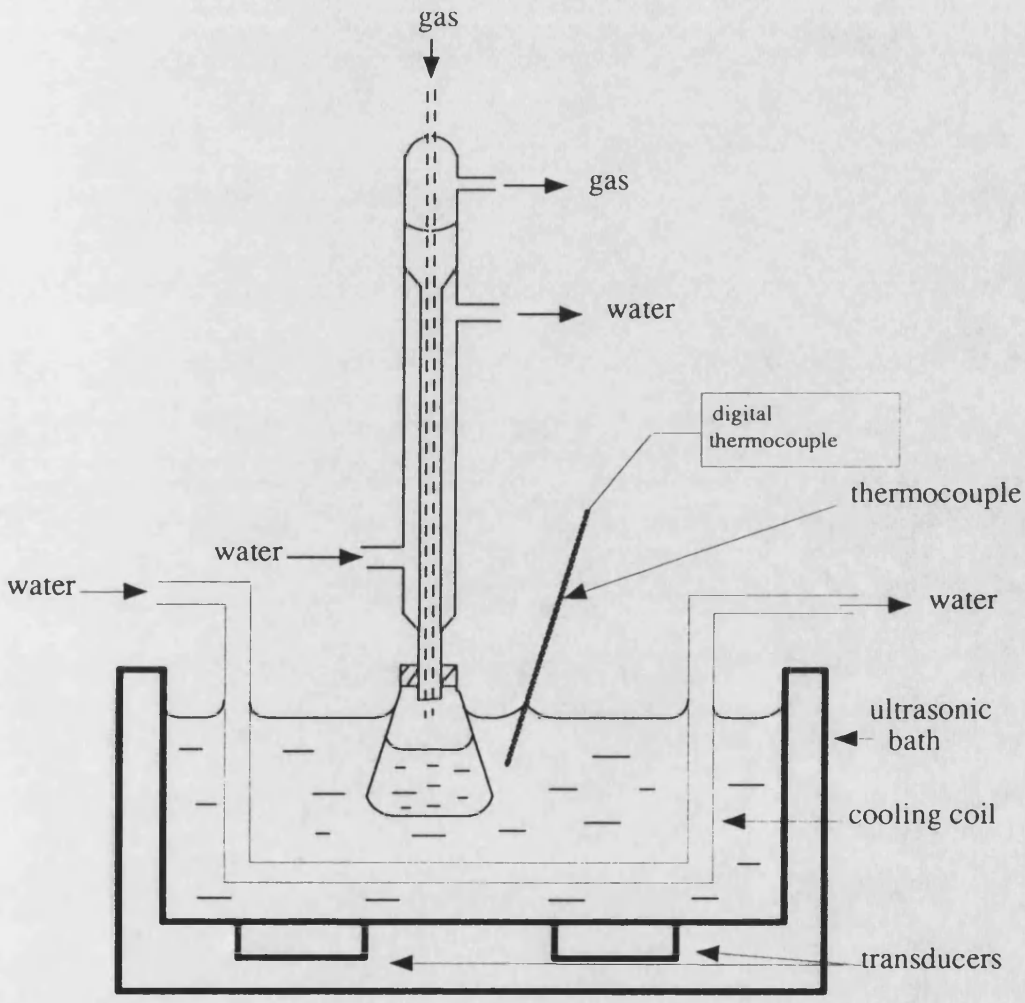

Figure 2.2 Ultrasonic bath reaction apparatus

In order to determine the region of maximum intensity in the ultrasonic bath, the erosion of aluminium foil at various locations was observed. This method is

based on the fact that the regions of maximum damage to the aluminium foil correspond with the areas of maximum sonochemical cavitation and has been outlined in more detail elsewhere.

c) Electrical Cable Modification Cell

The need to treat large samples of electrical cable (typically >15 cm strips are required for mechanical testing) meant that these reactions had to be performed in the ultrasonic bath. Reactions on these cables required the development of a further ultrasonic cell. This was based upon a cylindrical U-shaped tube having a 3 cm internal diameter and a capacity of 250 cm^3 as shown in figure 2.2b. This cell was then positioned in the ultrasonic bath as described above.

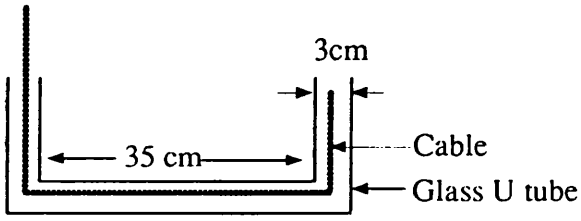

Figure 2.2b Electrical cable reaction cell

2.4.2 Calibration of Probe Intensity

There are various methods of reporting the ultrasonic intensity used during sonication. Some workers simply quote the nominal output as stated by the equipment manufacturers.[225] This value however, can be misleading as it refers only to the energy supplied to the transducers and not the energy reaching the reaction.

In the present work a calorimetric approach was adopted since this should give a direct relation to the amount of cavitation produced inside the reaction. A value is given for the time taken to heat a known volume of distilled water through a recorded temperature rise. This will enable other workers using different heat capacities to directly compare their results with the ones reported here. In order for a value to be given to the intensities used during the experiments, the temperature

rise was converted to an absolute value.

The ultrasonic reaction vessel was set up as for film reactions (fig 2.1a), but without the film holder present. A 150 cm^3 aliquot of distilled water was added to the vessel along with an electric heater and thermocouple probe the system was then allowed to equilibrate. The temperature was recorded and the electrical heater was switched on. The voltage and current were recorded using a Thandar TS3021S multimeter and the temperature rise was noted at sixty second intervals using a stop clock. The energy supplied by the heater is given by:

$$E = VIt \qquad 2.1$$

Where V is the voltage, I is the current and t is the time in seconds.

A total heat capacity, C, for the system was then calculated.

This procedure was then repeated using the Sonics and Materials VC600 ultrasonic probe in place of the electrical heater. The temperature rise was followed as before and the procedure carried out for each of the even numbered generator settings. The ultrasonic power was then calculated from:

$$P = \frac{C\,\Delta\Theta}{t} \qquad 2.2$$

Where C is the total heat capacity of the system, $\Delta\Theta$ is the temperature rise and t is the time in seconds. This value was then converted to power per unit area by dividing by the area of the probe tip.

Results for the Intensity Calibration

Volume of distilled water = 150 $cm^3 \pm 0.3$ cm^3

a) Electrical heater:

Time / s	Temperature / °C
0	20.8
60	22.1
120	23.2
180	24.2
240	25.1
300	25.8
$\Delta\Theta$	5.0

During heating: voltage=15.0 V and current=1.165 A

From equation 2.1, E = 5242.5 J and C = 1048.5 J K^{-1}

b) Ultrasonic probe:

Volume of distilled water = 150 ± 0.3 cm^3

Area of the ultrasonic probe tip = 1.202 cm^2

Time/s	Temperature /°C				
	Generator setting (arbitry units)				
	2	4	6	8	10
0	20.9	20.8	20.2	20.2	20.1
60	21.7	22.4	22.7	23.4	25.1
120	22.4	23.8	24.7	26.0	29.1
180	23.0	24.8	26.4	28.2	32.1
240	23.5	25.7	27.9	30.0	34.8
300	24.0	26.6	29.2	31.6	37.0
$\Delta\Theta$	3.1	5.8	9.0	11.4	16.9
Power (W)	10.83	20.27	31.46	39.84	59.07
Intensity W cm^{-2}	9.01	16.86	26.17	33.15	49.14

Estimation of the errors involved:

For the electrical heating process the error in recording the temperature was ± 0.1°C and the error in the time readings was ± 1 second. The total error in the the heat capacity then becomes:

$$\pm\left\{\left(\frac{0.2^\circ}{5.0^\circ}\right) + \left(\frac{2\ s}{300\ s}\right)\right\} \times 100\% = \pm 4.667\%$$

Therefore, C is $1048.5 \pm 48.9\ J\ K^{-1}$

The error in the ultrasonic intensity at, generator setting 6 is then:

$$\pm 4.667\% \pm\left\{\left(\frac{0.2}{9.0}\right) + \left(\frac{2}{300}\right)\right\} \times 100\% = \pm 7.6\%$$

Hence, the ultrasonic intensity is $26.17 \pm 1.99\ W\ cm^{-2}$

Whilst the percentage error would appear to be reduced by measuring values over larger temperature and time ranges, this procedure is to be avoided, since, at longer heating times and at higher temperatures, the contribution of thermal dissipation effects will be much greater thereby increasing the overall error.

2.5 Sonication Procedure for Polymer Particles

The sonication of polymer particles was performed using the same procedure in each experiment. Commercial polymer powders were sieved where necessary to obtain particles with a size of less than 500 μm as this was the instrumental measurement limit, see section

2.6 below. The required amount of polymer was then weighed into the

clean, dry, 100 cm^3 jacketed test tube, shown in figure 2.1b. To this sample was then added 50 cm^3 of distilled water and 0.1g of sodium dodecyl sulphate. The sodium dodecyl sulphate was used in order to reduce the surface tension of the water and allow wetting of the polymer particles.

The vessel was then connected to a water circulator and allowed to reach thermal equilibrium during which time the ultrasonic probe was clamped into position. All experiments were carried out at 35°C using an intensity of 26.2 W cm^{-2} (generator setting 6) for five hours, except where the effects of time have been investigated.

At the end of the sonication period the sample was filtered off, washed with, 2 x 50 cm^3, distilled water and dried under vacuum. The dried samples were then analysed directly by light scattering to determine their size distribution, see section 2.6.

2.6 Particle Size Measurements

Particle size distributions were recorded using a Malvern Instruments series 2600c particle size analyser operated in 'easy' mode. The optical unit was equipped with either a 300 or 100 mm focal length lense allowing measurement in the region 5.8 to 564 and 1.9 to 188 μm respectively.

The instrument was set up with a standard liquid flow cell (path length 2.0 mm) and connected to a stirred circulating reservoir. A suitable supporting liquid (99% ethanol for PMMA and 95% ethanol in all other cases) was added to the reservoir and pumped around the system. Solvent systems were selected on their ability to wet polymer particles completely without solvating them. Before sample

measurement calibration of the background solvent was necessary each time. After the solvent calibration, polymer powder samples were added slowly to the circulating solvent until the continually monitored obscuration level reached saturation point. At this point the system was allowed to stabilise for one minute, after which time particle size analysis was carried out. The results were calculated according to the Log-Normal distribution method and plotted as the percentage of particles versus particle size.

After each measurement, the equipment was drained and thoroughly cleaned before further use.

2.7 Reactions on Polyethylene

In the present thesis work has been primarily concerned with the modification of melt pressed polyethylene sheets. Subsequently, systems which showed promise were applied to polyethylene cable materials.

2.7.1 Polyethylene Film Reactions

Rectangles of polyethylene film, approximately 3 by 2 cm, were cut from the larger 0.2-0.3 mm thick melt pressed sheets using a scalpel. These samples were cleaned directly before use, firstly with methanol and then with a dichloromethane swab. The washed films were allowed to air dry at room temperature for about 30 minutes before being clamped into the purpose made stainless steel holder using retaining screws.

In the meantime, the required amount of reagents were weighed into the 250 cm^3 jacketed beaker along with the required volume of distilled water necessary to make the total volume up to 150 cm^3. The reagents were stirred with a glass rod until fully dissolved, where necessary, and allowed to reach thermal equilibrium.

After this time, the complete film holder was submerged in the reagents as

shown schematically in figure 2.1a. The ultrasonic probe was then clamped into position with the tip approximately 3 cm above the film surface. Throughout the course of these reactions, temperatures were maintained at 35 ± 1°C using a Tempette TE-8A water circulating thermostat and measured by a Digitron thermocouple.

All reactions in this series were conducted for five hours except where the effects of time have been studied. In addition, sonications were performed at an intensity of 26.2 W cm^{-2}, unless otherwise stated.

After the desired reaction period, the film holder and samples were removed from the "reactive" solution and rinsed with distilled water. The films were then extracted from the stainless steel holder and marked with a scalpel in order to indicate the sample face nearest to the ultrasonic probe tip during reaction. The films were then washed with a further 500 cm^3 of distilled water from a wash bottle followed by a 25 cm^3 aliquot of acetone. Finally, films were placed into clean glass specimen bottles and vacuum dried at 25°C, 0.05 mmHg for five hours.

Samples where the "reactive" solution displayed low water solubility, such as polymer solutions, were additionally stirred in 2 x 50 cm^3 hot (≈80°C) water for 5 minutes to ensure removal of any ungrafted material before being vacuum dried.

2.7.2 Derivatisation of Surface Hydroxyl Groups

a) Trifluoro Acetic Anhydride (TFAA): All derivatisation reactions were performed in the vapour phase following literature reports of unfavourable side reactions during solution phase derivatisations.[226] The method employed was that of Ratner *et. al.*,[226] although the same author has also shown that TFAA vapour reacts with both surface hydroxyl and epoxide groups.[227] Polymer samples were suspended in a glass test tube. TFAA (2 cm^3) was cautiously pipetted into the test tube below the sample without making contact. The test tube was then sealed with a teflon coated stopper and the reaction allowed to proceed for 15 minutes at 35°C.

After completion the reacted samples were removed and dried under vacuum 25°C, 0.05 mmHg for five hours and then analysed directly

2.8 Kinetics of Potassium Persulphate Decomposition

Potassium Persulphate decomposition studies were carried out in the 250 cm^3 jacketed beaker used for all film reactions and probe calibration measurements. (See figure 2.1a). Prior to each experiment the reaction cell was cleaned in an ultrasonic bath with water and surfactant, washed with copious quantities of distilled water, acetone and then dried in an oven.

The beaker was connected to a Tempette TE-8A water circulating thermostat which had been preset to the desired reaction temperature. A 150 ± 0.3 cm^3 aliquot of distilled water was then added to the beaker by pipette and the rubber lid fitted. The system was allowed to reach thermal equilibrium after which time 0.1966 ± 0.0002g of N-tButyl-α-phenyl nitrone and 0.150 ± 0.0002g of potassium persulphate were added. The solution was stirred vigorously with a glass rod until all the reagents had completely dissolved. The rubber lid was then re-fitted along with a thermocouple probe and a sampling syringe. The ultrasonic probe was clamped into position and a 0.2 cm^3 aliquot of the reaction mixture withdrawn using a 1 cm^3 gas tight syringe.

The ultrasonic probe was then switched on, initiating the reaction. The extracted sample was immediately delivered to a 25 cm^3 volumetric flask containing approximately 20 cm^3 of distilled water at 20°C, in order to quench the reaction. Further samples were removed at suitable time intervals throughout the course of the reactions and similarly quenched.

All diluted samples were analysed directly by transmission ultraviolet spectroscopy using a Perkin Elmer 330 double beam spectrometer with matching quartz cells and water as the reference. The N-t-Butyl-α-phenyl nitrone spin trap has a characteristic absorbance at 287nm which is removed upon reaction with a free

radical.

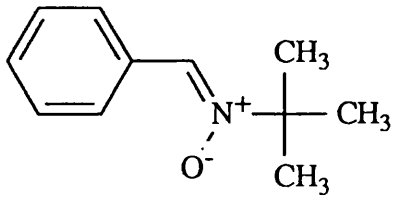

N-t-Butyl-α-phenyl nitrone. λ_{max}287

All thermal reactions in the absence of ultrasound were carried out in an identical manner, except in place of the ultrasonic probe an IKA magnetic stirrer and teflon magnetic flea were used.

Estimation of the errors involved in measuring the concentration of each sample:

error in sampling was: 0.2 ± 0.010 cm^3

error in the sample dilution was: 25 ± 0.1 cm^3

Total error in each point is therefore :

$$\pm \left(\frac{0.01}{0.2} + \frac{0.1}{25} \right) \text{ x } 100\ \% = \pm 5.4\ \%$$

2.9 Poly(vinyl chloride) Reactions

In the present work reactions have been carried out primarily on poly(vinyl chloride) powders and subsequently extended to moulded sheets of cable compound and finally actual cables.

2.9.1 Powder Reactions

Due to the number and diversity of reactions carried out on poly(vinyl chloride)

powders the following section has been divided into two main areas:

1. Substitution reactions:

This section was comprised of reactions carried out with "model" compounds and dyes as well as those grafting reactions with other polymers and monomers.

2. Elimination reactions:

This group of reactions was concerned with those transformations which proceed via an initial dehydrochlorination step.

1. Substitution Reactions

In all of these investigations the practical approach was similar depending on the ultrasonic source employed.

Ultrasonic bath reactions: In these experiments the required concentration of reagents dissolved in 25 cm^3 of an appropriate solvent were added to 1g of PVC powder contained in a 50 cm^3 conical flask. The flask was then clamped into the ultrasonic bath at the position of predetermined maximum intensity (see section 2.4.1). A reflux condenser and gas line were then fitted to the flask as shown in figure 2.2. After sonication at 35 ± 2°C for the chosen period of time, PVC powders were filtered off, washed with copious quantities (~10x50 cm^3) of the reaction solvent and vacuum dried at 60°C.

Ultrasonic probe: The required amount of reagents were dissolved in an appropriate amount of a chosen solvent and added to a weighed sample of PVC powder contained in the powder reaction cell, see figure 2.1b. The ultrasonic probe was clamped into position and the system allowed to reach thermal equilibrium at 35°C. After sonication for the desired period of time, the PVC powder was filtered off, washed and dried as described above for the ultrasonic bath reactions.

Reactions involving dyes and "model" compounds are presented in table 2.1, whilst those grafting reactions with other polymers and monomers are given in table 2.2.

Table 2.1

Experiment number	Reactant (weight g)	Solvent 25 cm^3	Gas	Sonication time (min)
1	4-Br-1-amino naphthalene[a]	2-propanol	N_2	60
2	Anthracene (1.4)	2-propanol	N_2	60
3	2-vinyl naphthalene (1.14)	2-propanol	N_2	60
4	2-vinyl naphthalene[b] (1.14)	2-propanol	N_2	60
5	2-vinyl naphthalene (1.14)	2-propanol	Air	60
6	2-vinyl naphthalene (0.25)	2-propanol	Air	60
7	Bromophenol blue (1.0)	H_2O	N_2	60
8	Bromophenol blue (0.25)	H_2O	N_2	60
9	Bromophenol blue (0.25)	H_2O	N_2	120
10	Bromophenol blue (0.25)	NaOH	N_2	60
11	Bromophenol blue (0.25)	NH_4OH	N_2	60
12	Bromophenol blue (0.25)	H_2SO_4	N_2	60
13	Bromophenol blue (0.25)	H_2O	Air	60
14	Bromophenol blue (0.25)	H_2O[c]	Air	60
15	Bromophenol blue (0.25)	THF	N_2	60
16	Bromophenol blue (0.25)	2-propanol	N_2	60
17	Bromophenol blue (0.25)	2-propanol	N_2	300
18	Bromophenol blue (0.25)	2-propanol	Air	60
19	Brilliant green (0.25)	2-propanol	N_2	60
20	Rose Bengal (0.25)	2-propanol	N_2	60
21p	Brilliant green (0.2)	H_2O	Air	5
22p	Rose Bengal (0.2)	H_2O	Air	5
23p	Bromophenol blue (0.2)	H_2O	Air	5
24p	Methylene blue (0.2)	H_2O	Air	5
25p	Crystal violet (0.2)	H_2O	Air	5
26p	Rhodamine B (0.2)	H_2O	Air	5

a- 1.75g; b - 0.06g of lithium wire added
c - 0.10g of sodium dodecyl sulphate added
p - Reaction carried out on an ultrasonic probe

Table 2.2

Experiment number	Ractant (g)	Solvent (ml)	Sonication time (min)
27	Acrylic acid (0.25g)	H_2O (25)	60
28p	Acrylic acid (1g)	H_2O (50)	5
29p	Polyacrylic acid (0.15g)	H_2O (50)	15
30	MMA (0.25g)	2-propanol (25)	60
31p	PMMA (0.25g)	Toluene (50)	5
32	Acrylamide (0.25g)	H_2O (25)	60
33	Polyacrylamide (0.25g)	H_2O (25)	60
34	Poly(ethylene oxide) (0.25g)	H_2O (25)	60
35p	Poly(ethylene oxide) (0.5g)	H_2O (50)	5
37	PVME[a] (0.25g)	H_2O (50)	60
38	Poly(vinyl alcohol) (0.25g)	H_2O (50)	60

p - Reaction carried out on an ultrasonic probe

a - Poly(vinyl methylether)

2. Elimination reactions: The procedure used for these experiments was similar throughout and a more detailed discussion of each system will be given in chapter 4.

To 1g of PVC powder contained in the appropriate reaction vessel were added 25 cm^3 of a known concentration of aqueous sodium hydroxide. The powder was sonicated for a given period of time, then filtered off, washed with 500 cm^3 of distilled water and vacuum dried.

The above procedure was repeated using 25 cm^3 of 2 mol dm^{-3} sodium hydroxide solution, but after a 1 hour sonication period 1.2 x 10^{-3}moles of a metal salt were added and the reaction stirred for a further 2 hours. A second series of experiments was carried out in an identical manner to this, but using distilled water as the reaction solvent. Finally, these experiments were duplicated using ultrasound

throughout and distilled water as the solvent.

Further investigations of the dehydrochlorination process were carried out using a phase transfer catalyst. In most experiments a 4% $^{w}/_{v}$ solution of tetra-butyl ammonium bromide in aqueous sodium hydroxide solution was employed, but sodium dodecyl sulphate has also been investigated. These experiments are presented in table 2.3 along with a number of base catalysed reactions in the presence of metal ions.

Finally a number of derivatisation reactions were carried out on PVC powder samples dehydrochlorinated according to the conditions in experiment 45p in table 2.3 above.

Reactions were carried out directly on 1g samples of the washed, dehydrochlorinated PVC according to the procedures outlined in table 2.4.

Table 2.3

Experiment No.	Reaction conditions[a]	Sonication time (min^{-1})
37	8% NaOH (50 cm^3) + $FeCl_3.6H_2O$ (0.05g)	60
38p	As above	60
39p	PVC film + 8% NaOH[d] + $FeCl_3.6H_2O$ (0.15g)	60
40p	PVC film + 8% NaOH[d] + $FeCl_3.6H_2O$ (0.30g)	120
41p	PVC film + 25% NaOH[d] + $FeCl_3.6H_2O$ (0.60g)	60
42	8% NaOH (50 cm^3) + $AlCl_3.6H_2O$ (0.045g)	60
43	8% NaOH (50 cm^3) + $ZnCl_2$ (0.025g)	60
44	25% NaOH (25 cm^3) + TBAB (0.1g)	60
45p	25% NaOH (50 cm^3) + TBAB (0.2g)	5
46	25% NaOH (50 cm^3) + SDS[b](0.4g)	
47p	PVC film + 8% NaOH[d] + TBAB (0.6g)	60
48p	PVC film + 25% NaOH[d] + TBAB (0.6g)	20 & 120

a- All % NaOH values refer to % $^{w}/_{v}$

b- Sodium dodecyl sulphate

p- Probe reaction

Table 2.4

Experiment No.	Reaction conditions[a]	Sonication time (min^{-1})
49p	Bromophenol blue (0.2g) in 50 cm^3 H_2O	5
50p	Brilliant green (0.2g) in 50 cm^3 H_2O	5
51p	Rose Bengal (0.2g) in 50 cm^3 H_2O	5
51p	Rhodamine B (0.2g) in 50 cm^3 H_2O	5
53p	Crystal violet (0.2g) in 50 cm^3 H_2O	5
54p	Methylene blue (0.2g) in 50 cm^3 H_2O	5
55p	Maleic Anhydride (0.2g) in 50 cm^3 H_2O	30
56p	50 cm^3 2% $^{w}/_{v}$ Acrylic acid in H_2O	5
57p	50 cm^3 2% $^{w}/_{v}$ Acrylic acid in H_2O	5
58p	Acrylic acid (1g) in 50 cm^3 25% NaOH + TBAB (0.2g)	5

a- All % NaOH values refer to % $^{w}/_{v}$

p- Reaction carried out on the ultrasonic probe

2.10 Analysis of Polymer Samples by Infrared Spectroscopy

All infrared spectra presented in this thesis were recorded on a Nicolet 510P optical bench fitted with a deuterated triglycine sulphate detector (DTGS). Interferograms were transformed using a Happ-Genzel apodization and the final spectra have been presented without further manipulation in absorbance units.

a) Attenuated Total Reflectance (ATR): The optical unit used for the measurement of all spectra was a Nicolet vertical variable angle ATR based upon a design by Gilby.[228] The unit was fitted to the Nicolet 510P base plate and adjusted to the desired angle of incidence, typically 45 or 60°. All spectra were obtained with

a 25 × 10 × 3 mm, 45° front face, KRS-5 (TlBr - TlI) prism, which was cleaned with a methanol swab prior to each measurement. The prism was fitted to the unit and before each set of measurements the mirrors were aligned to obtain the maximum intensity throughput.

The reacted, dried film samples to be analysed were cut into two 25 × 10 mm pieces. These were placed on either side of the KRS-5 prism with the top, reacted, face in contact (see section 2.7). To ensure good contact between the prism and the film surface samples were tightly clamped, taking care to avoid distortion of the soft KRS-5 crystal. Spectra were recorded at a resolution of $4cm^{-1}$ and obtained as the average of 150 scans using the crystal in air as a background.

b) Diffuse Reflectance (DRIFTS): The optical unit used for all measurements was "The Selector" Specac diffuse reflectance fourier transform accessory P/N 19900 series. The unit was fitted to the 510P baseplate and aligned for maximum energy throughput using ground KBr as the background sample.

A sample of the dried reacted polymer powder was mixed with previously ground KBr in the ratio 30% $^{w}/_{w}$. The sample mixtures were then used to fill a 11 mm diameter sample 'cup' which was subsequently levelled-off using a clean spatula. Spectra were recorded at a resolution of 4 cm^{-1}, for 500 scans using ground potassium bromide as the background.

c) Transmission: These spectra were recorded on either solution-cast thin films of the polymer samples or as potassium bromide discs of the polymer powder.

Hot decalin (80°C) was used for solution-casting all polyethylene samples, whilst tetrahydrofuran was used for poly(vinyl chloride) samples.

2.11 Diffuse Reflectance Ultraviolet Analysis of Polymer Powders

All ultra-violet spectral data was obtained using a Perkin Elmer 330 spectrometer fitted with a Hitachi 60mm diameter barium sulphate integrating sphere. Reacted, dried powder samples were placed in a 15 mm quartz-fronted screw-cell and tightly clamped. The cell was then fitted to the sphere and spectrum recorded over the range 190 - 860nm. All measurements were made using a previously collected reference of the pure untreated polymer.

2.12 Contact Angle Measurement

The equipment used for contact angle measurement was home-built and is shown schematically in figure 2.2

Reacted polyethylene film samples (see section) were gently wiped with a methanol swab and allowed to dry in air. The air dried films were then fixed to a horizontally level, heavy, stainless steel table using double sided sticky tape. The table was contained within a perspex box as shown in figure 2.3 and the whole unit was supported by a stone table. The inside of the box was maintained at relatively

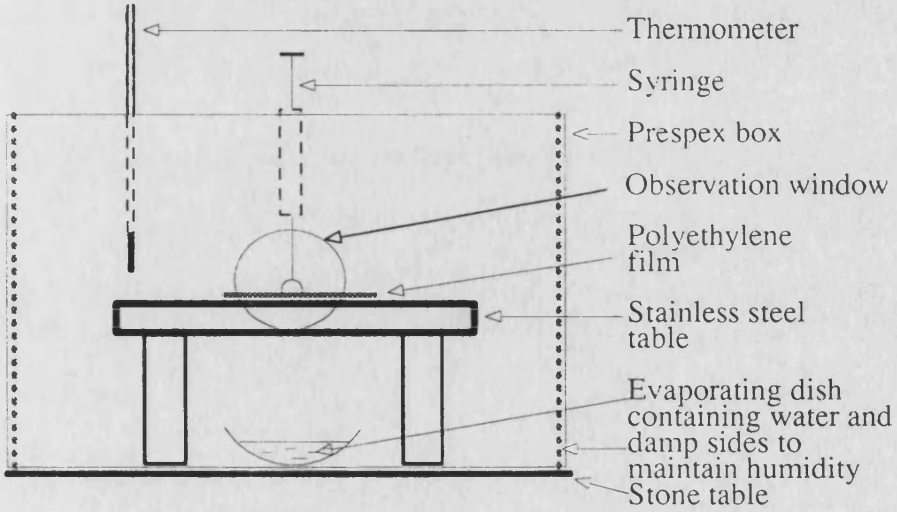

Figure 2.3 Apparatus for contact angle measurement

high humidity by using an open water vessel and moist material layers fixed to the

sides of the box. The enclosed system was allowed to equilibrate for fifteen minutes before measurement of each film sample.

The measurement technique employed was the observation of a sessile drop (see section 1). Water droplets were introduced onto the film surfaces via a 100 µl syringe needle inserted through the top of the perspex box. Droplets were observed, through an opening in the front of the box, using a travelling microscope fitted with a goniometer eye-piece. The newly formed drops were allowed to equilibrate for 30 seconds before being measured. Contact angle values were recorded using 10 ± 0.1 µl drops of pure water (see procedure in section 2.12.1 below). All measurements were recorded at 21 ± 1.5°C and values were determined from at least 10 drops at different positions across the surface.

2.12.1 Purification of Water for Contact Angle Measurement

Water was doubly distilled and then purified by passing through a Purite Standard Stillplus^{TM} clean up system. The system is comprised of a 0.2 µm bacterial filter, activated carbon cartridge and a mixed bed ion exchange column. The eluted water has a high purity and a pH of ≈6.

2.13 Analysis of Polymer Samples by Microscopic Methods

Microscopic analysis has been carried out in order to determine the effects of sonication on the surface morphology of polymer samples. Both optical and scanning electron microscopes have been used, the latter fitted with an x-ray analyser was also used to follow changes in elemental composition during some reactions.

2.13.1 Analysis of Polymer Samples by Scanning Electron Microscopy(SEM) and Energy Dispersive x-ray Analysis(EDX)

All electron microscopic analysis was performed on dried polymer samples using either a Jeol T330 or 35C scanning electron microscope.

Films: Typically 10 × 5 mm sections were cut from the reacted film samples using a scalpel. These sections were then attached, reacted face uppermost, to aluminium supports using colloidal graphite. The graphite was allowed to dry in air after which time the samples were coated with a conductive layer. All SEM imaging samples were coated with gold prior to analysis using an Edwards S150B sputter coater.

To avoid peak overlap during X-ray analysis however, some samples were coated with carbon using an Edwards E306 coater.

Powdered samples were also fixed to aluminium dishes using colloidal graphite and after drying, the dishes were inverted to remove the loose unattached particles. All samples were then coated as outlined above.

Energy dispersion x-ray data was obtained by using a link AN 10000 x-ray analyser coupled to the Jeol 35C scanning electron microscope.

2.13.2 Analysis of Polymer Samples by Optical Microscopy

Reflectance measurements were made on dried polymer powder samples only, owing to the low resolution which can be achieved with this technique (see section 1.3.3).

All optical microscopy was carried out using a Zeiss Stemi SV11 microscope. Samples were dispersed onto clean glass microscope slides using a spatula and observed directly. The magnification achieved was typically less than 66 times. Photographs were obtained with a 35 mm camera coupled to the microscope.

CHAPTER 3

THE PHYSICAL EFFECTS OF ULTRASOUND ON POLYMER PARTICLES AND SURFACES

It is inevitable that chemical modification of any polymer surface will promote, to some degree, structural reorganisation in the outermost regions of that surface. The extent of this transformation will be dependent upon the nature of the functionalising species, its penetration depth into the bulk polymer, both the reaction and storage conditions as well as the technique employed to bring about the modification.

In the present work, high power ultrasound has been investigated as a technique for introducing chemical functionality onto polymeric surfaces. In particular, studies were intended to assess the applicability of this method to the modification of moulded polyethylene and poly(vinyl chloride) electrical cables.

Owing to the origin and nature of the ultrasonic cavitation process, it was of great importance to establish not only the chemical, but also the physical, influence of this technique on the surface morphology of these polymers. Accordingly, a series of investigations concerning the effects of sonication on the size distribution and surface morphology of polymer particles suspended in aqueous media was carried out. Also, a survey of the effects of microstreaming-induced erosion on extended polyethylene film surfaces has been undertaken.

Many of the factors which influence bubble collapse and 'hot-spot' formation in homogeneous sonochemistry have a less pronounced effect in heterogeneous systems as outlined in chapter 1. The magnitude of heterogeneous sonochemical effects will, however, be influenced by the starting particle size, concentration, density, Tg(for polymers), ultrasonic intensity and irradiation time.

3.1 Polyethylene Powder

In the present study, the effects of ultrasonic irradiation time and concentration of polymer particles on the particle size distribution and limiting size have been investigated for low density polyethylene. All sonications were performed at an ultrasonic intensity of 26.2 Wcm^{-2} according to the procedure in

section 2.5

Figure 3.1 shows the change in mean particle size as function of sonication time for a $3\%^{w}/_{v}$ suspension of polyethylene particles. From this graph it can be clearly seen that the mean particle size decreases very rapidly during the initial stages of sonication. This decrease, however, rapidly approaches an asymptotic value (after approximately 60 minutes) and extended irradiation appears to have little or no further effect on that value. Greater information concerning the fragmentation process can be obtained from the distribution plots of percentage of particles versus particle size shown in figure 3.2. These data not only indicate the reduction in mean particle size, but also show that the size distribution narrows quite markedly with sonication time. Examination shows that this narrowing process arises primarily through loss of the larger particles, since the tailing off at this end of the curves becomes much sharper. Conversely, only a small increase in the percentage of particles below about 10 μm is apparent. This would suggest that either particle fragmentation occurs cleanly with no very small material being generated, or more probably that the very small particles undergo agglomeration. The agglomeration of very small particles has also been reported by Suslick *et al.*[179-81] during their studies of the fragmentation of metal powders in an ultrasonic field. In their work it was found that ultrasonically generated shock waves produced not only fragmentation of large particles, but also fusing of much smaller particles (<~10 μm). By using a number of different metals they were able to estimate that the maximum temperatures produced were between 2600 and 3400°C with collision velocities of between 100 and 500ms^{-1} for particles of ~10 μm in size. Whilst it is difficult to quantify the temperatures generated during collision between polymer particles, due to their being more readily deformed, the values must be significantly less than those reported by Suslick and co workers,[179-81] since at such temperatures polymer particles would become charred and carbonised. As no apparent degradation or char formation was observed during any of these studies, it would seem that the temperatures generated here must be only a few hundred degrees at

most. Accordingly, it can be argued that the density of the fragmenting particles will be responsible for the velocity of collisions and hence, the temperatures and pressures generated. Thus, the density would in turn be expected to greatly influence the final limiting particle size.

In the present work it is expected that the observed size reduction in polyethylene particles is also brought about by shock wave induced collisions and subsequent liquid turbulence. Measurements of laser induced cavitation in water have shown that shock wave pressures as high as 300 MPa may be produced. The resulting inter-particulate collisions must then deform the solid particles to such an extent that structural instability occurs with the resultant break up of the particles. It is unlikely that direct fragmentation via a shattering type process is responsible in view of the low Tg (-119°C) of the polyethylene sample used. Furthermore, that ultrasonically induced microstreaming cannot be the major cause is suggested by consideration of the size of a collapsing cavitation bubble in water. Calculations show the diameter of such bubbles to be of the order of 160 μm at 20 kHz,[157] therefore too large to promote direct fragmentation by a microstreaming mechanism.

On the basis of this evidence it follows that a reduction in the mean free path between colliding particles should result in fewer collisions having sufficient energy to induce deformation and hence, particle fragmentation. Accordingly, by increasing the concentration of suspended particulate matter an increase in the limiting particle size would be expected. Figure 3.3 shows a plot of the final mean particle size as a function of polymer powder concentration for samples sonicated for 5 hours. Clearly, the results shown in this plot support our suggested fragmentation mechanism. Figure 3.4 shows the distribution of particle sizes for each of the polymer loadings. From this data it is apparent that at higher concentrations more large particles remain. However, the percentage of particles smaller than 10 μm appears to be constant below a 5% $^{w}/_{v}$ loading. This would suggest that for low density polyethylene powder a loading of less than 4%$^{w}/_{v}$ is necessary to achieve a limiting particle size having a narrow distribution of sizes.

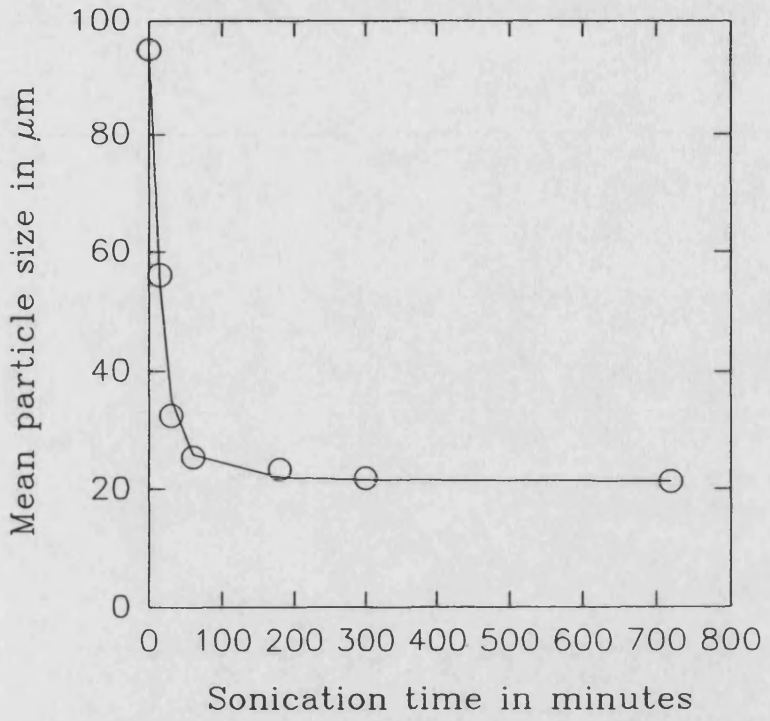

Figure 3.1 Showing the change in mean particle size as a function of sonication time for low density polyethylene powder.

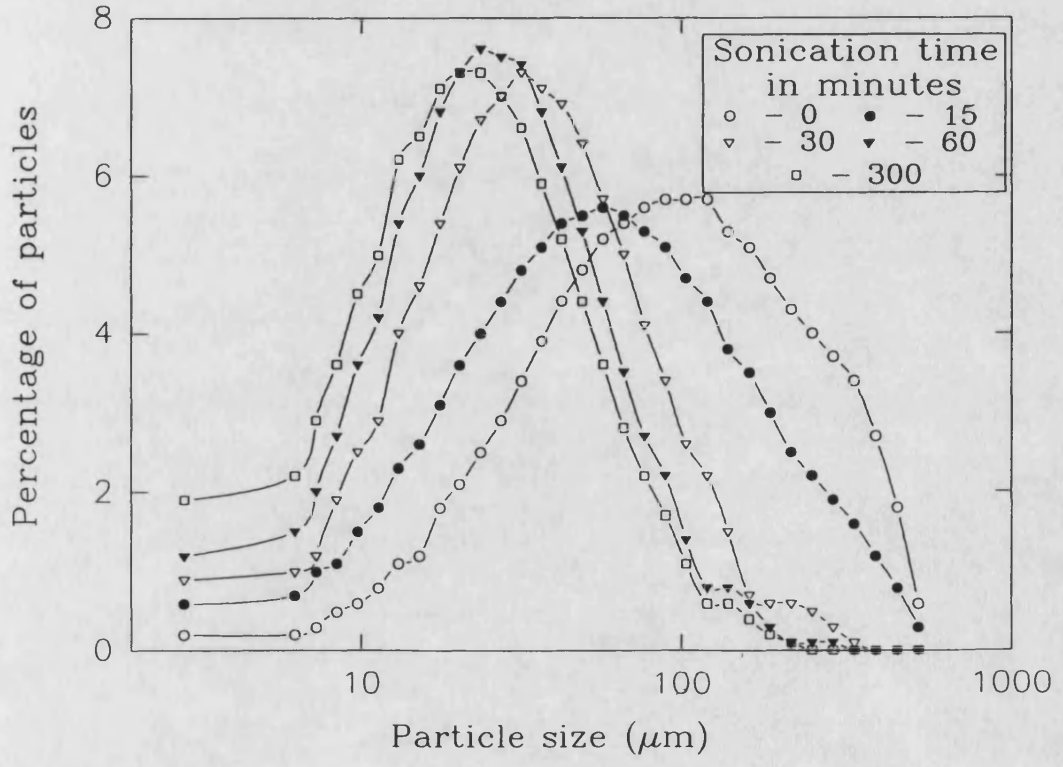

Figure 3.2 The distribution of particles versus the log particle size for polyethylene powder samples at varying sonication times.

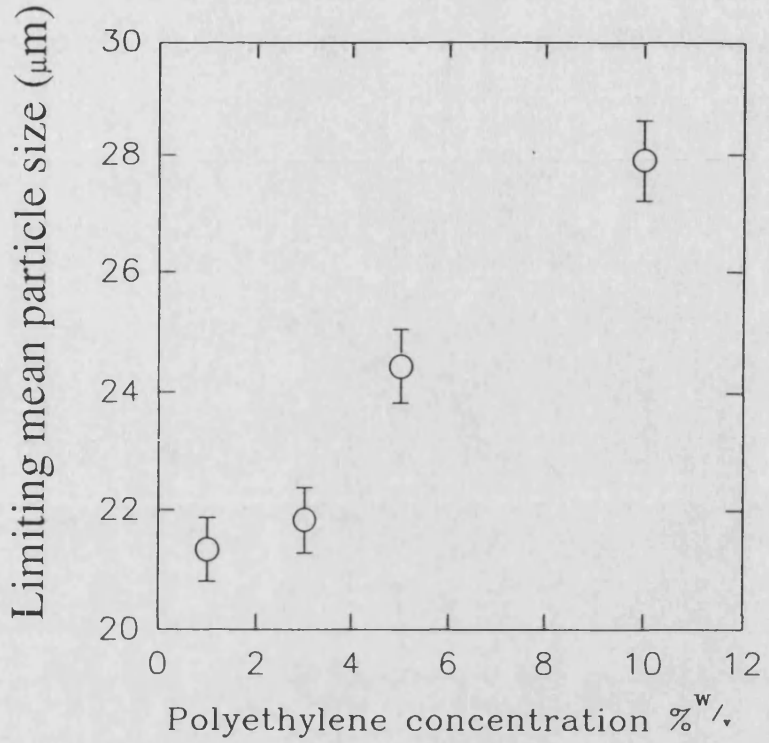

Figure 3.3 The change in final mean particle size as a function of polyethylene powder concentration.

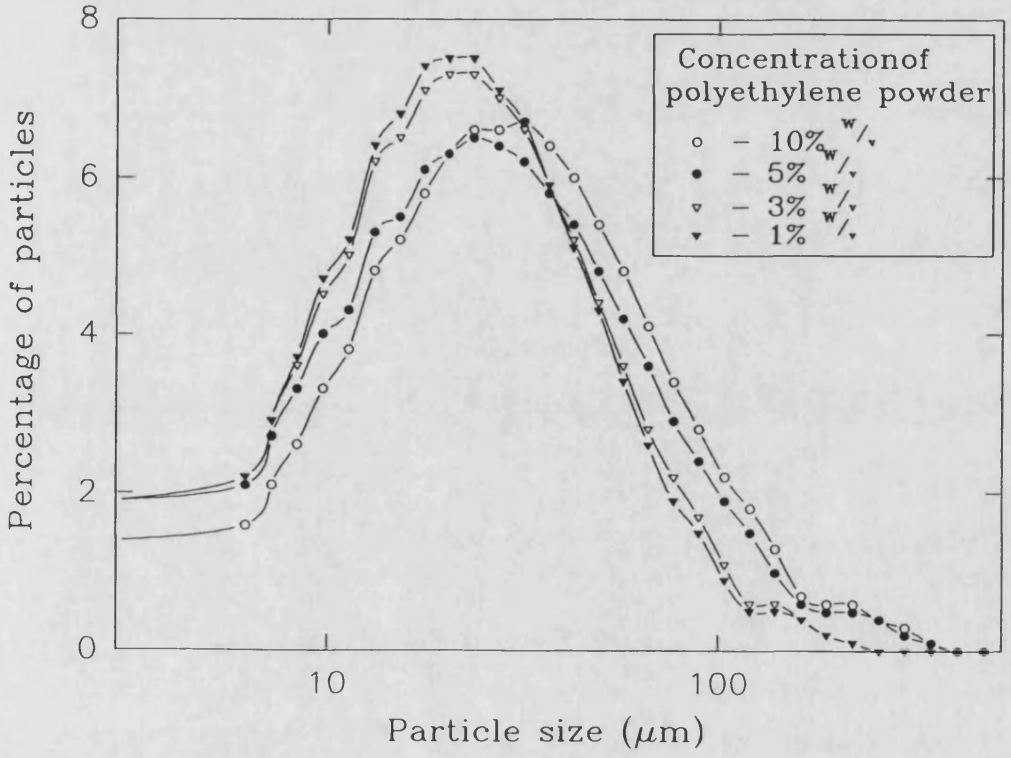

Figure 3.4 The distribution of particles versus the log particle size for varying concentrations of polyethylene powder.

3.2 Other Polymer Powders

In order to determine the contribution microstreaming may have on polymer particle fragmentation and surface erosion, polymer samples having greatly different sizes were a prerequisite. Particles with a size of much greater than 160μm were necessary for effective interaction with the imploding cavitation bubbles.[157] For comparison, however these samples needed an identical history (same Mwt, same Tg, same methods of manufacture etc). In the present work suitable samples of PMMA and polypropylene were available for use. To complete this set of investigations a sample of the PVC powder, used in sonochemical modification reactions, having a mean particle size of ~160μm was also used. The results of these experiments are given in table 3.1.

All of these sonications experiments were performed for five hours at 26.2 Wcm^{-2} using a 5 % $^{w}/_{v}$ loading of polymer particles as outlined in section 2.5. Whilst the precision of these mean values is uncertain, changes of ±5% can be considered significant although a more informative comparison of samples is obtained from their respective size distribution curves.

Table 3.1

POLYMER	PARTICLE SIZE		Size Decrease /%
	Initial	Final	
PMMA	450.1	455.0	-1.1
PMMA	49.7	54.7	+10.1
Polypropylene	381.0	291.4	+23.5
Polypropylene	159.3	139.6	+12.7
PVC	164.8	177.2	-7.0

3.2.1 Poly(methyl methacrylate)

Clearly, the larger PMMA sample showed no significant change in the mean particle size after the 5 hour sonication period. Analysis of the particle size distribution data presented in figure 3.5 further support the conclusion that ultrasound has little or no effect on the size of these large PMMA particles. Accordingly, this sample was analysed by optical and SEM methods to determine whether or not the microscopic surface morphology also remained unchanged during irradiation. Some SEM results are displayed in figures 3.6a and 3.6b for the unsonicated PMMA and 3.7a 3.7b for the sonicated material. Comparison of the two samples at both 200x and 1000x magnification clearly demonstrates that although the mean particle size remains unchanged the surface character has been significantly roughened and eroded. This effect is seen most strikingly with the optical microscope as shown in figure 3.8. Here both the sonicated and unsonicated material have been photographed together. The optical properties of the two materials are so vastly different that identification of each particle is possible.

The origin of this erosion might on first inspection appear to be the result of surface microstreaming, as evidenced by the size of the structures and the apparent pitting presented. However, examination of the much smaller PMMA samples shown in figures 3.9 and 3.10 indicates that a similar surface roughening has also occurred. These particles are $<<160$ μm and are, therefore, expected to be too small to experience any microstreaming effects. Thus, it must be envisaged that high-velocity collisions between particles results in the fracture and removal of the surface region. This result can perhaps be expected, since a high level of stress fractures will be formed in the outermost regions of the particle surface during manufacture, thus presenting a number of weak points for further fracture and removal of material. A similar type of process has been reported previously by Luche and co workers.[228] In their work the increased catalytic activity of a number of metal powders before and after sonication was studied. They found that the metal

oxide layer, which was apparent on almost all metals, was deformed or fractured and broke away from the underlying metal. In addition, the smaller PMMA sample shows a net size increase during sonication. Examination of the particle size distribution curves shown in figure 3.11 suggests that the origin of this increase is due to particle fusion and agglomeration generated during high speed collisions. Indeed, fused dumbell-type structures can be seen in the SEM images of the sonicated sample as shown in figures 3.12a and 3.12b, but were not apparent in the unsonicated material.

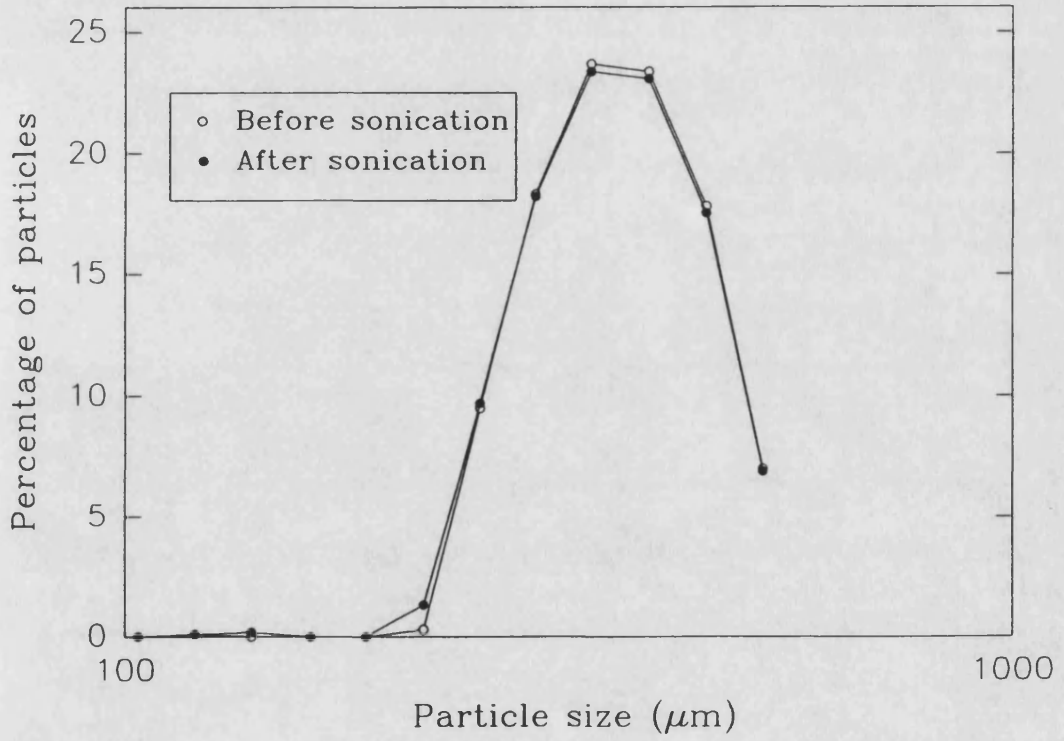

Figure 3.5 The distribution of particles versus log particle size for sonicated • and unsonicated ○ large PMMA particles.

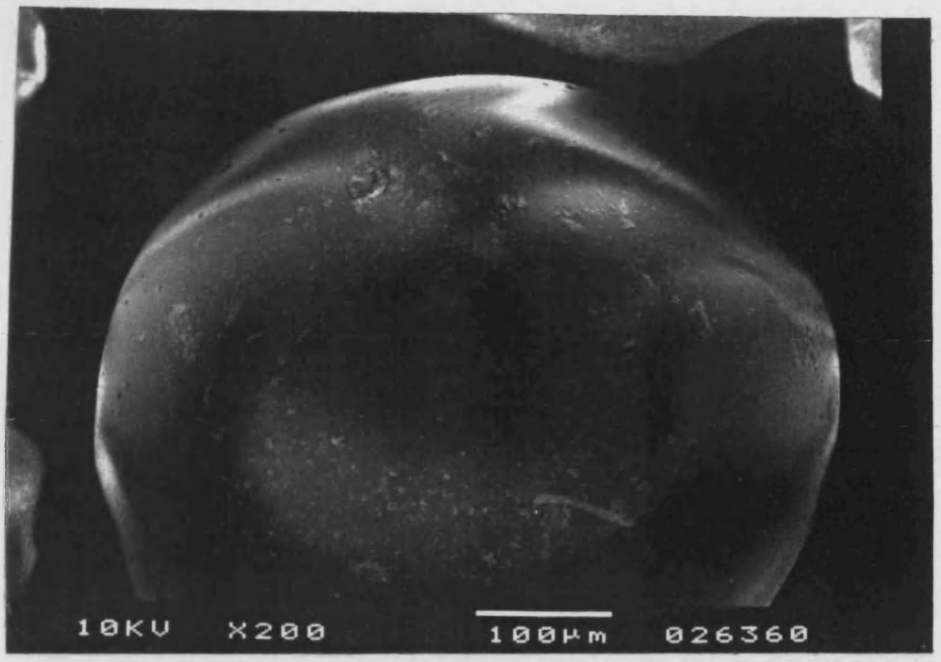

Figure 3.6a SEM image of a large PMMA particle before sonication.

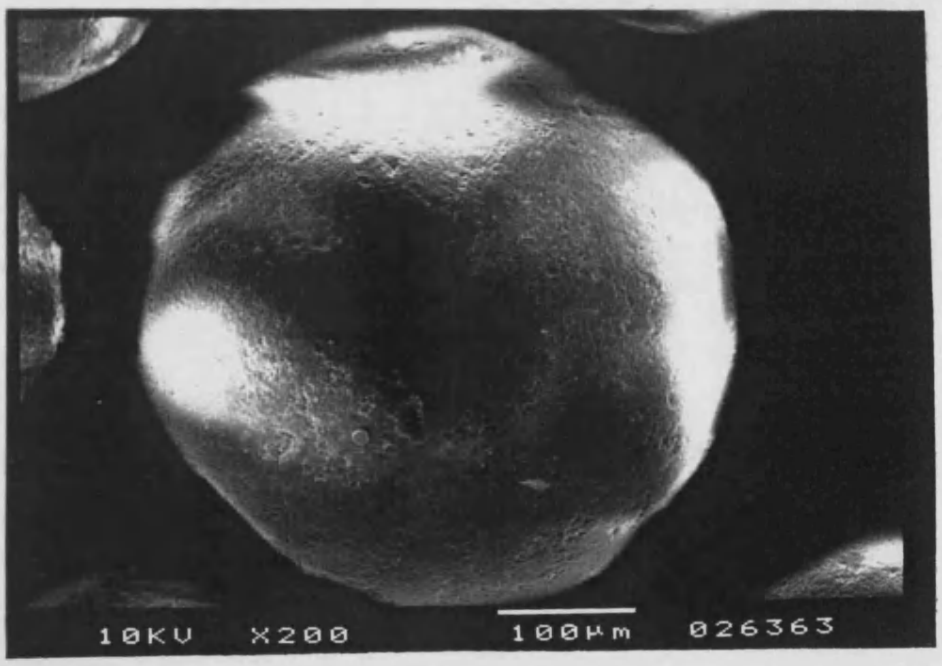

Figure 3.7a SEM image of a large PMMA particle after sonication for five hours.

1 Lighter
-4 Blk.

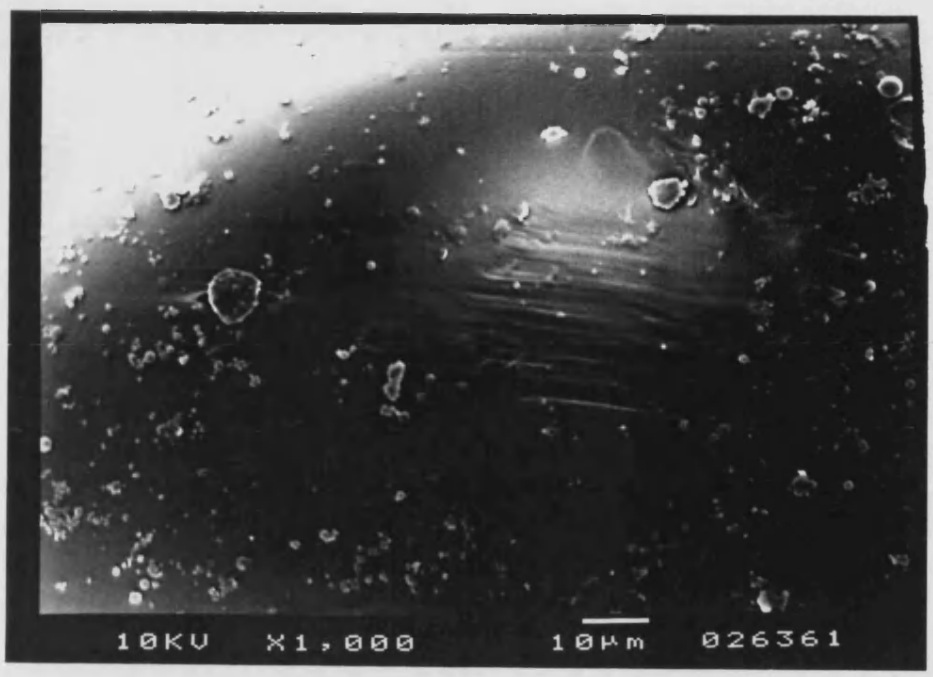

Figure 3.6b SEM image of a large PMMA particle before sonication.

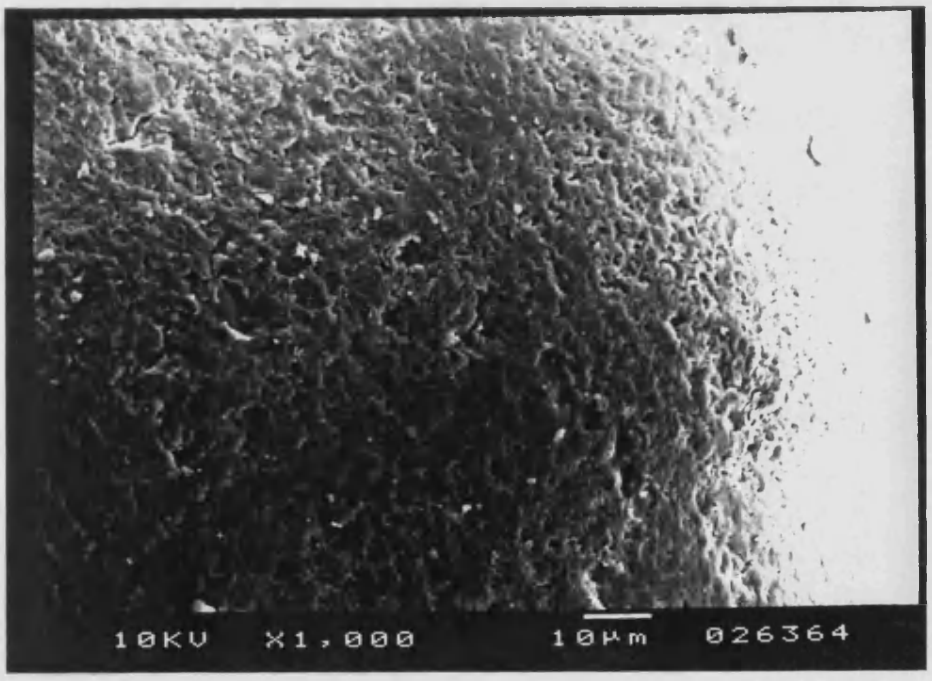

Figure 3.7b SEM image of a large PMMA particle after sonication for five hours.

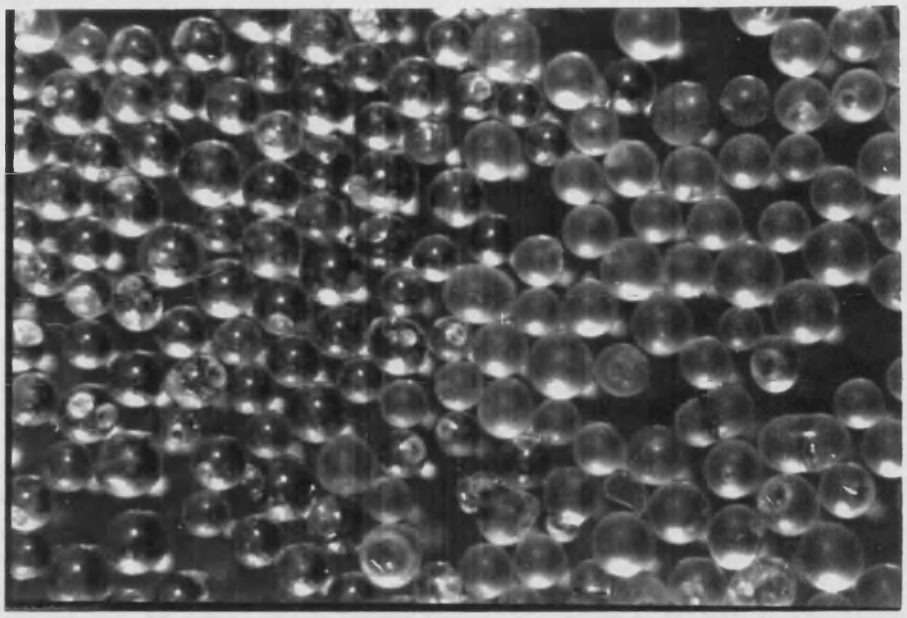

Figure 3.8 Optical microscope image of unsonicated and sonicated large PMMA particles at 32x magnification.

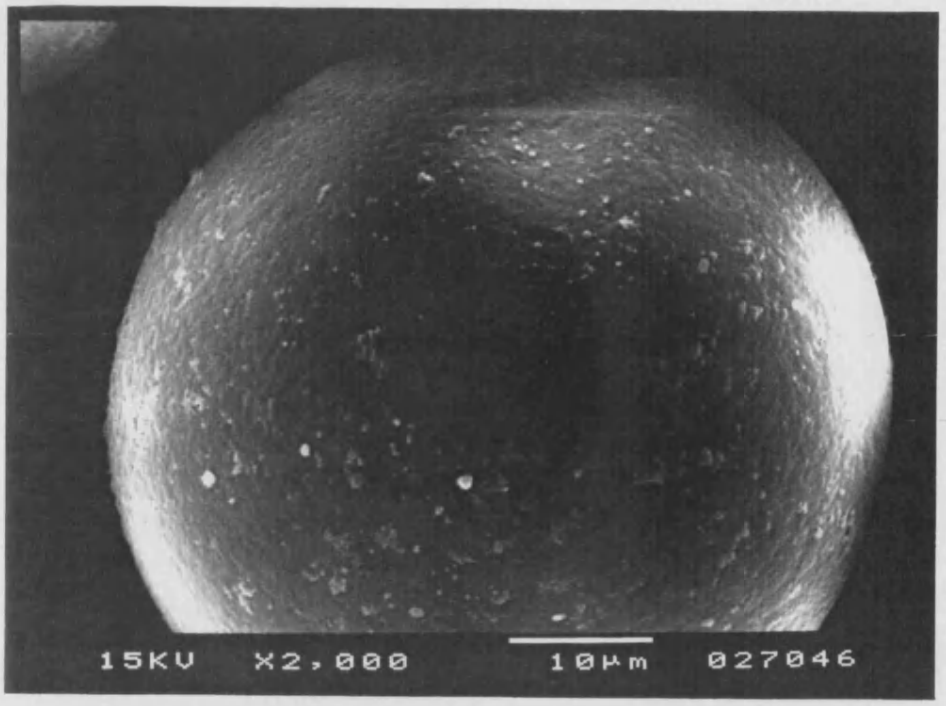

Figure 3.9 SEM image of a small PMMA particle before sonication.

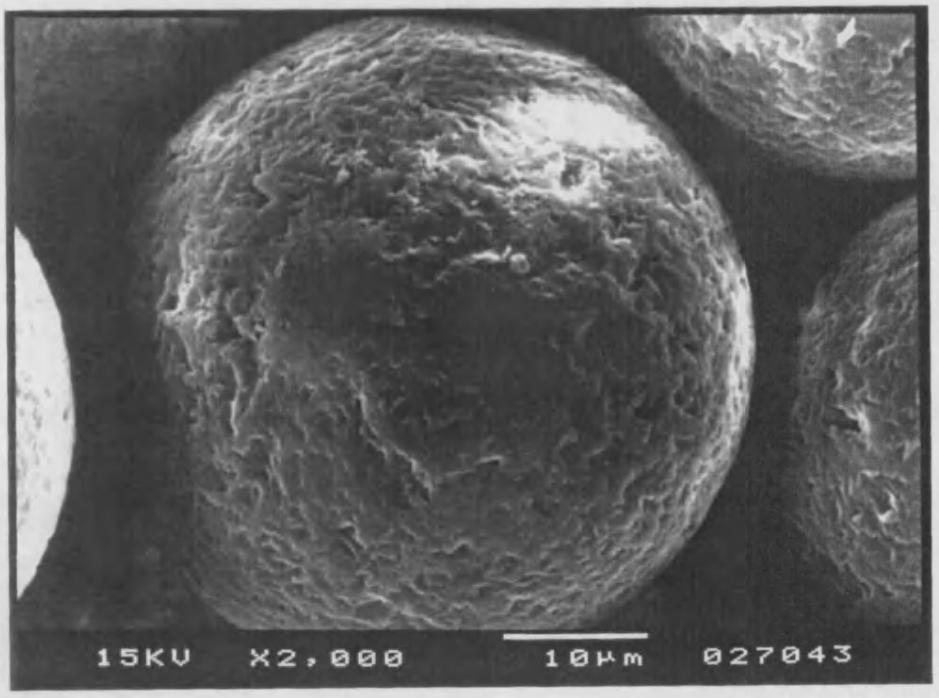

Figure 3.10 SEM image of a small PMMA particle after sonication.

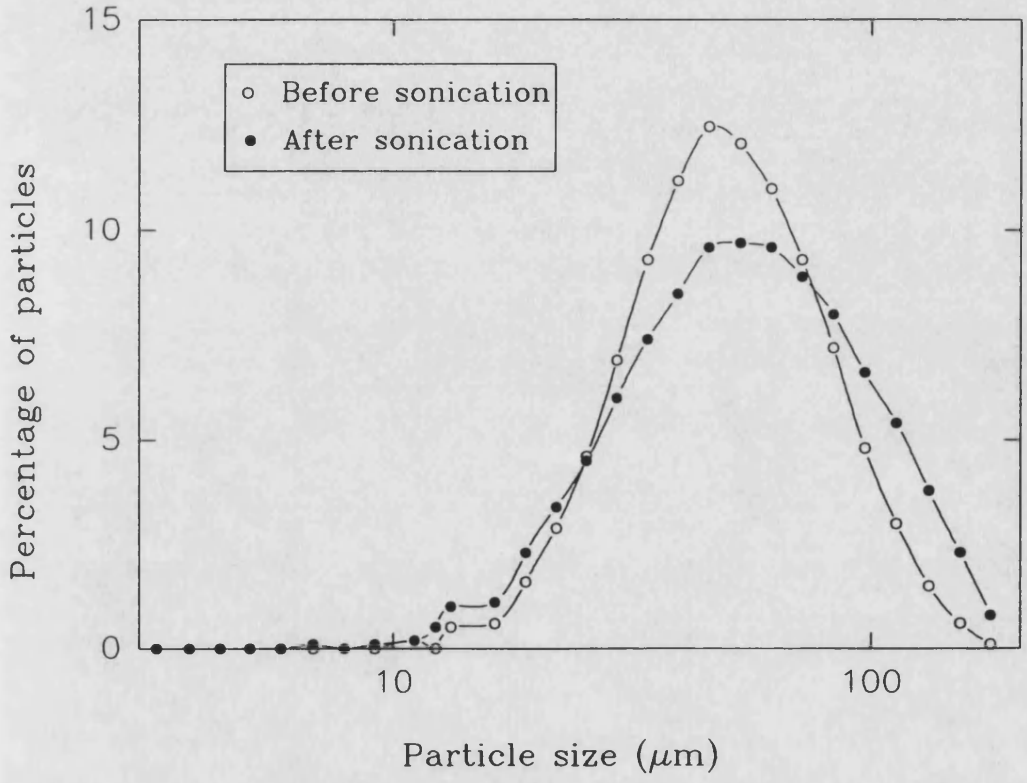

Figure 3.11 The distribution of particles versus log particle size for sonicated • and unsonicated ○ small PMMA particles.

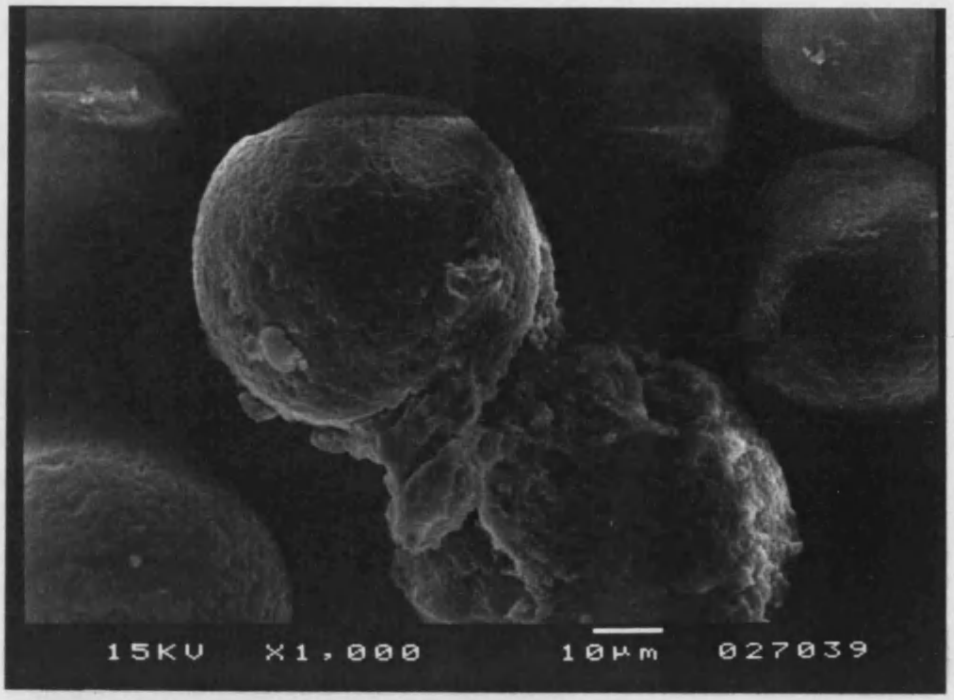

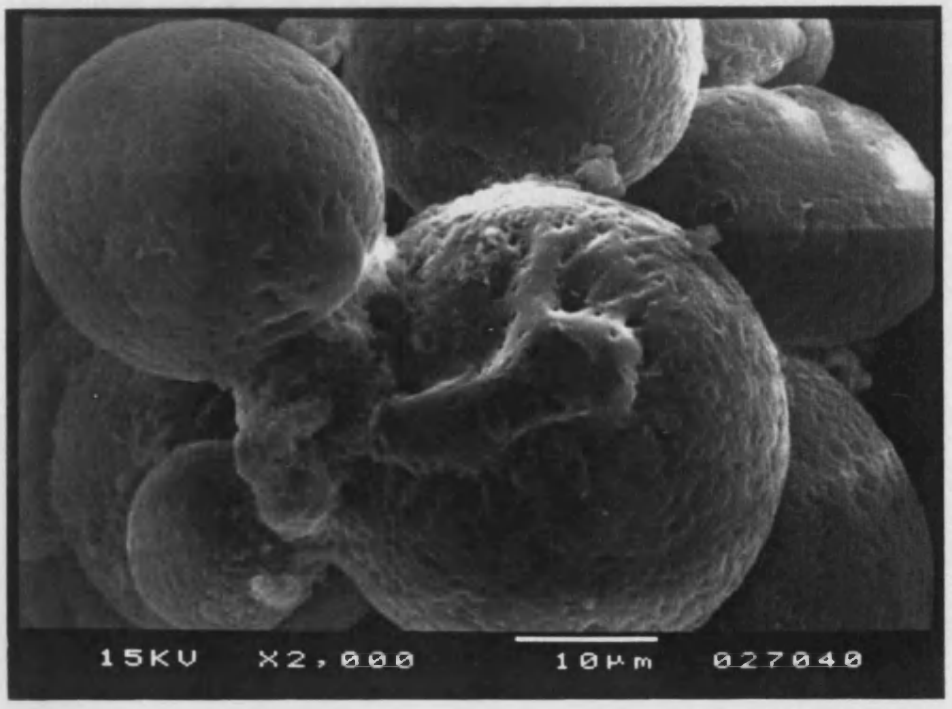

Figure 3.12a and 3.12b SEM images of small PMMA particles after sonication, clearly showing fused particle structures.

3.2.2 Polypropylene

From table 3.1 can be seen that both polypropylene samples undergo fragmentation leading to a reduction in their mean particle sizes. The particle size distribution curves for the smaller and larger samples are presented in figures 3.13 and 3.14 respectively. From these data it is apparent that the sample with the smaller mean starting size has a much broader distribution of particle sizes, which, after sonication, shows only a moderate decrease in the percentage of large particles and a subsequent increase in the percentage of particles below about 90μm. Conversely, the sample with the larger mean starting size has a much narrower distribution of sizes. Analysis of this system affords a more detailed understanding of the effects of ultrasound on this polypropylene sample. Clearly, those particles greater than about 250μm appear to be unstable in the ultrasonic field and are slowly reduced in size.

Optical micrographs of both the large and small polypropylene particles before and after sonication are shown in figures 3.15a, 3.15b, 3.16a and 3.16b respectively. In both cases the sonicated particles show a much smoother, more rounded geometry with the presence of much smaller particles.

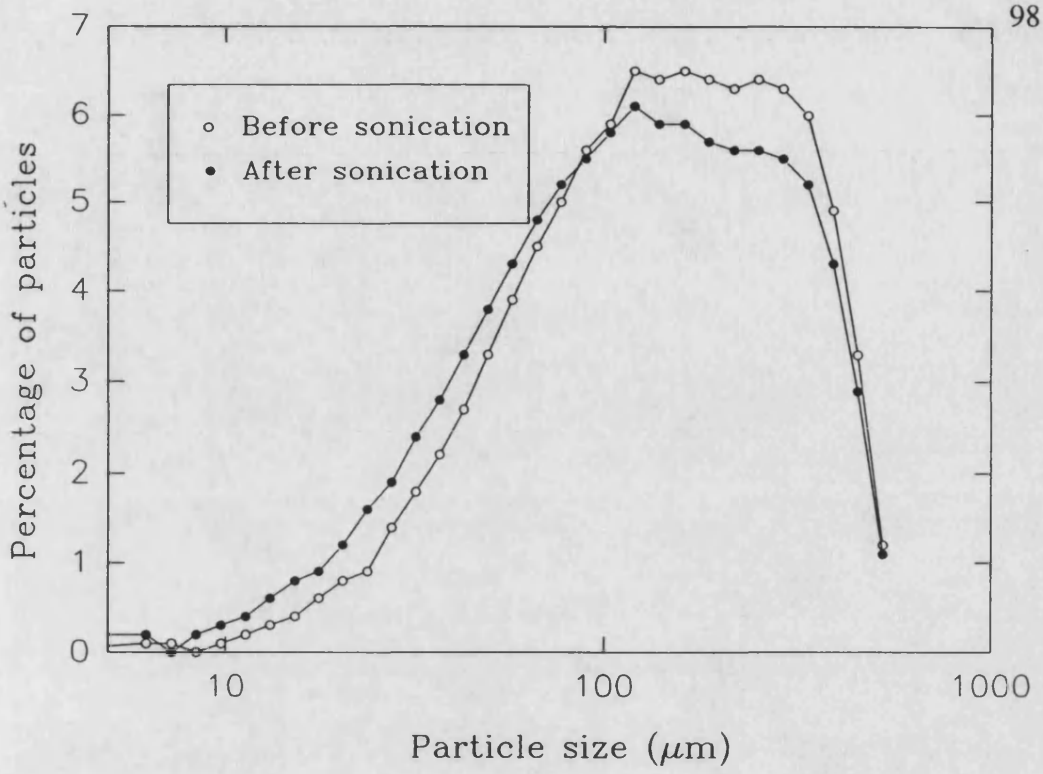

Figure 3.13 The distribution of particles versus log particle size for sonicated • and unsonicated ○ smaller polypropylene particles

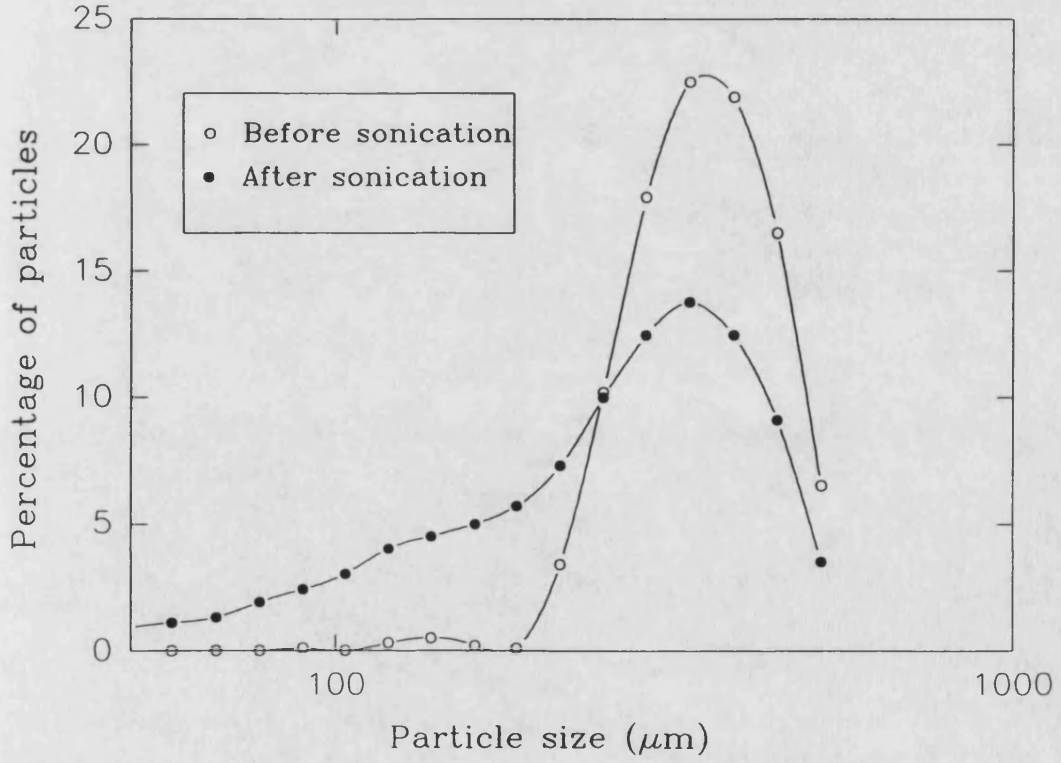

Figure 3.14 The distribution of particles versus log particle size for sonicated • and unsonicated ○ larger polypropylene particles

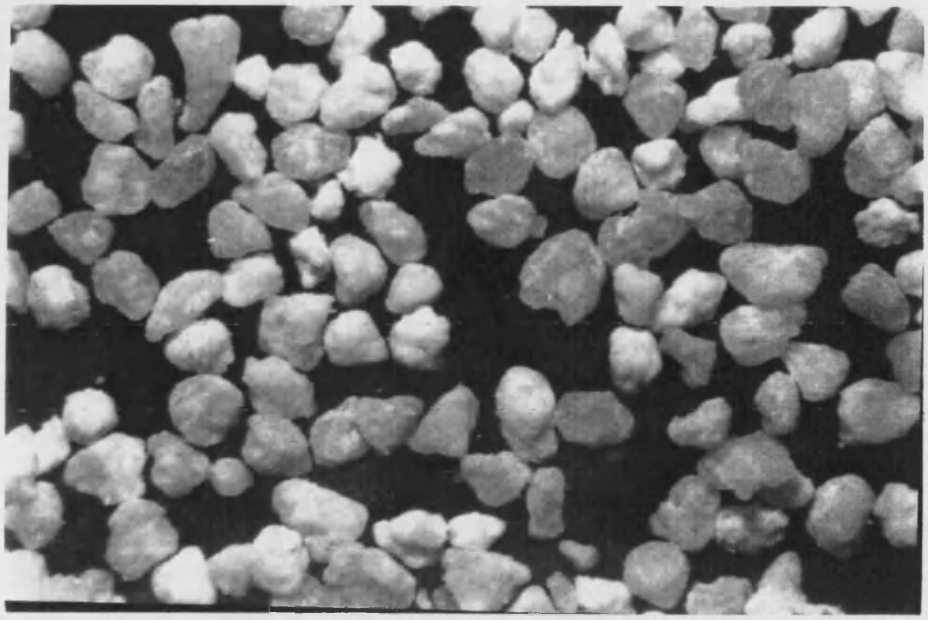

Figure 3.15a Optical microscope image of the larger polypropylene particles before sonication at 25x magnification

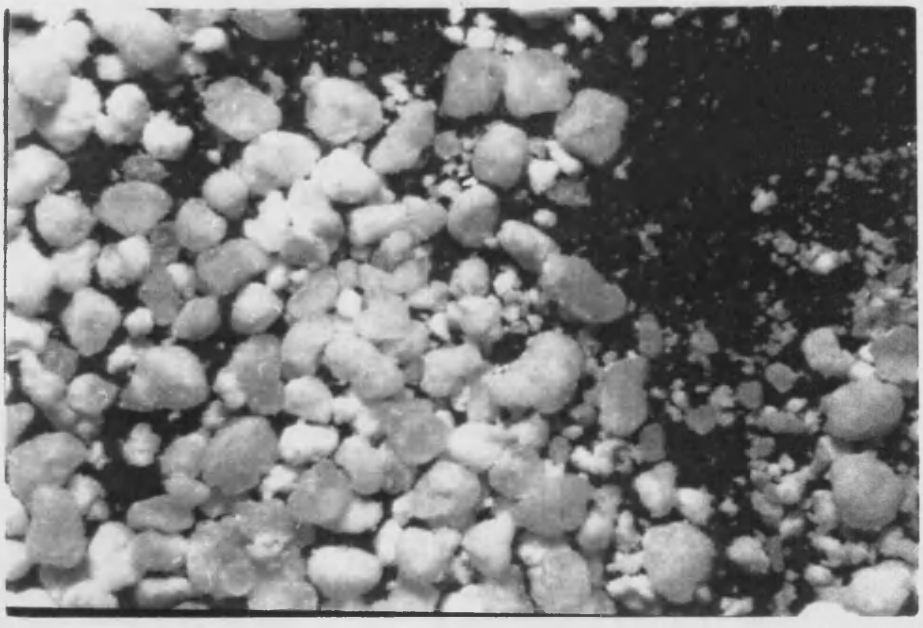

Figure 3.15b Optical microscope image of the larger polypropylene particles after sonication at 25x magnification

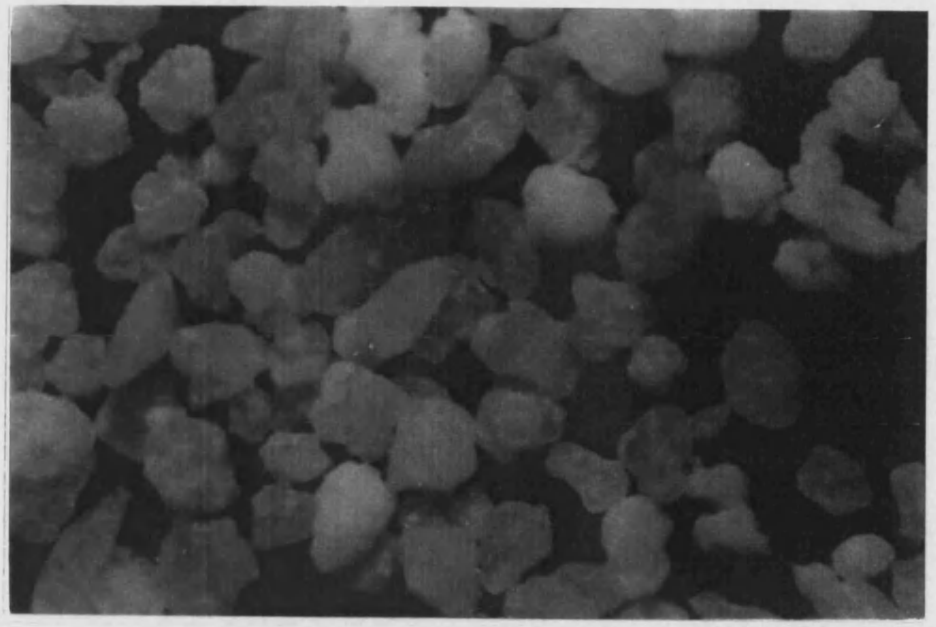

Figure 3.16a Optical microscope image of the smaller polypropylene particles before sonication at 66x magnification

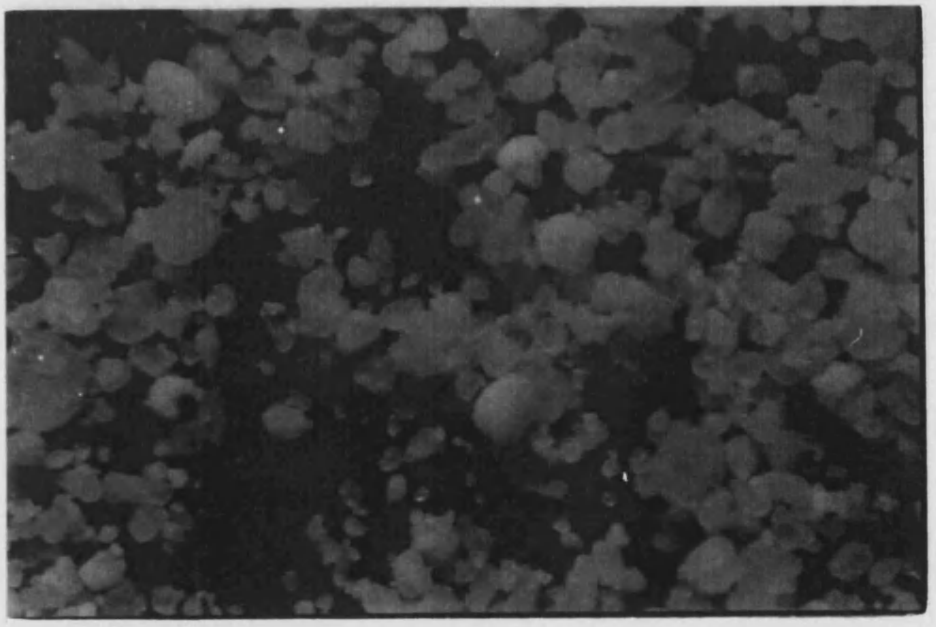

Figure3.16b Optical microscope image of the smaller polypropylene particles after sonication at 66x magnification

3.2.3 Poly(vinyl chloride)

From table 3.1 it can be seen that PVC powder also undergoes a small increase in mean particle size with sonication. The distribution of particle sizes, as shown in figure 3.17, is also shown to broaden implying both material agglomeration and fragmentation. The most lucid information concerning this sample is perhaps obtained from the SEM images displayed in figures 3.18a and 3.18b. Changes in the surface topography, including increased roughening are evident after sonication. The surface structures generated appear to have a lamellar type character and it may be these features which give rise to the increase in mean particle size. Closer examination reveals that agglomeration of very small particles has also taken place. These small particles appear to have become entrapped in rough heterogeneous structures on the surface of larger particles.

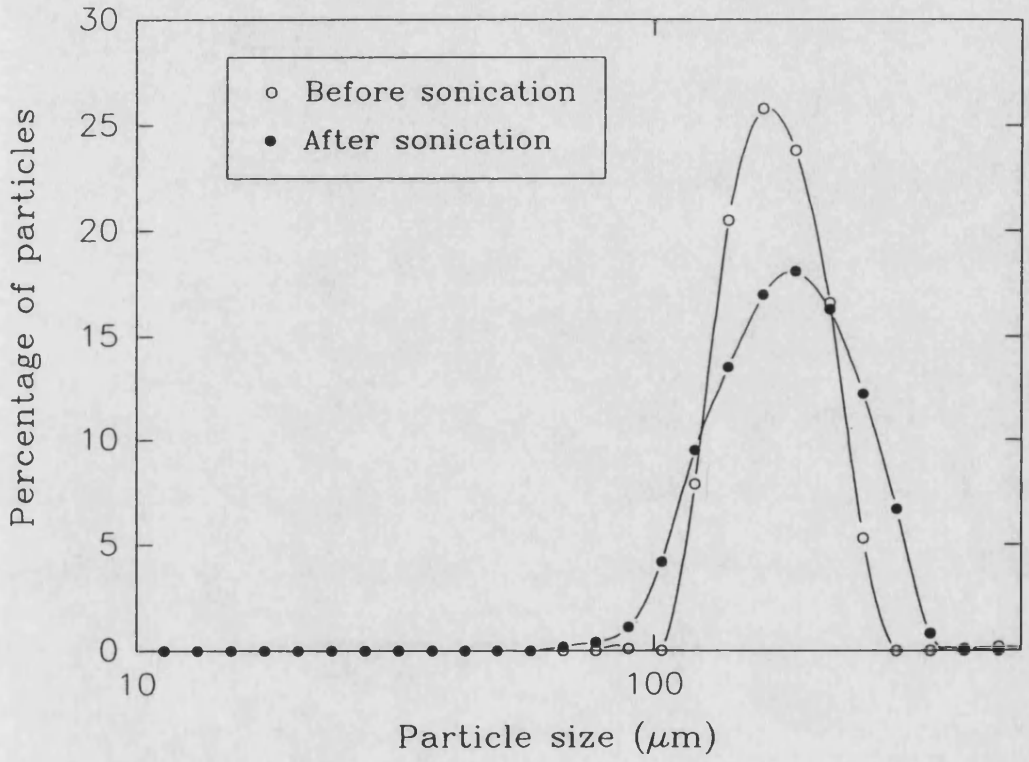

Figure 3.17 The distribution of particles versus log particle size for sonicated • and unsonicated ○ PVC particles.

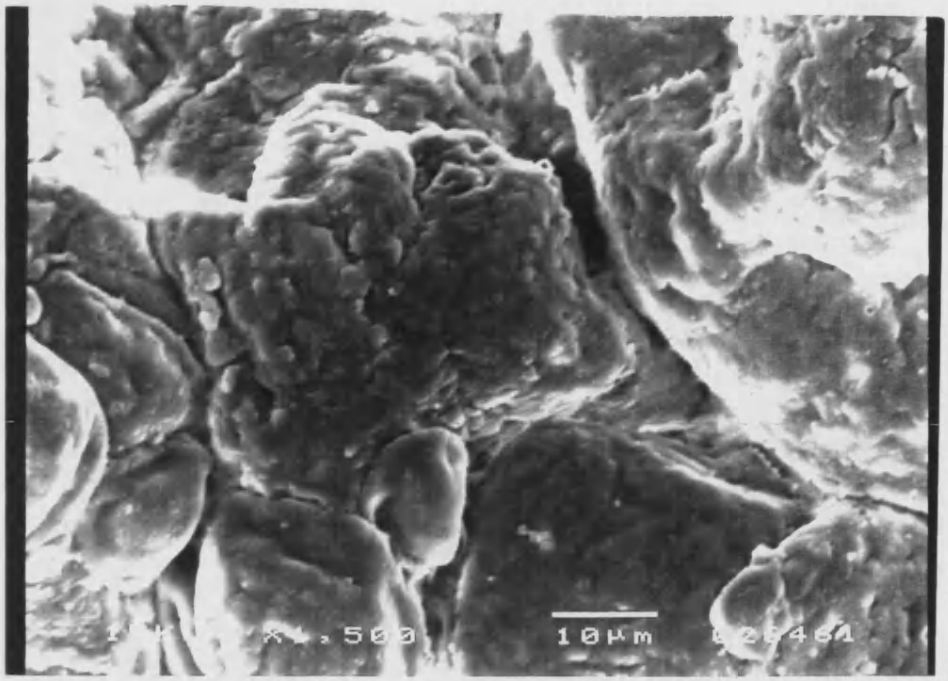

Figure 3.18a SEM image of a PVC particle before sonication.

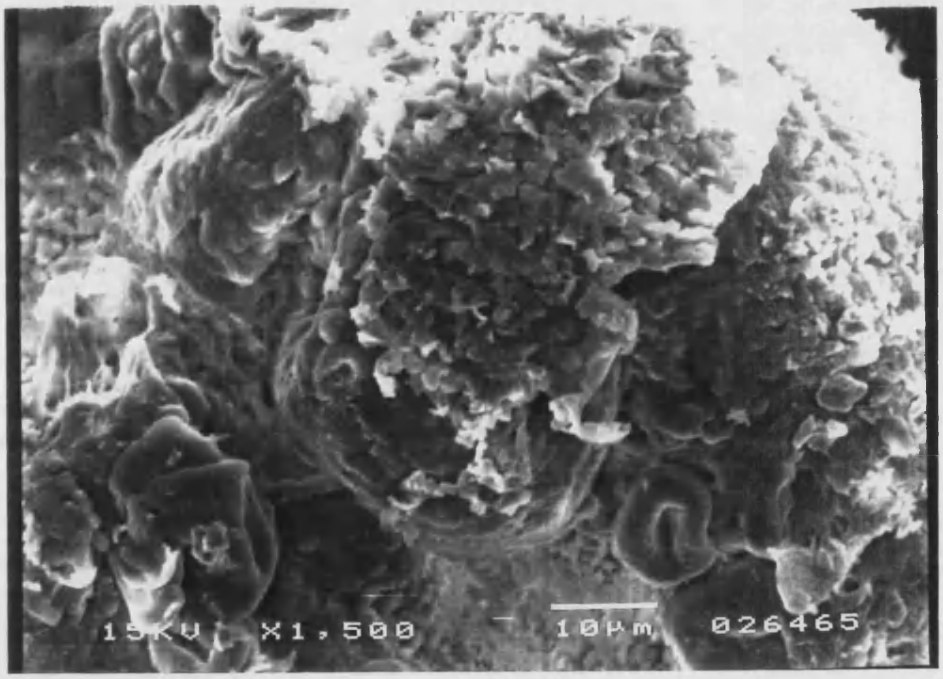

Figure 3.18b SEM image of a PVC particle after sonication.

3.3 Extended Polyethylene Surfaces

From the studies with small polymer particles it was found that the contribution of ultrasonically induced microstreaming on their surface character could not be conclusively established. In the present study the effects of sonication time and distance from the ultrasonic probe tip have been investigated for low density polyethylene melt-pressed films. These samples more closely represent the surface of a "real" electrical cable and should also enable the contribution of microstreaming to be determined.

The surface topography of melt-pressed polyethylene films is rarely smooth on a microscopic level and consequently, may present a number of nucleation sites for cavitation, see section 1.6.1. In this instance, cavitation bubbles would be expected to grow directly on the surface of the films and during collapse generate microjets of liquid which will impinge upon the surface. This process would then give rise to 'pockets' or isolated regions of damage across the surface at point where the heterogeneity was present in the original film.

Figures 3.19a, b and c show typical electron micrographs of the untreated polyethylene film. The surface topography in each instance appears to have a 'grainy' structure. Figures 3.20a, b and c show the surface of the film after a five hour sonication at 26.2Wcm^{-2} in distilled water at distances of 5, 15 and 30mm from the probe tip respectively. Clearly, in each instance, damage to the surface is apparent.

In an attempt to understand this effect in more detail, the survey was extended to include an actual reaction system. For this purpose the sonication of polyethylene films in aqueous potassium persulphate solution at an intensity of 26.2 Wcm^{-2}, as described in detail in chapter 5, was performed at various sonication times. The results from the one, three and twenty-four hour sonications performed in this series are shown in figures 3.21, 3.22 and 3.23 respectively. After sonication for one hour no changes were apparent in the sample when viewed at 1000x

magnification. At much higher magnification(5000x) however, a small amount of surface structure is evident. The three hour sonication as depicted in figure 3.22 clearly shows the presence of surface structure and erosion at both 1000x and 3500x magnification. After extensive sonication for a period of 24 hours only a small increase in the surface roughness is observed over the three hour sample.

3.19a

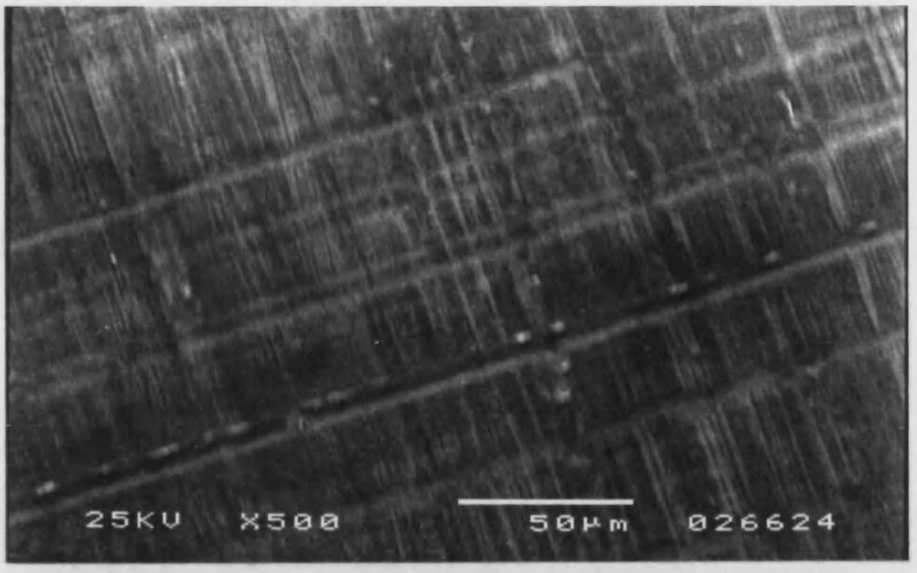

3.19b

3.19c

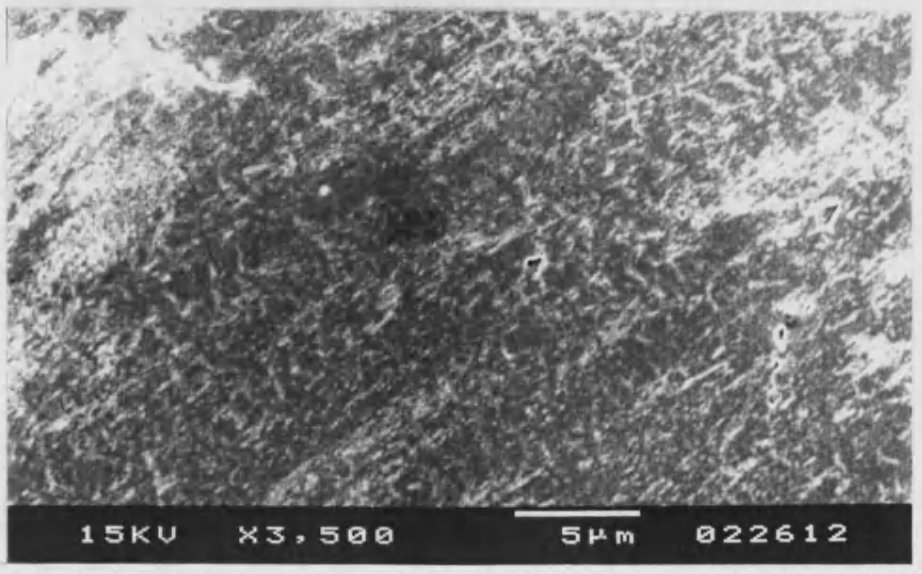

Figure 3.19a, 3.19b and 3.19c SEM images of melt pressed polyethylene films.

1 lighter
-4 BLK.

3.20a

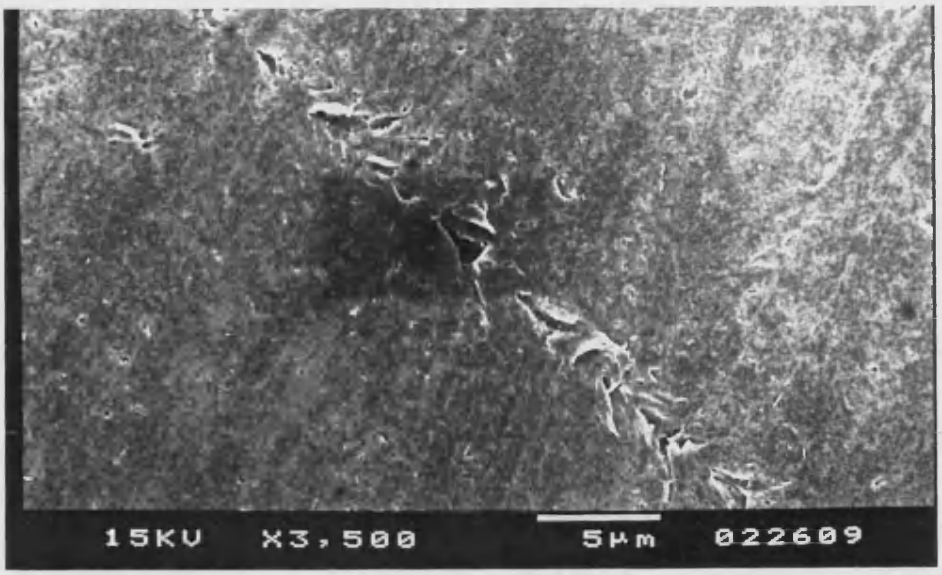

3.20b

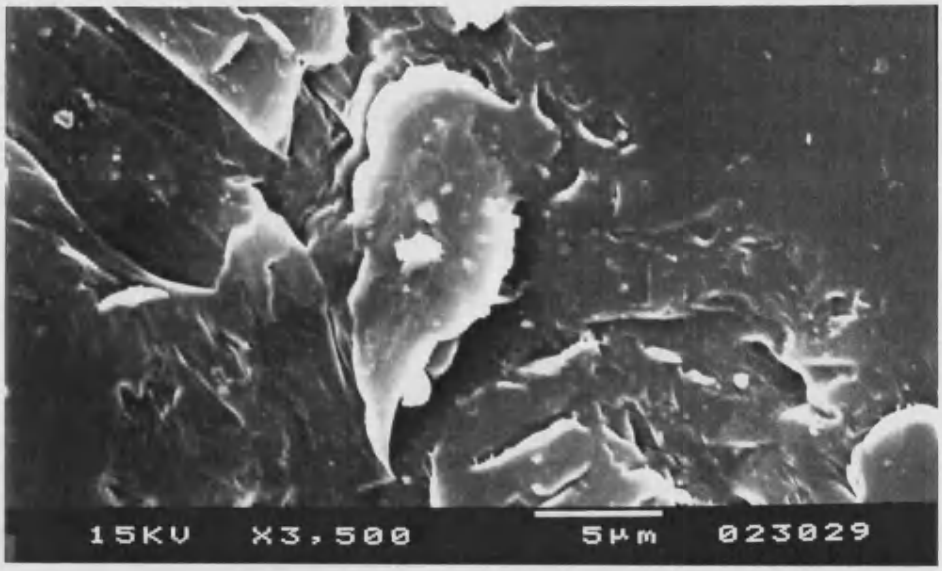

3.20c

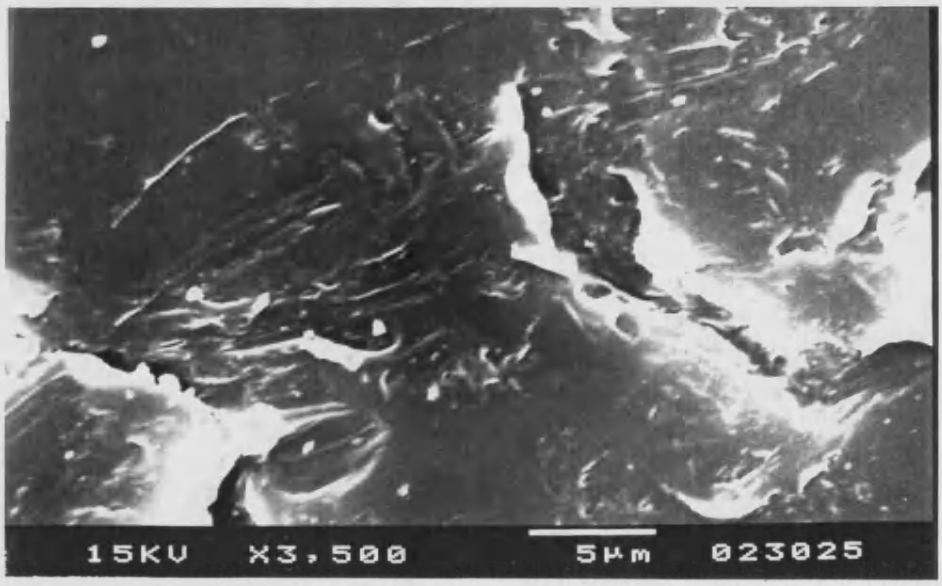

Figure 3.20a, 3.20b and 3.20c SEM images of melt pressed polyethylene films after sonication at a distance of 5, 15 and 30mm from the probe tip respectively.

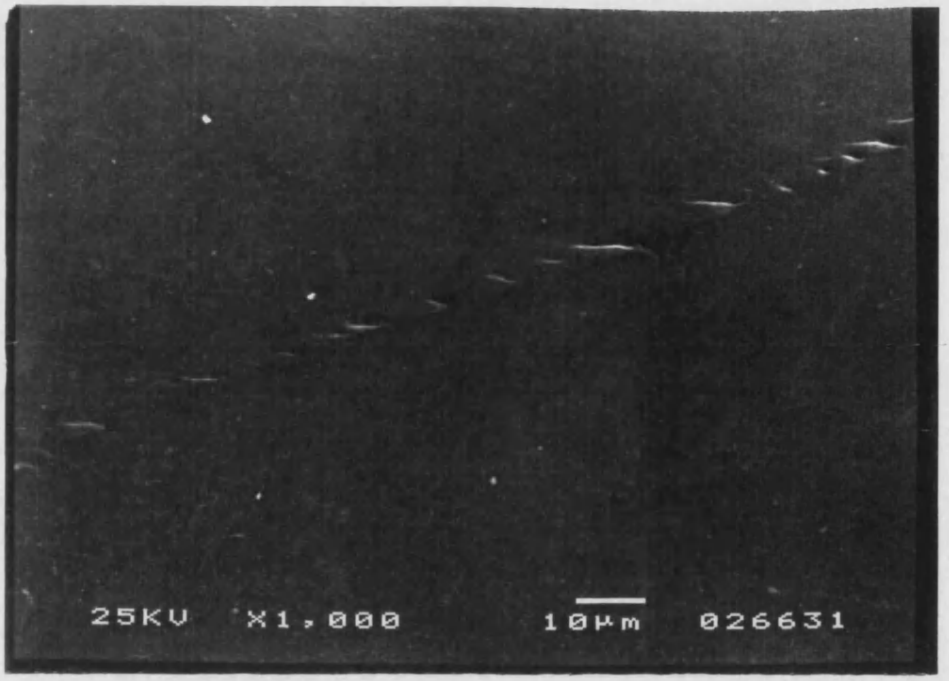

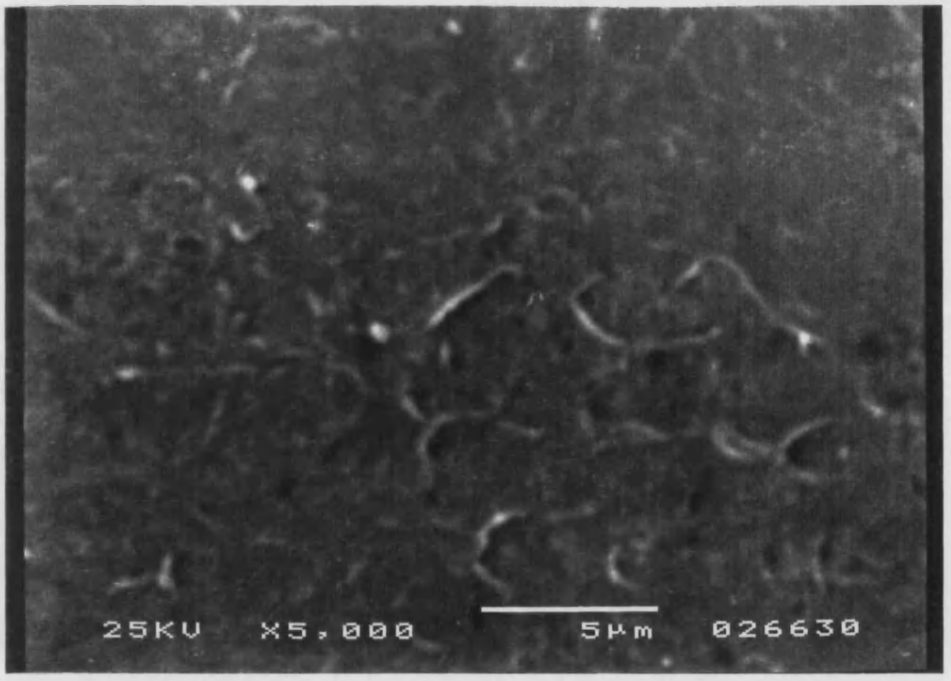

Figure 3.21 SEM images of melt pressed polyethylene films after 1 hours sonication.

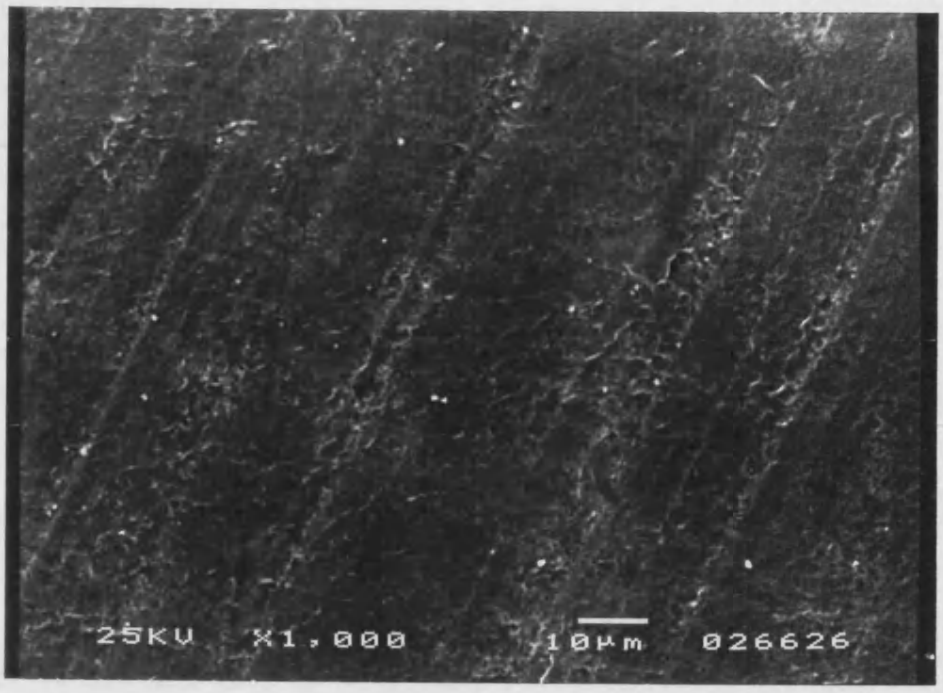

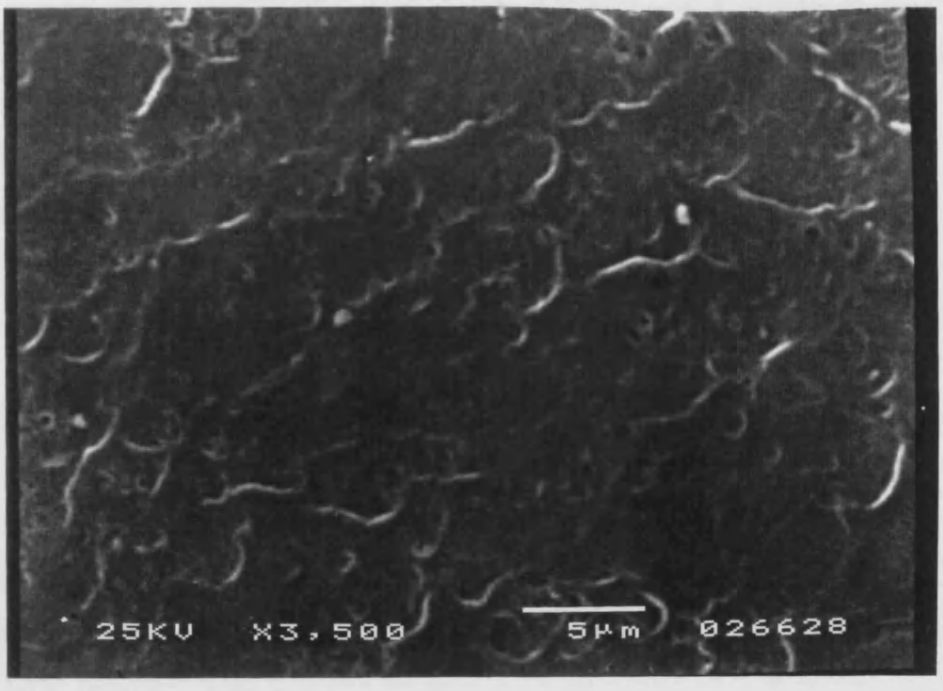

Figure 3.22 SEM images of melt pressed polyethylene films after 3 hours sonication.

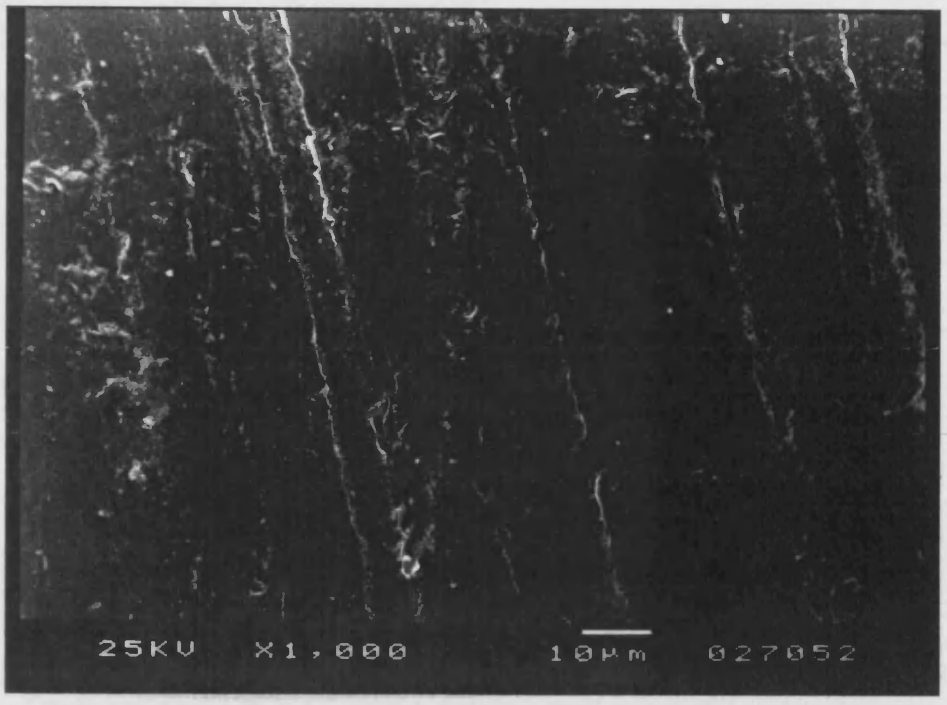

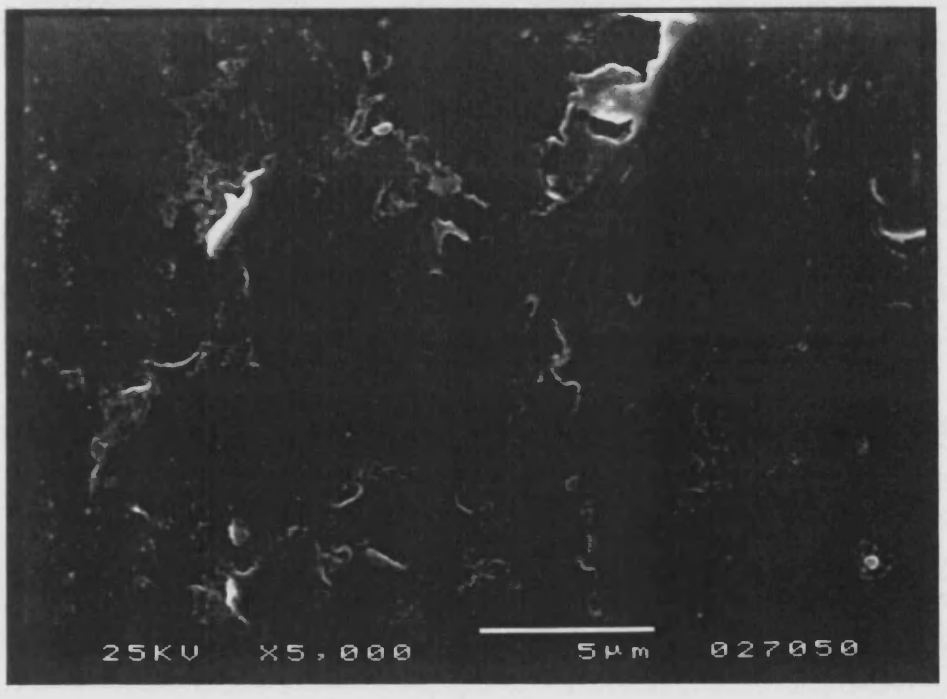

Figure 3.23 SEM images of melt pressed polyethylene films after 24 hours sonication.

From the above observations it can be concluded that the mechanism by which roughening and surface erosion of particles occurs is one in which collapse of the ultrasonic cavitation bubbles generates shock waves which induce high speed particulate collisions. The temperatures and pressures generated during these collisions must be significantly lower than those reported for metals[179-81] and are insufficient to cause charring and thermal degredation of the polymers. The fragmentation process appears to be related to the Rockwell hardness and Izod impact strengths of the polymers as shown in table 3.2. Analysis of the data in tables 3.1 and 3.2 shows that the 'harder' the polymer is, the more difficult it is to fragment. Conversely, the higher the impact strength the more the polymer will be deformed by these collisions, resulting in the formation of unstable structures which are subsequently broken up. The contribution of microstreaming effects, however, remains unclear for the range and size of polymer powders studied.

Table 3.2

Impact strength and hardness of polymers

Polymer	Izod Impact strength Jm^{-1}	Rockwell Hardness
Polyethylene	700	10
Polypropylene	80	100
PVC	43	115
PMMA	27	125

The extent of surface erosion produced by ultrasonic microstreaming, whilst clearly apparent, appears to be much less significant than is generally observed with other 'wet' chemical modification reactions for polyethylene. More significantly, the present levels of surface etching failed to show any significant changes in the optical properties and lustre of these films. This result is clearly important and signifies that modification can be achieved with no apparent change to the finish of moulded polymer structures.

The observation of erosion on these films also signifies the need to exercise

caution when analysing samples for chemical modification by contact angle measurement, see chapter 5 for a more detailed discussion on this subject.

CHAPTER 4

MODIFICATION OF POLY(VINYL CHLORIDE) SURFACES

Before examining the reactions carried out on PVC it is perhaps pertinent to consider the fundamental chemical properties of the vinyl chloride repeat unit. The repeat unit in poly(vinyl chloride) is a relatively simple molecule consisting of only C-H, C-C and C-Cl bonds all of which are covalent, although C-Cl shows a large degree of polarisation. The data for these bonds including average dissociation energies are given in table 4.1 below.

Table 4.1

Average properties of PVC bonds[230]

Bond	Bond length nm	Dipole moment D	Bond dissociation energy kJ/mol
C-C	0.154	0	≈346
C-H	0.109	0.4	≈413
C-Cl	0.177	1.46	≈339

By examination of the vinyl chloride repeat unit it can be seen that PVC will initially react by either a substitution or elimination type process.

In the present study the applicability of ultrasound for use in the modification of PVC surfaces has been investigated and, in view of the growing pressures placed upon the chemical industry to reduce both environmental waste and the use of corrosive chemicals, reactions have mostly been carried out in either distilled water or 2-propanol. And, to enhance the effects of any transformation and increase the ease of product analysis, all preliminary studies were carried out on powder samples with a high surface area.

Finally, as a point of clarity the modification reactions have been divided into either substitution or elimination type transformations. Some features will, however, be common to both and these will be discussed as appropriate.

4.1 Substitution Reactions

There are several mechanisms by which substitution reactions can occur in an organic molecule: the most well known of these being the S_N1 and S_N2 types. For the purpose of polymer reactions it is necessary to consider each mechanism with respect to the segments in the polymer chain. Second order substitution at a carbon centre is hindered by the presence of bulky substituents and accordingly, substitution of chlorine atoms by this mechanism could be expected to proceed more readily at secondary than at tertiary centres. Hence, branch points in the polymer chain will hinder S_N2 type substitution reactions. Conversely, due to the formation of an intermediate carbonium ion, S_N1 type mechanisms will be more favourable at tertiary than secondary centres.

Substitution can also be achieved through a free radical type mechanisms. In this instance, reaction can arise either through homolytic fission of bonds in the polymer or by attack from a radical species. The second of these processes occurs during the chlorination of polyethylene and PVC. Furthermore, in view of the report by Luche,[166] that ultrasound will favour radical pathways over traditional ones these routes are perhaps the most pertinent to the present work.

4.1.1 Reactions with Chromophore Containing Molecules

Ultrasound is known to promote dehalogenation of halogenated organics in aqueous suspension via free radical type processes.[204,205] If this situation could be achieved at the surface of halogenated polymers such as PVC then the following situation might arise:-

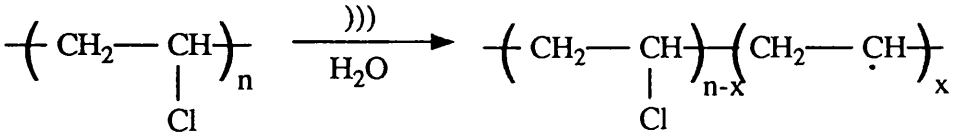

Scheme 4.1

The macro-radical produced in this way could then be expected to either react with the solvent or any reagents contained in it.

In the present work, samples of the PVC powder were initially sonicated for five hours using the ultrasonic probe at an intensity of 26.2 Wcm^{-2} in both water and 2-propanol in order to determine the reaction, if any, with these solvents. In neither case were any changes apparent in the DRIFT spectra, thus implying that little or no reaction can be expected with these solvents during reactions performed at lower ultrasonic intensity in the bath.

Subsequently, a number of preliminary investigations using "model" compounds were carried out. For this purpose the following series of aromatic chromophores having zero, one or two functional groups were chosen, since detection of the chromophore unit by diffuse reflectance uv spectroscopy should afford a facile means of following any grafting.

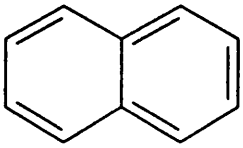

Naphthalene

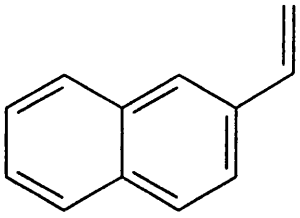

2-vinyl naphthalene

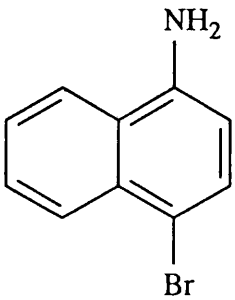

1-amino-4-bromonaphthalene

Figure 4.1

The diffuse reflectance uv spectrum of the product from the reaction with naphthalene showed no absorbance bands. This result was expected since the naphthalene nucleus has no functional groups through which reaction could be achieved.

The reaction of 2-vinyl naphthalene in 2-propanol with PVC was performed under varying conditions (see experiments 3-6 in table 2.1) and the reflectance ultraviolet spectra are shown in figure 4.2. All spectra were recorded against a background of untreated PVC, see section 2.11. Although these spectra cannot be used directly to obtain quantitative results, since changes in the particle size and morphology will effect the absorbance characteristics, a comparison between similarly treated samples should be possible. Clearly, in all cases absorbance bands due to the naphthalene nucleus are present. The reaction however, appears to be influenced by the gaseous atmosphere (experiments 3 & 5) to a much greater extent than would be expected by consideration of changes in the ultrasonic cavitation process resulting from differences in the physical properties of oxygen and nitrogen, see section 1.6. The origin of this feature may perhaps be attributed to the nature of the gases concerned, since oxygen is known to rapidly quench free radical species. This would suggest, therefore, that radical species are involved at some stage during the reaction. In this instance reaction of the 2-vinyl naphthalene molecule may give rise to the formation of a graft copolymer according to scheme 4.2.

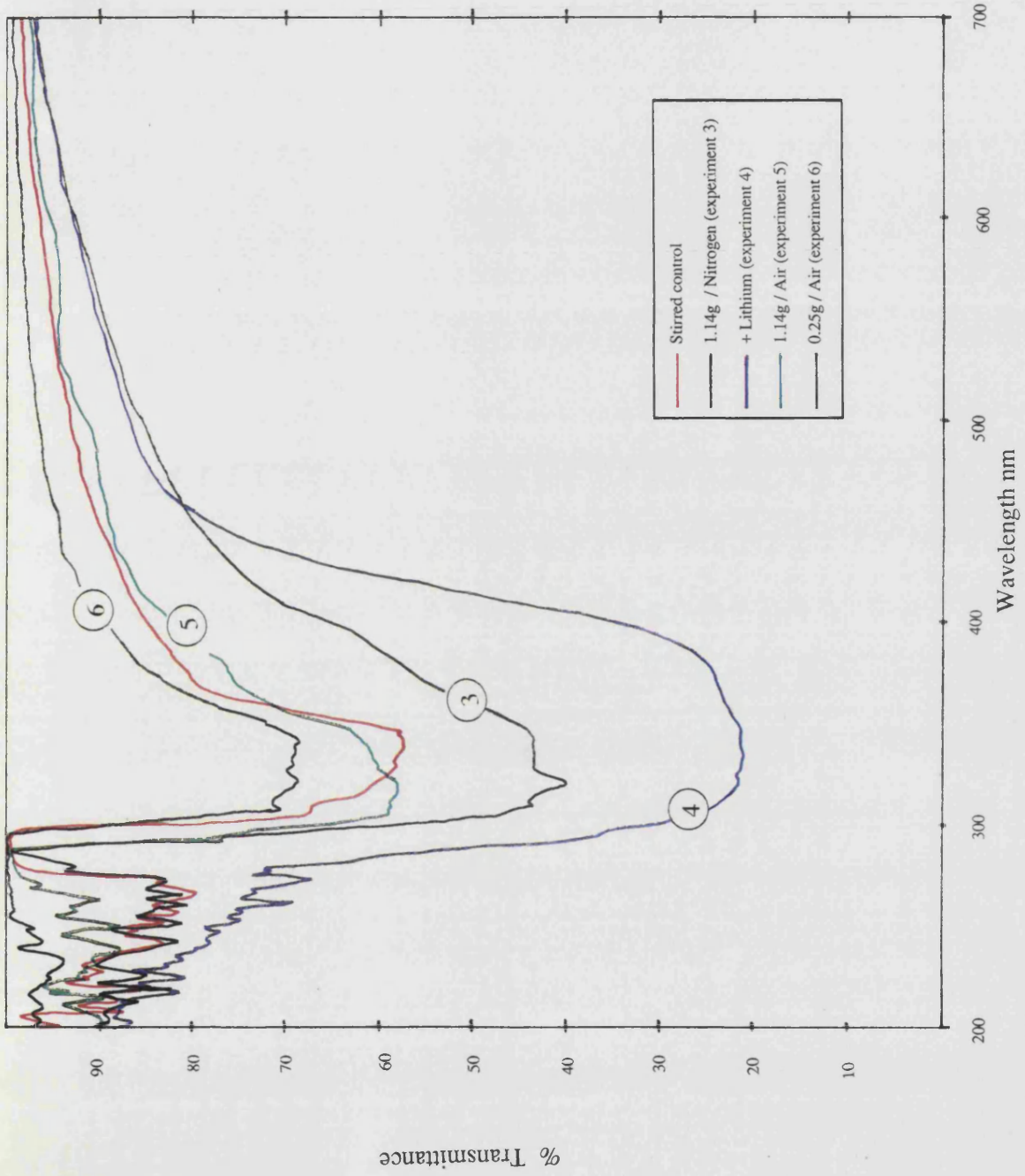

Figure 4.2 Diffuse reflectance ultraviolet spectra of PVC powder after reaction with 2-vinylnaphthalene under varying conditions

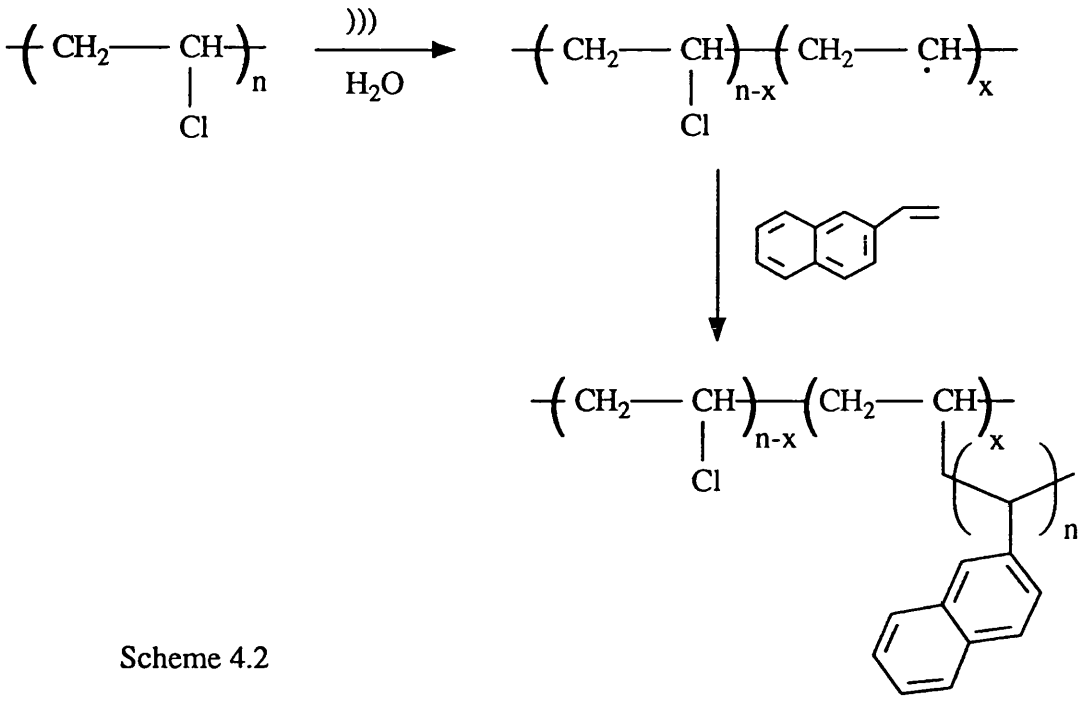

Scheme 4.2

A number of workers have reported that block copolymers can be produced by adding vinyl monomers during the ultrasonic degradation of a second homopolymer in solution.[231] Degradation of the polymer in solution is known to produce macroradicals which are reported to initiate polymerisation of the vinyl containing molecules. A number of other workers however, have shown that vinyl monomers can be polymerised by ultrasound in the absence of any further initiating species.[217-20] The formation of poly(vinyl naphthalene) in the present reaction would have produced a 2-propanol insoluble material which might have precipitated on the PVC surface. It was necessary, therefore, to carry out a more detailed examination of this system in order to verify whether or not the observed spectral features were due to ungrafted homopolymer.

A closer examination of the spectra presented in figure 4.2 shows that the λ_{max} value is at higher wavelength (340nm) in the stirred control than in the sonochemical samples (330nm), thus implying a reduction in the conjunction length of the chromophore unit during sonication. This observation is consistent with the anticipated graft polymerisation of the 2-vinylnapthalene. That the observed results

were not due to unremoved homopolymer was further confirmed by the sonication of 2-vinylnapthalene in 2-propanol. After sonication the 2-propanol was removed and the resulting solid analysed by ^{1}H and ^{13}C nmr. Both spectra indicated the presence of starting material only, thereby eliminating the possibility of homopolymer formation and supporting the grafting mechanism shown in scheme 4.2 The observed lack of homopolymer in this system can perhaps be attributed to the low ultrasonic intensities achieved by using the bath in these experiments, since, polymerisation in the absence of any further initiating species is reported to require quite high ultrasonic intensities.[220]

By adding a small amount of lithium wire to the reaction, experiment 4 in table 2.1, the absorbance band at 330nm was found to increase quite markedly. The lithium is thought to aid in the breaking of C-Cl bonds in the PVC according to scheme 4.3 below.

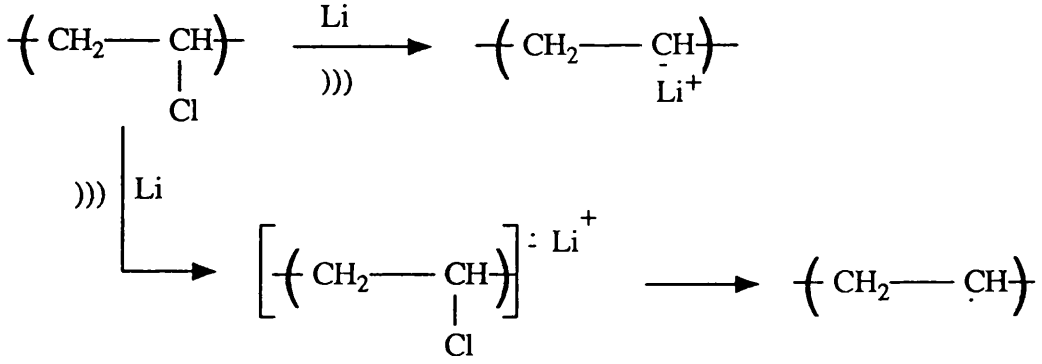

Scheme 4.3

Thus an increase in the number of radical sites might be expected, thereby explaining the observed increase in the absorbance.

The final reaction in this series involved the grafting of 1-amino-4-bromonaphthalene, which it was anticipated might also allow grafting through homolytic fission of the C-Br bond. Figure 4.3 shows the dispersion ultraviolet spectrum of the reaction product. The broad absorbance peak clearly shows the presence of the chromophore unit. The grafting mechanism however, remains unclear but two possibilities may be identified as shown in schemes 4.4 and

4.5.

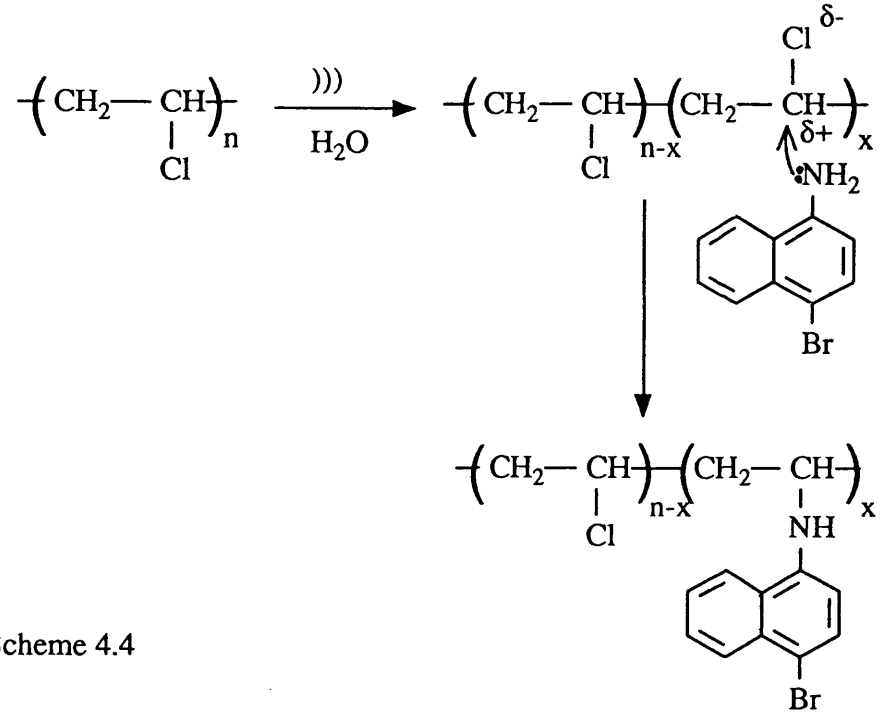

Scheme 4.4

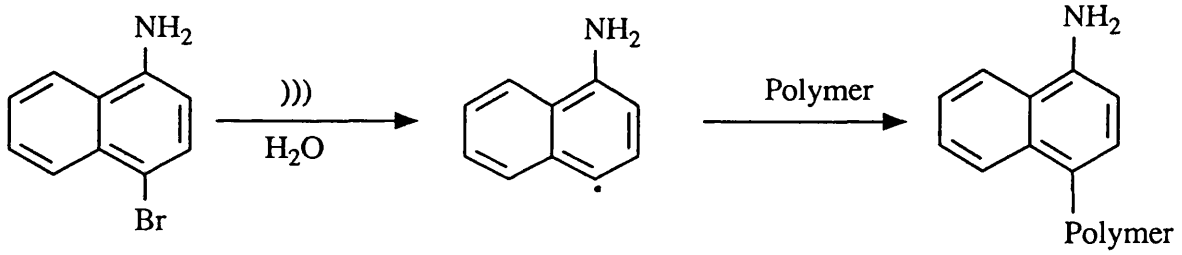

Scheme 4.5

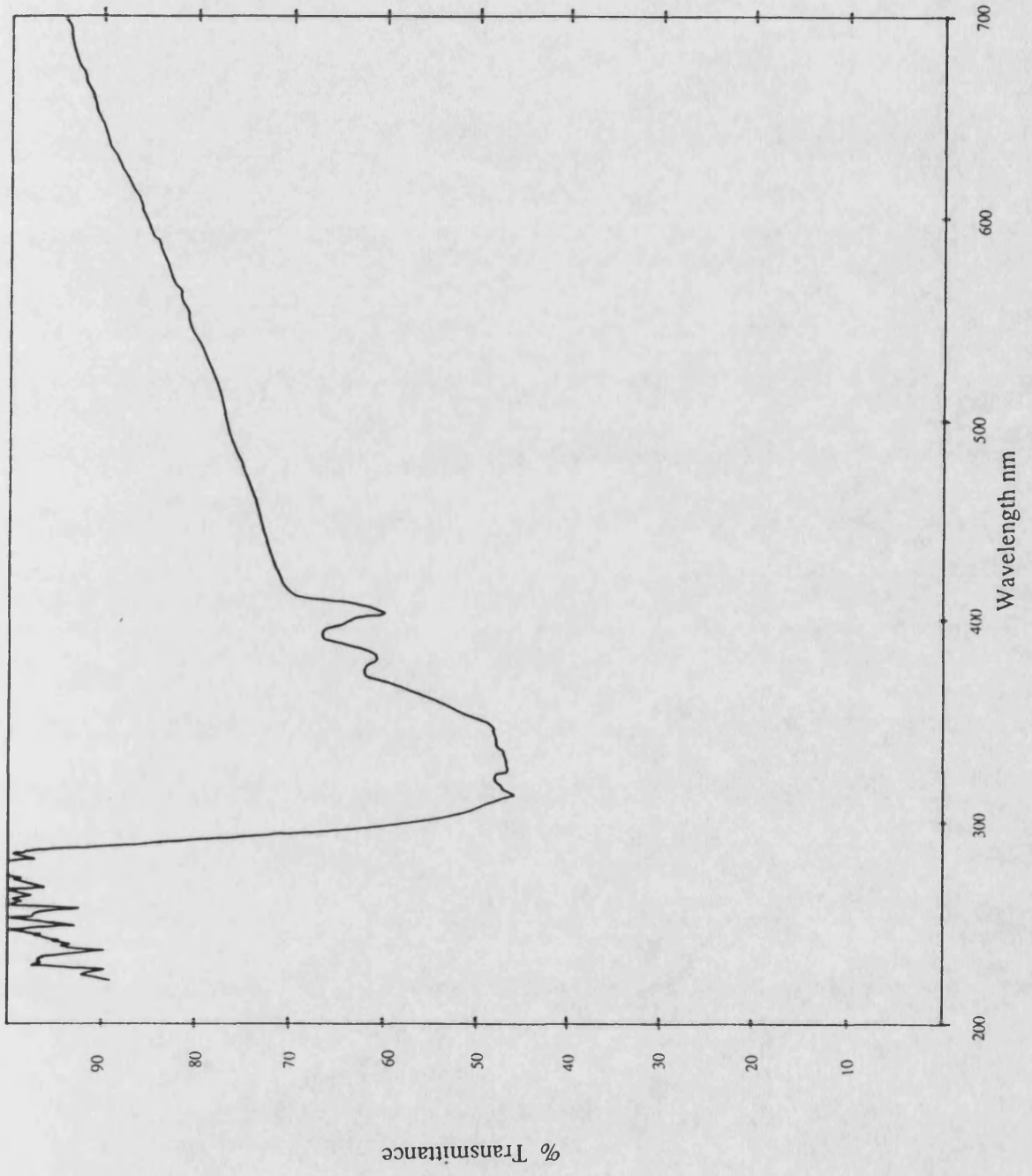

Figure 4.3 Diffuse reflectance ultraviolet spectrum of PVC powder after reaction with 1-amino-4-bromonaphthalene

Whilst the first of these schemes provides a clear point of attachment of the graft molecule to the polymer chain the second one is more ambiguous, with reaction at either carbon of the vinyl chloride repeat unit being possible.

The isolated 2-propanol soluble product from the reaction was dried under vacuum and recrystallised twice from ethanol. The melting point was then recorded and found to be 101-102°C (Lit. 102°C),[232] confirming the presence of unreacted starting material. This observation is consistent with the first of the two reactions schemes since, the aromatic radical in scheme 4.5 might also be expected to abstract a proton from the solvent to give 1-aminonaphthalene. Thus, a mixture of 2-propanol soluble products would be expected with a subsequent lowering of the melting point.

In this reaction the ultrasound may serve to act solely as a phase transfer catalyst, although perhaps the C-Cl bond in the polymer backbone is again broken before reaction with the chromophore.

4.1.1.1 Reactions With Dye Molecules

Following the observed grafting with "model" compounds investigations were extended to include more complex dye molecules. Initial studies were carried out using bromophenol blue in either aqueous solution or 2-propanol and then extended to include a number of other water soluble dyes. The structures of these dyes are shown in figure 4.4 A-F.

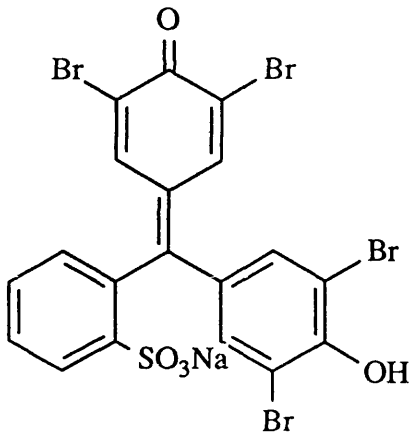

A. Bromophenol Blue

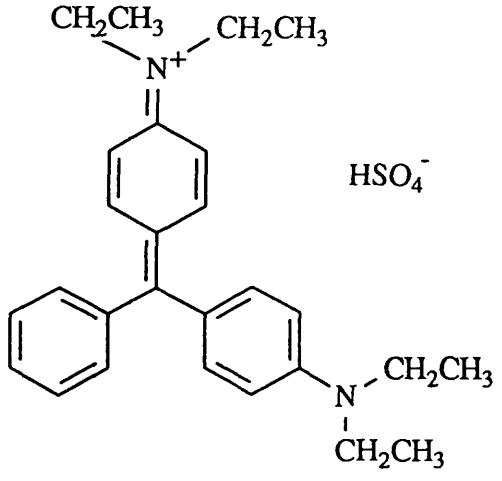

B. Brilliant Green

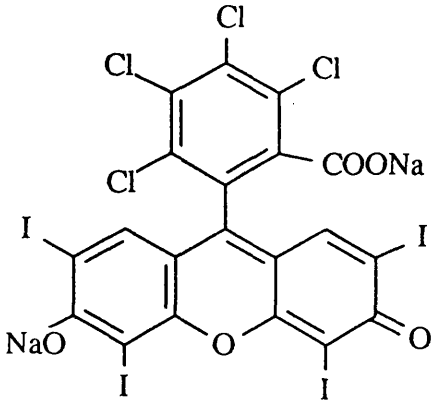

C. Rose Bengal

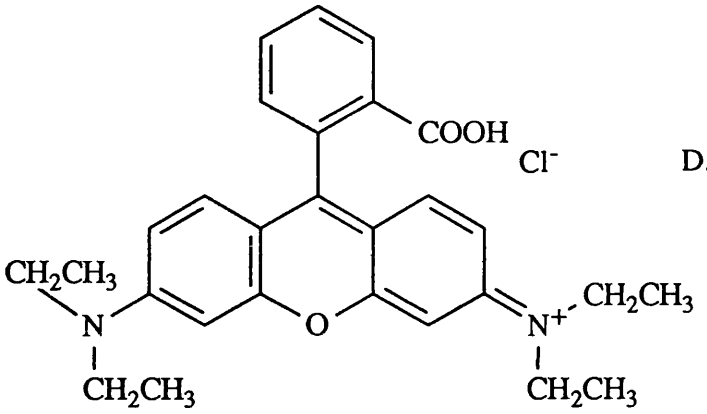

D. Rhodamine B

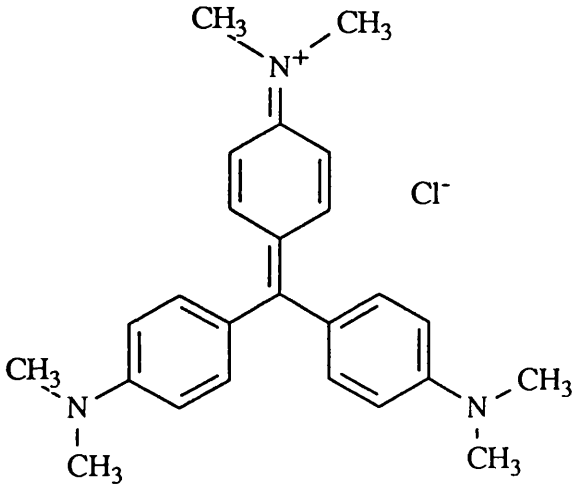

E. Crystal Violet

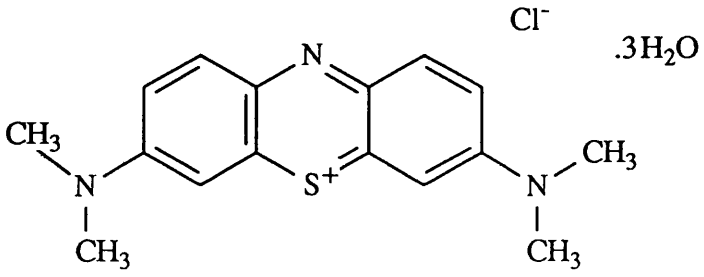

F. Methylene Blue

The diffuse reflectance ultraviolet spectra from the reactions of bromophenol blue with PVC are presented in figures 4.5 to 4.9.

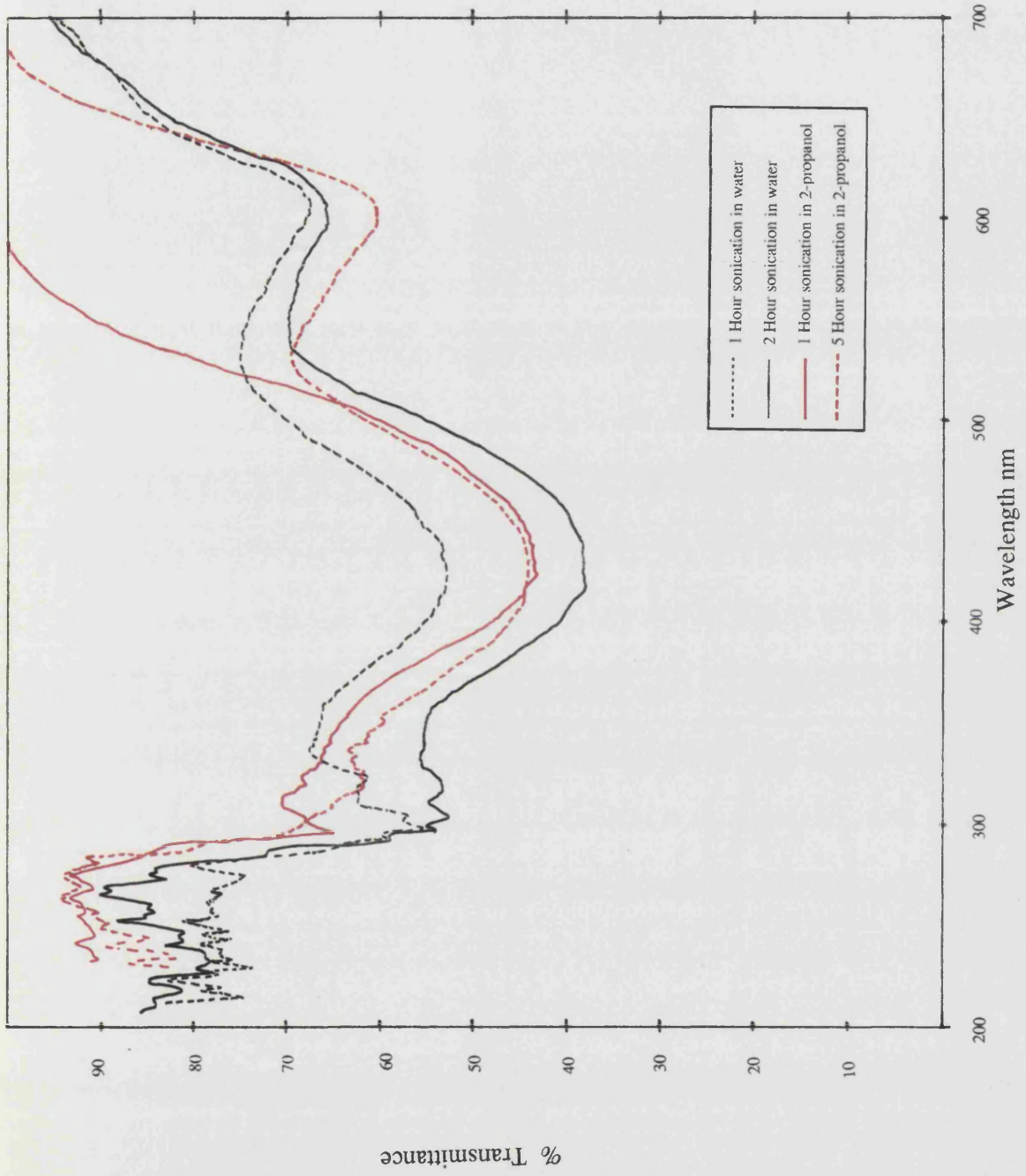

Figure 4.5 Diffuse reflectance ultraviolet spectra of PVC powder after reaction with bromophenol blue for varying sonication times in both water and 2-propanol

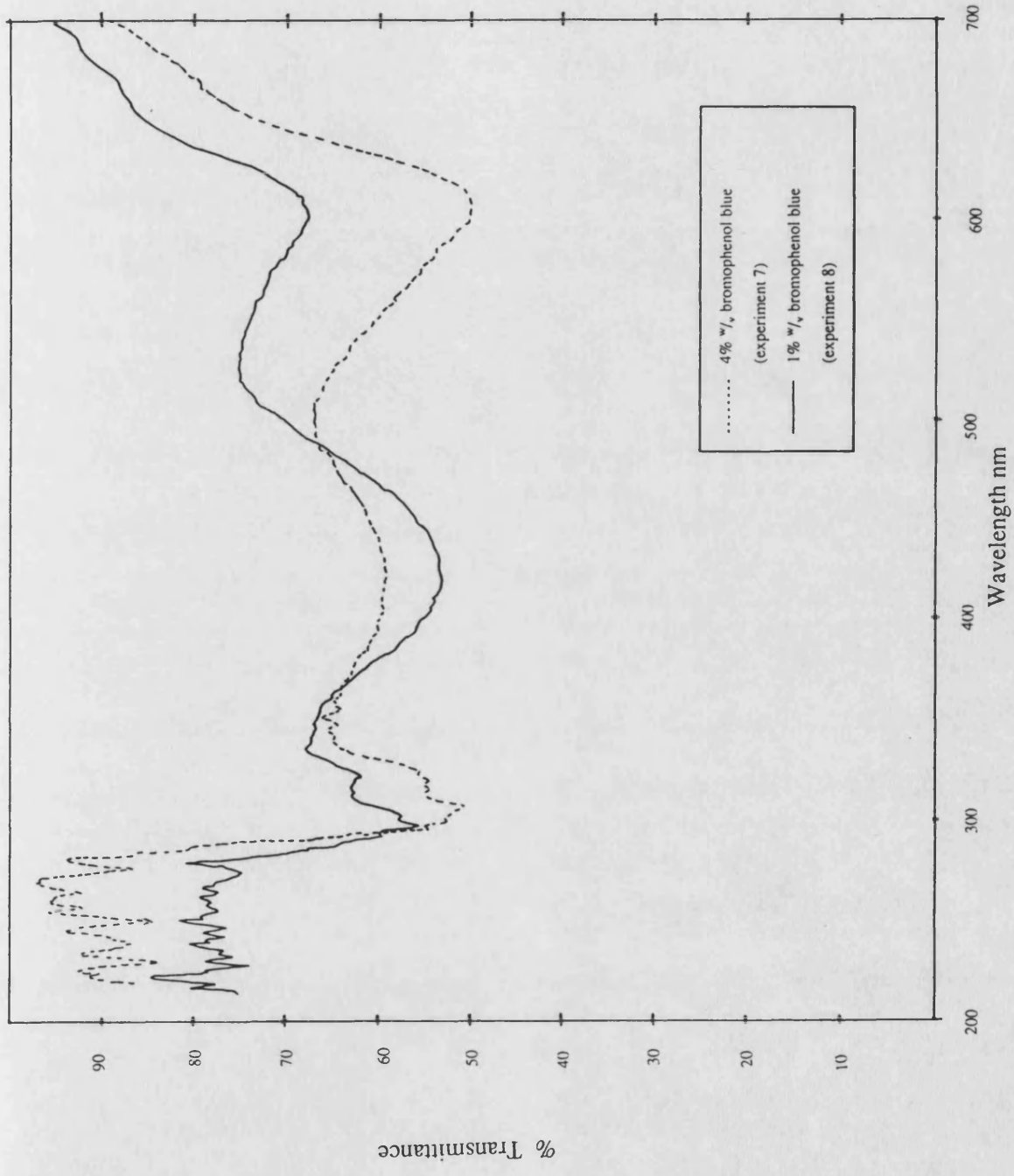

Figure 4.6 Diffuse reflectance ultraviolet spectra of PVC powder after reaction with bromophenol blue at various concentrations

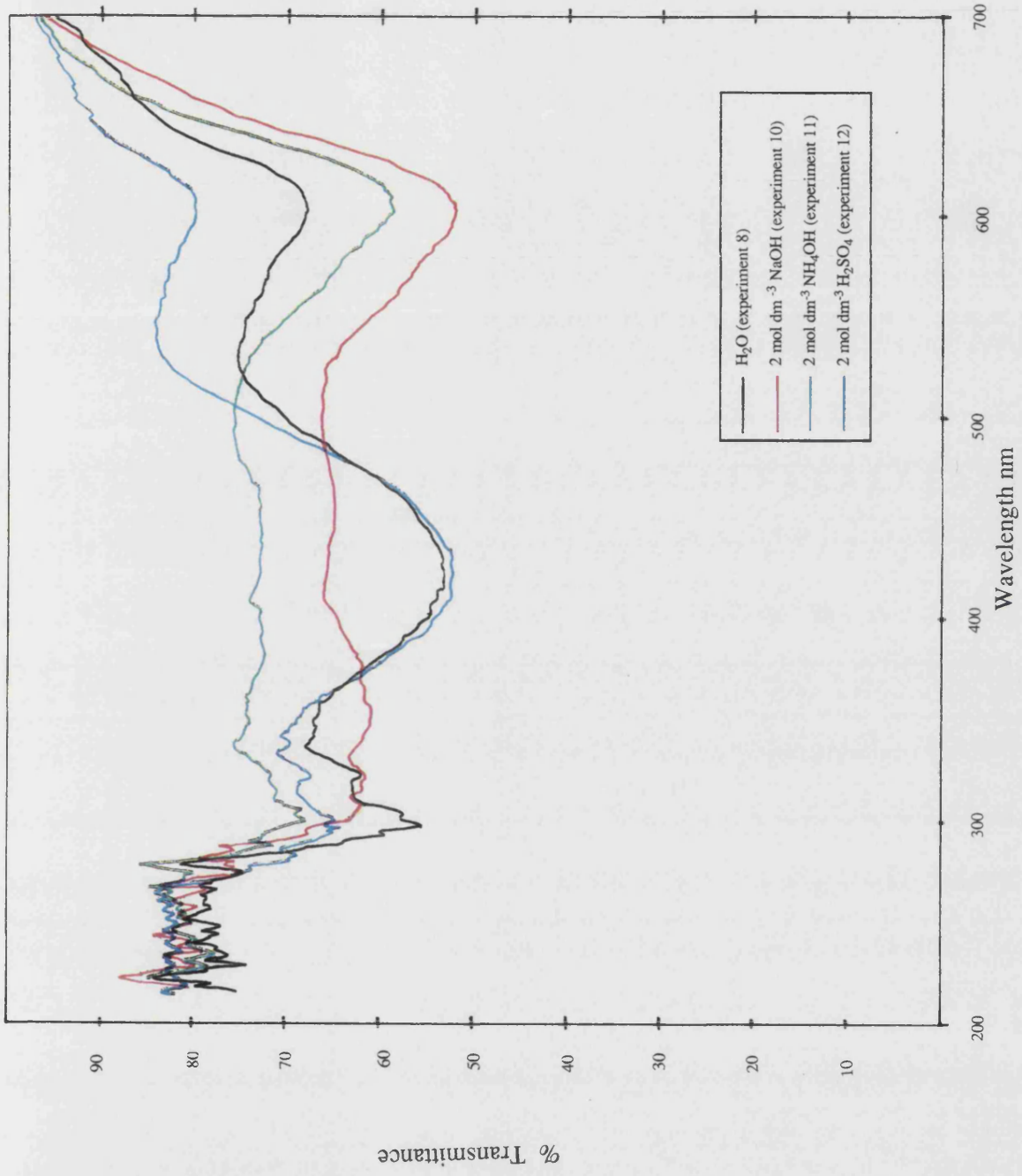

Figure 4.7 Diffuse reflectance ultraviolet spectra of PVC powder after reaction with bromophenol blue under various conditions of pH

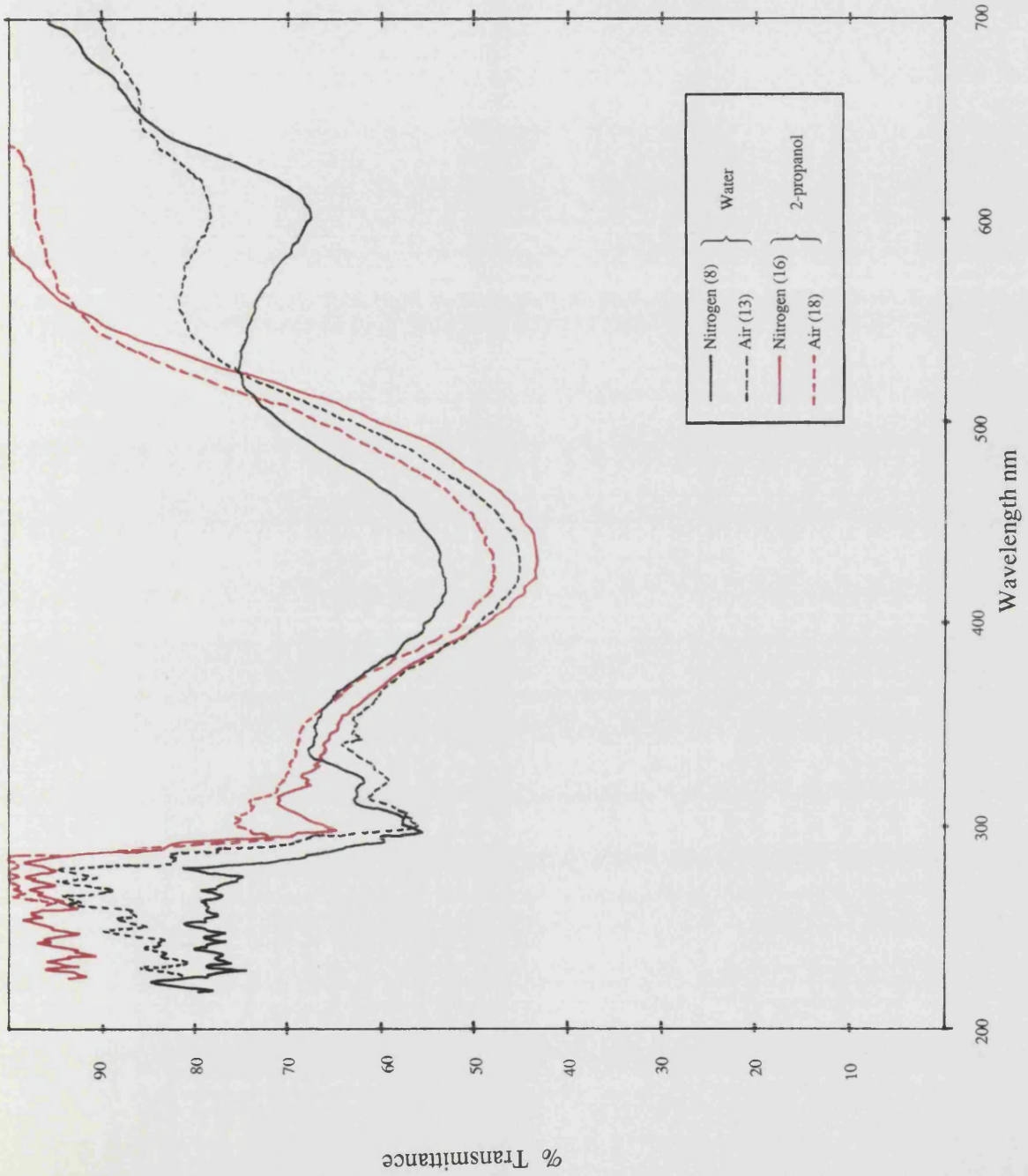

Figure 4.8 Diffuse reflectance ultraviolet spectra showing the effects of gaseous environment on the ultrasonic reaction of PVC powder with bromophenol blue in both water and 2-propanol

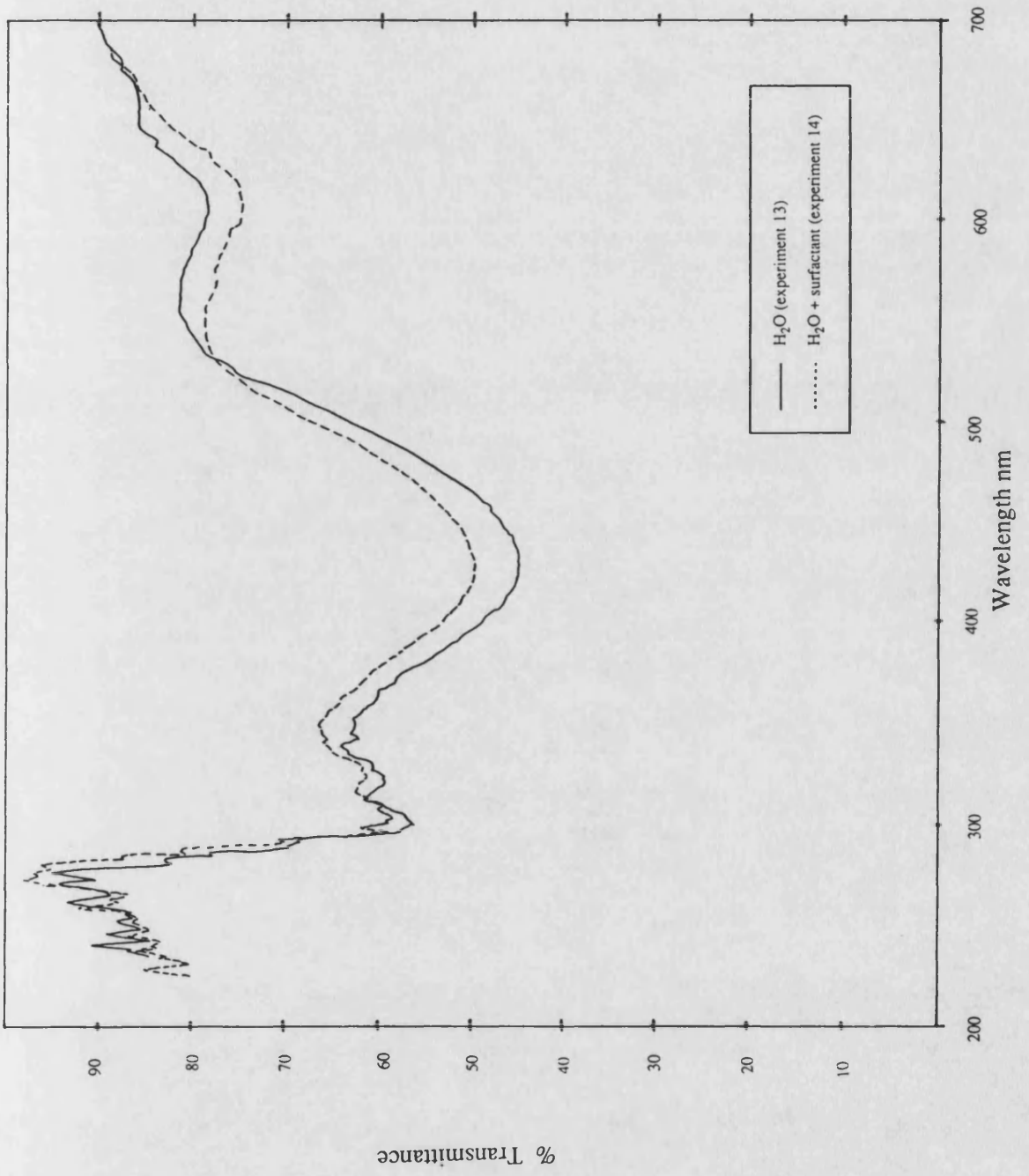

Figure 4.9 Diffuse reflectance ultraviolet spectra showing the effects of surfactant on the ultrasonic reaction of PVC powder with bromophenol blue in water

Figure 4.5 shows the effect of sonication time on the reaction in both water and 2-propanol. After one hour sonication in water the two characteristic absorbance peaks of bromophenol blue are observed at ≈420 and ≈605nm. Extending the sonication time to two hours appears to cause a small change in the relative intensity of each of these bands. Sonication experiments 16 and 17 in 2-propanol show a more marked change. After one hour only one band at ≈420nm is present, but after five hours irradiation a second band at ≈605nm is again evident. All experiments were carried out under nitrogen and it would seem, therefore, that reaction occurs in each solvent despite the changes in their respective cavitational intensities. In this respect, Niemczewski has reported that the cavitation intensity in 2-propanol is only about 38% of that in pure water.[140] It could then be argued that although 2-propanol is a poorer solvent for ultrasound, it allows better wetting, and hence, transfer of the dye to the polymer surface. As outlined earlier, however, direct comparison of these absorbance values cannot be made as samples were treated in different solvents and will consequently have different absorbance characteristics.

The spectra presented in figure 4.6 show the effects of bromophenol blue concentration. Two broad absorbance bands are evident at ≈420 and 605nm in each spectrum, but the relative intensity of the higher wavelength band is seen to increase quite markedly with increasing concentration.

For bromophenol blue, the following equilibrium can be presented:

$$R\text{-}SO_3Na \rightleftharpoons R\text{-}SO_3^- + Na^+ \qquad \text{Scheme 4.6}$$

Blue (605nm) Yellow (420nm)

The equilibrium constant, Ka, is then given by:

$$Ka = \frac{[R\text{-}SO_3^-]\,[Na^+]}{[RSO_3Na]}$$

If the degree of dissociation is α at a concentration C, then;

$$Ka = \frac{\alpha^2 C}{1-\alpha}$$

Hence, if $\alpha << 1$ then, $Ka \approx \alpha^2 C$ and so as C increases α must decrease.

Accordingly, at higher dye concentrations the intensity of the absorption band at 605nm would be expected to increase.

This variation in intensity of the two characteristic bromophenol blue absorption bands is also seen strikingly in figure 4.7 where the effects of pH have been presented. In acidic media only the band at 420nm is present. In distilled water both bands are evident, but the 420nm band is still the stronger. In basic media however, the band at 420nm has been surpressed and an increase in the intensity of the 605nm band is observed. The origin of these changes can be ascribed to the position of the equilibrium given in scheme 4.6. In acidic media the equilibrium will be pushed to the right hand side, whilst in the basic media it will be pushed to the left hand side. Accordingly, the band at ≈420nm will be due to the R-SO_3H species whilst the one at 605nm can be ascribed to the R-SO_3Na group. Thus, the colour of the reacted polymer surface was selectively controlled by varying the pH of the aqueous dye solution.

From figure 4.8 it can be seen that the gaseous environment also influences the intensity of each of the absorbance bands. In both solvents, reaction under nitrogen favours the formation of the acidic band at ≈420nm, whilst air shows an increase in relative intensity of the basic band at ≈605nm. This effect is seen to be much more pronounced in water than 2-propanol and may also arise through concentration changes induced by ultrasonic degradation of the dye molecules.

Finally, the reaction of bromophenol blue with PVC was studied in air with the addition of a small amount of sodium dodecyl sulphate present to possibly act as a phase transfer agent (experiment 14). The diffuse reflectance uv spectra from this investigation are shown in figure 4.9. The addition of surfactant appears to have only limited effect on the absorbance values, but a small shift in the relative intensity of each of the bands is again present. The origin of this shift can be ascribed to the ionised surfactant molecules which in turn will push the equilibrium shown in scheme 4.6 to the left hand side and hence, result in a decrease in the band at ≈420nm and corresponding increase in the band at ≈605nm.

Other dyes: The grafting onto PVC powder surfaces was extended to include brilliant green and rose Bengal, experiments 19 and 20 in table 2.1. The diffuse reflectance uv spectra of the reacted polymer samples, presented in figure 4.10, clearly show the presence of each of the dye molecules. Although perhaps the most vivid characterisation of these samples is obtained by consideration of their respective colours.

In order to produce a reaction system for commercial use, however, it was necessary to greatly reduce the time scale of these reactions. To effect this, a higher power ultrasonic horn was used. Reactions were carried out in water under air at $26.2Wcm^{-2}$ using all six dyes (experiments 21p to 26p in table 2.1) shown in figure 4.4 and the diffuse reflectance uv spectra were recorded. All samples showed the presence of dye molecules. To better understand the stability of these dyed polymers, samples were soxhlet extracted for 24 hours with methanol. The diffuse reflectance spectra from these products are shown in figure 4.11. Clearly in each case some dye remains bound to the polymer surface, although the characteristic visible colour of the respective dyes is significantly lower in intensity in all cases except with brilliant green. The diffuse reflectance uv spectrum of this sample was relatively unchanged by the soxhlet extraction process and the polymer powder was visibly seen to retain its characteristic bight green colour.

The positive charge on this dye would serve to rule out the possibility of chlorine substitution by either a S_N1 or S_N2 type mechanism. Whilst radical substitution remains a possibility, it would seem unlikely since crystal violet has a similar structure and charge to brilliant green, but shows much lower levels of grafting. The origin of the increased reactivity of brilliant green can perhaps be attributed to the counter ion which might serve to remove an acidic β proton from the PVC. A mechanism for the reaction might then be:

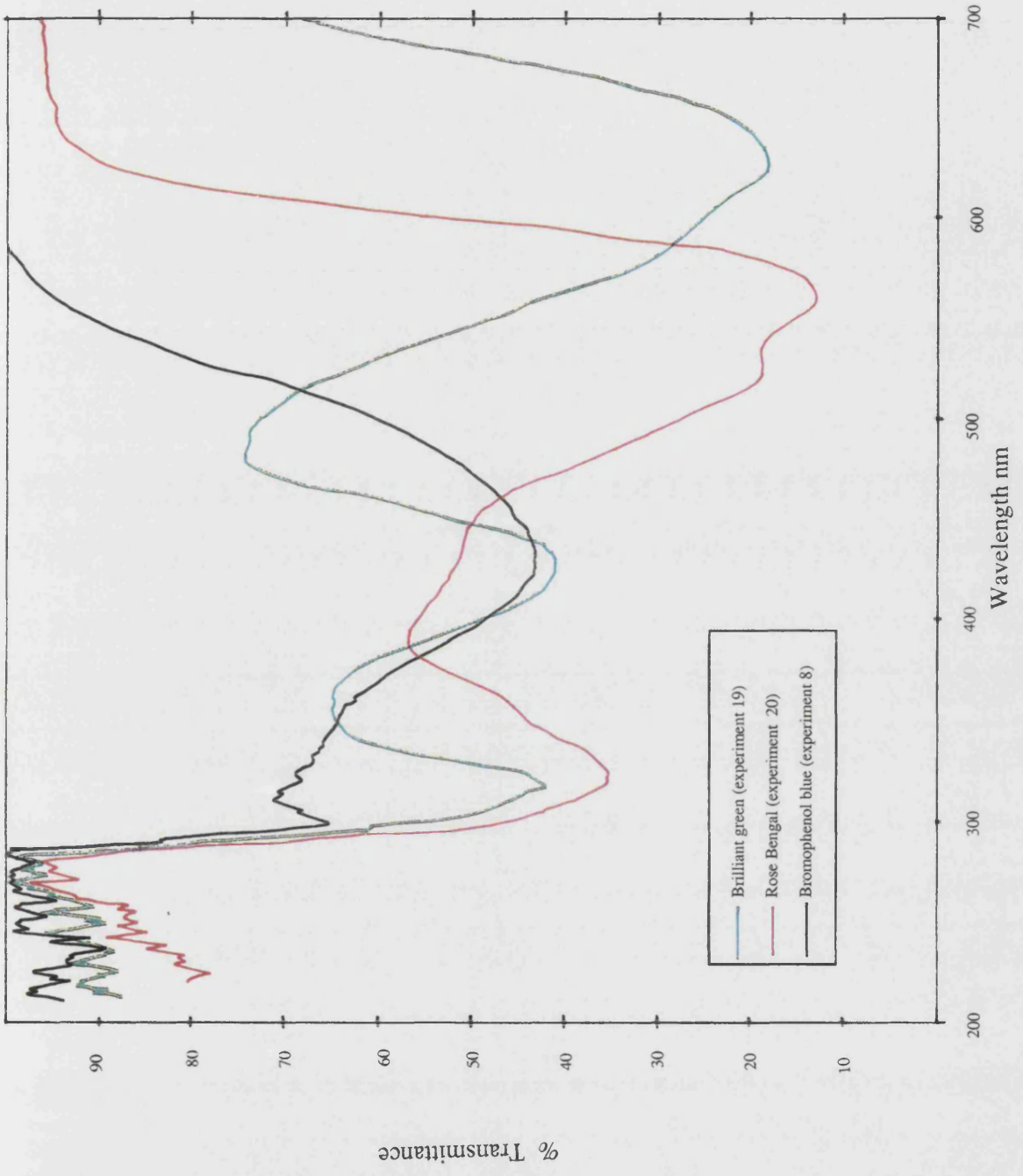

Figure 4.10 Diffuse reflectance ultraviolet spectra of PVC powder samples after reaction with various dyes in water

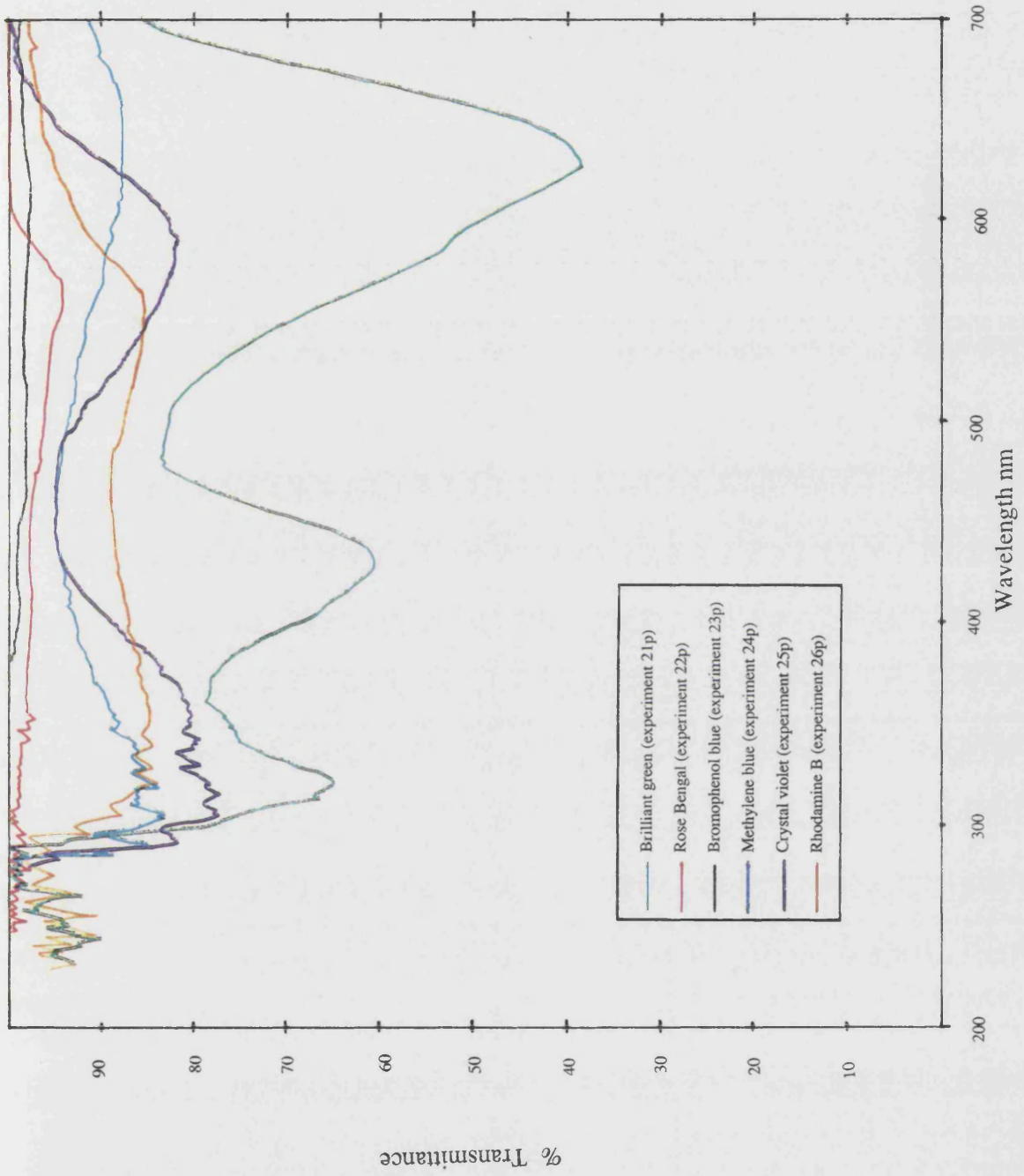

Figure 4.11 Diffuse reflectance ultraviolet spectra of PVC powder samples after ultrasonic reaction with various dyes in water following 24 hour soxhlet extractions with methanol

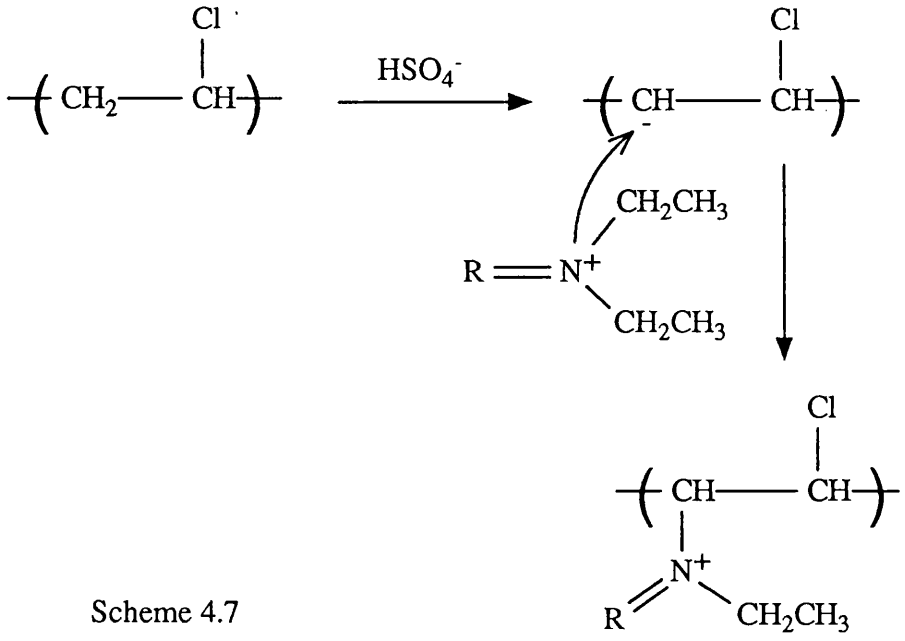

Scheme 4.7

The first step in this sequence is synonymous with the base catalysed elimination mechanism, E1cB, discussed later in section 4.2.

Thus, it has been shown that ultrasound can be used effectively to generate surface colour on PVC powders, thereby achieving one of the project targets. The application of these reaction systems for the modification of real PVC electrical cables is discussed below in chapter 6.

4.1.2 Reactions With Other Polymers and Monomers

It was expected that many of the desired end properties for PVC cable surfaces could be achieved most successfully by grafting a second polymer or monomer on to the surface. To effect this, with regard to our environmental constraints, a number of aqueous soluble polymers and monomers were examined along with two organic systems other than 2-vinylnaphthalene described earlier.

A number of workers have studied the ultrasonic degradation of polymers in solution. As outlined in chapter 1 the degradation process generates macroradicals in solution which can then be used to form block copolymers having known and

controllable, block lengths. In the present work it was expected that the in situ generation of macroradical species could perhaps also be used for the production of heterogeneous graft copolymers.

In the present series of investigations none of the water soluble polymers employed (see table 2.2 section 2.9.1) were found to undergo grafting at the surface of PVC by either diffuse reflectance infrared or uv spectroscopy. Similarly neither acrylamide or acrylic acid were found to undergo grafting by these analytical methods.

Owing to the limited success obtained with aqueous polymers and monomers, reactions were carried out using PMMA in toluene (experiment 31p) and MMA in 2-propanol (experiment 30). The end PVC product in each case was filtered off and then soxhlet extracted for two hours with 2-propanol. The DRIFT spectra of the resulting powders are shown in figures 4.12b and 4.12c respectively and that of untreated PVC in 4.12a. All three spectra show the presence of a carbonyl stretching band at $\approx$1740 cm^{-1}, although the intensity of this band is significantly higher in samples reacted with both PMMA and MMA. The origin of this band in experiment 31p with PMMA, however, remains in some doubt since, a similar stirred control experiment also showed the presence of residual homopolymer even after soxhlet extraction for twenty four hours with 2-propanol. Reaction with MMA, however, clearly demonstrates that during sonication the monomer undergoes polymerisation even at the low ultrasonic intensities generated in the bath, since unreacted monomer would have been removed during extraction with 2-propanol. Hence, it would appear that polymerisation is initiated by reaction with the solid surface. Although it remains difficult to characterise fully the nature of this material, it can be expected that the growing polymer would partition preferentially at the PVC surface since 2-propanol is a non-solvent for PMMA at low temperatures. Accordingly, polymerisation might be initiated by reaction at the surface or, growing macroradicals may be terminated by reaction with the solid surface. Thus, the capacity for grafting onto the PVC powder is greatly increased.

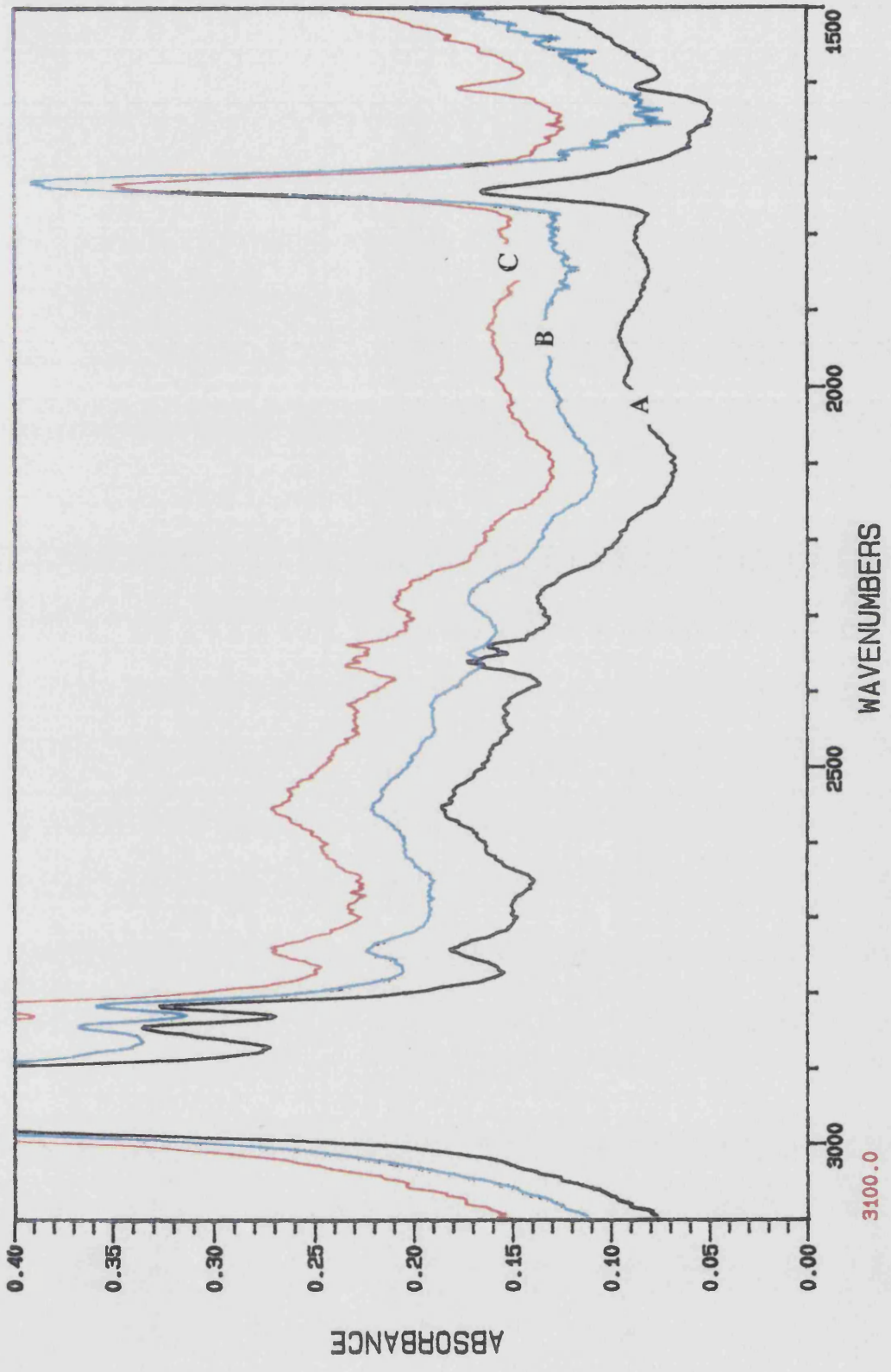

Figure 4.12 DRIFT spectra of PVC powder (A), PVC powder after reaction with PMMA in toluene (B) and PVC powder after reaction with MMA in 2-propanol (C)

Consideration of these observations with monomers and polymers leads to a number of conclusions. First, macroradicals generated by the ultrasonic degradation of water soluble polymers in solution do not appear to undergo significant surface grafting onto PVC. Secondly, surface grafting with monomers appears to be more favourable when the polymers formed are insoluble in the reaction solvent.

These observations might then be explained by one or more of the following situations:-

1. Macroradicals in solution do not react with the solid polymer, but instead react preferentially with the solvent.

2. Macroradicals react readily with the heterogeneous polymer surface, but due to the solubility of the polymer chains in the reaction solvent, present favourable points for ultrasonic cleavage. This situation is represented schematically in figure 4.13:

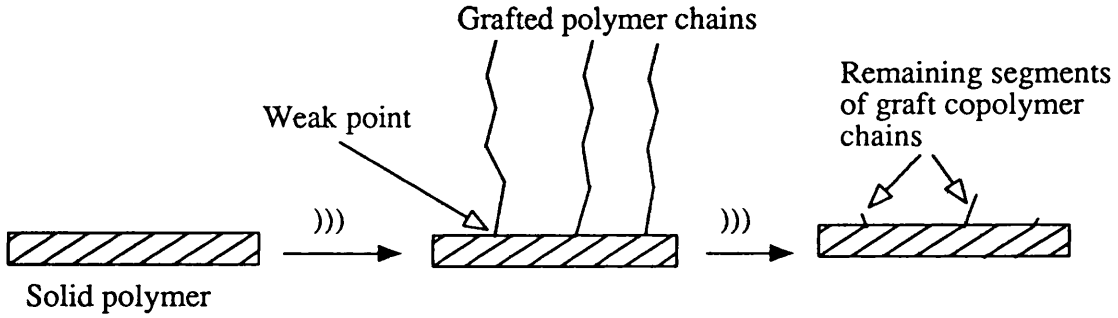

Figure 4.13 A model for the ultrasonic grafting of a solvated polymer onto a heterogeneous polymer surface

During ultrasonic irradiation the macroradicals generated react with the solid surface. In subsequent cavitation cycles the shock waves produced by bubble collapse will sweep the surface, preferentially removing any unbound material or solvated polymer chains.

3. The reaction of monomers with the polymer surface presents a greater number of possibilities. Firstly, the interaction of the solvent with the monomer will

be very important in these systems, since it will greatly affect the partitioning of the reagents throughout the system. Secondly, the interaction of the solvent with the growing macroradical will also be of paramount importance.

For a solvated monomer, reaction at the polymer surface may be random. If the growing macroradical is then solvated by the reaction medium the situation in point 1 above will arise. If, however, the growing macroradical is insoluble in the reaction solvent, then the stability of the graft copolymer, to subsequent cavitation cycles, would be greatly enhanced to a degree dependent upon the interaction between the growing polymer, the solid polymer surface and the reaction medium.

Conversely, a monomer in a poor solvent might position itself between the solvent and heterogeneous polymer. In this instance reaction with the solid surface will be much more favourable during cavitation at the surface.

Finally, the initiation site for grafting reactions involving monomers must also be considered. The ultrasonic polymerisation of vinyl monomers in solution is reported to be initiated by radical species generated in the 'hot spots' formed during collapse of the cavitation bubbles.[217-20] The growing macroradical then propagates in a conventional way and will be subject to the possible fates discussed above.

Conversely, polymerisation of vinyl monomers may be initiated by reaction sites on the heterogeneous polymer surface. In this instance three possible initiation mechanisms may arise, (i) radical, (ii) anionic and (iii) cationic.

(i). Radical sites may be generated on the solid polymer surface by sonochemical homolysis of C-C, C-Cl or C-H bonds as discussed in section 4.1.1 for 2-vinyl naphthalene.

(ii). Anionic polymerisation may arise in the presence of a base by removal of acidic β protons according to the first step of an E1cB type mechanism.

(iii). Cationic initiation may result if the C-Cl bond is broken with charge separation, according to the rate limiting stage of an S_N1 type substitution, see section 4.1.1.

Alternatively, cavitation at the surface of PVC has been shown to promote surface roughening, (see chapter 3). This process will result in mechanical dislocation and chain breakage at the surface, which in turn may present suitable sites for the initiation of vinyl monomers.

In the present series of studies it is expected that radical type initiating processes will be prevalent, but other methods will be discussed in section 4.2 concerning elimination reactions. Irrespective of the initiating step, the fate of the growing macroradical can be expected to proceed according to the earlier arguments.

In conclusion, it is believed that all of the above mechanisms may be occurring simultaneously. The contribution of each these will, however, be dependent upon a number of factors such the interaction between the solid polymer, solvent and solvated polymer or monomer.

4.2 Elimination Reactions

In the present work, the base catalysed dehydrochlorination[117] of both pure PVC films and powders has been studied. The influence of metal ions on the elimination process and secondary reactions of the double bonds formed have also been examined.

To better understand the potential of HCl elimination as a suitable first step for the modification of PVC surfaces it is necessary to consider the mechanisms of the reactions that might arise.

Elimination reactions proceed in general via either a first or second order process. First order elimination of the E1 type will proceed through the intermediary of a carbonium ion and might then lead to the sequence of reactions shown in scheme 4.8, where B is a base. This type of mechanism will be favoured by good leaving groups and polar solvents.

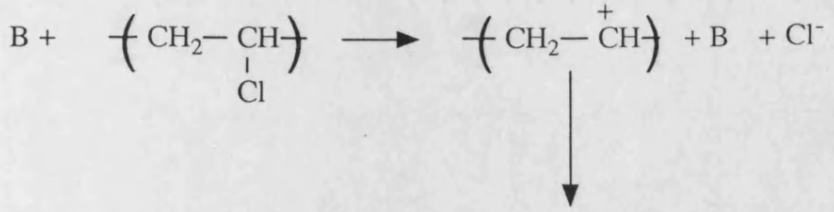

Scheme 4.8

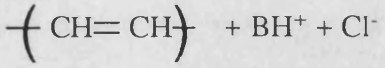

The elimination by the E1cB mechanism includes the formation of a carbonium ion intermediate generated by abstraction at the acidic β proton as mentioned earlier in scheme 4.7.

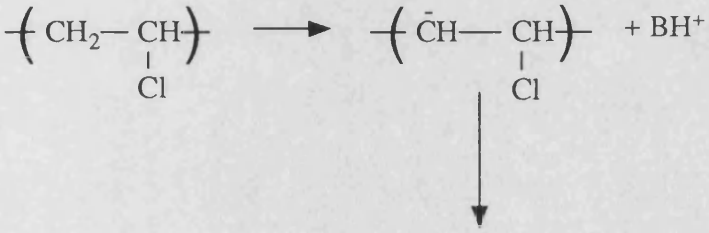

Scheme 4.9

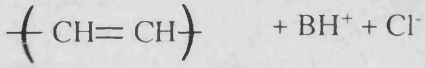

Second order elimination of the E2 type will proceed through a bimolecular transition state which may vary accordingly:

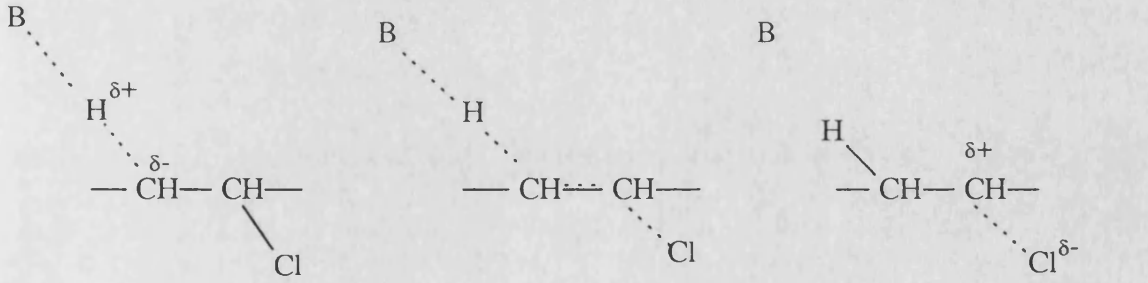

Carbanion character

Central character

Carbonium ion character

Scheme 4.10

In the case of PVC, the HCl leaving group will stabilise the carbanion structure in relation to the carbonium ion and hence increase C-H bond breakage. Electron withdrawing substitutes such as double bonds in the β position will also serve to increase the carbanion character and favour C-H bond breakage.

Another elimination mechanism known in the literature is the four centre H-X elimination. The essence of this mechanism may be explained by the following sequence:

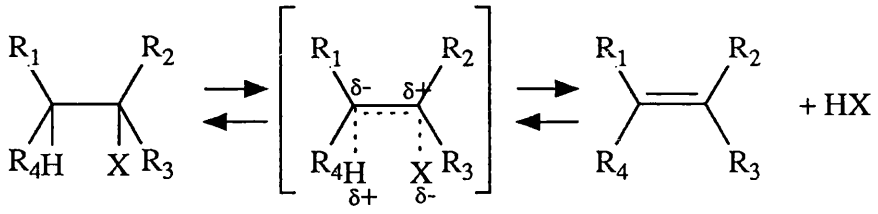

Scheme 4.11

Owing to the nature of the PVC chain, reaction by this mechanism would be expected to proceed by a "zipper-like" mechanism until an irregularity was encountered, thus producing a fully conjugated polymer.[113]

4.2.1 Base Catalysed Elimination Reactions

Initially, the stability of PVC powder samples towards aqueous sodium hydroxide was investigated. Samples of the polymer were sonicated at 26.2Wcm^{-2}, 35°C for five hours then washed, vacuum dried and analysed by both diffuse reflectance infrared and ultraviolet spectroscopies. Both 2 mol dm^{-3} and 6.25 mol dm^{-3} (8 and 25% ^{w}/v respectively) sodium hydroxide solutions failed to produce any changes in the resulting spectra. These observations would suggest that no significant amount of HCl is eliminated from the PVC surface in the presence of base alone.

Subsequently, samples of PVC suspended in sodium hydroxide were sonicated in the ultrasonic bath for one hour after which time a known weight of a metal salt was added, see the experimental procedure in section 2.9.1. The resulting slurry was stirred for a further two hours to allow complexation of the metals with any double bonds formed. The diffuse reflectance uv spectra of some of these samples, recorded against an unreacted PVC reference, are shown in figure 4.14.

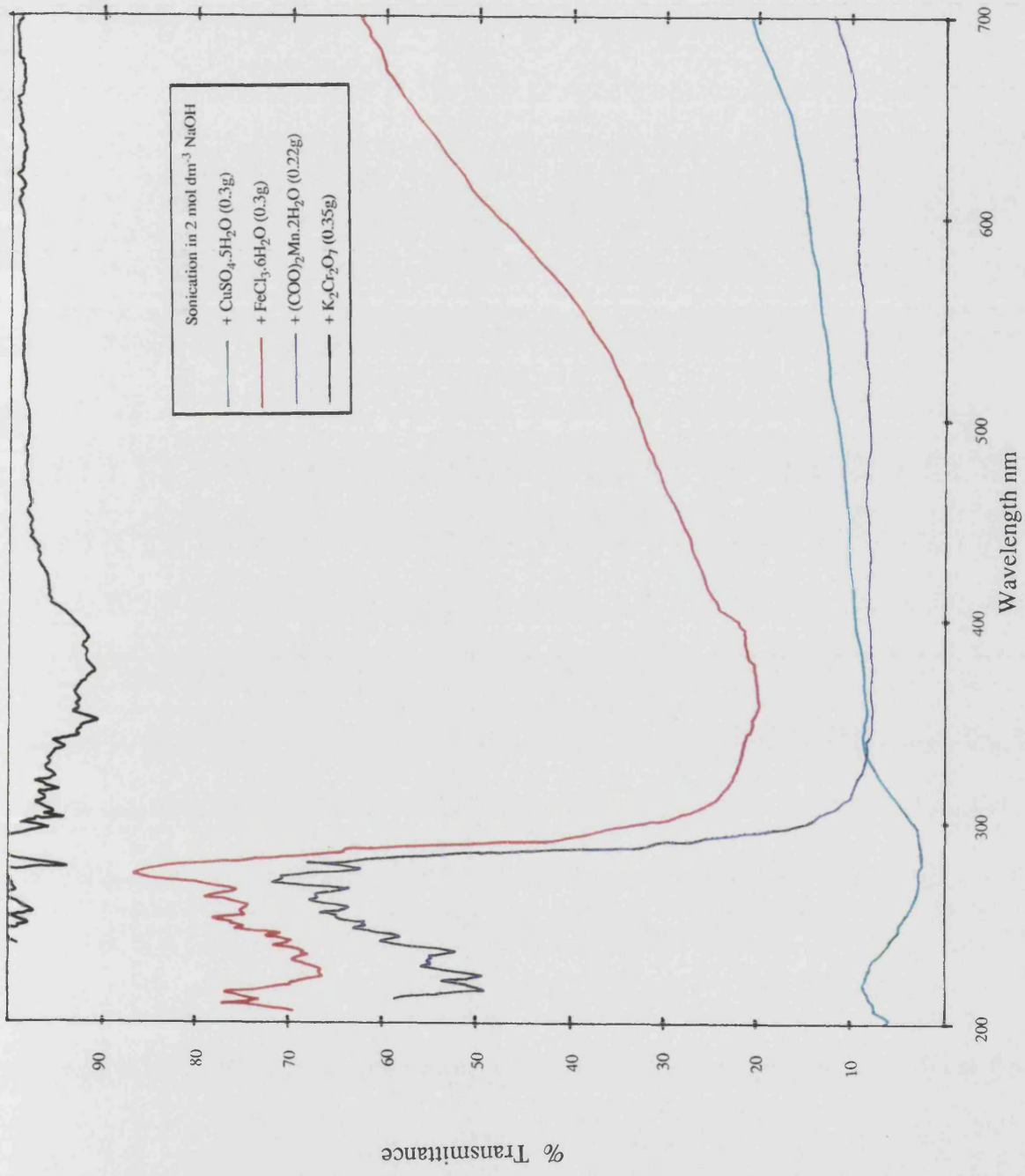

Figure 4.14 Diffuse reflectance ultraviolet spectra of PVC powder samples after ultrasonic reaction with sodium hydroxide and subsequent stirring with metal salts

Clearly, samples stirred with $CuSO_4.5H_2O$, $FeCl_3.6H_2O$ and $(COO)_2Mn.2H_2O$ show broad absorbance bands which remain even after the samples were subjected to 24 hour soxhlet extractions with water. Only potassium dichromate appeared to have little or no effect.

To obtain further information on the chemical interactions involved in these systems a series of control experiments wwas performed. The same weights of metal salts used previously were added to suspensions of PVC in water and the systems sonicated for two hours in the ultrasonic bath. The reflectance ultraviolet spectra of the soxhlet extracted samples are shown in figure 4.15. Only the sample treated with $FeCl_3.6H_2O$ showed the presence of an absorption band, although much weaker than that generated in sodium hydroxide solution. These results suggest that some unsaturation might be produced by the hydroxide base, the extent of which may perhaps be increased by the addition of metals, although the metals may be simply chelated with the double bonds formed.[7]

Subsequently, a number of reactions involving iron (III) chloride were undertaken (experiments 37 to 41). Both experiment 37 and 38p on PVC powder showed large absorbance bands in the reflectance ultraviolet spectra as given in figure 4.16. The sample from the experiment performed with the ultrasonic probe, 38p, was then analysed by EDX and the resulting spectrum is presented in figure 4.17b with that of untreated PVC in figure 4.17a. Trace levels of iron can only be seen in the reacted sample (4.17b) suggesting that chelation of the metal with surface double bonds may be occurring.

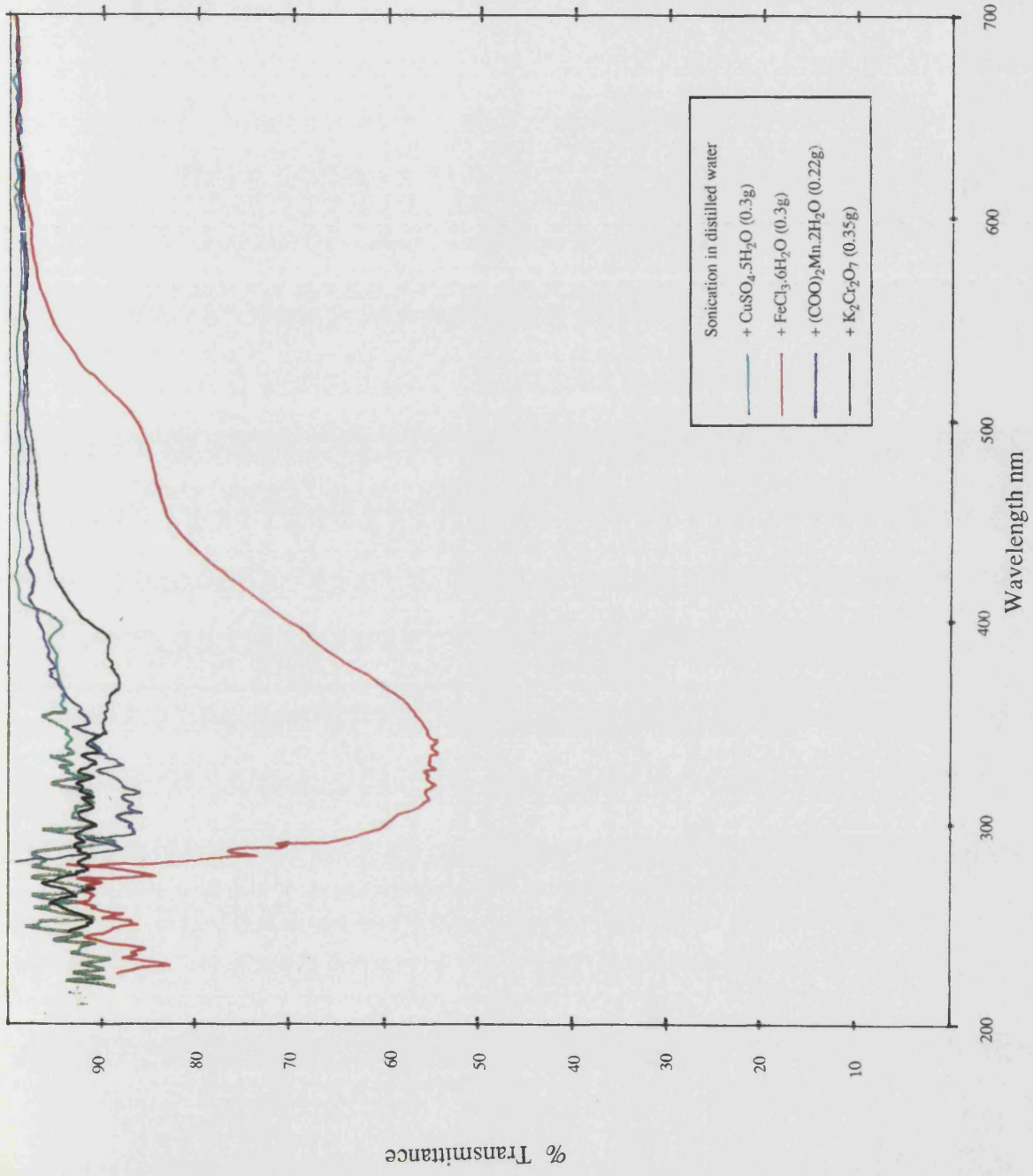

Figure 4.15 Diffuse reflectance ultraviolet spectra of PVC powder samples after ultrasonic reaction with aqueous metal salts

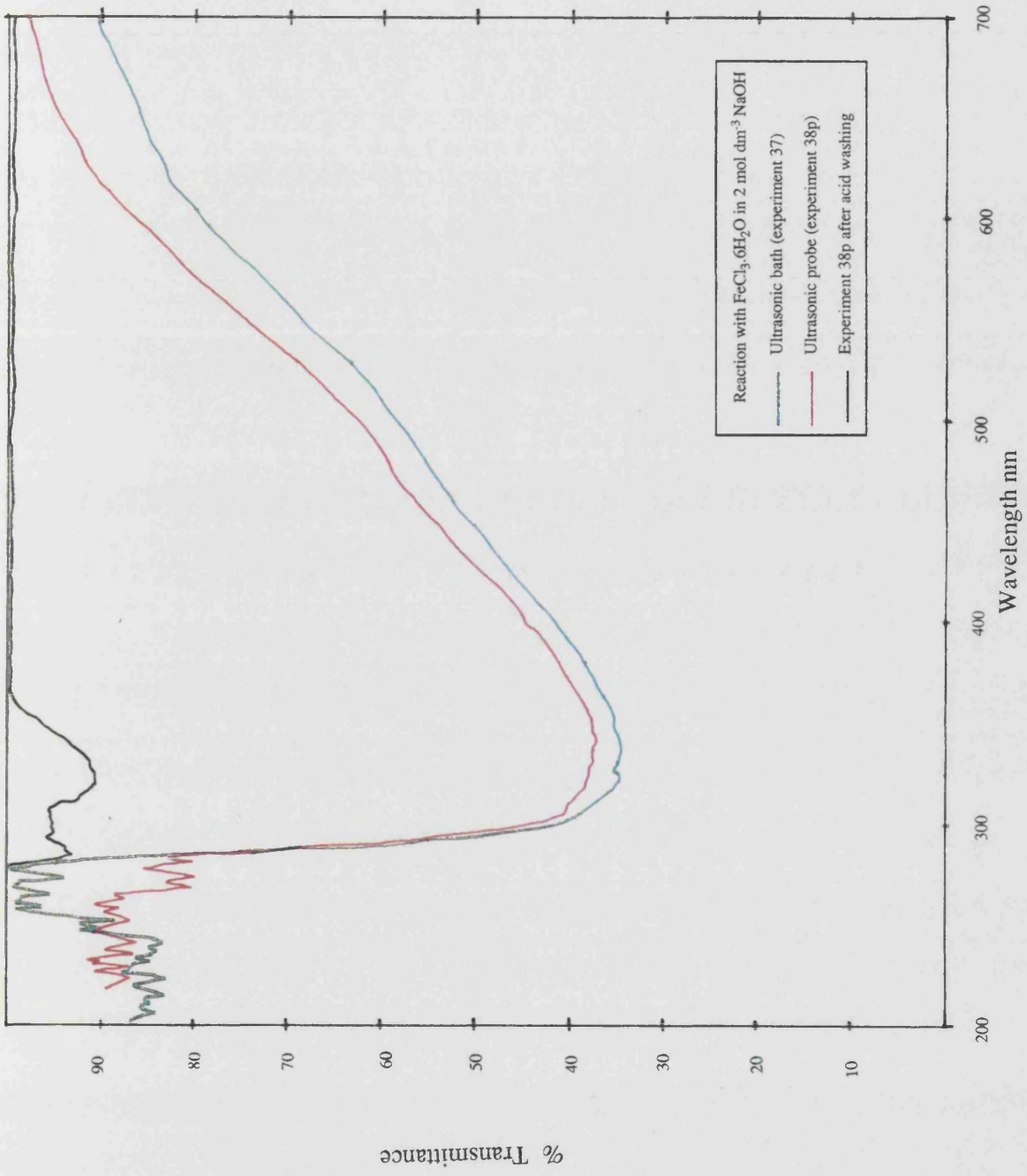

Figure 4.16 Diffuse reflectance ultraviolet spectra of PVC powders after reaction with NaOH in the presence of $FeCl_3.6H_2O$

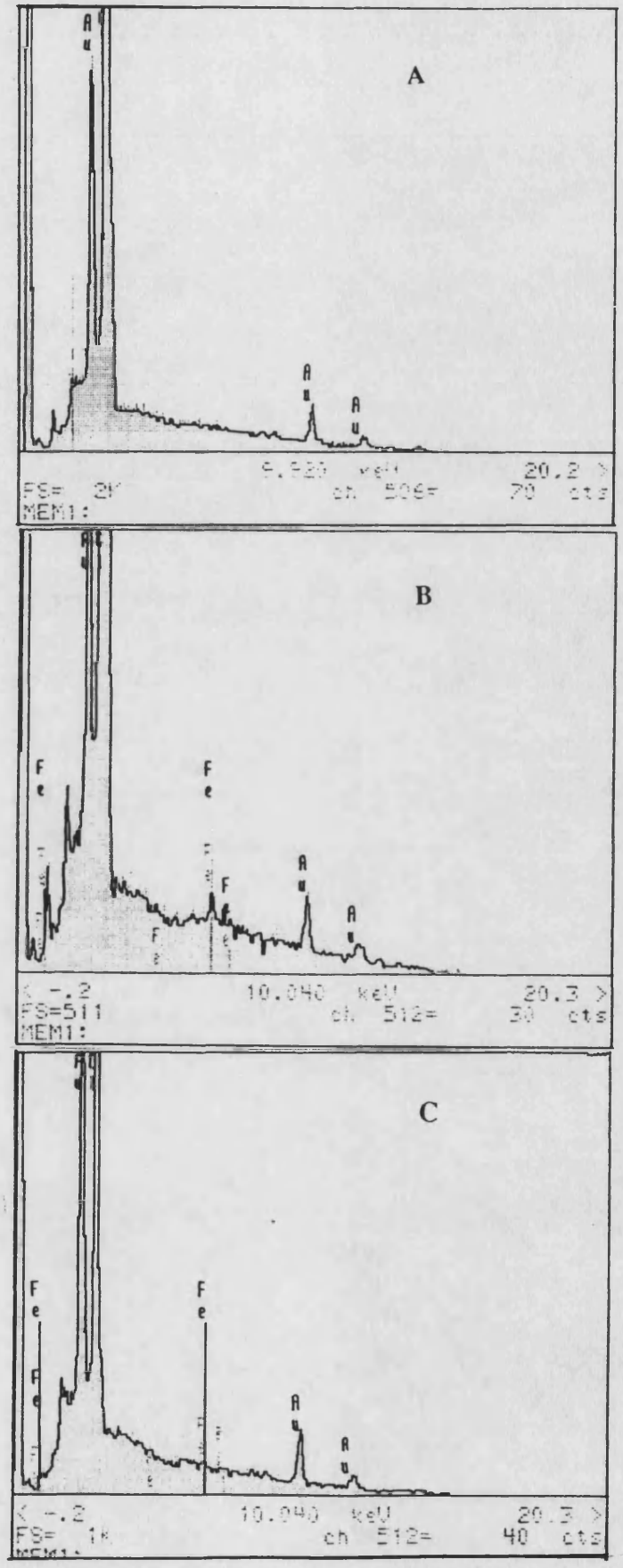

Figure 4.17 EDX spectra of PVC powders; **A** untreated PVC, **B** after reaction with NaOH in the presence of $FeCl_3.6H_2O$, **C** sample **B** after acid washing

In basic media, however, iron(III) chloride will form hydrous ferric oxide precipitates at very slow rates and these may be present as an unbound layer on the polymer surface. These species are yellow in colour due to charge transfer bands which extend into the visible region and may therefore be responsible for the above observations. Accordingly, the sample from experiment 38p was washed with 2 mol dm^{-3} hydrochloric acid to remove any such precipitate. The resulting polymer showed little absorbance in the diffuse reflectance uv spectrum as shown in figure 4.16 and no residual iron was found in the EDX spectrum as shown in figure 4.17c. This would suggest that hydrous ferric oxide was responsible for the absorbance bands seen in experiment 37 and 38p, although it could be argued that the rate of precipitation is too low to be observed and the acid serves only to remove the chelated iron.

In a recent report by Carty *et al.*[233] the catalytic effect of iron (III) chloride on the thermal dehydrochlorination of PVC was discussed and a cross linking mechanism for the process was proposed. It was thought that a similar process might be possible during the sonochemical reaction of PVC with base in the presence of $FeCl_3.6H_2O$. A possible mechanism for this reaction would then involve $FeCl_3.6H_2O$ catalysed E1 elimination to give a carbonium ion which could then react internally with the double bonds formed by the competing base catalysed, E1cB, elimination of HCl.

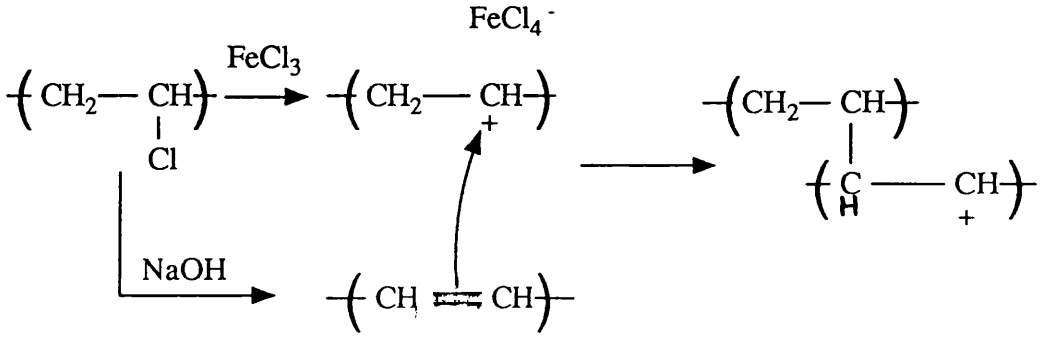

Scheme 4.12

As the sodium hydroxide - PVC interface is sharp, reaction would be

expected to occur only in the outer few monolayers of the surface. Accordingly, a cross-linked surface region would be expected. To verify this theory, samples of PVC powder from experiment 38p were stirred in THF, a good solvent for the PVC starting material. At concentrations of less than 1% $^{w}/v$ some polymer remained visibly undissolved even after stirring overnight at elevated temperature (≈50°C). This insolubility, however, is characteristic of the conjugated polymers produced by elimination of HCl. Whilst elimination can be anticipated in this system, the levels are expected to be below those which would be necessary to cause insolubility, since no double bond stretching bands were discernible in the DRIFTS spectrum of this sample. Hence, it is thought that the observed insolubility results from surface cross linking.

This reaction system was then extended to include PVC films solution cast from THF, experiments 39p to 41p in table 2.3. ATR analysis of the film samples from both experiments, 39p and 40p, with 2 mol dm^{-3} (8% $^{w}/v$) sodium hydroxide failed to show any changes from the pure PVC film. At 25% $^{w}/v$ sodium hydroxide concentration (experiment 41p) the ATR spectrum, as given in figure 4.18, showed the presence of a broad absorbance band centred around 1770 cm^{-1} characteristic of the stretching frequency of carbonyl groups. It would seem therefore, that increasing base concentration promotes the elimination of HCl, but this is also accompanied by concurrent oxidation reactions. The air oxidation of unsaturated sequences formed during dehydrochlorination of PVC has been reported previously by Campbell and Rauscher.[115] In view of this observation, it can be argued that reaction of PVC powders with the more dilute base may also have generated surface oxygen species which promoted chelation of the metal ions.

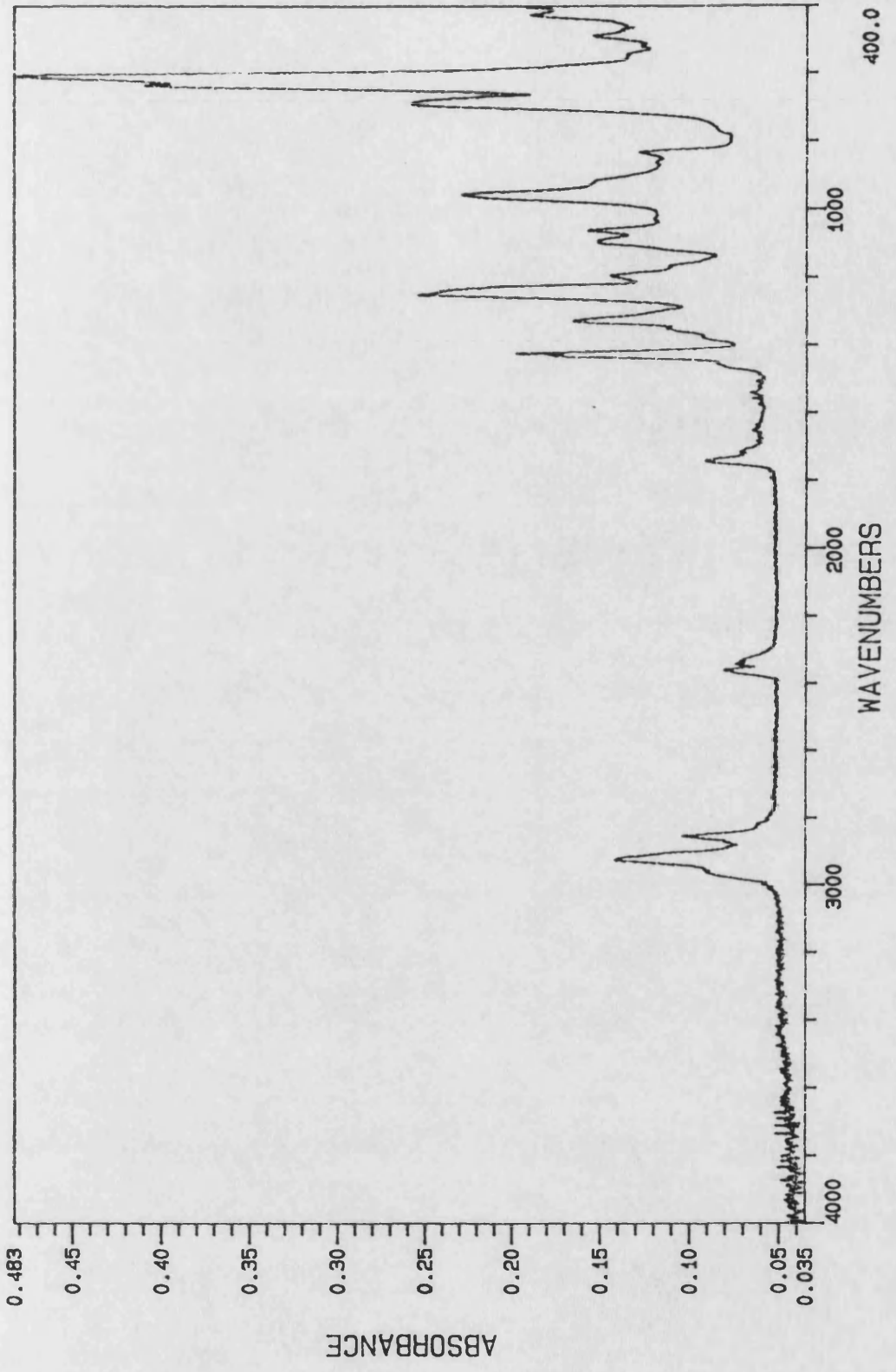

Figure 4.18 The 45° ATR spectrum of a PVC film after reaction with 25% $^{w}/_{v}$ NaOH in the presence of $FeCl_3.6H_2O$

Following the success with iron (III) chloride two other Lewis acids, $AlCl_3$ and $ZnCl_2$, were employed (experiments 42 and 43 respectively), but failed to produce any changes in the diffuse reflectance ir and uv spectra from the untreated base PVC. Subsequent analysis by EDX also failed to detect any residual aluminium or zinc on the polymer samples. Finally, samples were found to dissolve completely in THF. On the basis of this evidence it would seem that, at best, only very low levels of modification were obtained with $AlCl_3$ and $ZnCl_2$.

4.2.1.1 The Generation Of Surface Double Bonds

In the present work dehydrochlorination reactions were carried out on PVC surfaces primarily to generate double bonds which it was anticipated could then be used as a starting point for secondary reactions.

The base catalysed dehydrochlorination of PVC using a phase transfer catalyst such as tetrabutyl ammonium bromide has been widely reported in the literature.[115-7,119] In addition, the elimination of HF from PVF_2 using an aqueous base and phase transfer catalyst has also been reported to exhibit a rate enhancement during the application of ultrasound.[121] These reactions are reported to occur by a "zipper-like" mechanism as outlined in scheme 4.11, producing conjugated sequences of 7-12 double bonds.

An initial attempt at sonochemical dehydrochlorination (experiments 44 to 46) was carried out on PVC powders. The reflectance ultraviolet spectra from these studies are presented in figure 4.19 and the DRIFT spectrum of the product from experiment 45p in figure 4.20. The intensity and λ_{max} of the uv absorbance band suggests that high levels of conjugation can be achieved on the polymer surface in only 5 minutes using the ultrasonic probe at an intensity of 26.2 W cm^{-2}. This is further supported by the intensity of the broad absorbance band between 1600cm^{-1} and 1750cm^{-1} in the DRIFT spectrum, 4.20 compared with untreated PVC in figure 4.12A , which indicates the formation of both a number of environmentally different carbon-carbon double bonds, but also suggests the presence of a number of carbonyl

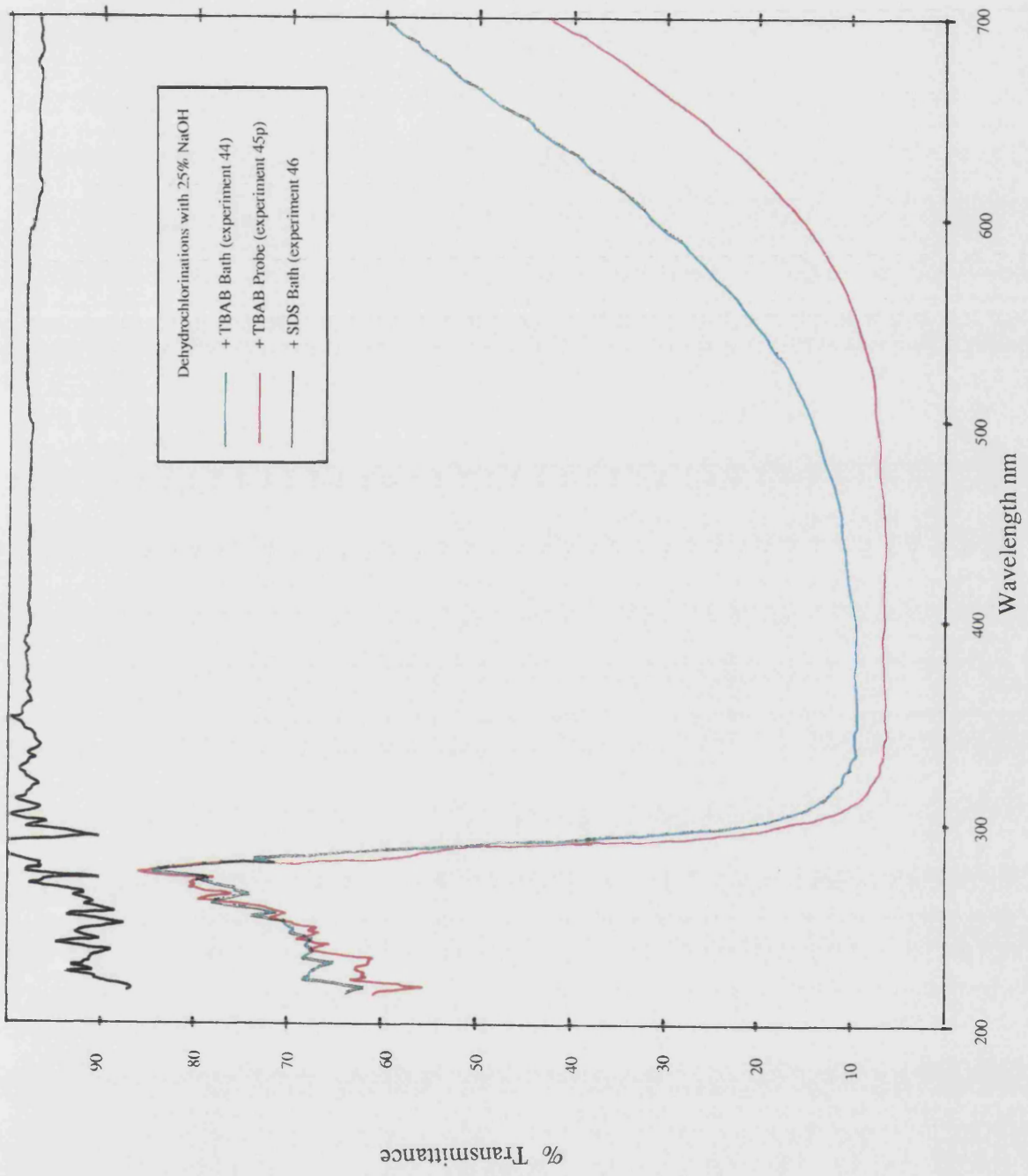

Figure 4.19 Diffuse reflectance ultraviolet spectra of PVC powders after reaction with 25% $^{w}/_{v}$ NaOH and TBAB

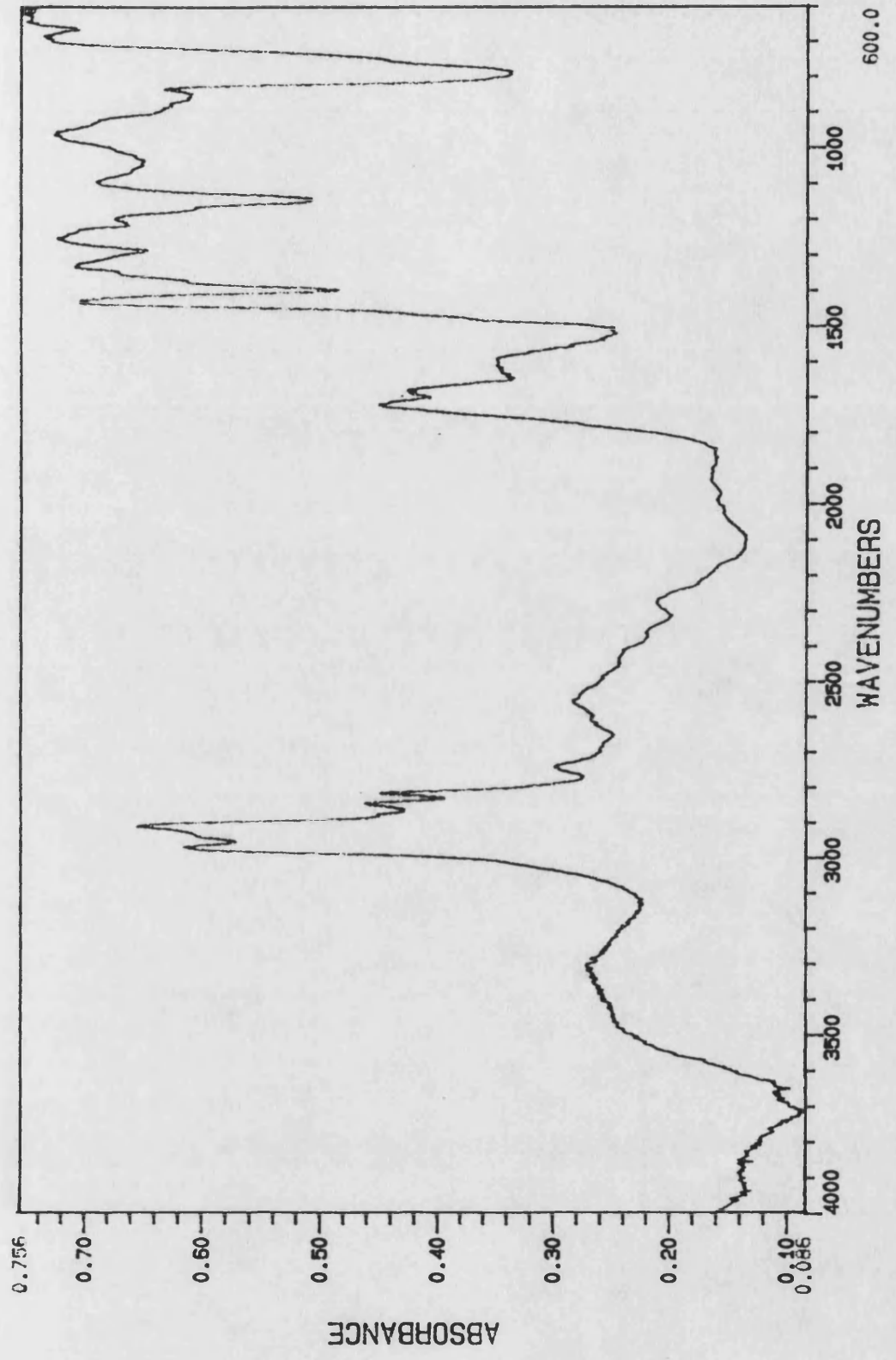

Figure 4.20 The DRIFT spectrum of PVC powder after 5 minutes reaction with 25% $^{w}/_{v}$ NaOH and TBAB using an ultrasonic probe

species. The air oxidation of unsaturated sequences generated by dehydrochlorination of PVC has been observed in experiment 41p above and has also been reported earlier.[115]

Analogous reactions were then carried out on solution cast PVC film samples (experiments 47p and 48p). The diffuse reflectance uv spectra of these samples, figure 4.21, show that sequences of unsaturated carbon-carbon bonds were formed with 25% $^{w}/_{v}$ sodium hydroxide, but not when 8% $^{w}/_{v}$ sodium hydroxide was used. The ATR spectrum from experiment 48p with 25% $^{w}/_{v}$ NaOH, shown with that of pure PVC in figure 4.22, showed no absorbance bands due to carbon-carbon double bonds. This would suggest that under these dehydrochlorinating conditions, reaction is limited to a very shallow surface layer much less than 1μm thick.

These results suggest that high levels of conjugation can be readily achieved at the surface of PVC powders and films with 25% NaOH and TBAB, but this conjugation is limited to a very thin surface layer. Furthermore, the above evidence also indicates that these double bonds are reactive and become readily oxidised in air.

4.2.1.2 Reaction Of Surface Double Bonds

The ability to react these double bonds in a secondary transformation would clearly present the ability of selectivity modifying PVC to within 1μm of the surface.

With regard to this aim samples of PVC powder, dehydrochlorinated according to experiment 44p, were washed and sonicated directly in aqueous solutions of each of the dyes displayed in figure 4.4, experiments 49 to 54 in table 2.4.

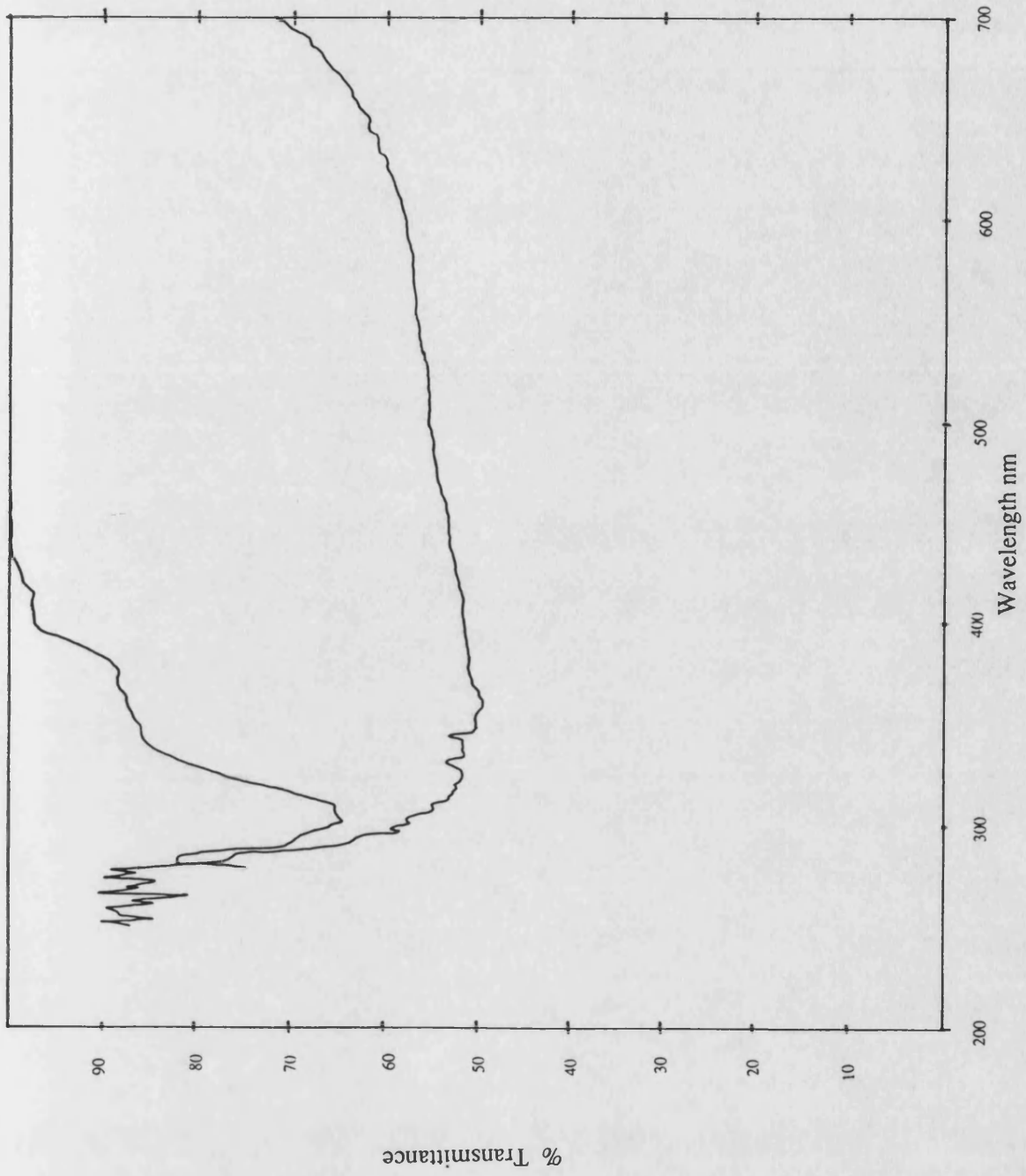

Figure 4.21 Diffuse reflectance ultraviolet spectra of PVC films after reaction with; **A** 8% $^{w}/_{v}$ NaOH and **B** 25% $^{w}/_{v}$ NaOH

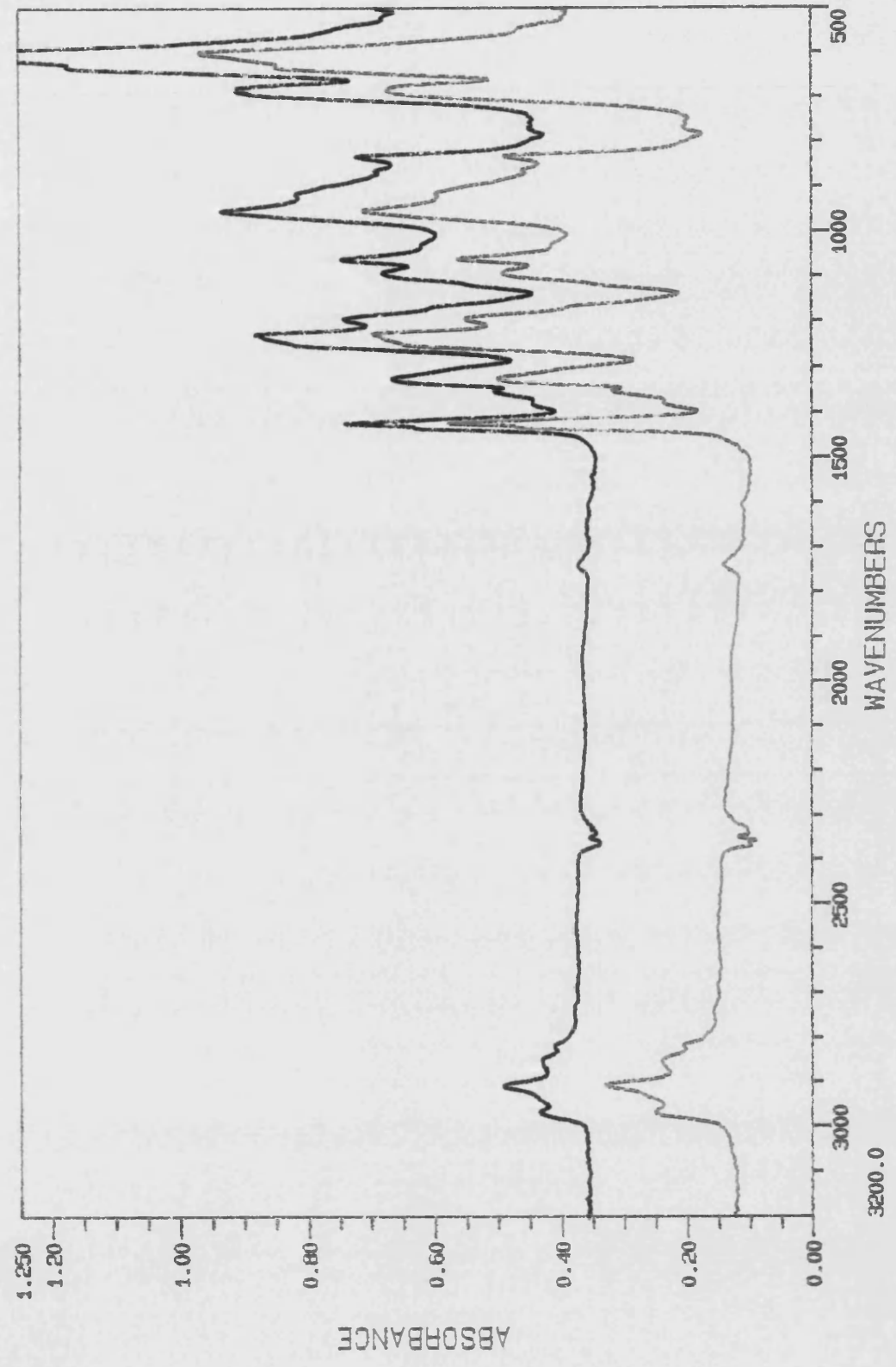

Figure 4.22 The 45° ATR spectrum of PVC after sonochemical dehydrochlorination with 25% $^{w}/_{v}$ NaOH and TBAB ——

The diffuse reflectance uv spectra of the products from these reactions, after 24 hour soxhlet extractions with water, are shown in figure 4.23. Although some absorption bands are present, the major contribution in each spectrum appears to be due to conjugated sequences. The variation in the conjugation absorbance bands between samples is expected to arise through differences in the amount of air oxidation.

In an attempt to increase the hydrophilicity of the PVC surface, reaction was carried out with a 0.4% $^{w}/_{v}$ solution of maleic anhydride, a known dienophile (experiment 55). The DRIFT spectrum of the product from this reaction, figure 4.24, showed a marked decrease in the C=C stretching band from that observed for the dehydrochlorinated sample, figure 4.20. No apparent increase in carbonyl species, however, was observed. The origin of this feature remains unclear, but might arise through solubilisation and removal of the outermost layers of material. Since, it can be envisaged that reaction with maleic anhydride would increase the water solubility of the reacted polymer surface, which ultimately may have become solvated and removed. A similar observation has also been reported for oxidised polyethylene surfaces.[66]

Finally in an attempt to prepare hydrophilic PVC surfaces after dehydrochlorination, reactions were carried out using aqueous acrylic acid solutions, experiments 56 to 58 in table 2.4.

The end PVC sample from experiment 57, in which TBAB was present, is shown in figure 4.25C with that of untreated PVC(A) and dehydrochlorinated PVC(B). This sample showed an increase in the carbonyl absorbance band at ~1725 cm^{-1}. The position of this band is consistent with the carbonyl stretching frequency of acrylic acid and would, therefore, suggest that some reaction occurred in this system. None of the other experiments in this series showed any significant changes with respect to the untreated PVC. Although the mechanism for this transformation is uncertain, it must be concluded that the reaction is facilitated in some way by the

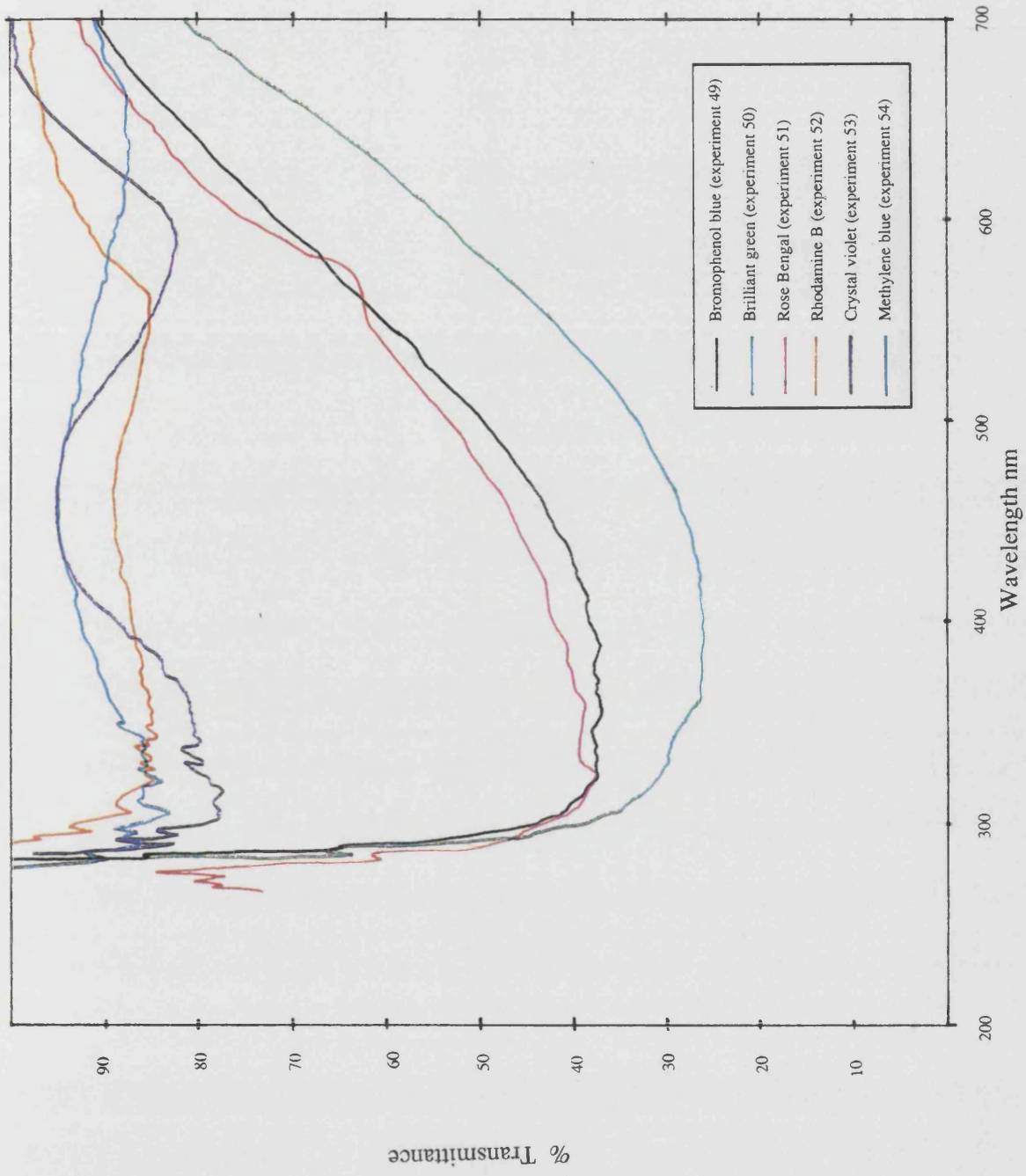

Figure 4.23 Diffuse reflectance ultraviolet spectra of dehydrochlorinated PVC (as experiment 44p) after reaction with aqueous dyes

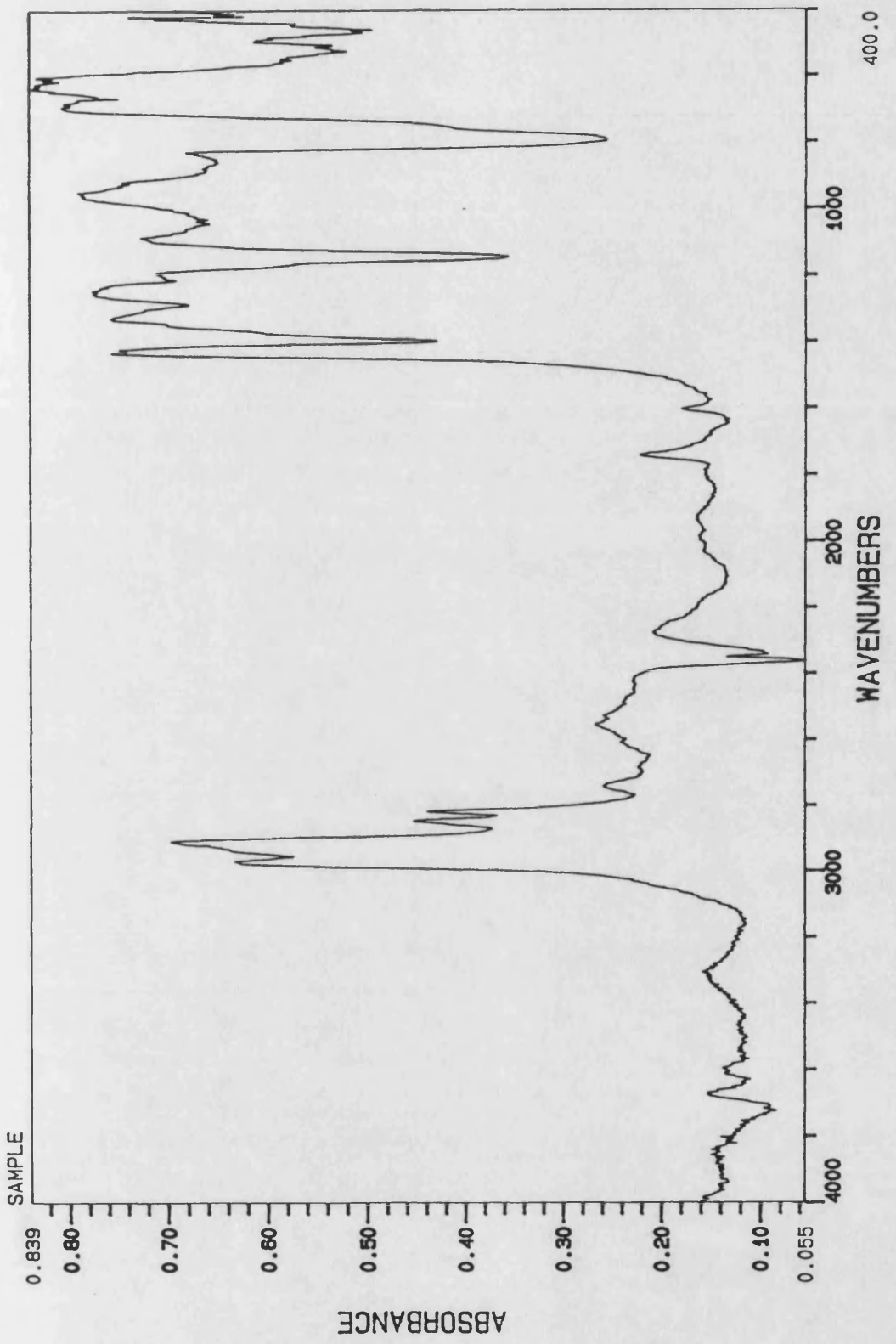

Figure 4.24 The DRIFT spectrum of dehydrochlorinated PVC (as experiment 44p) after reaction with maleic anhydride

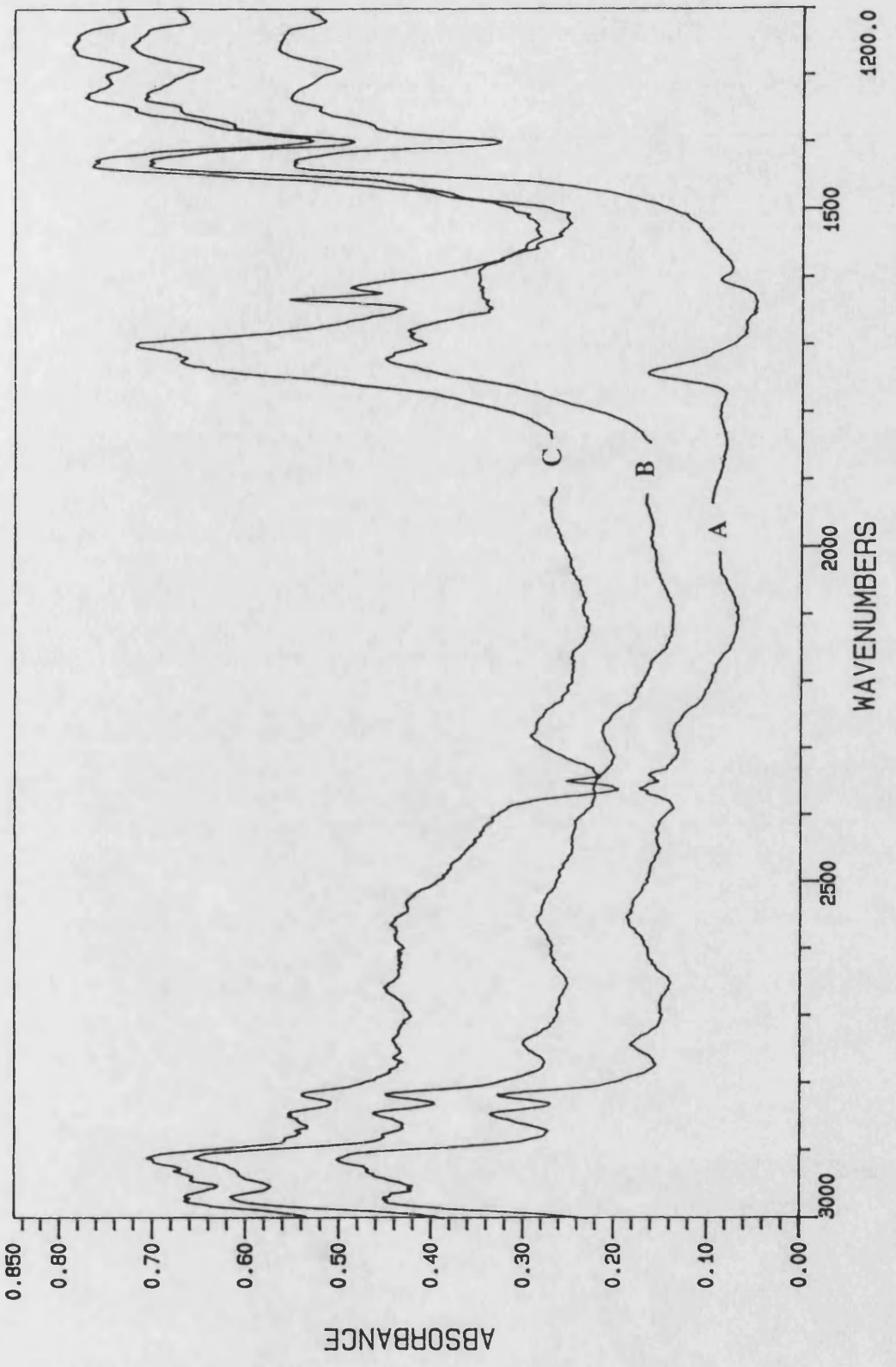

Figure 4.25 DRIFT spectra of, **A** untreated PVC, **B** dehydrochlorinated PVC and **C** sample **B** after reaction with acrylic acid in the presence of ultrasound

presence of the phase transfer catalyst.

In this system it might be argued that the acrylic acid monomer reacts with the PVC surface to initiate polymerisation. The growing macroradicals formed might also react with surface double bonds to form branch points or may simply be terminated. In either instance the grafted material would be much more stable to cavitation since the polymer chains would no longer be extended into the solution.

4.3 Conclusions

In conclusion, it has been shown that ultrasound can be used effectively to colour the surface of PVC powder samples by promoting surface reactions with aqueous solutions of dyes. The final colour of the dyed powder was found to be dependent upon the concentration of dye, sonication time, gaseous atmosphere and the pH of the dye solution for bromophenol blue. Reaction was found to occur with a number of aqueous dyes, allowing several colours to be generated. The most successful coloration was obtained with brilliant green, the reaction mechanism for which is thought to involve the counter ion of the dye in solution.

Direct grafting of aqueous polymers from solution appeared to be less successful, possibly because only a limited number of chain breaks occur near the solid surface. However, it can also be argued that grafting occurs but the grafted polymer surface is unstable towards successive cavitation cycles and is subsequently eroded. Functionalisation seems to be most successful when monomers are polymerised at the surface and the resulting polymers are insoluble in the reaction solvent.

Base catalysed elimination of HCl from PVC can be readily achieved using ultrasound and TBAB as a catalyst. In the presence of metal ions chelation and surface crosslinking is seen to occur. The secondary sonochemical reaction of surface double bonds has shown some promise with acrylic acid in the presence of a small amount of TBAB and maleic anhydride.

These results clearly demonstrate that a number of the targets suggested in section 1.10 can be achieved by using ultrasound. The application of these reactions to "real cable samples" is discussed in chapter 6.

CHAPTER 5

MODIFICATION OF POLYETHYLENE SURFACES

Polyethylene is chemically the simplest of all polymers, consisting of only carbon and hydrogen. Unfortunately, this simplicity renders it relatively inert towards chemical reaction as outlined in section 1.4.1.

To date, only one report in the open literature has addressed the application of ultrasound to heterogeneous polymer modification.[121] It was necessary therefore, to adopt a broad approach to the objectives of modifying the surface hydrophilicity, hardness and colour of polyethylene films and cables.

At the present time it is generally regarded that to chemically modify polyethylene surfaces it is better to first generate some kind of oxidised layer which can be subsequently derivatised.[63] In the present work a number of ultrasonic oxidation routes for polyethylene have been investigated and the most promising of these used to generate the starting material for further sonochemical derivatisation studies. Finally, the ability of ultrasound to bring about grafting and chemical modification in a single step has been investigated for a few systems.

Since most sonochemical processes are reported to be accelerated at lower temperature and in view of the report by Niemeczewski that water has a cavitation maximum at 35°C,[140] it was considered pertinent to carry out oxidation reactions in the present work at this temperature.

The oxidation of polyethylene by wet chemical methods generally requires very strong oxidising agents. Those systems chosen for use in the present studies are shown in table 5.1 along with their respective redox potentials.[234]

Table 5.1

Oxidising agent	Redox reaction	Potential
Dichromate	$Cr_2O_7^{2-} + 14H^+ + 6e^- \longrightarrow 2Cr^{3+} + 7H_2O$	$E^o = 1.36$ v
Peroxide	$H_2O_2 + 2H^+ + 2e^- \longrightarrow 2H_2O$	$E^o = 1.763$ v
Persulphate	$S_2O_8 + 2e^- \longrightarrow 2SO_4^{2-}$	$E^o = 1.96$ v
	$S_2O_8 + 2e^- + 2H^+ \longrightarrow 2HSO_4^-$	$E^o = 2.08$ v

These systems clearly present a strong oxidising ability and each will be dealt with below.

5.1 Reactions With Dichromate

One of the most successful chemical methods for the modification of polyethylene surfaces has been that of chromic acid oxidation.[235] This system results in the formation of a number of oxygen containing species, the relative concentration of which can be controlled to some degree by varying the reaction conditions.[56-7] The mechanism for alkane oxidation in the absence of ultrasound has been described by Wiberg and Eisenthal and is outlined in scheme 5.1.[236]

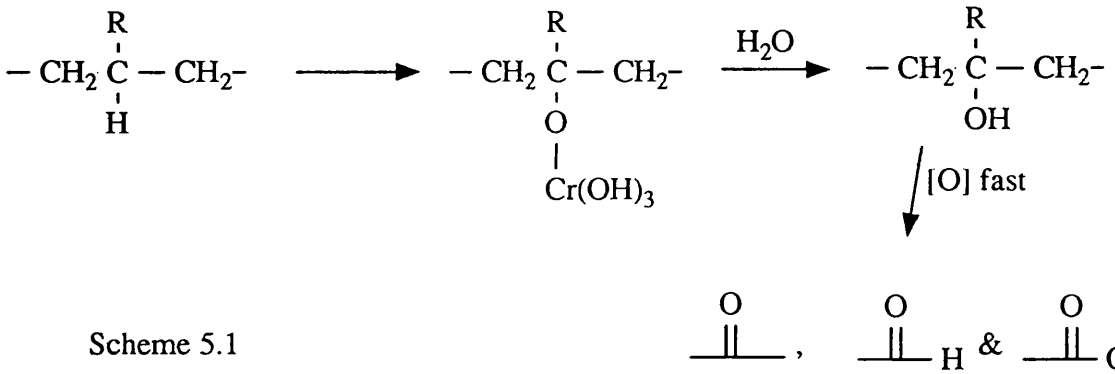

Scheme 5.1

In the present work chromic acid oxidations were performed in an identical manner to that of Rasmussen *et al.*, the end samples being used as a guide to establish the accuracy of the contact angle measurement technique.

Contact angle values obtained from these oxidised polyethylene samples are shown in table 5.2 along with those obtained for the starting polyethylene and a typical literature range for this system.

Table 5.2

Contact angle values for oxidised polyethylene

Polyethylene	Oxidised polyethylene	Literature range[56,58]
98.6°	62.2°	45-66°
97.4°	58.6°	

Clearly, the contact angle values obtained in the present work compare favourably with those reported in the literature and, moreover, are significantly different from the starting material to allow changes in surface character to be followed.

The highly corrosive nature of the chromic acid oxidising system rendered it unsuitable for use in the present study, as targets were to develop modification systems with a lower capacity for corrosion. Accordingly, ultrasonic reactions were carried out using a more dilute solution consisting of 5g $K_2Cr_2O_7$ dissolved in 150 cm^3 of 32.0% $^w/_v$ H_2SO_4. Sonication and stirred control reactions were conducted for five hours after which time the films were removed, washed and dried as described in section 2.7.1. Contact angle measurement and ATR-ir analyses were then carried out according to the procedures in sections 2.11 and 2.10 respectively.

The contact angle values for the ultrasonic and stirred samples were 93.5 and 94.4° respectively. Thus, both samples showed a small decrease in value from the starting polyethylene, but remained within the ± 5° level of accuracy predicted for

these measurements. Neither sample showed any signs of oxidation by ATR-ir in the region 2000-1500 cm^{-1}.

These results would suggest that some oxidation might be achieved with this acidified dichromate solution, although the levels can be expected to be low. Furthermore, ultrasound appears to have little accelerating affect on the oxidation process.

Accordingly, on the basis of these results and those reported by other workers, it was anticipated that this system would be unable to meet the present requirements of a rapid, low or non-corrosive functionalising system for polyethylene surfaces.

5.2 Reaction With Hydrogen Peroxide

Fragmentation of hydrogen peroxide yields highly reactive hydroxyl radicals according to:

$$H_2O_2 \longrightarrow 2OH\cdot \qquad (5.2)$$

This decomposition process is reported to be accelerated by the presence of trace amounts of metal ions such as iron(II).[62]

$$Fe^{2+} + H_2O_2 \longrightarrow Fe^{3+} + OH^- + OH\cdot \qquad (5.3)$$

In the present study samples of polyethylene film were sonicated in a variety of hydrogen peroxide solutions according to the procedure outlined in section 2.7.1. The water contact angle values of the resulting films were then measured and are shown in table 5.3 along with the values obtained for stirred control samples.

Table 5.3

Water contact angle values for polyethylene films oxidised by hydrogen peroxide.

Hydrogen peroxide system *	Contact angle °	
	Stirred	Ultrasound
H_2O	97.1	94.1
6%	96.1	94
30%	95.4	89.8
6% + $FeSO_4$(0.15g)	100.8	91.8
30% + $FeSO_4$(0.15g)	------	89.7
30% + $FeCl_3$ (0.1g)	93	89.7
6% + Maleic anhydride (5g)	------	84.9

* Concentration values are %by volume

All of the stirred control reactions gave water contact angles to within five degrees of the starting polyethylene film (~98°). The most significant change was observed with 30% peroxide containing iron(III) chloride, indicating that some reaction occurred with this system. No signs of oxidation were, however, observed in the ATR spectrum of this sample. However, extremely low levels of oxidation can be expected in these systems, since oxidation of polyethylene is known to occur at very slow rates in aqueous media.[61,62] The oxidation levels achieved in these stirred control systems remain low over the five hour time scale employed. Accordingly, acceleration of this oxidation process by ultrasound could present a useful modification method.

The application of ultrasound to these systems clearly presents a marked change in the water contact angle values. As described in chapter 3, sonication of polyethylene film samples at the intensity used here (26.2 Wcm^{-2}) has been shown

to cause surface erosion and roughening. The presence of surface damage cannot, however, be responsible for the changes in contact angles observed here. Since polyethylene has an intrinsic contact angle of greater than 90°, any change in the surface roughness would be expected to produce an increase in the observed contact angle according to Wenzel's equation (1.5),[19] as discussed in section 1.3.3.3, rather than the decrease observed in these experiments. Furthermore, the relatively large droplet size used for measurements would be expected to reduce inaccuracies incurred by the formation of a tortuous perimeter as outlined in section 1.3.1.3.[20]

From table 5.3 it can be seen that the biggest change in contact angle was obtained at 30% peroxide concentration, whilst 6% peroxide produced little significant change. Addition of trace amounts of Fe^{2+} or Fe^{3+} appeared to have little or no further effect on the oxidation process with 30% peroxide, but gave a more marked effect with 6% peroxide. However, analysis of the polyethylene film samples oxidised with 6% peroxide both with and without metals present failed to show any oxidation by ATR-ir.

Reaction with 30% peroxide alone also failed to show any oxidation by ATR-ir, but the product from the reaction with iron(II) sulphate present clearly shows the presence of a broad absorbance band at ~1725 cm^{-1}. The position of this band is consistent with the formation of mainly ketone groups. This spectrum is shown in figure 5.1B along with those of virgin polyethylene (5.1A) and a TFAA derivatised sample of the oxidised film (5.1C)

This experiment was then repeated under identical conditions, but the product was reacted with trifluoroacetic anhydride (TFAA) vapour according to the procedure in section 2.7.2. This derivatisation should selectively label any hydroxyl groups present, generating trifluoro esters. This was necessary, since it was expected that reaction with sonochemically generated hydroxyl radicals would generate surface hydroxyl groups. The resulting ATR-ir spectrum of this sample is also shown in figure 5.1 along with the spectra for the oxidised sample and starting polyethylene. The reacted sample has an absorbance band at ~1786 cm^{-1} which is

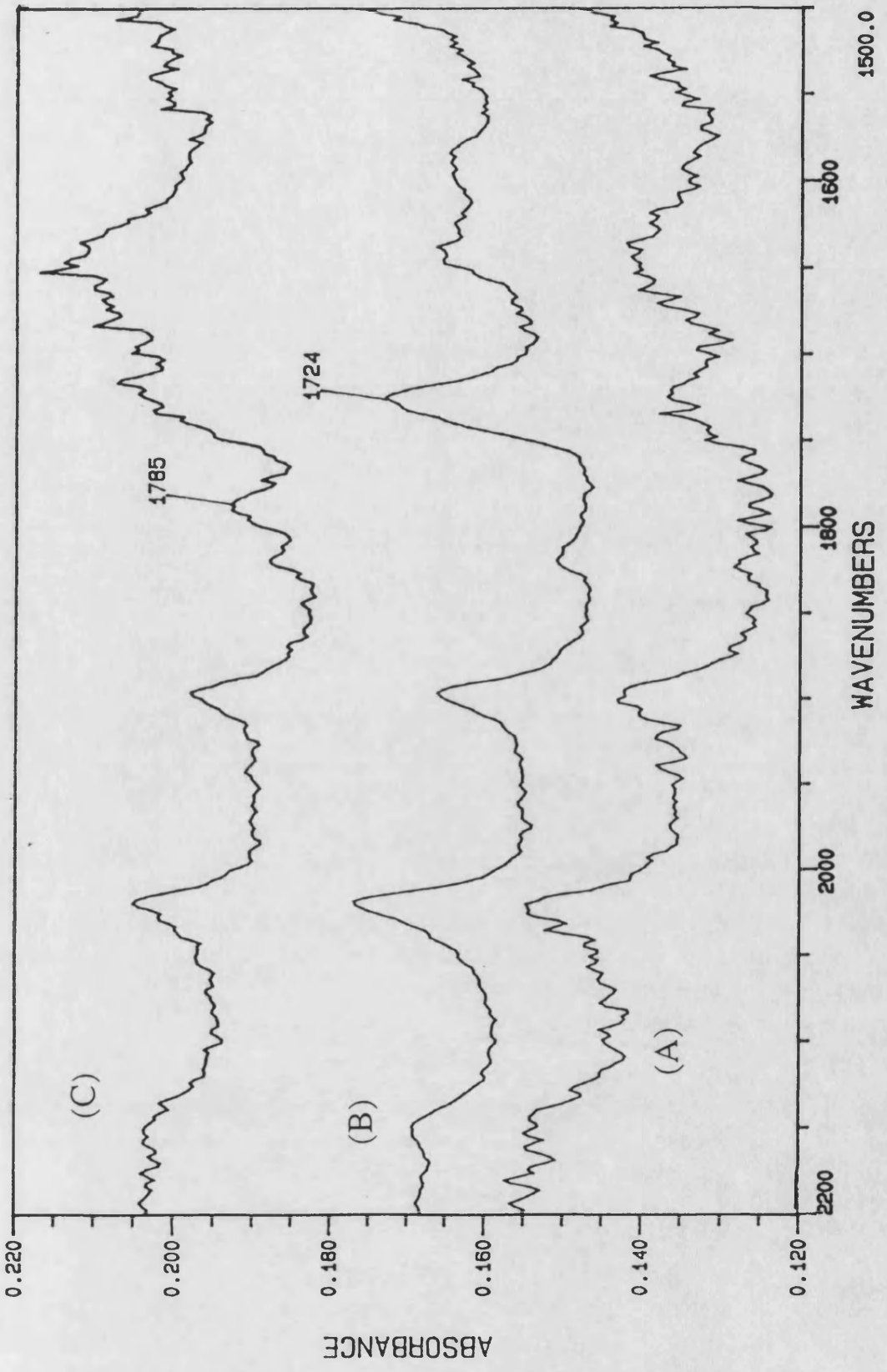

Figure 5.1 ATR spectra at 60° of polyethylene (A), polyethylene oxidised with 30% H_2O_2 and $FeSO_4$ (B) and sample (B) after derivatisation with TFAA (C)

characteristic of the carbonyl group of the fluoroesters formed by the reaction of hydroxyl groups with TFAA as shown in scheme 5.4.

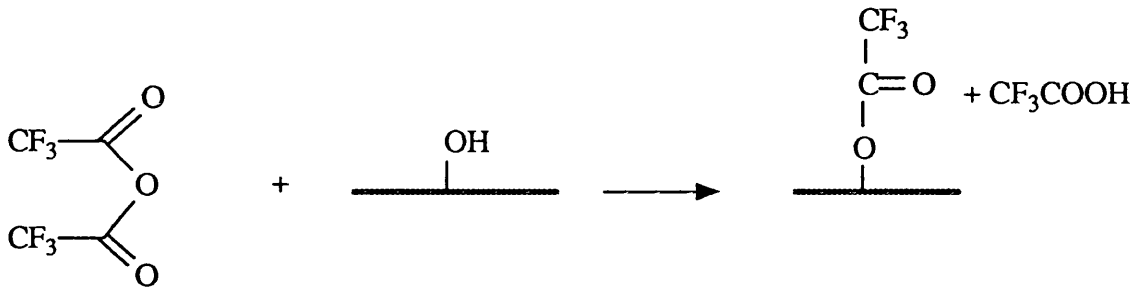

Scheme 5.4

The relatively weak intensity of this band would suggest that only a small proportion of hydroxyl groups are generated during reaction with peroxide, although the initial step of oxidation might involve the formation of a hydroxyl group which is subsequently oxidised further to give a ketone. Moreover, the formation of mainly ketone groups would serve to suggest that only limited scission of the polymer chains occurs during oxidation by this method.

5.3 Reaction With The Persulphate Oxidising System

5.3.1 Rate of Persulphate Decomposition

Persulphates are well known free radical initiators for polymerisation reactions. During heating the persulphate molecule splits homolytically with first order kinetics according to scheme 5.5.

$$S_2O_8^{2-} \xrightarrow{\Delta} 2SO_4^{\cdot -} \qquad (5.5)$$

Schumb and Ritner reported that the decomposition of potassium persulphate underwent a slight rate increase (~10%) during sonication at 8.7 kHz.[202] Later,

Lorimer *et al.* reported that the decomposition underwent a rate increase between 50 and 70°C during sonication at several ultrasonic intensities, although the decomposition was only studied above 50°C.[203] In this study, the temperature range has been extended because sonochemical reactions are often more efficient at low temperature.

Initially, a survey of the decomposition kinetics for potassium persulphate was undertaken at several temperatures and ultrasonic intensities according to the procedure outlined in section 2.8. The first order rate constants for these experiments are presented in tables 5.4 and 5.5 and the raw data have been presented graphically in appendix 1. The Arrhenius plots of these data are shown in figures 5.2a and 5.2b for the thermal and ultrasonic decompositions respectively.

Table 5.4 ·

First order rate constants for the thermal and ultrasonic decomposition of potassium persulphate

Temperature °C	Rate constant $min^{-1} \times 10^{-3}$	
	Thermal	Ultrasonic
25	---	0.510
35	0.060	0.663
45	---	1.028
55	0.541	1.432
65	4.263	4.260
75	12.487	8.985

From table 5.4 it can be seen that the rate for the ultrasonic decomposition of potassium persulphate is increased quite markedly over the thermal decomposition below ~65°C. Above this temperature the effect appears to be negligible and the

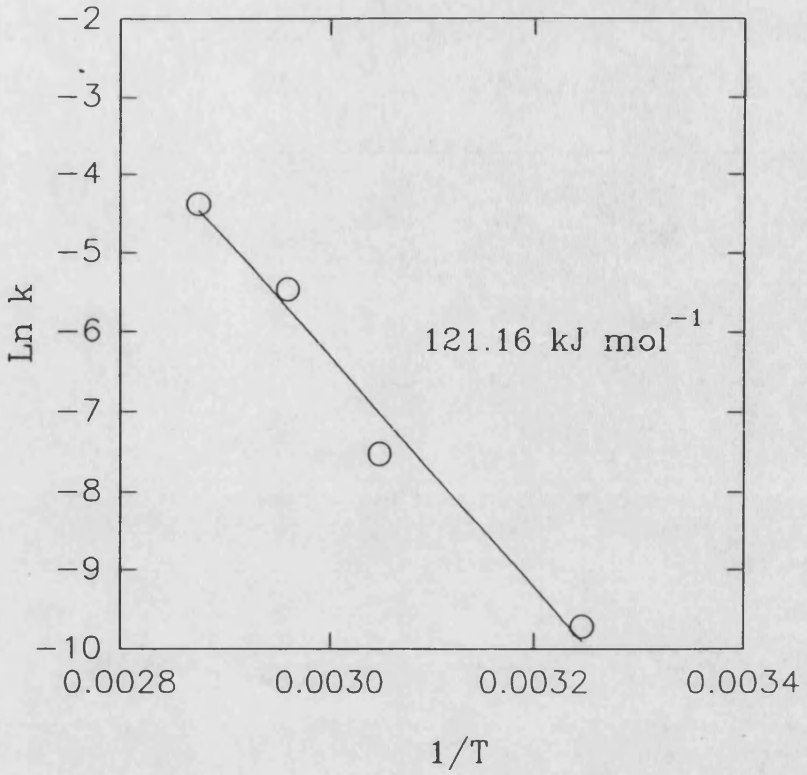

Figure 5.2a Arrhenius plot for the thermal decomposition of potassium persulphate

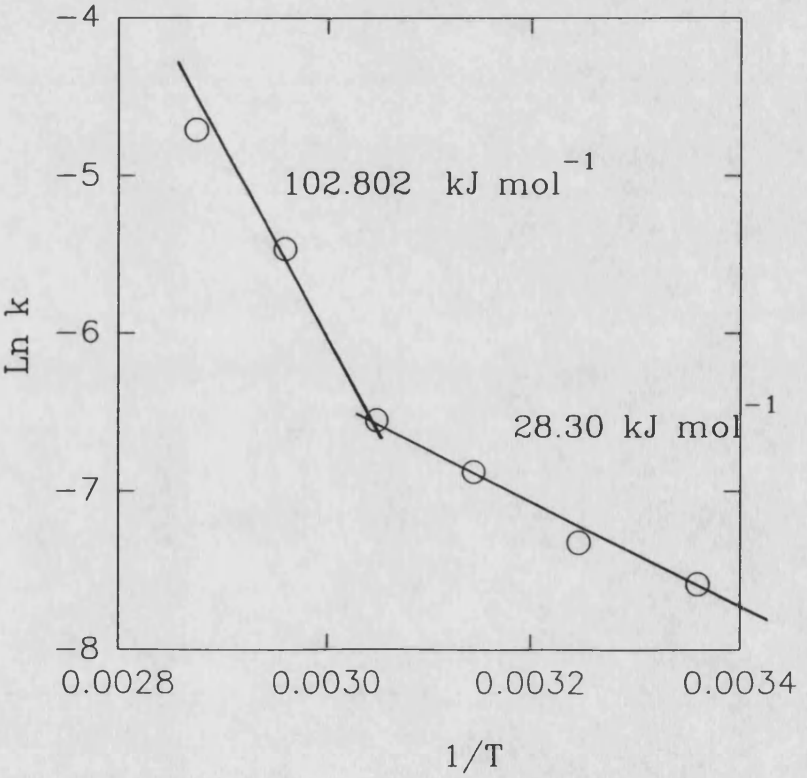

Figure 5.2b Arrhenius plot for the ultrasonic decomposition of potassium persulphate

rate constant at 75°C is less than that observed for the thermal process alone. This feature is possibly due to poor mixing in the ultrasonic experiment as a result of the much lower cavitation intensity obtained at this temperature.

The Arrhenius plot of the thermal decomposition process gives a value of 121.2 kJ mol^{-1} for the activation energy, which compares favourably with a literature value of 140 kJ mol^{-1} in basic media.[237] The ultrasonic decomposition however, appears to produce two linear regions giving values of 102.8 kJ mol^{-1} and 28.3 kJ mol^{-1} for the reaction above and below 55°C respectively. Thus, it would seem that above 55°C the decomposition is thermally controlled, but below this the ultrasonic contribution becomes increasingly more important.

Table 5.5

First order rate constants for the decomposition of potassium persulphate at 35°C using various ultrasonic intensities.

Ultrasonic Intensity Wcm^{-2}	Rate constant min^{-1} x 10^{-3}
16.8	0.488
26.2	0.663
33.2	1.002
49.1	0.810

The data in table 5.5 and figure 5.3 show the change in rate constant as a function of the ultrasonic intensity. Clearly, k passes through a maximum value ~33 W cm^{-2}. This feature, noted by several workers, can be attributed to the ultrasonic cavitation process, since an increase in the intensity will cause an increase in both the number and size of the cavitation bubbles. This relationship does not continue indefinitely, because these bubbles may become too large to collapse during the compression cycle of the cavitation process.[126,134] In addition, the presence of large

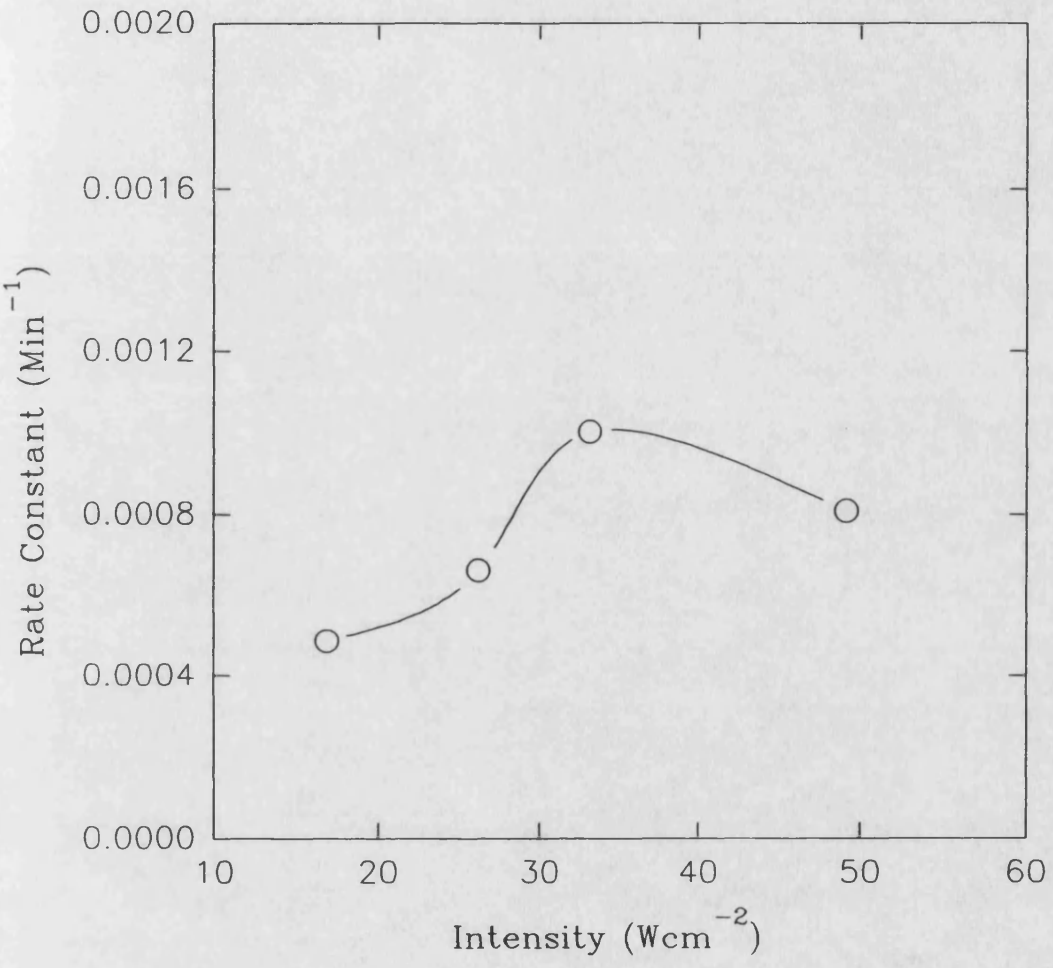

Figure 5.3 The variation in rate constant as a function of ultrasonic intensity for potassium persulphate decomposition at 35°C

numbers of bubbles at the surface of the ultrasonic source will give rise to inefficient coupling of the sound waves with the liquid, hence reducing the effective energy input as discussed in section 1.6.

Finally, it can be expected that hydroxyl radicals produced by the ultrasonic fragmentation of water will also react with the N-^{t}butyl-α-phenyl nitrone spin trap. The contribution of these reactions to the overall rate of disappearance of the nitrone spin trap in the present study is expected to be negligible, since previous workers, using the dosimeter systems outlined in section 1, have shown that the number of radicals generated by the homolysis of water are of the order $5x10^{-7}$ moles per hour in 150 cm^3 of water at an ultrasonic intensity of 27.6 Wcm^{-2}. Whilst the change in concentration of the nitrone spin trap used for the present study was of the order of $\sim 1x10^{-3}$ moles. Thus, the error obtained through the non-consideration of water fragmentation can be expected to be less than 0.1%.

Thus, it has been shown that ultrasound accelerates the decomposition of potassium persulphate by a factor of ~10 at 35°C. Ultrasound can, therefore, be used to increase both the rate of production of reactive species in solution as well promoting mass transfer across the surface.

5.3.2 Oxidation of Polyethylene By Aqueous Persulphate

Initially, a preliminary survey of the potential of aqueous potassium and ammonium persulphate solutions for the ultrasonic oxidation of polyethylene films was undertaken. Experiments were then carried out in the presence of a number of reagents known to affect the decomposition rate of the persulphate systems.[238] These reactions are given in table 5.6 along with the water contact angle values of the resulting film samples.

Table 5.6

Water contact angle values of polyethylene films after reaction with a number of aqueous persulphate systems using ultrasound.

Reactants	Water contact angle °	
	Ultrasound	Stirred
1. 5g $K_2S_2O_8$ in 150 cm^3 water	81.8	96.1
2. As 1 but under nitrogen	92.4	99.5
3. As 1 but 75°C stirring	83.8	94.7
4. 5g $(NH_4)_2K_2S_2O_8$ in 150 cm^3 water	92.2	98.2
5. As 1 + 0.05 g sodium metabisulfite	90.4	---
6. As 2 + 0.05 g sodium metabisulfite	92.5	---
7. As 1 but in 0.05 mol dm^{-3} NaOH	92.9	---
8. As 1 but in 0.05 mol $dm^{-3}H_2SO_4$	89.1	---
9. As 1 + 0.3g $FeCl_3.6H_2O$	81.9	---
10. As 1 + 0.05g sodium dodecyl sulphate	---	93.1
11. as 1 + 5g Maleic Anhydride	84.5	---

From table 5.6 it can be seen that all of the ultrasonic oxidation reactions gave contact angle changes of greater than ± 5° with respect to untreated polyethylene, whilst none of the stirred control reactions at 35°C showed significant changes.

As discussed in section 5.2 for hydrogen peroxide, the origin of these changes cannot be ascribed to either the aqueous environment alone or the increase in surface roughness, since sonication in pure water failed to give a significant change in contact angle and an increase in surface roughness would be expected to give an increase in the intrinsic contact angle according to Wenzel's equation (1.5).[19]

Previously, Morris has studied the effects of ammonium persulphate treatment on polyethylene adhesive joint strengths.[239] Large increases in joint strength were achieved using 0.26 mol dm^{-3} (8.89g/150 cm^3) aqueous persulphate solution, although only a small change in the critical surface tension of wetting was observed. In all cases small carbonyl peaks were reported to be visible in the ATR-ir spectra although no spectra or location for these bands were given. Reacted samples were reported to be partially insoluble in p-xylene and the increased adhesive joint strength was attributed to surface cross-linking.

The first conclusion to be drawn from table 5.6 is that ultrasound clearly plays a significant role in the surface reactions. Reaction with potassium persulphate both under air and nitrogen gave similar results, with the contact angle in each case being reduced by about 16° respectve to untreted polyethylene. The same reaction in air at 75°C using stirring, which would yield a similar quantity of radical species, gave a much smaller change of about 5° in the contact angle. Hence, ultrasound is promoting a surface reaction as well as accelerating the production of radical species. The ATR spectrum from the 75°C reaction, however, showed the presence of a carbonyl stretching band at 1744 cm^{-1} as displayed in figure 5.4. No such bands were apparent in the sonochemically treated samples. This can perhaps be attributed to the much softer surface and increased mobility of polymer chains at high temperatures resulting in deeper penetration of reagents into the film. In addition, this mobility may lead to reorganisation of the modified surface, again leading to deeper levels of functionalisation. At 35°C the polymer is much harder and hence functionalisation will be more localised at the surface.

The contact angle changes in table 5.6 also signify that some reaction occurred with ammonium persulphate alone (experiment 4), although modification appeared to be more substantial with the potassium salt. Analysis of this sample by ATR-ir also showed the presence of a new absorbance band at ~1745 cm^{-1}, (figure 5.5). The position of this band is consistent with the carbonyl stretching of organic esters.

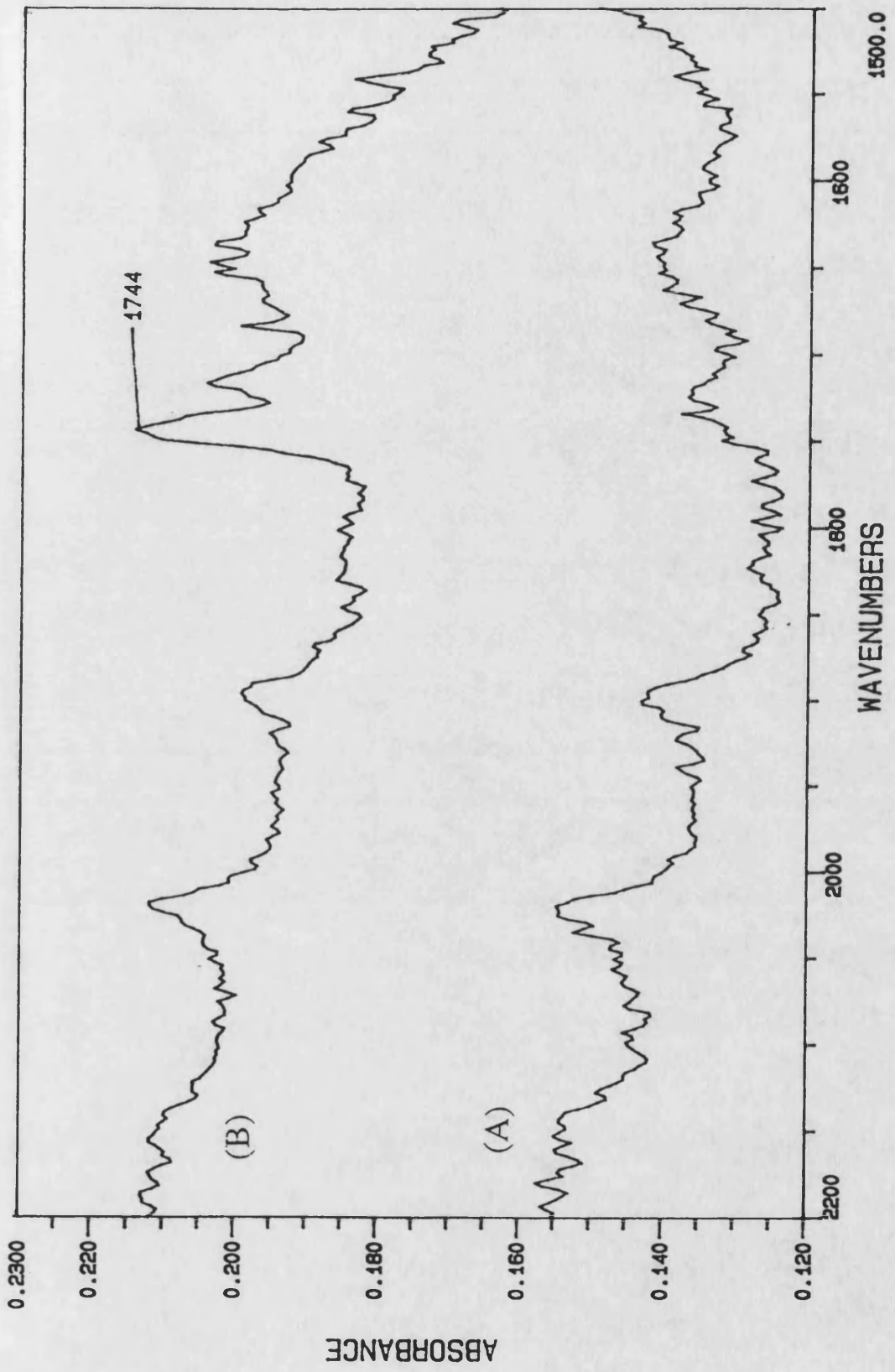

Figure 5.4 The 60° ATR spectrum of polyethylene (A) and polyethylene oxidised with potassium persulphate at 75°C (B)

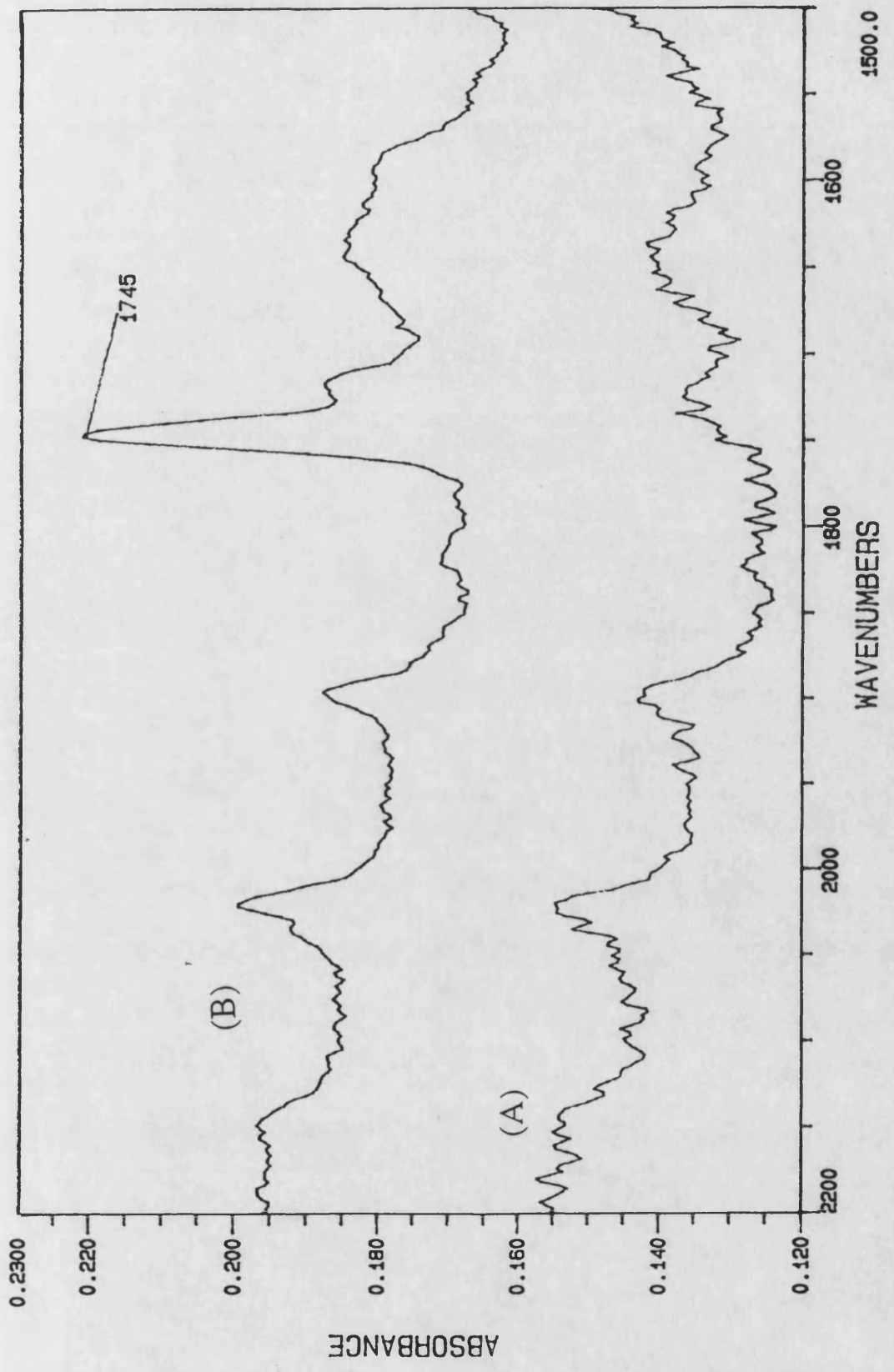

Figure 5.5 The 60° ATR spectrum of polyethylene (A) and polyethylene oxidised with ammonium persulphate at 35°C using ultrasound (B)

These observations suggest that a greater level of oxidation is achieved with ammonium persulphate than with potassium persulphate. The contact angle data, however, indicate that the degree of oxidation is lower with ammonium persulphate. Cumulatively these features suggest that the oxidation layer is more diffuse but distributed over a deeper region of the infrared sampling depth (~0.75μm) with the ammonium salt, but is confined to the outermost molecular layer with the potassium salt and therefore undetected by ATR-ir. The origin of these differences remains unclear, but may be attributable to the ability of ammonium salts to act as phase transfer catalysts. Thus, the ammonium persulphate may penetrate into the polymer surface much more readily, thereby allowing a greater depth of reaction to occur.

The oxidised film samples from the above experiment with potassium persulphate were subsequently analysed for changes in the surface oxygen content with respect to untreated polyethylene by EDX. No significant changes in the oxygen to carbon ratio were detected and these spectra are shown in figures 5.6a and 5.6b for polyethylene and the oxidised sample respectively. No evidence for crosslinking was obtained with either sample 1 or 4, since both these samples and the untreated polyethylene were found to dissolve completely in hot decalin.

Addition of sodium metabisulphite, a known accelerator for persulphate decomposition, failed to cause any changes in the wetting characteristics of either film sample (experiments 5 & 6 in table 5.6) from those obtained with each of the persulphate salts alone. Again, carbonyl activity was only present with the ammonium persulphate treated film giving further credence to the above discussion.

Studies of the thermal decomposition kinetics for sodium and potassium persulphate in basic, neutral and dilute acid solutions by Green and Mason[240] and later by Kolthoff and Miller[237] showed that the reaction is catalysed by the addition of acids.

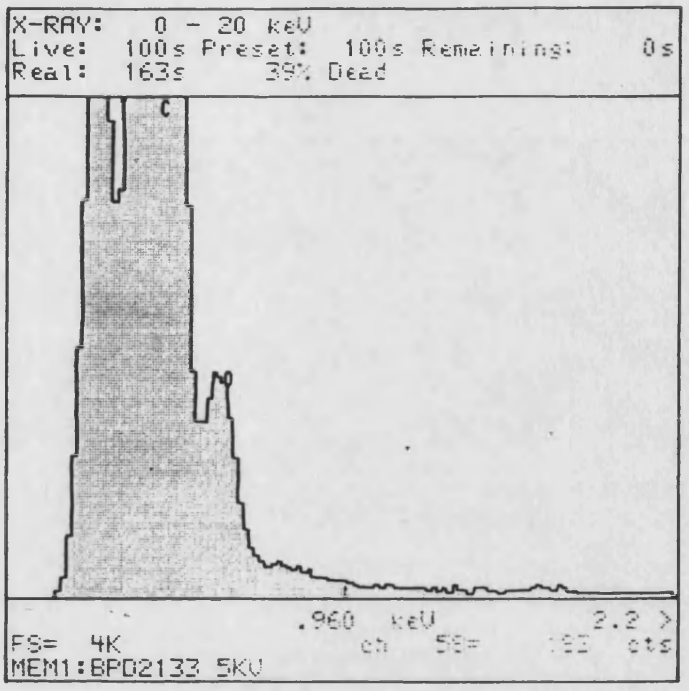

Figure 5.6a EDX spectrum of untreated polyethylene

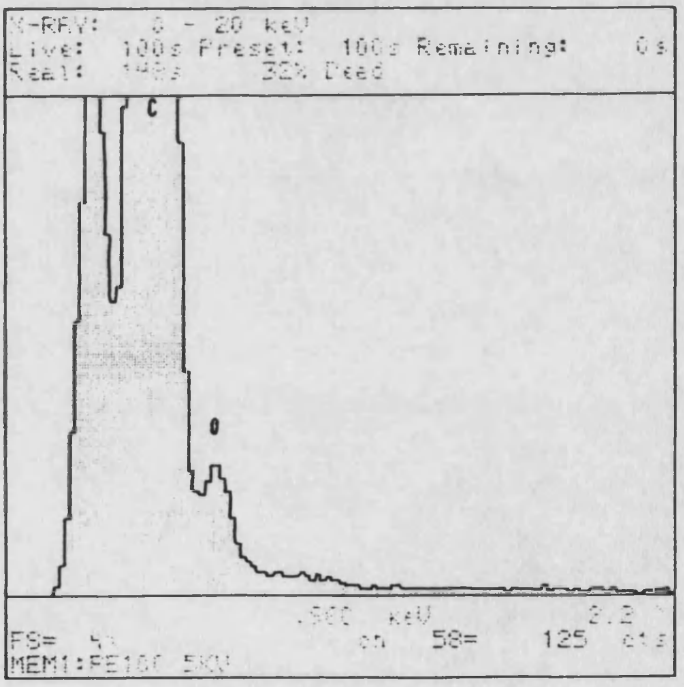

Figure 5.6b EDX spectrum of polyethylene oxidised with potassium persulphate

In the present work, oxidation reactions were performed with potassium persulphate in dilute acid and base solutions, experiments 7 & 8 in table 5.6 respectively. In each case the water contact angles of the treated films were significantly different from the starting polyethylene, but the changes were less than those obtained in neutral media. No oxidation was apparent in either sample by ATR-ir analysis.

These results are consistent with the mechanism for persulphate decomposition in acidic media proposed by Kolthoff and Miller,[237] and would support the theory that the oxidation of polyethylene occurs via a radical pathway:

A. Neutral media:

$$S_2O_8^{2-} \longrightarrow 2SO_4^{\cdot -} \qquad (5.6)$$

$$2S_2O_4^{\cdot -} + H_2O \longrightarrow 2HSO_4^- + 2HO\cdot \qquad (5.7)$$

$$2HO\cdot \longrightarrow H_2O + \tfrac{1}{2} O_2 \qquad (5.8)$$

B. Acid solution:

$$S_2O_8^{2-} + H^+ \longrightarrow HS_2O_8^- \longrightarrow SO_4 + HSO_4^- \qquad (5.9)$$

$$SO_4 \longrightarrow SO_3 + \tfrac{1}{2} O_2 \qquad (5.10)$$

Clearly, the acid catalysed decomposition proceeds via a solely ionic route, whilst the decomposition in neutral media leads to the formation of two different radical species. Reaction of these radicals with the polyethylene surface might then proceed according to the following schemes:

Reaction with the hydroxyl radical would be expected to form surface hydroxyl groups directly. Alternatively, the sulphate radical anion might react with the polymer surface initially and then be hydrolysed to produce surface hydroxyl groups according to scheme 5.12. The hydrolysis of sulphate end groups in a similar manner during persulphate initiated polymerisations has been reported earlier.[241]

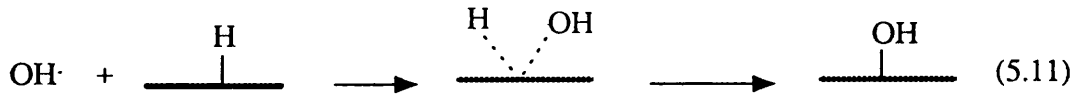

(5.11)

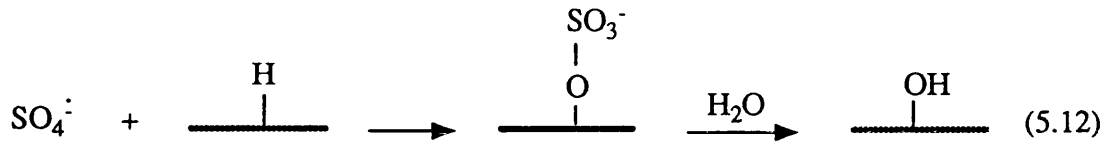

(5.12)

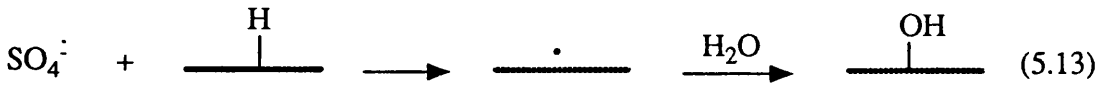

(5.13)

Finally, the sulphate radical might abstract a hydrogen from the polymer surface to generate a radical site which subsequently reacts with a water molecule to produce a surface hydroxyl group. These mechanisms are consistent with sonochemically enhanced reactions since a number of workers have reported that single electron transfer reactions are accelerated by ultrasound, whilst those proceeding by solely ionic pathways are relatively unaffected.[66]

In each case a hydroxylated surface would be produced which might be responsible for the lack of carbonyl bands in the ir spectra of potassium persulphate oxidised films. Accordingly, samples of the polyethylene film oxidised with 5g of potassium persulphate in 150 cm^3 of distilled water at an ultrasonic intensity of 26.2 Wcm^{-2} for five hours were derivatised with trifluoroacetic anhydride vapour (TFAA) as described in section 2.7.2. The TFAA is known to react selectively with surface hydroxyl groups to form fluoroesters according to scheme 5.4.[227]

The ATR-ir spectrum of the derivatised polyethylene sample is shown in figure 5.7C along with starting polyethylene(5.7A) and unoxidised polyethylene after exposure to TFAA vapour (5.7B). The characteristic fluoroester peak at ~1785 cm^{-1} is clearly present in the oxidised polyethylene sample to a much greater degree than in the virgin polyethylene derivatised sample. This indicates that

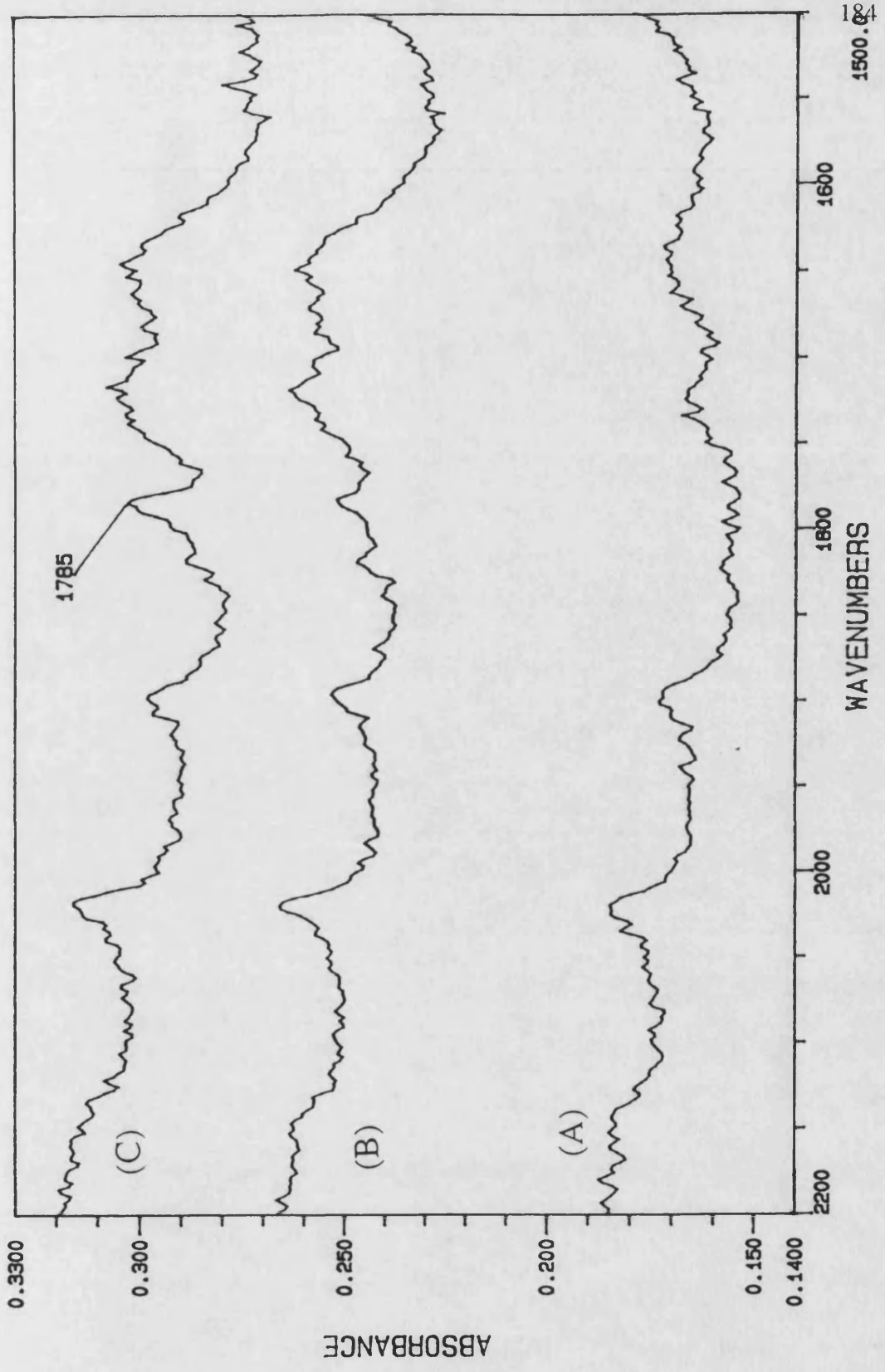

Figure 5.7 The 60° ATR spectrum of polyethylene (A), polyethylene after exposure to TFAA (B) and polyethylene oxidised with potassium persulphate and exposed to TFAA (C)

although very low levels of surface hydroxyl groups are present in the starting material, there are clearly many more after the ultrasonic reaction with potassium persulphate.

Addition of trace amounts of metals has also been reported to increase the rate of decomposition of the persulphate system.[241] In the present work iron(III) chloride was added to the oxidation system (experiment 9 in table 5.6), but the resulting contact angle value for the reacted polyethylene film, although significantly less than untreated polyethylene, was higher than that observed with the persulphate alone. Again, no infrared activity was evidenced by ATR analysis. It would seem therefore, that either the iron(III) chloride competes with the polyethylene surface to react with the radicals produced or presents an alternative non-radical decomposition pathway.

The addition of sodium dodecyl sulphate (SDS) to the reaction system as a possible phase transfer agent (experiment 10 in table 5.6) also gave rise to a film having a contact angle value between that of the untreated polyethylene and the aqueous persulphate oxidised film. This would suggest that either the transfer of reagents to the surface is not the major limiting factor in this oxidation route or, the SDS limits the reaction in some way. The presence of SDS is known to reduce the intensity of cavitation in water by lowering the cavitation threshold and for this reason is usually added to the bulk water in ultrasonic baths, see section 1.7.1.1. It might also be argued that the hydrophobic chains of the SDS molecules will accumulate at the polymer surface and prevent reaction, or perhaps react preferentially with any radical species.

The effects of time, ultrasonic intensity and persulphate concentration on the oxidation process were then studied. The water contact angle values of the film samples from each of these studies are presented in figures 5.8 to 5.10 respectively. Each of the contact angle values in these figures is the mean of at least 10 measurements across the film surface and values have been plotted with error bars calculated from the standard deviation of these values.

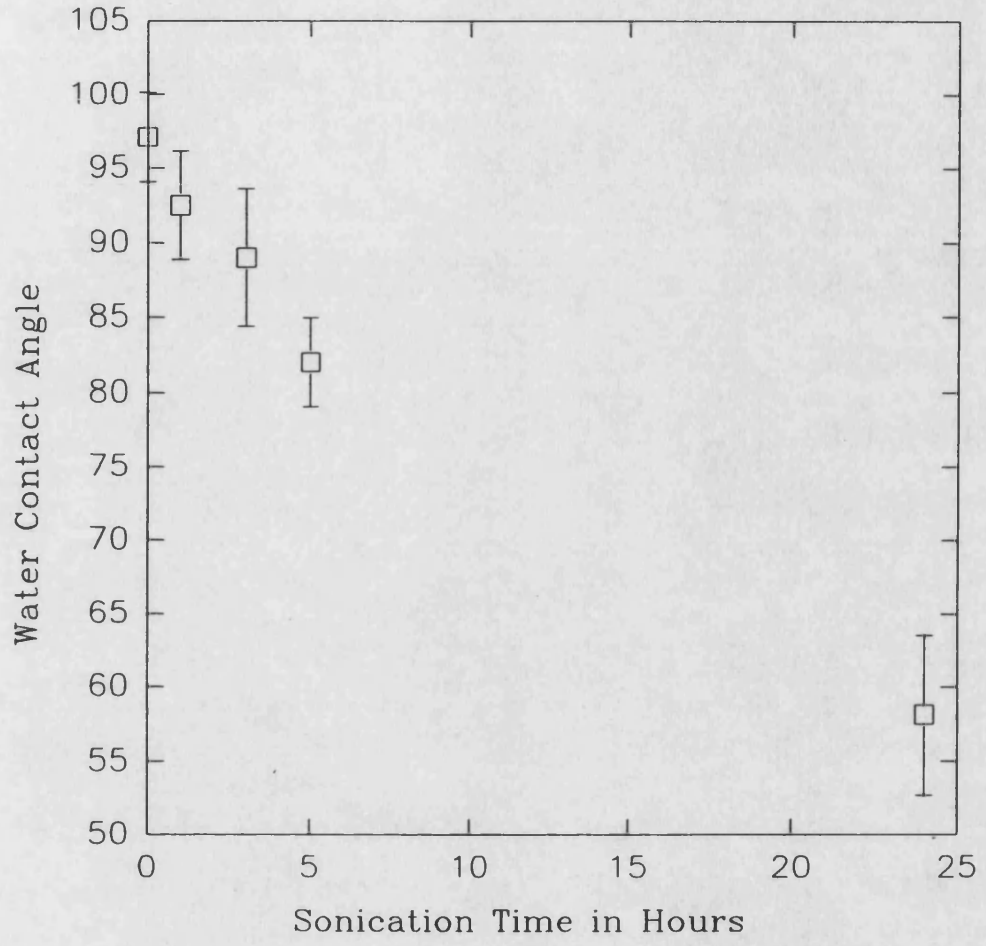

Figure 5.8 The change in water contact angle with sonication time for potassium persulphate oxidised polyethylene films

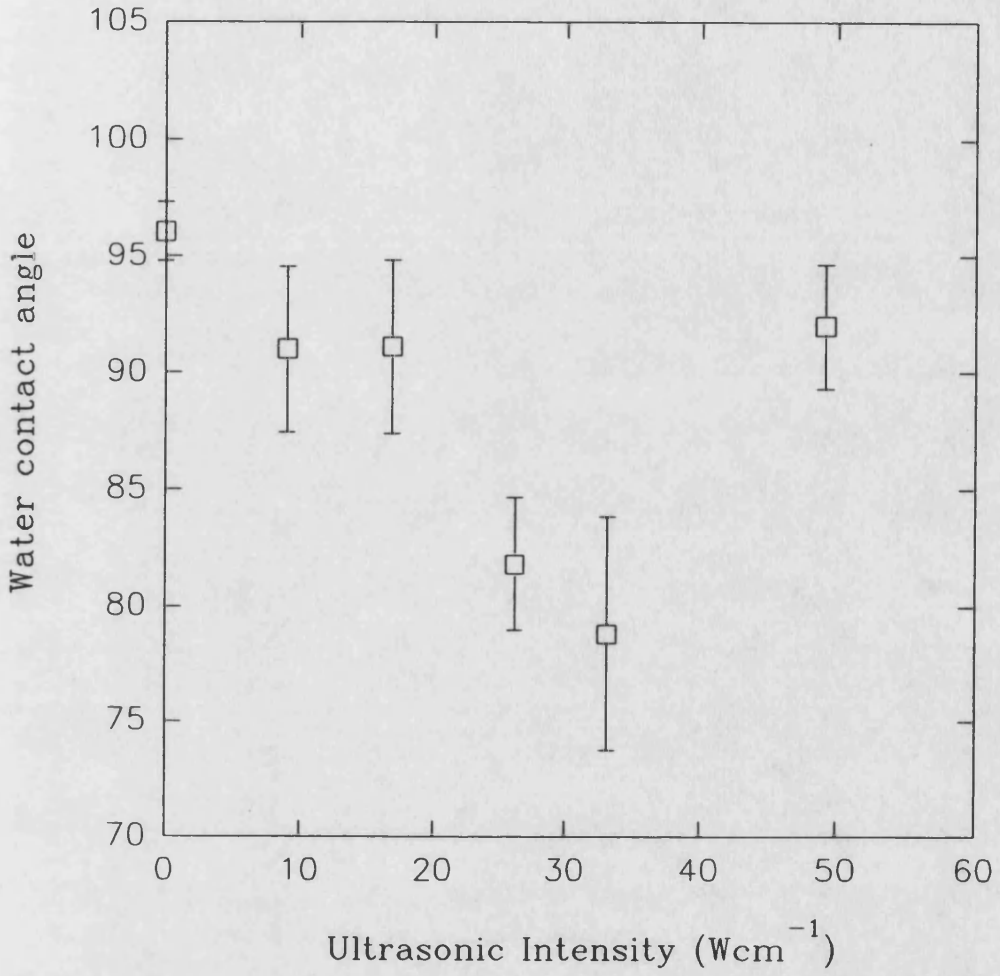

Figure 5.9 The change in water contact angle as a function of ultrasonic intensity for potassium persulphate oxidised polyethylene films

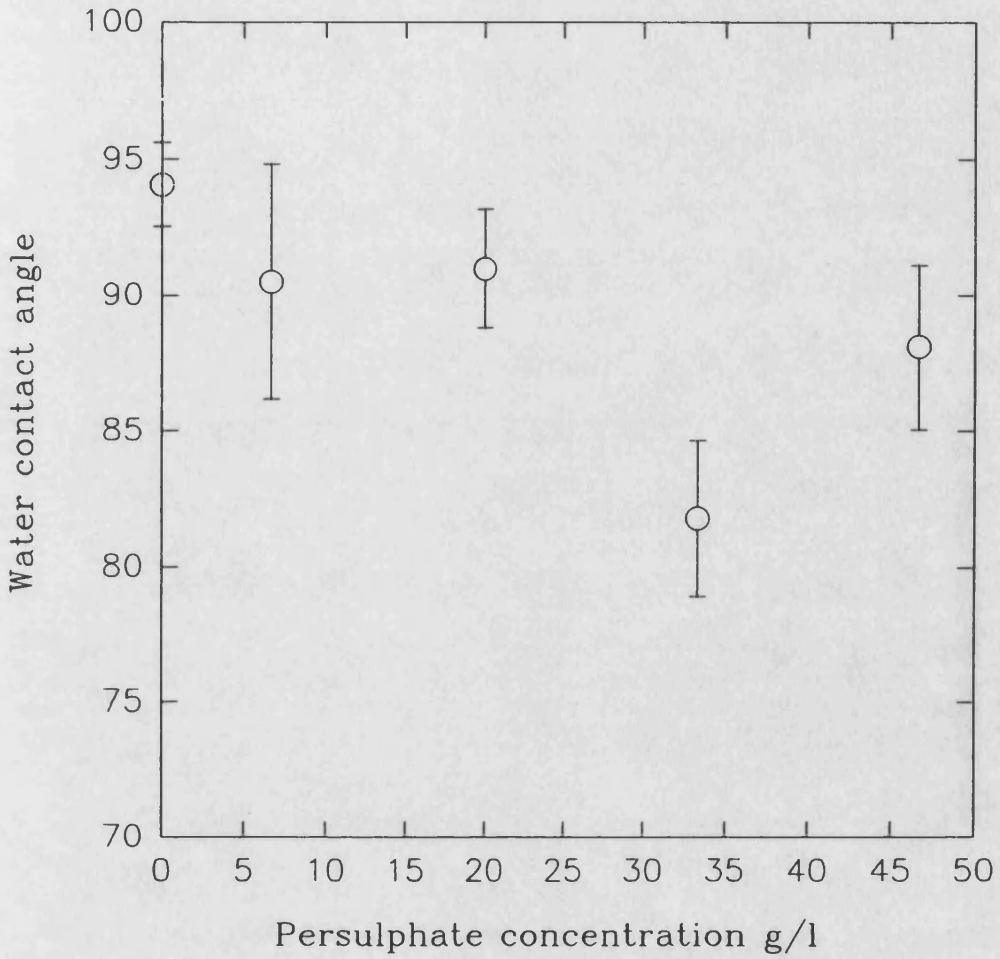

Figure 5.10 The change in water contact angle as a function of potassium persulphate concentration for ultrasonically oxidised polyethylene films

The plot of sonication time versus water contact angle for polyethylene films, oxidised using the same conditions as experiment 1 in table 5.6., figure 5.8, shows a marked change in the surface wettability of the polymer film after 24 hours. The ATR-ir spectrum of the resulting polyethylene film sample, displayed in figure 5.11, showed the presence of two carbonyl absorption bands at 1716 cm^{-1} and 1736 cm^{-1}. The position and intensity of these bands would suggest that the oxidation layer is still very thin and composed of mainly carboxylic acid and ester groups. This result can perhaps be expected, since Gallopo and co workers have shown that alcohols can be oxidised by persulphate.[242] In addition, the above observations would suggest that the nature of the surface functionality could be controlled to some degree by varying the sonication time and reaction temperature.

It would appear from the contact angle data that sonication for 24 hours in aqueous persulphate solution produces levels of oxidation similar to those obtained during chromic acid etching. The selectivity of the persulphate system however, appears to be significantly higher with reaction being limited to the outermost layers of the polyethylene surface.

These conclusions are further supported by the results in chapter 3 where oxidised film surfaces were analysed by scanning electron microscopy. The levels of surface erosion and etching observed with the ultrasonic persulphate oxidation system in this study were found to be significantly less than is generally seen with chromic acid solutions, even after 24 hours sonication.

The data in figure 5.9 shows the effect of ultrasonic intensity on the water contact angle for oxidised polyethylene films. These data clearly correspond to the rate of decomposition of the potassium persulphate as a function of ultrasonic intensity shown in figure 5.3. Thus, the rate of oxidation appears to be limited by the number of cavitational events resulting in homolysis of the persulphate.

Finally, the dependence of the ultrasonic oxidation on persulphate concentration was investigated at an intensity of 26.2 W cm^{-2} over five hours. These data, figure 5.10, show no clear dependence on concentration.

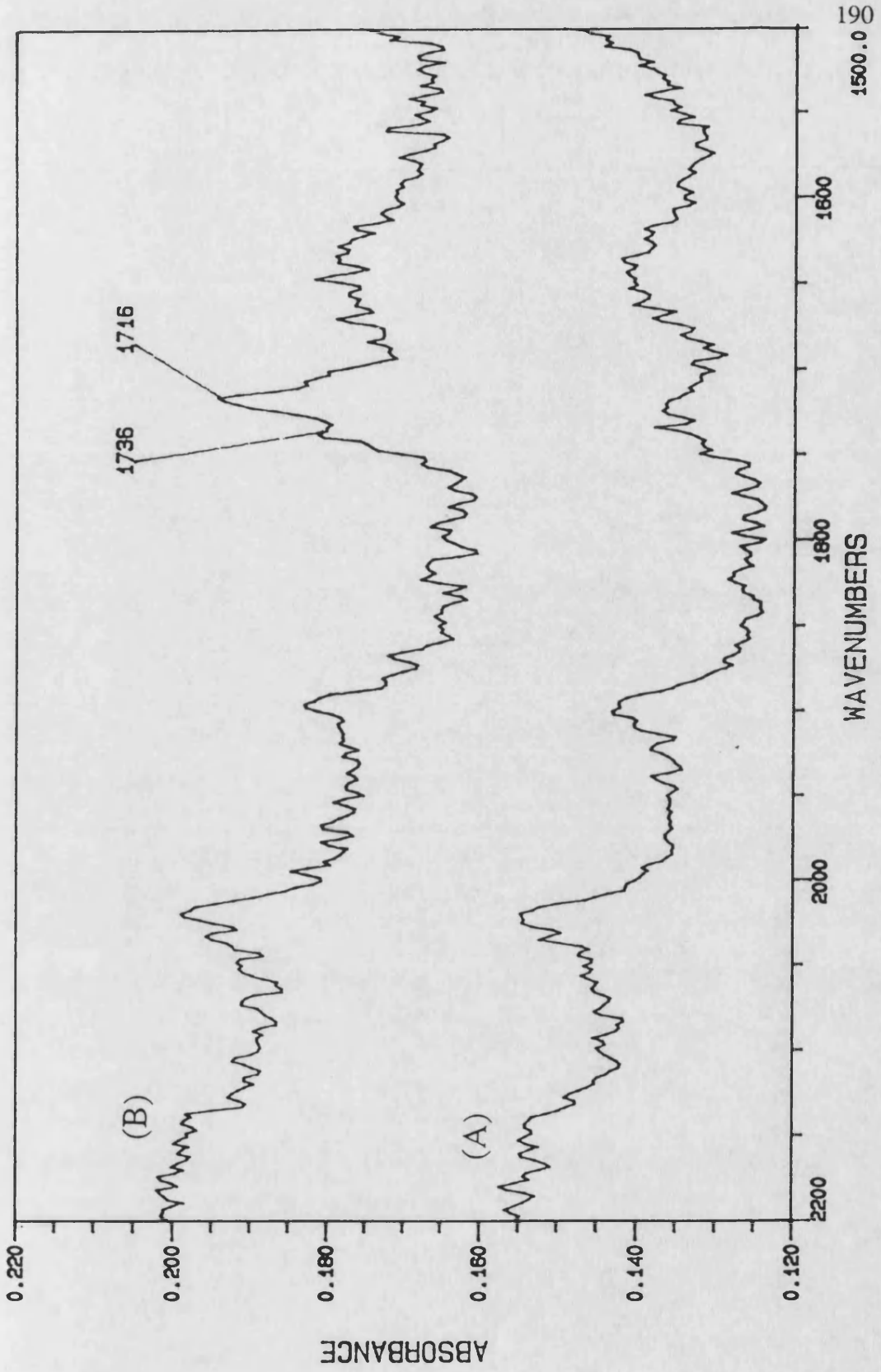

Figure 5.11 The 60° ATR spectrum of polyethylene after 24 hours sonication with potassium persulphate (B) and untreated polyethylene (A)

In conclusion, it must be argued that the ultrasonic oxidation of polyethylene film surfaces by potassium persulphate proceeds initially through the generation of surface hydroxyl groups. These groups are then oxidised further by the persulphate to give carboxylic acids and esters. At extended sonication times the oxidation layer produced gives a similar contact angle to chromic acid oxidised samples, but the oxidation is limited to a region of the polymer surface much less than 1μm.

5.3.2.1 Changes in Surface Crystallinity

Previous workers have reported that oxidation of polyethylene surfaces occurs initially in the crystalline regions.[32] The characteristic doublet at 720-730 cm^{-1} in the infrared spectrum has been shown to be sensitive to crystallinity changes in the polymer surface during the acid etching of polyethylene.[32] The 730 cm^{-1} component of this doublet is associated with the crystalline regions and the 720 cm^{-1} component mainly with the amorphous regions. The absorbance ratio, $R=I_{720}/I_{730}$ can be taken as a measure of the crystallinity. The values of R obtained in the present work for polyethylene films oxidised in the standard way with persulphate are displayed in table 5.7.

Table 5.7

Absorbance ratio of the amorphous crystalline bands, $R=I_{720}/I_{730}$, for polyethylene films oxidised by aqueous potassium persulphate

Sample	R from ATR
Polyethylene	1.25
5 hour oxidation	1.27
24 hour oxidation	1.36

The values of R presented in table 5.7 compare favourably with the changes

reported by Haridoss and Perlman during the acid etching of polyethylene films.[32] In their work the values of R varied from 1.09 for the untreated polyethylene to 1.45 for chromic acid oxidised samples. While the changes in the present work are lower, they also suggest that the ultrasonic oxidation of the polyethylene films in the present work occurs preferentially in the crystalline regions of the polymer. Furthermore, the smaller value of R observed in the present work is to be expected since the persulphate oxidation has been shown to be much more surface selective than chromic acid treatments. Although recently, Urban and co workers have suggested that this method is not entirely accurate for studying crystallinity changes in the surface,[33] since the absorbance ratio of these bands is sensitive to the sample and crystallite orientation. Accordingly, they reported that accurate determination of surface crystallinity requires detailed polarisation studies. The results from this work can, therefore, only be regarded as approximate, although a the trend in values is evident.

5.3.3 Reaction of Oxidised Polyethylene Films

The ability of the potassium persulphate system to generate surface oxidation on polyethylene films was used as starting point for secondary reactions. Film samples were initially oxidised for five hours using the same conditions as for experiment 1 in table 5.6. The oxidised films were then washed and dried as described earlier, see section 2.7.1, before being reacted further.

The contact angle results for reactions performed in this section are given in table 5.8

Table 5.8

Contact angle data for oxidised polyethylene films after secondary grafting reactions.

Reactants	Water contact angle °
10% $^{w}/_{v}$ acrylic acid[a]	78.0
0.01% $^{w}/_{v}$ polyacrylic acid	71.1
0.1% $^{w}/_{v}$ polyacylamide	88.6
10% $^{w}/_{v}$ hydroxy ethyl methacrylate[a]	78.9
0.6g Brilliant green	85.8
0.6g Methylene blue	82.1

Inhibitor was removed, see section 2.2

All sonication reactions displayed in table 5.8 were carried out for one hour at 35°C using an ultrasonic intensity of 26.2 Wcm^{-2} according to the procedure in section 2.7.1. The water contact angle data for the resulting films, also shown in table 5.8, indicated that only reaction with poly(acrylic acid) produced a value significantly less than that of the oxidised polyethylene film, although some reaction was also suggested with both acrylic acid and hydroxyethyl methacrylate.

Analysis of all of these samples by ATR-ir failed to show any new bands in the spectral region 500-4000 cm^{-1}. The reason for this apparent lack of reactivity may perhaps be attributed to the mechanism outlined in figure 4.13 in chapter 4, since it can be envisaged that any water soluble reagents grafted onto the polyethylene surface will extend into the solution. They will then be vulnerable to microstreaming and erosional effects and may be "swept" clear of the surface by subsequent acoustic cycles.

Accordingly, one further reaction was carried out using 5% $^{w}/_{v}$ trimethylsilyl methacrylate in 25% $^{v}/_{v}$ 2-propanol:water, as this would be expected to generate an

insoluble polymer layer as the reaction proceeded. Reaction was also carried out for one hour at 35°C using an intensity of 26.2 W cm^{-2}. The resulting film sample was found to give a water contact angle of 44°, clearly showing that a much higher degree of reaction had occurred with this system. The ATR-ir spectrum of this sample (figure 5.12) however, showed only a weak absorbance band at 1742 cm^{-1}. This would imply that some reaction had indeed occurred, but again the modification layer remained very thin.

Neither reaction with brilliant green nor methylene blue (see figure 4.4 for structures) gave any significant changes in the respective water contact angles from that of the oxidised polyethylene film. Analysis of these samples by diffuse reflectance ultraviolet spectroscopy also failed to show the presence of either chromophore, thus implying that very little or no reaction occurred.

In conclusion, it has been shown that ultrasound can be used to accelerate the decomposition of potassium persulphate in aqueous solution by a factor of about 10 times at 35°C. The radical species formed during this decomposition react with polyethylene film surfaces to give initially a hydroxylated polymer surface. At longer sonication times further oxidation takes place leading to the formation of mainly carboxylic acid and ester groups. The low temperature used for this sonochemical oxidation reaction, 35°C, causes only a limited increase in mobility of the polymer chains such that the polymer surface remains relatively hard, confining oxidation to a much shallower surface region. Grafting onto the oxidised surface is more difficult, however, but appears to be most successful when the grafted species is incompatible with the reaction solvent.

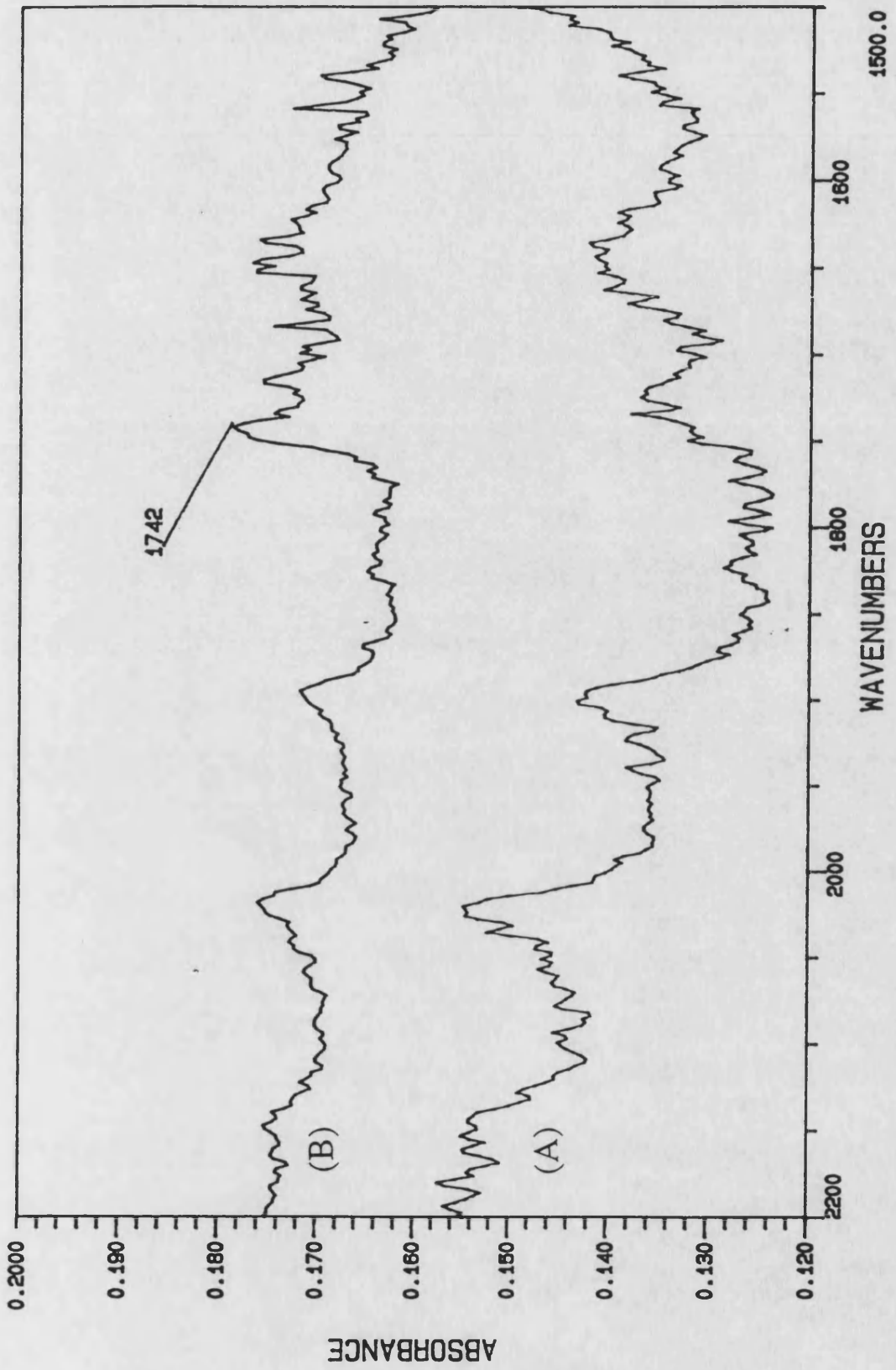

Figure 5.12 The 60° ATR spectrum of potassium persulphate oxidised polyethylene after reaction with trimethylsilyl methacrylate

CHAPTER 6

MODIFICATION OF "REAL" ELECTRICAL CABLES

The final stages of the work in this thesis involved the application of the those systems developed in the previous chapters to "real" cables. Samples of melt pressed PVC and polyethylene, prepared from actual cable materials, and commercial cables with polyethylene or PVC sheaths were supplied by BICC.

The results in chapters 4 and 5 have shown that a number of chemical modifications could be readily achieved on base polyethylene and PVC samples. The most promising of these have been applied to "real" systems. Caution should, however, be exercised in the interpretation of these results since the commercial samples contained plasticisers, fillers and other additives in addition to the base polymer.

As outlined in chapter 1, the ultimate target of the project was to develop cables with significantly different surface properties such as chemical resistance, coloration and slippability. A number of processed samples were submitted to BICC for testing but results were not received in time to be included in this thesis. Accordingly, the results in this chapter have been based upon the chemical characterisation methods used for model systems in chapter 4 and 5.

6.1 Modification of Polyethylene Cables

The feasibility of the ultrasonic potassium persulphate oxidation process for modification of polyethylene cable samples was assessed. Reactions were carried out in an identical manner to experiment 1, table 5.6, on extruded sheets of both very low density polyethylene (VLDPE) and polyethylene cable compound.

The contact angle results for the oxidised and unoxidised samples from these reactions are shown below in table 6.1.

Table 6.1

Contact angle values for polyethylene cable samples before and after ultrasonic treatment with potassium persulphate.

Polyethylene sample	Starting	Oxidised
VLDPE	84.0	82.0
polyethylene cable compound	86	<30

Whilst the accuracy of contact angle data for these samples is expected to be lower than with melt pressed polyethylene films, there is clearly a significant change in surface wettability with the polyethylene cable compound. No significant change was observed, however, with the VLDPE sample. The polyethylene cable compound was subsequently analysed by both ATR-ir and EDX. Analysis was complicated by the presence of additives, plasticisers and carbon black and no significant changes in the amount or number of oxygen containing species could, however, be detected by either of these techniques.

It has been shown that polyethylene cable compound can also be sonochemically oxidised by potassium persulphate. Indeed, reaction with this material appears to be more successful than with the base polyethylene. This result may be due to the greater starting surface wettability seen with this sample, through the presence of additives. This may in turn allow better transfer of reagents to the polymer surface and hence, increase the rate of reaction. No significant changes in the surface property were observed, however, for the VLDPE sample. Reaction in these systems is clearly more complex than with pure polyethylene and it would seem that the additives play some role in the transformation processes.

6.2 Modification of Poly(vinyl chloride) Cables

Following the success of sonochemical modification reactions on pure PVC powders and films, as discussed in chapter 4, extension was made to include melt pressed sheets of PVC and samples of white PVC household cable. Due to the physical nature of the household cable samples, these reactions were carried out in the Kerry PUL 325 ultrasonic bath using the reaction cell described in section 2.4.1C.

6.2.1 Reaction With Dyes

In chapter 4 it was shown that the most successful coloration of PVC powders was achieved with the brilliant green dye. Accordingly, samples of the white household cable were sonicated for one hour in the same concentration of aqueous dye solution used for experiment 20 in table 2.1. For a comparison, samples were also sonicated in aqueous solutions of bromopheneol blue and rose Bengal.

The end cable sample from reaction with brilliant green was then analysed by diffuse reflectance ultraviolet spectroscopy, using barium sulphate as a reference, and the resulting spectra are displayed in figure 6.1a and b. The reacted sample, figure 6.1b, shows the presence of an absorbance band at 630 nm, clearly indicating the presence of the dye chromophore unit. The most vivid characterisation of this sample, however, is perhaps obtained by eye, since the sample is visually green as shown in figure 6.2 (samples 4 & 5). Further analysis was then carried out by ATR-ir at a 45° incident angle but no changes were apparent. This observation would suggest that reaction on household cable is also very surface selective and limited to a very shallow surface region. By consideration of figure 6.2 it can be seen that reaction with both bromophenol blue and rose Bengal produced significantly less coloration on the cable surface. These results are also consistent

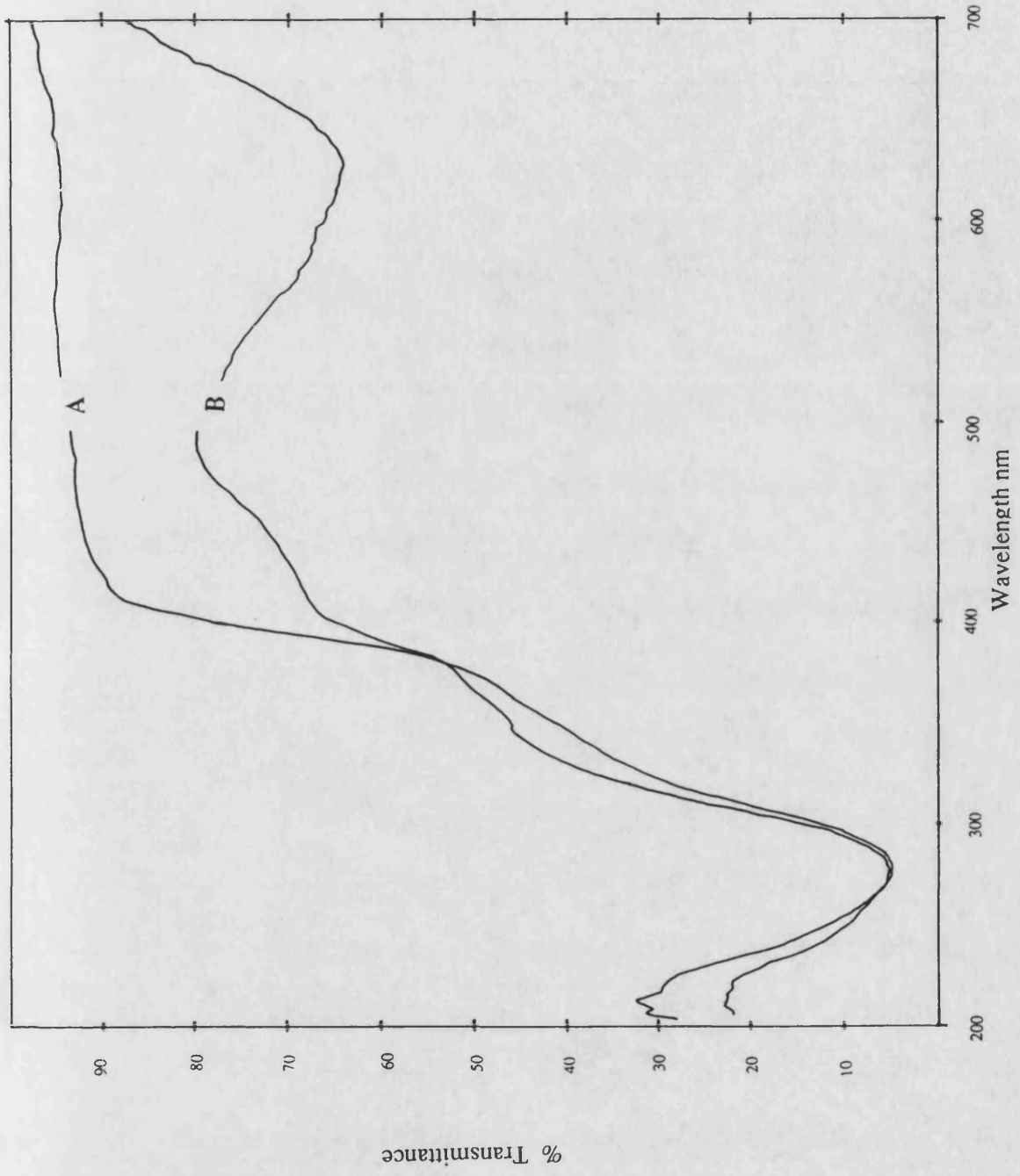

Figure 6.1 Diffuse reflectance spectra of poly(vinyl chloride) household cable; (**A**) untreated and (**B**) after reaction with brilliant green

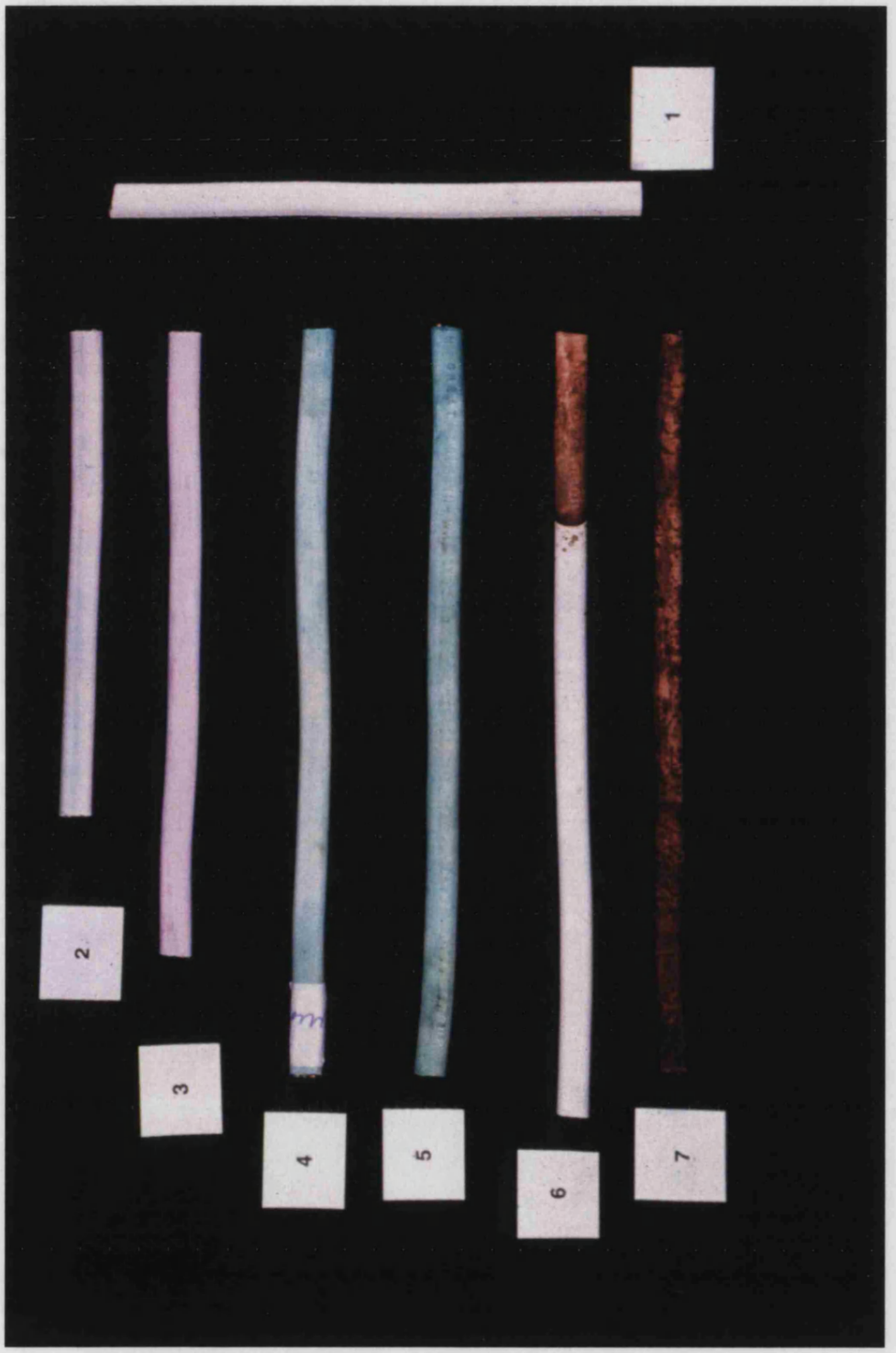

Figure 6.2 Photograph of PVC cable samples: (1) Untreated, reacted with; (2) Bromophenol Blue, (3) Rose Bengal, (4) Brilliant Green (20 minutes), (5) as (4) but 60 minutes, (6) NaOH and TBAB (20 minutes), (7) as (6) but 60 minutes.

with those observed with base PVC in chapter 5.

In conclusion it must be stated that despite the presence of a number of additives and antioxidants PVC cables can be coloured by sonochemically induced reaction with aqueous solutions of brilliant green.

6.2.2 Elimination Type Reactions

It was shown in chapter 4 that reaction of PVC surfaces with NaOH in the presence of trace amounts of $FeCl_3$ resulted in some surface crosslinking.

The ability to chemically cross-link the outermost layers of a preformed PVC cable would present a number of useful properties. Accordingly, reactions with aqueous base in the presence of iron (III) chloride were carried out according to the conditions in experiment 41p, on sheets of PVC cable compound (PM134 and GHI219) supplied by BICC.

The ATR-ir spectra from these investigations showed no discernable changes in the region 4000 to 500 cm^{-1}. This observation is consistent with the anticipated crosslinking mechanism, since very few inter chain bonds need to be formed in order to generate an insoluble cross-linked surface. Hence, surface crosslinking is suggested in this system although complete characterisation has not been achieved.

Dehydrochlorination With NaOH and TBAB

Dehydrochlorination reactions were applied to both films of PVC cable compound and household cable samples supplied by BICC, since in order for the reaction of double bonds to present a feasible modification route, the initial dehydrochlorination step must be applicable to "real" production samples. Reactions were carried out for one hour using the same conditions as those in experiment 47.

The ATR-ir spectra from these experiments with PVC PM134 and GHI219

are presented in figures 6.3 and 6.4 respectively. A broad absorbance band at $\approx$1600-1700cm^{-1} is apparent in both reacted samples suggesting that reaction occurred to a much greater degree than with the pure PVC films. The conjugation produced on the surface of these samples resulted in the formation of a brown-black cable and these sample are also shown in figure 6.2.

The origin of the increased reactivity of these samples over solution cast PVC films can perhaps be ascribed to changes in the topography and, particularly with actual cable samples, chemical composition of the surface region.

Solution cast films exhibited a much smoother surface than the extruded cable samples. This feature would then serve to present a greater interfacial area of contact between the reagents and surface. Furthermore, the calcium carbonate filler used in the cable samples might be expected to present a much more open and porous structure, thereby, allowing greater penetration of reagents into the polymer surface. That roughness is responsible, is perhaps evidenced most clearly by the reactions with powder samples where conjugation is also more readily detectable,

Conversely, it might be argued that the increased surface roughness seen with cables would give rise to an increase in the number of ultrasonic cavitation nuclei according to the crevice model outlined in section 1.6.1.[133-5] Whilst this may have some contribution to the process it is felt that surface area and porosity are the major reasons for the present results. Powder samples also present a greater detectable degree of unsaturation, but an increase in cavitation at the surface is not expected in these systems because collapsing cavitation bubbles have a diameter similar to that of the PVC particles (~160μm) and are therefore too large to interact with the PVC particles directly.[160] See also chapter three for a more detailed discussion of the interaction of collapsing cavities with PVC powders.

Furthermore, the presence of the plasticiser and other additives in these polymer samples may allow better wetting and hence, transfer of reagents to the polymer surface.

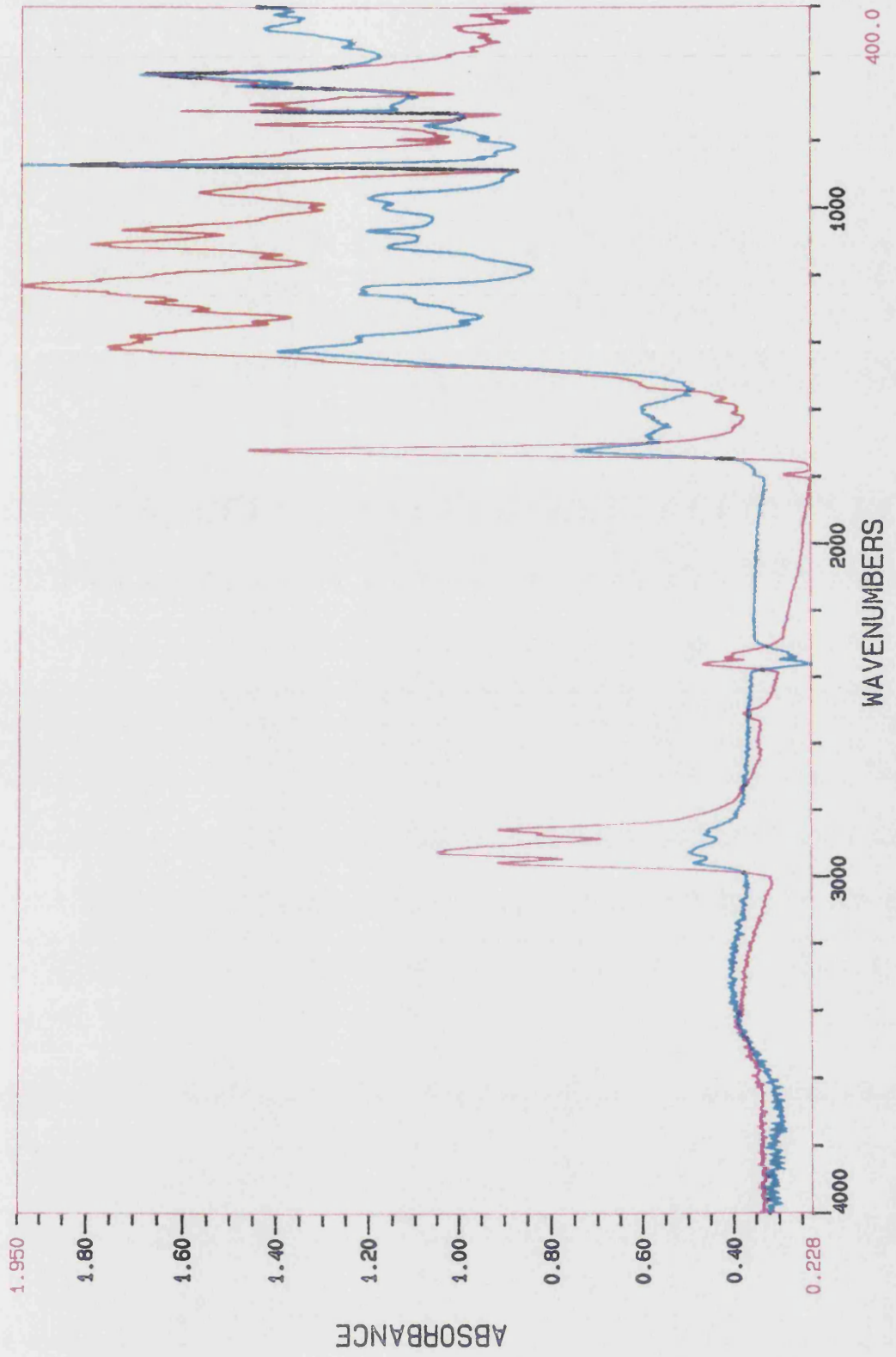

Figure 6.3 The 45° ATR spectra of PVC cable compound PM134 before reaction and after reaction with 25% $^{w}/_{v}$ NaOH and TBAB

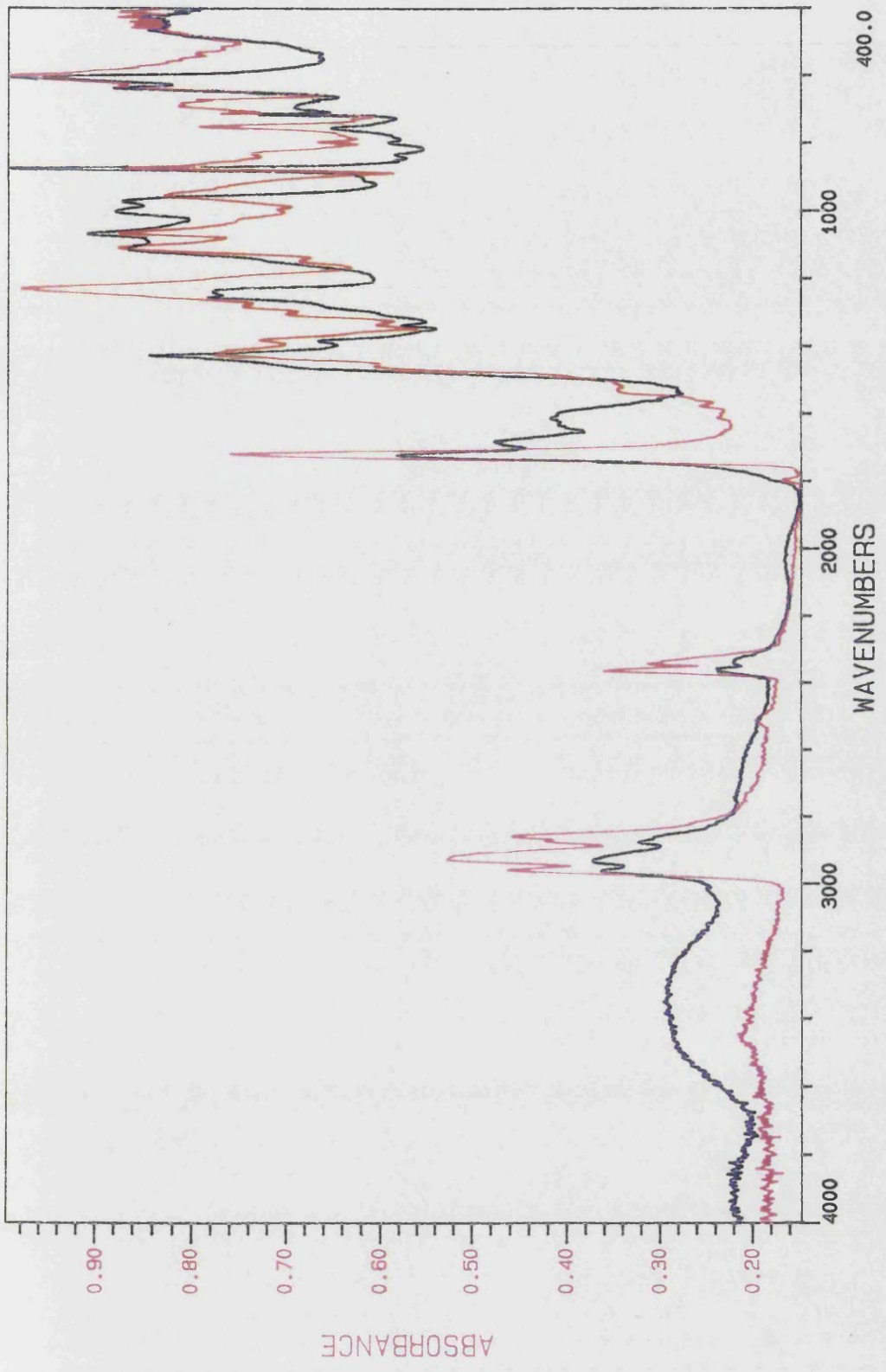

Figure 6.4 The 45° ATR spectra of PVC cable compound GHI219 before reaction —— and after reaction with 25% $^{w}/_{v}$ NaOH and TBAB ——

To gain more information about the depth of this reaction a sample of the dehydrochlorinated PM134 film was freeze fractured and the resulting edge analysed by SEM and EDX. The modification layer was however, shallower than the resolution (~1μm) of this technique, implying that reaction is very surface selective even with the actual cable materials.

In conclusion, it has been shown that PVC cable materials containing plasticisers, fillers and other additives can be reacted in a similar way to the pure base polymer. In this way, surface colour and dehydrochlorination has been achieved and reacted samples of household cable are shown in figure 6.1.

CHAPTER 7

CONCLUSIONS AND FURTHER WORK

The work described in the preceding chapters has clearly demonstrated that ultrasound can be used effectively to promote the introduction of new chemical functionality at the surface of polyethylene and PVC base polymers. Successful extension of several of the most promising ultrasonic transformations to "real" electrical cable materials has also been achieved.

The application of ultrasound has been shown to accelerate some conventional chemical processes, but moreover, has also provided a number of new routes. In addition, ultrasonic cavitation near a solid surface allows improved mass transfer of reagents, but the levels of surface etching and erosion were shown to be lower than those obtained with many conventional 'wet' chemical treatments.

The strength of water as a solvent for cavitation at relatively low temperatures and its poor wetting ability for these, and many other organic polymers, gives rise to a sharp reaction interface. This feature in turn allows reaction to proceed to only a very shallow depth into the surface.

The ability to carry out low temperature ultrasonic surface modification reactions in non-corrosive aqueous media clearly presents a new branch of technology. Before successful commercial production is achieved, however, several areas need development.

i. Work should be carried out with a commercial reaction system where a uniform high intensity ultrasonic field can be generated. This should remove the 'patchy' appearance exhibited by the reacted cable samples in figure 6.2 above.

ii. A more detailed understanding of the reaction rates would be necessary in order to establish the required exposure time. This in turn could be controlled by increasing the length of the sonochemical reactor or by changing the extrusion rate of the cable.

iii. Finally, an economic comparison between the improvement in the cable properties and the production costs must be analysed.

CHAPTER 8

REFERENCES

1. R.J. Young and P. Lovell in "Introduction to Polymer Science", 2nd Edn., Chapman and Hall, 1991
2. F.G. Thorpe in "New Methods of Polymer Synthesis", Ed., J.R. Ebdon, Blackie, 1991.
3. D.C. Sherrington, Encyclopedia of Polymer Science and Engineering, 2nd Edn., Wiley, New York, **14**, 101.
4. E. Leonhardi, "Chemisches Wortebuch der Allgemeine Bergriffe der Chemie", Leipzig 1781, 27.
5. J. Blyth and A.W. Hofmann, Liebigs Ann. Chem., 1845, **53**, 316.
6. H. Staudinger "From Organic Chemistry to Macromolecules", Wiley, New York, 1970.
7. E. Maréchal Comprehensive Polymer Science, 1989, **6**, 1.
8. T.J. McCarthy, Chima, 1990, **44**, 316
9. R.J. Good, J. Am. Chem. Soc., 1953, **74**, 5041.
10. R.E. Johnson, J. Phys. Chem., 1959, **63**, 1665.
11. T. Young, Phil. Trans. Roy. Soc., (London), 1805, **95**, 65.
12. D.H. Bangham and R.I. Razouk, Trans. Faraday Soc., 1937, **33**, 1459.
13. D.G. Rance in "Surface Analysis and Pretreatment of Plastics and Metals", Ed., D.M. Brewis, Applied Science, London 1982.
14. A.W. Neumann and R.J. Good, J. Surf. Coll. Sci., 1979, **11**, 31
15. G.L. Mack, J. Phys. Chem., 1936, **40**, 159
16. W.A. Zisman, J. Paint Technol., 1972, **44**, 42.
17. R.J. Good in "Surface and Colloid Science", Ed., R.J. Good and R.R. Stromberg, Plenum, New York, **11**, 1979.
18. R.E. Johnson and R.H. Dettre in "Contact Angle Wettability and Adhesion", ACS Adv. Chem. Ser., 1964, **43**, 112.
19. R.N. Wenzel, Ind. Eng. Chem., 1936, **28**, 988.
20. R.J. Good and M.N. Koo, J. Coll. Interface Sci., 1979, **71**, 283.

21. A. Baszkin and L. Ter-Minassian-Saranga, Polymer, 1978, **19**, 1083.

22. S.R. Holmes-Farley, R.H. Reamey, T.J. McCarthy, J. Deutc and G.M. Whitesides, Langmuir, 1985, **1**, 725.

23. Atlas der Polymer und Kunstoffanalyse, Carl Hanser Verlag, 2nd Edn., Ed., D.O. Hummel and F. Scholl, 1978-87.

24. P.R. Griffiths in "Chemical Infrared Fourier Transform Spectroscopy", Wiley Interscience, 1975.

25. W.T.M. Johnson, Official Digest of Oil and Colour Chemists Association, 1960, **32**, 1067.

26. H.A. Wills and V.J.I. Zichy in "Polymer Surfaces", Ed., D.T. Clark and W.J. Feast, Wiley, Chichester, 1978.

27. W.Wm. Wendlandt and H.G. Hecht, "Reflectance Spectroscopy", Interscience, 1966.

28. M.P. Fuller and P.R. Griffiths, Anal. Chem., 1978, **50**, 1906.

29. N.J. Harrick, "Internal Reflection Spectroscopy", Interscience, New York, 1967.

30. D. Briggs, V.J.I. Zichy, D.M. Brewis, J. Comyn, R.H. Dahm, M.A. Green and M.B.Konieczko, Surf. Interface Anal., 1980, **2**, 107.

31. J.P. Luongo and H. Schonhorn, J. Polym. Sci., A, 1968, **6**, 1649.

32. S. Haridoss and M.M. Perlman, J. Appl. Phys., 1984, **55**, 1332.

33. J.B. Huang, J.W. Hong and M.W. Urban, Polymer, 1992, **33**, 5173.

34. L.C. Sawyer and D.T. Grubb in "Polymer Microscopy", Chapman and Hall, London, 1987.

35. D.A. Hemsley, "The Light Microscopy of Synthetic Polymers", Oxford University Press, 1984.

36. J.R. White and E.L. Thomas, Rubber Chem. Technol., 1984, **57**, 457.

37. H.B. Haas, Proc. Indiana Acad. Sci., 1939, **48**, 104.

38. E.M. Cross and T.J. McCarthy, Macromolecules, 1992, **25**, 2603.

39. M. Lutinger and C.W. Cooper, J. Polym. Sci., C, 1968, **24**, 257.

40. G.D. Adams and R.L. Dawson, Encyclopedia of Polymer Science And Engineering, 2nd Edn., Wiley, New York, **6**, 494.

41. A. Puszynski and E. Godniak, Makromol. Chem. Rapid Commun., 1980, **1**, 617.

42. A. Peterlin and G. Meinel, J. Polym. Sci., B, 1969, **3**, 1059.

43. B. Bikson, J. Jagur-Grodzinski and D. Vofsi, Polymer, 1979, **20**, 215.

44. D.A. Olsen and A.J. Osteraas, J. Polym. Sci., A, 1969, **7**, 1921.

45. W.E. Walles U.S. Pat., 4,220,739, (1978).

46. J. Ihata, J. Polym. Sci., A, 1988, **26**, 167.

47. D.A. Olsen and A.J. Osteraas, J. Appl. Polym. Sci., 1969, **13**, 1523.

48. D.A. Olsen and A.J. Osteraas, J. Appl. Polym. Sci., 1969, **13**, 1537.

49. H. Ravel, Y.P. Singh, M.H. Mehata and S. Devi, Polm Int., 1992, **29**, 261.

50. F.M Rugg, J.J. Smith and R.C. Bacon, J. Appl. Polym. Sci., 1954, **13**, 535.

51. F.P. LaMantia and D, Curto, Polymer Degredation and Stability, 1992, **36**, 131.

52. D.M. Brewis and D. Briggs, Polymer, 1981, **22**, 7.

53. H. Schonhorn and F.W. Ryan, J. Polym. Sci., A, 1968, **6**, 231.

54. H. Schonhorn and F.W. Ryan, J. Appl. Polym. Sci., 1974, **18**, 235.

55. D. Briggs, D.M. Brewis and M.B. Konieczko, J. Mat. Sci., 1977, **12**, 429.

56. P. Blais, D.J. Carlsson G.W. Csullog and D.M. Wiles, J. Coll. Interface Sci., 1974, **47**, 636.

57. J.R. Rasmussen, E.r. Stedonski and G.M. Whitesides, J. Am. Chem. Soc., 1977, **99**, 4736.

58. D. Briggs, D.M. Brewis and M.B. Konieczko, J. Mat. Sci., 1976, **11**, 1270.

59. D. Bergbreiter, N. White and Z. Zhou, J. Polym. Sci., A, 1992, **30**, 389.

60. D.L. Allara and C.W. White, Adv. Chem. Ser., 1978, **169**, 273.

61. J.L. Henry and A. Garton, J. Polym. Sci., A, 1990, **28**, 945.

62. J.L. Henry, A.L. Ruaya and A. Garton, J. Polym. Sci., A, 1992, **30**, 1693.

63. J.M. Lane and D.J. Hourston, Prog. in Org. Coatings, 1993, **21**, 269.

64. A.R. Blythe, D. Briggs, C.R. Kendall, D.G. Rance and V.J.I. Zichy, Polymer, 1978, **19**, 1273.

65. D. Briggs, C.R. Kendall, A.R. Blythe and A.B. Wootton, Polymer, 1983, **24**, 47.

66. L.J. Gerenser, J.F. Elman, M.G. Mason and J.M. Pochan, Polymer, 1985, **26**, 1162.

67. D.T. Clark, A. Dilks and D. Shuttleworth, Ref. 26, Chapter 9, p.185.

68. J. Peeling and D.T. Clark, J. Polym. Sci., A, 1983, **21**, 2047.

69. D. Briggs, D.M. Brewis and M.B. Konieczko, J. Mat. Sci., 1979, **14**, 1344.

70. Z. Foltynowicz, K. Yamaguchi, B. Czajka and S.L. Regen, Macromolecules, 1985, **18**, 1349.

71. K. Allmér, A. Hult and B. Rånby, J. Polym. Sci., A, 1988, **26**, 2099.

72. K. Allmér, A. Hult and B. Rånby, J. Polym. Sci., A, 1989, **27**, 1641.

73. K. Allmér, A. Hult and B. Rånby, J. Polym. Sci., A, 1989, **27**, 3405.

74. K. Allmér, A. Hult and B. Rånby, J. Polym. Sci., A, 1989, **27**, 3419.

75. P. Zhang and B. Rånby, J. Appl. Polym. Sci., 1991, **43**, 621.

76. H. Kubota, K. Kobayashi, J.F. Ding and Y. Ogiwara, Eur. Polym. J., 1988, **24**, 441.

77. J.F. Ding, H. Kubota and Y. Ogiwara, Eur. Polym. J., 1992, **28**, 49.

78. C. Batich and A. Yahiaoui, J. Polym. Sci., A, 1987, **25**, 3479.

79. D.S. Everhart and C.N. Reilly, Anal. Chem., 1981, **53**, 665.

80. D. Bergbreiter and J. Zhou, J. Polym. Sci., A, 1992, **30**, 2049.

81. J. Zhou and D. Bergbreiter, Polymer Preprints, 1992, **33** , 266.

82. D. E. Bergbreiter, B. Srinivas and H.N. Gray, Macromolecules, 1993, **26**, 3245.

83. S. Margel, E. Cohen, Y. Dolitzk and O. Sivan, J. Polym. Sci., A, 1992, **30**, 1103.

84. S. Martin and G. Levin, J. Appl. Polym. Sci., 1981, **26**, 3295.

85. I.M. Plitz, R.A. Willingham, and J. Starnes, Macromolecules, 1976, **9**, 633.

86. I.M. Plitz, R.A. Willingham, and J. Starnes, Macromolecules, 1977, **10**, 499.

87. S. Marian and G. Levin, J. Appl. Polym. Sci., 1981, **26**, 3295.

88. G. Levin, Makromol. Chem., 1984, **5** , 513.

89. M. Takeishi, Y. Naito and M. Okawara, Die Angew. Makromol. Chem., 1973, **28**, 111.

90. E.E. Gilbert, J. Polym. Sci., A, 1984, **22**, 3603.

91. H. Zimmerman, A. Holländer and J. Behnisch, Polymer Degredation and Stability, 1992, **36**, 149.

92. A.H. Frye and R.W. Horst, J. Polym. Sci., 1959, **40**, 419.

93. W.I. Benough and M. Onozuka, Polymer, 1965, **6**, 625.

94. J. Lewis, M.K. Naqvi and G.S. Park, Makromol. Chem. Rapid Commun., 1980, **1**, 119.

95. J.M.J Fréchet, J. Makromol. Sci. Chem., 1981, **A 15**, 877.

96. N.P. Allen, R.P. Burns, J. Dwyer and C.M. McAuliffe, J. Mol. Catal., 1978, **3**, 325.

97. K. Hiratani, Y. Matsumoto and T. Nakagawa, J. Appl. Polym. Sci., 1978, **22**, 1787.

98. A. Gal, M. Cais and D.H. Kohn, J. Polym. Sci., A, 1978, **16**, 71.

99. A. Dondos and P. Rempp, Compt. Rend., 1962, **254**, 1064.

100. A.J. Dias and T.J. McCarthy, Macromolecules, 1987, **20**, 2068.

101. K-W. Lee and T.J. McCarthy, Macromolecules, 1988, **21**, 2318.

102. B.U. Kolb, P.A. Patton and T.J. McCarthy, Macromolecules, 1990, **23**, 366.

103. T.G. Bee and T.J. McCarthy, Macromolecules, 1992, **25**, 2093.

104. W.F. Maddams in "Degredation and Stabilisation of Poly(vinyl chloride)", Ed., E.D. Owen, Elsevier Applied Science, London, 1984.

105. W.H. Starnes, F.C. Schilling, K.B. Abbas, I.M. Plitz, R.L. Hartless and F.A. Bovey, Macromolecules, 1979, **12**, 13.

106. P.C. Deb and S. Sankokholkar, Makromol. Chem. Rapid Commun., 1980, **1**, 63.

107. G. Lechermeier, C. Pillot, J.Gole and A. Revillon, J. Appl. Polym. Sci., 1975, **19**, 1979.

108. G. Lechermeier, A. Revillon and C. Pillot, J. Appl. Polym. Sci., 1975, **19**, 1989.

109. A. Vidal, J.B. Donnet and J.P. Kennedy, J. Polym. Sci., Polym. Lett. Ed., 1977, **15**, 585.

110. N.G. Thame, R.D. Lundberg and J.P. Kennedy, J. Polym. Sci., A, 1972, **10**, 2525.

111. R.T. Sikorski and E. Czerwinska, Eur. Polym. J., 1986, **22**, 179.

112. D. Braun in "Degradation and Stabilisation of Polymers", Ed., G. Geuskens, Applied Science, London, 1975.

113. J. Wypych in "Polyvinylchloride Degradation", Ed., A.D. Jenkins, Elsevier, 1985.

114. C.S. Marvel, J.H Sample, and M.F. Rov, J. Am. Chem. Soc.,1939, **61**, 3241.

115. J.E. Campbell and W.H. Rauscher, J. Polym. Sci., 1955, **18**, 461.

116. E. Tschida, C-N. Shih, I. Shionara and S. Kambara, J. Polym. Sci., A, 1964, **2**, 3347.

117. J.P. Roth, P. Rempp and J. Parrod, J. Polym. Sci., C, 1963, **4**, 1347.

118. F. Tüdös, T. Kelen, T.T. Nagy and B. Turcsányi, Pure. Appl. Chem., 1974, **38**, 201.

119. H. Kise, J. Polym. Sci., A, 1982, **20**, 3189.

120. F-F. He and H. Kise, J. Polym. Sci., A, 1983, **21**, 1729.

121. M.W. Urban and E.M. Salzar-Rojas, Macromolecules, 1988, **21** , 372.

122. A. Henglein, Ultrasonics, 1978, **25**, 6.

123. H.G. Flynn, "Physical Acoustics", Academic Press, New York, 1964, **1B**, 57.

124. G. Kirchoff, Ann. Phys., 1868, **134**, 177.

125. J. Thorneycroft and S. Barnaby, Inst. C. Eng., 1895, **122**, 51.

126. B.E. Notlingk and E.A. Neppiras, Proc. Phys. Soc., (London), 1950, **B63**,679.

127. E.A. Neppiras and B.E. Notlingk, Proc. Phys. Soc., (London), 1950, **B63**, 1032.

128. E.A. Neppiras, Phys. Rep., 1980, **61**, 160.

129. D. Srinivasan and L.V. Holroyd, J. Appl. Phys., 1961, **32**, 446.

130. K.S. Suslick, R.E. Cline and D.A. Hammerton, J. Am. Chem. Soc., 1986, **108**, 5641.

131. M.A. Margulis, Adv. Sonochem, 1990, **1**.

132. Lord Rayleigh, Phil. Mag., 1917, **34**, 94.

133. L.A. Crum, Nature, 1979, **278**, 149.

134. R.E. Apfel in "Methods of Experimental Physics : Ultrasound", Ed., P.D. Edmonds, Academic Press, New York 1964, **19**, 356.

135. R.H.S. Winterton, J. Phys. D: Appl. Phys., 1977, **10**, 2041.

136. M. Greenspan and T. Tschiegg, J. Res. Natl. Bur. Stds., 1967, **71C**, 299.

137. A. Weissler, I. Pecht and M. Anbar, Science, 1965, **150**, 1288.

138. K.S. Suslick and P.F. Schubert, J. Am. Chem. Soc., 1983, **105**, 6042.

139. A. Henglein and C.H. Fischer, Ber. Bunsen Ges. Phys. Chem., 1984, **88**, 1196.

140. B. Niemczewski, Ultrasonics, 1980, **18**, 107.

141. J-L. Luche, Ultrasonics, 1987, **25**, 40.

142. V. Griffing, J. Chem. Phys., 1950, **18**, 997.

143. V. Griffing, J. Chem. Phys., 1952, **20**, 939.

144. L.A. Crum, Appl. Sci. Res., 1982, **38**, 101.

145. H.W.W. Brett and H.H. Jellinek, J. Polym. Sci., 1954, **13** , 441.

146. H.J. Eyring, J. Chem. Phys., 1936, **4**, 283.

147. P. Renaud, J. Chim. Phys., 1953, **50**, 135.

148. M. Margulis and L.M. Grundel, Zh. Fiz. Khim., 1982, **56**, 1445.

149. G. Cum, G. Galli, R. Gallo and A. Spadaro, Ultrasonics, 1992, **30**, 267.

150. J. Curie and P. Curie, Compt. Rend., 1880, **91**, 294.

151. J. Curie and P. Curie, Compt. Rend., 1881, **93**, 1137.

152. T.J. Goodwin in "Chemistry with Ultrasound", Ed., T.J. Mason, Elsevier Applied Science, 1990.

153. T.J. Mason, J.P. Lorimer and J.P. Moorehouse, Educ. in Chem., 1989, **26**, 13.

154. B. Pugin, Ultrasonics, 1987, **25**, 49.

155. Lucas Dawe Ultrasonics, Pentagonal Liquid Processor

156. W.T. Richards and A.L. Loomis, J. Am. Chem. Soc., 1927, **49**, 3086.

157. "Ultrasound, Its Chemical, Physical and Biological Effects", Ed. K.S. Suslick, VCH, 1988.

158. C.M.R. Low and S.V. Ley, "Ultrasound in Synthesis", Springer Verlag, 1989.

159. T.J. Mason and J.P. Lorimer, "Sonochemistry: Theory, Applications and Uses of Ultrasound in Chemistry", Ellis Horwood, 1988.

160. "Current Trends in Sonochemistry", Ed., G.J. Price, Royal Society of Chemistry, Cambridge, 1992.

161. T.J. Mason, Ultrasonics, 1986, **24**, 245.

162. J. Lindley and T.J. Mason, Chem. Soc. Rev., 1987, **16**, 275.

163. Y. Goldberg, R. Sturkovich and E. Lukevics, Heterocycles, 1989, **29**, 597.

164. K.S. Suslick, Science, 1990, **247**, 1439.

165. R.F. Abdulla, Aldrichimia Acta, 1988, **21**, 31.

166. J-L. Luche, C. Einhorn, J.C. Souza-Barbosa, C. Petrier, C. Depuy, P. Delair and T. Tuschi, Ultrasonics, 1990, **28**, 317.

167. K.S. Suslick and K.A Kemper, Ultrasonics, 1993, **31**, 463.

168. M. Kornfeld and L. Suvorov, J. Appl. Phys., 1944, **15**, 495.

169. C.F. Naudé and A.T. Ellis, J. Basic Eng., 1961, **83**, 648.

170. T.B. Benjamin and A.T. Ellis, Phil. Trans. Roy. Soc. London Ser. A, 1966, **260**, 221.

171. M.S. Plesset and R.B. Chapman, J. Fluid Mech., 1971, **47**, 283.

172. W. Lauterborn and W. Hentschel, Ultrasonics, 1985, **23**, 260.

173. W. Lauterborn and W. Hentschel, Ultrasonics, 1986, **24**, 59.

174. W. Lauterborn and H. Bolle, J. Fluid Mech., 1975, **72**, 391.

175. B. Vyas and C.M. Preece, J. Appl. Phys., 1976, **47**, 5133.

176. R.W. Wood and A.L. Loomis, Phil. Mag., 1927, **4**, 417.

177. K. Söllner, Trans. Faraday Soc., 1938, **34**, 1170.

178. J. Lindley, J.P. Lorimer and T.J. Mason, Ultrasonics, 1986, **24**, 292.

179. K.S. Suslick, D.J. Casadonte, M.L.H. Green and M.E. Thompson, Ultrasonics, 1987, **25**, 56.

180. K.S. Suslick, D.J. Casadonte and S.J. Doktycz, Solid State Ionics, 1989, **32/33**, 444.

181. S.J. Doktycz and K.S. Suslick, Science, 1990, , 1067.

182. E.C. Hughes and F. Veatch, US. Pat. 2,800,444; Chem. Abstr., 1957, **51**, 17151g.

183. T.S Mertes, US. Pat. 2,899,414; Chem. Abstr., 1959, **53**, 23093.

184. M.A. Margulis, Russian Pat., 1959, 631,372.

185. N. Moriguchi, J. Chem. Soc. Jpn., 1934, **55**, 749.

186. N. Moriguchi, J. Chem. Soc. Jpn., 1934, **55**, 751.

187. T.D. Lash, J. Chem. Ed., 1985, **62**, 720.

188. S. Regen and A. Singh, J. Org. Chem., 1982, **47**, 1587.

189. S. Prakash and J. D. Pandy, Tetrahedron, 1965, **21**, 903.

190. F.O. Schmitt, C.H. Johnson and R.A. Olson, J. Am. Chem. Soc., 1929, **51**, 370.

191. A. Weissler, J. Am. Chem. Soc., 1959, **81**, 1077.

192. A. Weissler, H.W. Cooper and S. Snyder, J. Am. Chem. Soc., 1950, **72**, 1769.

193. M.E. Fitzgerald, V. Griffing and J. Sullivan, J. Chem. Phys., 1956, **25**, 926.

194. N. Miller, Trans. Faraday Soc., 1950, **46**, 546.

195. K. Makino, M.M. Mossoba and P. Reisz, J. Am. Chem. Soc., 1982, **104**, 3537.

196. K. Makino, M.M. Mossoba and P. Reisz, J. Phys. Chem., 1983, **87**, 1369.

197. See K.S. Suslick In Reference 157, p. 141.

198. H. Ficke, E.J. Hart and P. Smith, J. Chem. Phys., 1938, **6** , 229.

199. N. Miller, J. Chem. Phys., 1950, **18**, 79.

200. W.A. Armstrong, R.A. Facey, D.W. Grant and W.G. Humphreys, Canad. J. Chem.,1963, **41**, 1575.

201. G.J. Price and E.J. Lenz, Ultrasonics, 1993, **31**, 451.

202. W.C. Schumb and E.S. Rittner, J. Am. Chem. Soc., 1940, **62**, 3416.

203. J.P. Lorimer, T.J. Mason, K. Fiddy, R. Groves and D. Dodgson, Ultrasonics International Conference Proceedings, 1989, 1283.

204. L. Zechmeister and E.F. Morgan, J. Am. Chem. Soc., 1955, **78**, 2149.

205. G.J. Price, P. Matthias and E.J. Lenz, Env. Protection and Proc. Safety, in press.

206. E.W. Flosdorf and L.A Chambers, J. Am. Chem. Soc., 1933, **55**, 3051.

207. A. Szalay, Z. Physik. Chim., 1933, **A164**, 231.

208. A. Szent-Gyorgyi, Nature, 1933, **131**, 278.

209. G.J. Price, Adv. Sonochem, 1990, **1**, 231.

210. A.M. Basedow and K.H. Ebert, Adv. Polym. Sci., 1977, **22**, 83.

211. A. Henglein, Makromol. Chem., 1954, **14**, 15.

212. A. Henglein, Makromol. Chem., 1955, **15**, 188.

213. H.W. Melville and A.J. Murray, Trans. Faraday Soc., 1950, **46**, 996.

214. M. Tabata, T. Miyazawa and J. Sohma, Proc. 3rd. Yamada Conference on Free Radicals, Yamadi Sci. Found., Osaka, 1979, 243.

215. M. Tabata, T. Miyazawa, J. Sohma and O. Kobayashi, Chem. Phys. Lett., 1980, **73**, 178.

216. J.R. Thomas and D.L. de Vries, J. Phys. Chem., 1959, **63**, 254.

217. P. Kruus, Ultrasonics, 1983, **21**, 193.

218. P. Kruus, J. Lowrie and M.L. O'Neil, Ultrasonics, 1988, **26**, 352.

219. G.J. Price, P.F. Smith and P.J. West, Ultrasonics, 1991, **29**, 166.

220. G.J. Price, D.J. Norris and P.J. West, Macromolecules, 1992, **25**, 6447.

221. T. Allen 'Particle Size Measurement' Powder Technology Series, Chapman and Hall, 4th Edn., 1990.

222. Lord Rayleigh, Phil. Mag., 1881, **12**, 81.

223. Lord Rayleigh, Proc. Roy. Soc. (London), 1911, **A84**, 25 : 1914, **A90**, 219.

224. R. Gans, Ann. Physik., 1908, **25**, 377.

225. T.J. Mason and J.P. Lorimer, "Sonochemistry", Ellis Horwood, 1988.

226. A. Chilkoti, B.D. Ratner and D. Briggs, Chem. Mater., 1991, **3**, 51.

227. A. Chilkoti and B.D. Ratner, Surf. Interface Anal., 1991, **17**, 567.

228. A.C. Gilby, Appl. Optics, 1974, **13**,2479

229. J.L-Luche, work presented at a one day Sonochemistry Symposium to Commemorate the Centenery of The Institute Meurice, Brussels, March 1993.

230. Nuffield Advanced Science Book of Data, Ed., R.D. Harrison, 1972.

231. P.F. Smith PhD Thesis, University of Bath 1991 and references therein.

232. CRC Handbook of Chemistry and Physics, Ed., R.C. Feast, 52nd Edn., 1971.

233. P. Carty, E. Metcalfe and S. White, Polymer, 1992, **33**, 2704.

234. Standard Potentials in Aqueous Solution, Ed., A.J Bard, K. Parsons and J. Jordan, Marcel Dekker, 1985.

235. D. Briggs in "Surface Analysis and Pretreatment of Metals and Plastics", Ed., D.M. Brewis, Applied Science, 1982.

236. K.B. Wiberg and R. Eisenthal, Tetrahedron, 1964, **20**, 1151.

237. I.M Kolthoff and I.K. Miller, J. Am. Chem. Soc., 1951, **73**, 3055.

238. J.M. Anderson and J.K. Kochi, J. Am. Chem. Soc., 1970, **96**, 1651.

239. C.E.M. Morris, J. Appl. Polym. Sci., 1970, **14**, 2171.

240. L. Green and O. Mason, J. Chem. Soc., 1910, **97**, 2083.

241. T.C. Hunter PhD Thesis University of Lancaster 1991.

242. R. Curci, G. Delano, F. Difuria, J.O. Edwards and A.R. Gallopo, J. Org. Chem., 1974, **39**, 3020.

APPENDIX 1

RAW DATA PLOTS FOR THE THERMAL AND ULTRASONIC DECOMPOSITION OF POTASSIUM PERSULPHATE

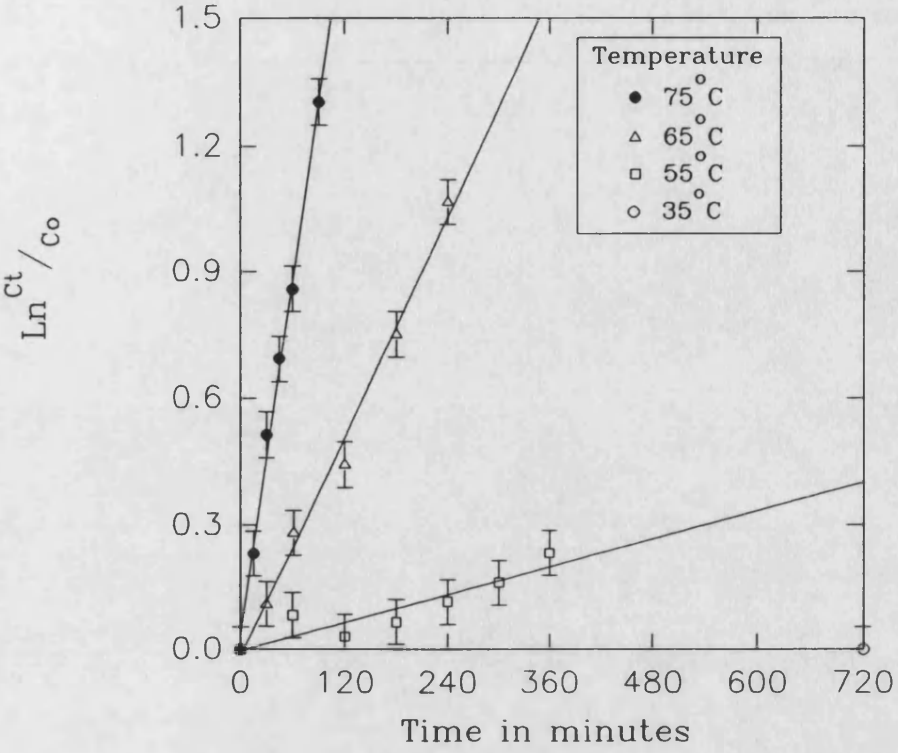

Thermal decomposition

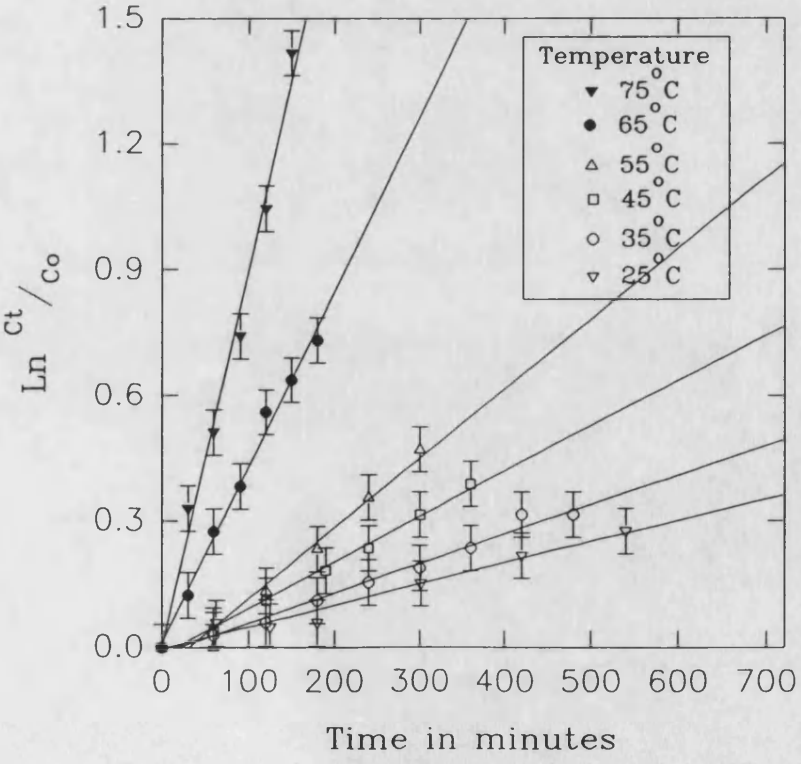

Ultrasonic decomposition